

VNIVERSITAT DE VALÈNCIA

Departament de Física Teòrica, IFIC – CSIC



Exotic properties of neutrinos  
using effective Lagrangians  
and specific models

PhD dissertation by

Alberto Aparici Benages

Under the supervision of

Arcadi Santamaria i Luna

Valencia, December 16<sup>th</sup> 2013

*There is no love of life without despair about life.*

ALBERT CAMUS, on PhD's.

*They wanted the end to be comforting, to say that it was not an end, but a beginning. But it's not a beginning, it is the real end; there will be nothing afterwards, nothing.*

DMITRI SHOSTAKOVICH, on postdoctoral positions.

*Of course it is happening inside your head, Harry, but why on earth should that mean that it is not real?*

ALBUS DUMBLEDORE, on renormalisation.

*I find your lack of faith disturbing.*

LORD DARTH VADER, after presenting his latest neutrino mass model.

This doctoral dissertation is based on the research presented in the following publications:

- [1] *Right-handed neutrino magnetic moments*  
A. A., Kyungwook Kim, Arcadi Santamaria, José Wudka  
[Phys.Rev.](#)**D80** 013010 (2009)
  
- [2] *A model for right-handed neutrino magnetic moments*  
A. A., Arcadi Santamaria, José Wudka  
[J.Phys.](#)**G37** 075012 (2010)
  
- [3] *Right-handed neutrino magnetic moments*  
A. A., Kyungwook Kim, Arcadi Santamaria, José Wudka  
[J.Phys.Conf.Ser.](#)**259** 012089 (2010)
  
- [4] *A realistic model of neutrino masses with a large neutrinoless double beta decay rate*  
Francisco del Águila, A. A., Subhaditya Bhattacharya, Arcadi Santamaria, José Wudka  
[JHEP](#) **1205** 133 (2012)
  
- [5] *Effective Lagrangian approach to neutrinoless double beta decay and neutrino masses*  
Francisco del Águila, A. A., Subhaditya Bhattacharya, Arcadi Santamaria, José Wudka  
[JHEP](#) **1206** 146 (2012)
  
- [6] *Neutrinoless double  $\beta$  decay with small neutrino masses*  
Francisco del Águila, A. A., Subhaditya Bhattacharya, Arcadi Santamaria, José Wudka  
[PoS Corfu2012](#) 028 (2013)

## ABBREVIATIONS

This is a list of abbreviations used throughout the text:

$0\nu\beta\beta$  neutrinoless double beta decay

**BAO** baryon acoustic oscillations

**CHAMP** charged massive particle

**CL** confidence level

**CMB** cosmic microwave background

**EFT** effective field theory

**EWSB** electroweak symmetry breaking

**LFV** lepton flavour violation

**LFV-ing** lepton-flavour-violating

**LN** lepton number

**LNV** lepton number violation

**LNV-ing** lepton-number-violating

**NP** new physics

**QCD** quantum chromodynamics

**QED** quantum electrodynamics

**QFT** quantum field theory

- SM** Standard Model
- SSB** spontaneous symmetry breaking
- VEV** vacuum expectation value

# CONTENTS

<i>Abbreviations</i> . . . . .	iv
1. <i>Overview</i> . . . . .	1
2. <i>Introductory concepts</i> . . . . .	3
2.1 Elements of the Standard Model: the weak interactions . . . . .	3
2.1.1 The weak interactions: a broken $SU(2)$ symmetry . . . . .	4
2.1.2 Doublets and singlets . . . . .	5
2.1.3 The trouble with masses, and a solution . . . . .	7
2.1.4 Hypercharge . . . . .	12
2.1.5 Concluding remarks . . . . .	17
2.2 Effective theories . . . . .	18
3. <i>Neutrinos</i> . . . . .	25
3.1 Neutrino masses . . . . .	25
3.1.1 Masses and the nature of fermionic particles . . . . .	26
3.1.2 Neutrino oscillations . . . . .	30
3.1.3 Writing masses and mixings . . . . .	32
3.2 Our knowledge of the mass sector . . . . .	36
3.2.1 Oscillation experiments . . . . .	37
3.2.2 Tritium beta decay and the magnitude of neutrino masses . . . . .	45
3.2.3 Cosmological bounds . . . . .	48
3.2.4 Neutrinoless double beta decay . . . . .	50
3.3 Seesaw mechanism . . . . .	58
3.3.1 Type I Seesaw . . . . .	59
3.3.2 Type II Seesaw . . . . .	60
3.3.3 Type III Seesaw . . . . .	63

---

3.4	Neutrino magnetic moments . . . . .	65
4.	<i>Right-handed neutrino magnetic moments</i> . . . . .	69
4.1	An effective theory capable of parametrising all neutrino mass scenarios . . . . .	69
4.2	Heavy physics content of the effective vertices . . . . .	72
4.3	The Lagrangian in terms of mass eigenfields . . . . .	75
4.4	Collider effects . . . . .	79
4.4.1	General considerations . . . . .	79
4.4.2	Decay mechanisms for the new neutral fermions . . . . .	80
4.4.3	Heavy neutrinos in $e^+e^-$ colliders . . . . .	84
4.4.4	Neutral heavy lepton production at the LHC . . . . .	88
4.4.5	Higgs decays into heavy neutrinos . . . . .	89
4.5	Astrophysical and cosmological considerations . . . . .	92
4.5.1	Astrophysical effects . . . . .	92
4.5.2	The electroweak moments as a source of CP asymmetry in the early universe . . . . .	95
4.6	Summary of bounds and conclusions . . . . .	99
4.7	Appendix: Decay rates and cross sections . . . . .	103
5.	<i>A model for right-handed neutrino magnetic moments</i> . . . . .	109
5.1	The model . . . . .	110
5.2	Generation of the dimension-five operators . . . . .	113
5.2.1	The right-handed neutrino electroweak moments . . . . .	113
5.2.2	The effective Higgs boson interaction . . . . .	115
5.3	Phenomenological analysis . . . . .	116
5.3.1	Considerations on the mass of the right-handed neutrinos . . . . .	116
5.3.2	$E$ or $\omega$ as CHAMP's . . . . .	118
5.3.3	Allowing for CHAMP decays . . . . .	119
5.3.4	Lepton Flavour Violating processes . . . . .	122
5.3.5	The model at colliders . . . . .	125
6.	<i>Neutrinoless double beta decay and neutrino masses</i> . . . . .	127
6.1	Violating lepton number through leptons and bosons . . . . .	127
6.2	Identification of the relevant operators. The role of chirality . . . . .	132

---

6.2.1	Preliminary remarks . . . . .	132
6.2.2	Notation . . . . .	134
6.2.3	Operators with two left-handed leptons . . . . .	137
6.2.4	Operators with one left- and one right-handed lepton . . . . .	138
6.2.5	Operators with two right-handed leptons . . . . .	139
6.2.6	A note to the model builder . . . . .	139
6.3	Implications for neutrinoless double beta decay . . . . .	141
6.4	Implications for neutrino masses . . . . .	145
6.5	Preeminence of the $W\nu e$ and $WWee$ mechanisms in neutrinoless double beta decay . . . . .	150
6.6	Modeling the lepton-boson mechanisms . . . . .	152
7.	<i>A model realising the <math>W\nu e</math> mechanism</i> . . . . .	159
7.1	A model with spontaneous and explicit breaking of lepton number . . . . .	160
7.2	Generation of $\mathcal{O}^{(7)}$ . . . . .	163
7.3	Neutrino masses and neutrinoless double beta decay . . . . .	165
7.4	Phenomenological constraints on the model parameters . . . . .	168
7.5	Collider effects . . . . .	172
8.	<i>A model realising the <math>WWee</math> mechanism</i> . . . . .	174
8.1	A model with lepton number softly broken . . . . .	175
8.2	The scalars of the theory . . . . .	178
8.2.1	Boundedness of the potential . . . . .	178
8.2.2	Vacuum expectation values . . . . .	182
8.2.3	Physical scalar spectrum . . . . .	185
8.2.4	Some couplings of phenomenological interest . . . . .	189
8.3	Neutrinoless double beta decay . . . . .	190
8.4	Lepton flavour violation constraints . . . . .	193
8.5	Constraints from naturality and perturbative unitarity . . . . .	196
8.6	A very constrained neutrino spectrum . . . . .	197
8.6.1	Calculation of the two-loop neutrino masses . . . . .	200
8.6.2	The structure of the neutrino mass matrix . . . . .	204
8.6.3	Consequences for the neutrino mass spectrum . . . . .	206
8.7	Constraints on the parameters of the model . . . . .	212



---

8.8	The model at colliders . . . . .	216
8.9	Domain walls and alternatives . . . . .	218
9.	<i>Conclusions</i> . . . . .	221
10.	<i>En la lengua de Cervantes</i> . . . . .	228
10.1	El título . . . . .	228
10.2	Neutrinos . . . . .	230
10.3	Momentos magnéticos de neutrinos dextrógiros . . . . .	233
10.4	Desintegración doble beta sin neutrinos . . . . .	236
11.	<i>Agradecimientos</i> . . . . .	242
	<i>Bibliography</i> . . . . .	248

## 1. OVERVIEW

In the past fifteen years oscillation experiments have unveiled the massive character of neutrinos; their results, combined with the enduring efforts to directly measure neutrino masses –not yet successful–, picture an image of three extremely light neutrinos, lighter by several orders of magnitude than the rest of the known particles. This mass gap calls for an explanation, and suggests that neutrinos might hide other unexpected properties related to the physics that endows them with this very special personality.

In this work we study several nonstandard features of neutrinos, first focusing on their phenomenological consequences and then progressing towards a more complete explanation. This scheme is realised in the interplay between effective field theory and concrete models. Effective interactions are powerful tools that allow to study the low-energy effects of heavy particles without having to specify the details of the heavy physics; they provide, so, a natural way to carry out model-independent analyses of exotic low-energy features. However, they are known to be limited: whenever some knowledge of the high-energy physics is needed, effective theories fail to yield predictions. Models, on the other hand, provide a complete specification of the low- and high-energy physics, thus allowing to calculate all and every feature of the theory; at the same time, and for this reason, they are limited: they must commit to one and just one family of new particles and can only yield predictions about them. Our aim is to combine the most powerful qualities of both approaches: to use effective operators to spot and study new neutrino properties in a model-independent way, and to complement that vision with concrete models which provide sharp high-energy predictions and maybe additional low-energy features that the effective theory cannot predict.

---

The text is organised as follows: chapters 2 and 3 introduce the basic concepts on which our study lies: the Standard Model, effective field theory and neutrino physics. Chapters 4 and 5 give a prominent role to right-handed neutrinos: we discuss in them effective operators that involve right-handed neutrinos as *low*-energy fields. We find a dimension-five interaction that has remained essentially unnoticed to date and which provides magnetic moments for the  $\nu_R$ 's, opening a plethora of scenarios where they might be relevant. In chapter 4 we address the question from the effective theory viewpoint, while in chapter 5 we discuss one model that realises the magnetic moment interaction. Chapters 6, 7 and 8 study a family of effective interactions that provide neutrinoless double beta decay and may overpower the usual contribution mediated by Majorana neutrino masses. We find two alternative mechanisms: one involving one  $W$  boson, one electron and one neutrino ( $W\nu e$  mechanism) and one involving two  $W$ 's and two electrons ( $WWee$  mechanism), both with explicit violation of lepton number. In chapter 6 we study how to characterise these effective interactions, how they contribute to  $0\nu\beta\beta$  and how they mediate the generation of neutrino masses. We find a remarkable connection between the chirality of the leptons involved in the effective interaction and the suppression of both the interaction and the generated neutrino masses. In chapters 7 and 8 we discuss models that realise the two effective mechanisms: in chapter 7 the  $W\nu e$  interaction is considered and chapter 8 is devoted to the  $WWee$  interaction. The latter model presents several interesting phenomenological features and can provide signals in a variety of different experiments.

## 2. INTRODUCTORY CONCEPTS

In this chapter we present the Standard Model and motivate some of its properties. While we introduce the notation for the SM fields we will discuss the topic of spontaneous symmetry breaking and the origin of mass in the Standard Model, as it plays an important role in the following chapters. We also introduce the concept of effective theory and explain how it applies to quantum field theory. The aim of these disquisitions is introductory, but the interested reader will find throughout the text references to specialised reviews where these topics are treated in more depth.

### *2.1 Elements of the Standard Model: the weak interactions*

The Standard Model is the main framework of modern particle physics. It is a quantum field theory that successfully describes the electromagnetic, weak and strong interactions of the known particles by using internal symmetries of the associated fields – see in [7–18] the original work, and also for instance [19, 20] for modern reviews. The fundamental fields include twelve fermions: six quarks,  $u$ ,  $d$ ,  $s$ ,  $c$ ,  $b$  and  $t$ ; three charged leptons,  $e$ ,  $\mu$  and  $\tau$ ; and three neutrinos,  $\nu_e$ ,  $\nu_\mu$  and  $\nu_\tau$ . The number of fundamental bosons may depend on how you count, but let's say we have eleven gauge bosons: eight coloured gluons for QCD, a massless photon for electromagnetism, and the  $W$  and  $Z$  for the weak interactions. And then the Higgs boson.

All these fields are organised in multiplets with well-defined internal symmetries; the symmetries are gauged, and this introduces naturally the gauge bosons into the theory and yields the right interaction vertices. That is strictly true for the strong interactions, and electromagnetism

---

might in principle be accommodated. The weak interactions, however, pose a more difficult challenge because their associated bosons are known to be massive and pure gauge theories yield strictly massless bosons; besides, the properties of the weak symmetries towards chirality make it impossible to construct a proper mass term for the fermions. These problems are solved at once by introducing the Higgs field and making it break the weak symmetries spontaneously. Let us explain how this happens, as we will deal mostly with the weak interactions in the chapters that follow.

### 2.1.1 *The weak interactions: a broken $SU(2)$ symmetry*

The weak interactions are accurately described at low energies by the effective Fermi interaction, which couples two fermionic currents into a dimension-six operator [21–23]. The celebrated experimental work of Madame Wu, carried out in the fifties, came to show that these interactions violate parity maximally [24, 25], which has to be implemented in the effective interaction. This can be done if the aforementioned fermionic currents only involve one of the fermion chiralities; by convention, the left-handed chirality is chosen to participate in the weak Fermi interactions whereas the right-handed one is transparent to them.

The Fermi interaction, however good it is at low energies, cannot be the final theory of the weak interactions: it is an effective interaction, and as such it fails at high energies, where the underlying particles should manifest. The sixties saw the development of several proposals for the high-energy content of the weak interactions, and finally it was the theoretical framework of Weinberg, Glashow and Salam [7, 13, 14] which proved to be the most successful – as of summer 2013, some might find it even *too* successful. This model gathers the left-handed components of the fermions in doublets and invokes upon them a  $SU(2)$  gauge symmetry. Intuitively, we know from the Fermi interaction that there’s a high-energy interaction connecting electrons to electron neutrinos and  $u$  quarks to  $d$  quarks, together with one or more heavy particles; grouping the fields into multiplets and invoking a gauge symmetry is a natural way to generate interactions among the fields

and, besides, provides new particles –the gauge bosons– that hold up the whole structure of new interactions. So, it seems a fairly good idea; but why doublets and why precisely  $SU(2)$ ? Indeed, originally it was not the only option, and ultimately it was the experiment who established the better proposal, but some valuable information can be extracted from an analysis of the currents in the Fermi interaction, as the reader can find, for instance, in chapter 11 of [26]. Let us here skip these details and focus on the notation that we are to use along the text and on the process of spontaneous symmetry breaking, which will recur over and over in the forthcoming chapters; but as a necessary caveat, we propose to the reader the following question: so, we are to group electrons and electron neutrinos into a doublet and then we are to say the doublet is  $SU(2)$ -symmetric. But how? Would not that imply that electrons and neutrinos should be indistinguishable? Indeed it would; so we already know, from the start, that the story cannot end with  $SU(2)$ . In due time this and other issues will be too strident to be ignored; but first things first: we promised some notation and here it comes.

### 2.1.2 Doublets and singlets

As we already argued, our theory of the weak interactions has the left-handed components of the fermions grouped into doublets which will be made  $SU(2)$ -invariant; we will denote the leptonic doublets by  $\ell_L$  and the quark doublets by  $Q_L$ :

$$\begin{aligned} \ell_{Le} &= P_L \begin{pmatrix} \nu_e \\ e \end{pmatrix} & \ell_{L\mu} &= P_L \begin{pmatrix} \nu_\mu \\ \mu \end{pmatrix} & \ell_{L\tau} &= P_L \begin{pmatrix} \nu_\tau \\ \tau \end{pmatrix} \\ Q_{L1} &= P_L \begin{pmatrix} u \\ d \end{pmatrix} & Q_{L2} &= P_L \begin{pmatrix} c \\ s \end{pmatrix} & Q_{L3} &= P_L \begin{pmatrix} t \\ b \end{pmatrix}, \end{aligned} \quad (2.1)$$

where  $P_L$  is the left-handed chiral projector, and the doublets may bear a family index that we will denote in general by a greek letter,  $\ell_{L\alpha}$  or  $Q_{L\alpha}$ ; in most cases, though, this index will be omitted in order to avoid overburdening the notation. The charge carried by these doublets, and represented by their  $SU(2)$  properties, is called *weak isospin*, and we will denote it by  $T$ . Hence, the doublets carry  $T^2(\ell_L) = T^2(Q_L) = 1/2$ ,

while the components possess a well-defined value for the isospin along the  $z$ -axis; for instance, we have  $T_3(e_L) = T_3(d_L) = -1/2$  and  $T_3(\nu_{Le}) = T_3(u_L) = +1/2$ .

The right-handed components of the fermions are singlets, that is, chargeless under  $SU(2)$ ; they will be denoted by  $e_R, \tau_R, u_R$  and so on, or sometimes as  $e_{R\alpha}, u_{R\alpha}, d_{R\alpha}, \nu_{R\alpha}$ , when we want to express them as components of a vector in flavour space. The existence of right-handed neutrinos is not proven yet, as we will discuss in more detail in section 3.1.1, and usually they are not considered part of the Standard Model. They can be added to the SM content in order to account for the existence of neutrino masses, but that is not the only option – again, see section 3.1.1.

The fermionic Lagrangian of the Standard Model, thus, considering only the weak  $SU(2)$  symmetry, will read

$$\begin{aligned} \mathcal{L}_W = & i \bar{\ell}_{L\alpha} \gamma_\mu D^\mu \ell_L^\alpha + i \bar{Q}_{L\alpha} \gamma_\mu D^\mu Q_L^\alpha + \\ & + i \bar{e}_{R\alpha} \gamma_\mu \partial^\mu e_R^\alpha + i \bar{u}_{R\alpha} \gamma_\mu \partial^\mu u_R^\alpha + i \bar{d}_{R\alpha} \gamma_\mu \partial^\mu d_R^\alpha, \end{aligned} \quad (2.2)$$

where Einstein's convention is understood for family and Lorentz indices; from now on, in simple expressions such as this one we will omit these indices. Note that there are no masses in Lagrangian (2.2): since mass terms are of the form  $\bar{e}_R e_L$ , they involve fields with different  $SU(2)$  charges and therefore they're not gauge invariant. This is another issue that points to the necessity of breaking  $SU(2)$ .

But let us come back to this just in a moment; before we need to fix the notation for the gauge bosons: begin by noticing that, whereas the singlet right-handed fields have a usual kinetic term with a spacetime derivative, the doublets, charged under the gauge symmetry, need a covariant derivative that we denote by  $D^\mu$ . This derivative contains a usual  $\partial^\mu$  plus other terms involving the gauge fields, that transform appropriately in order for  $SU(2)$  to be respected even locally. We write these terms as

$$D_\mu = \partial_\mu - ig T_a W_\mu^a,$$

where  $g$  is the coupling for the  $SU(2)$  interactions,  $T_a$  are the generators of  $SU(2)$  (the Pauli matrices halved,  $T_a = \frac{1}{2} \sigma_a$ ), and  $W_\mu^a$  are three real vector fields, the gauge bosons of  $SU(2)$ . The covariant kinetic terms

for the doublets in (2.2) yield interactions among the fermions and the gauge bosons, of the form

$$g \bar{\ell}_L \gamma^\mu T_a \ell_L W_\mu^a \qquad g \bar{Q}_L \gamma^\mu T_a Q_L W_\mu^a,$$

which are the embryos of the weak interaction vertices. The kinetic term for the gauge bosons can be devised by looking at their transformation properties under  $SU(2)$  and writing the most general bilinear gauge-invariant term that contains two derivatives, as it must be for bosonic fields. We will not enter into the details, which can be consulted for instance in [19], or in chapter 8 of [26], but we provide the form of these kinetic terms:

$$\mathcal{L}_{kW} = -\frac{1}{4} W_{\mu\nu}^a W_a^{\mu\nu}, \quad W_{\mu\nu}^a \equiv \partial_\mu W_\nu^a - \partial_\nu W_\mu^a + g \epsilon^a_{bc} W_\mu^b W_\nu^c. \quad (2.3)$$

### 2.1.3 The trouble with masses, and a solution

It is important to note that the same gauge transformations that define the gauge fields, as we see in (2.3), explicitly forbid a mass term for them. So, at this point of the story we are left with a symmetry that provides some fields which quite resemble the particles we observe, but none of them can have mass at all; besides, the symmetry renders the neutrino and the electron undistinguishable, which certainly doesn't resemble at all the situation in the real world. One could conclude that a symmetry that yields the correct elements for the model ends up restricting too much their properties. The question is: is there a way to relax these requirements so that we can reconcile the theory with reality?

The Higgs mechanism provides such a means; and, incidentally, one that remarkably matches the experimental data. The idea is to introduce a scalar field, the Higgs field, which shifts the vacuum of the theory to a non-gauge-invariant state; as a consequence, some fields with well-defined  $SU(2)$  properties will no longer represent physical excitations of the theory – for instance, excitations with definite mass. The fields that describe the actual particles of the theory will be combinations of the primordial fields, so we may say that the shift in the vacuum induces a shift in the fields. The new fields will happen to



have mass terms, and will successfully describe the particles we observe. At the end of the day it all happens *as if* there was no  $SU(2)$  symmetry at all, because fields that should be undistinguishable end up being rather different, and terms which seemed forbidden appear in a natural fashion. We say that the symmetry has been broken *spontaneously*, for we have not introduced any term that breaks  $SU(2)$ ; rather, it is the fact that we live in a noninvariant vacuum what makes us see the world as if  $SU(2)$  was not a symmetry. But the underlying laws of physics remain  $SU(2)$ -invariant, and the symmetry pervades most of the properties of the particles and their interactions.

Let us tell this story in a somewhat more rigorous way. The Higgs field is introduced as a complex scalar field with  $SU(2)$  charge; this last requirement is crucial, for it must displace the vacuum to a state with definite  $SU(2)$  properties. The simplest option is to choose the Higgs to be a doublet, like the other  $SU(2)$ -charged fields in the theory. We write it as  $\phi$ , and it contains four real-valued degrees of freedom; we can arrange them in several ways,

$$\phi(x) = \begin{pmatrix} \phi_1(x) + i\phi_2(x) \\ \phi_3(x) + i\phi_4(x) \end{pmatrix} = e^{i\sqrt{2}T_a\theta^a(x)/f} \begin{pmatrix} 0 \\ \rho(x) \end{pmatrix}. \quad (2.4)$$

Maybe the right-hand side reordering proves to be the most useful<sup>1</sup>; in it,  $T_a$  are the generators of  $SU(2)$ ,  $\rho$  and the  $\theta_a$  are real scalar fields, and  $f$  is some mass scale, needed for dimensional consistency. We endow the Higgs field with a quartic self-coupling,  $\lambda(\phi^\dagger\phi)^2$ , and an ‘anomalous’ mass term which apparently contains an imaginary mass,  $-\mu^2\phi^\dagger\phi$ . Summarising, the Lagrangian for the Higgs field is

$$\mathcal{L}_{\text{Higgs}} = (D_\mu\phi)^\dagger D^\mu\phi + \mu^2\phi^\dagger\phi - \lambda(\phi^\dagger\phi)^2, \quad (2.5)$$

but of course  $\phi$  cannot represent a real particle with such an unphysical mass. The introduction of this mass term forces us to look for the physical fields somewhere else. Thinking a little bit semiclassically, one may notice that  $\phi = 0$  is not a minimum of the scalar potential

---

<sup>1</sup> Of course there are infinitely many possible locations for  $\rho$  – some sort of ‘modulus of  $\phi$ ’. The convenience of this particular choice will be seen in due course, when we discuss electric charge.

of the theory,  $V(\phi) = \lambda(\phi^\dagger\phi)^2 - \mu^2\phi^\dagger\phi$ , and this is due precisely to the anomalous sign of  $\mu^2$ . It is possible to prove rigorously<sup>2</sup> that when the potential is minimised by nonzero values of some fields, then these fields acquire finite vacuum expectation values; this, in turn, implies that the vacuum of the theory corresponds to a state which is not invariant under some of the symmetries felt by the relevant fields. In other words: due to the sign of  $\mu^2$ , the symmetries under which  $\phi$  is charged should become spontaneously broken.

Let's see how this affects the properties we're interested in: first, notice that  $V(\phi)$  depends solely on  $\rho$ , as defined in (2.4), and that  $V(\rho)$  is minimised for  $\rho = \sqrt{\mu^2/2\lambda} \equiv v$ ; this is the value of the VEV for  $\rho$  and, hence, for  $\phi$  we have

$$\langle\phi\rangle = \begin{pmatrix} 0 \\ v \end{pmatrix}.$$

Then we may identify a field with a physically meaningful mass term by shifting  $\rho$  and defining a new field around the minimum:

$$\rho(x) = v + \frac{H(x)}{\sqrt{2}} \quad V(H) = \mu^2 H^2 + \sqrt{2}\lambda v H^3 + \frac{\lambda}{4} H^4,$$

where the  $\sqrt{2}$  factor accounts for a proper normalisation of the kinetic term of  $H$ , which is a real field. This way defined, the measured VEV of the Standard Model is  $v \simeq 246$  GeV [32]; some authors prefer to define the VEV with a  $\sqrt{2}$  normalisation too, and then a value of 174 GeV is given.

The  $H$  field, needless to say, is the now-superstar Higgs boson, whose mass has been recently measured to  $m_H = \mu \simeq 125$  GeV [33, 34]. But the interesting story is what happens to the other three degrees of freedom of the Higgs doublet: if we come back to equation (2.4), what we have done is just

$$\phi = e^{i\sqrt{2}T_a\theta^a/v} \begin{pmatrix} 0 \\ v + \frac{H}{\sqrt{2}} \end{pmatrix}, \quad (2.6)$$

---

<sup>2</sup> Though we won't do so here; the interested reader may look into [27–29], chapter 2 of [30], and also chapter 5 of [31].

where we have fixed  $f$  to the natural mass scale of the problem,  $f = v$ . If we substitute now this expression into the kinetic term in (2.5), a great deal of new pieces appear. We select here some of them:

$$(D_\mu \phi)^\dagger D^\mu \phi = \frac{1}{2} \partial_\mu \theta^a \partial^\mu \theta_a + \frac{g^2 v^2}{4} W_\mu^a W_a^\mu - \frac{gv}{\sqrt{2}} W_\mu^a \partial^\mu \theta_a + \dots, \quad (2.7)$$

and from them we point out three important features: first, the  $\theta$ 's are revealed as the Goldstone bosons associated to the spontaneous breaking, as they're massless, propagating scalar fields that transform in the adjoint representation of  $SU(2)$ . Second, the gauge bosons develop mass terms due to the shift of  $\rho$  to  $H$ , or, equivalently, due to the shift of the vacuum to a non- $SU(2)$ -invariant state. Third, the Goldstone bosons mix with the gauge bosons, thus providing the longitudinal degree of freedom needed to construct a consistent massive vectorial field<sup>3</sup>. The terms in equation (2.7) prove how deep has been the introduction of that anomalous sign in equation (2.5).

Going a step further, the Higgs field can also help in giving masses to the fermions. Notice that the  $SU(2)$  charges allow to write Yukawa interactions of the form  $\bar{\ell}_L Y_e e_R \phi$ , where  $Y_e$  is a matrix in flavour space, and that after SSB these interactions provide, among others, terms that exactly resemble a fermion mass term:

$$\bar{\ell}_L Y_e e_R \phi = v \bar{\ell}_L Y_e e_R + \bar{\ell}_L \frac{Y_e}{\sqrt{2}} e_R H, \quad (2.8)$$

where we have expressed the interactions after the breaking in the unitary gauge. Through this mechanism, the Higgs field emerges as the necessary piece to understand mass in the Standard Model: its VEV is the common scale for the masses of the gauge bosons and the fermions; the complex spectrum we observe is the consequence of the

---

<sup>3</sup> In fact, we can always, if we want, eliminate the Goldstone bosons from the description of the physics and consider just three vectorial bosons with definite nonzero mass. Formally, this is justified by the fact that the interactions remain  $SU(2)$ -invariant and we can choose to express them in any  $SU(2)$  gauge we like; for instance, a gauge that cancels the  $\theta$ 's in every spacetime point. Such gauge is called the *unitary gauge*. For more information on gauge fixing in spontaneously broken gauge theories the reader may refer to [26] or [35].

modulation of  $v$  by the gauge and Yukawa couplings. As a side effect, the Higgs boson, the only excitation of the Higgs field that retains individuality, inherits couplings to the fermions that are correlated to their mass spectrum: the heavier the fermion mass, the larger the Yukawa coupling and the larger the coupling to the Higgs boson, as we can see in (2.8).

The mechanism described above could be thought to provide masses only for the fields in the second component of the weak isodoublet, as the VEV is located in that position (the way we chose it, see equation (2.6), imposes a zero in the first component). This is not quite correct, for there is one more way to couple the Higgs field to the fermion doublets. To see it, remember that the fundamental representation of  $SU(2)$  is pseudoreal, that is, we can transform isovectors in the fundamental representation to isovectors in the complex-conjugate of the fundamental representation; to do so we only need an appropriate  $SU(2)$  matrix, which happens to be  $i\sigma_2$ . We often call this matrix  $\epsilon$ , as it is the totally antisymmetric  $2 \times 2$  matrix. Then consider the Yukawa couplings we can construct not with  $\phi$ , but with  $\phi^*$ : since we want to couple it to fundamental-representation doublets, say  $Q_L$ , we will need the mediation of  $\epsilon$ . As a result:

$$\begin{aligned} \overline{Q_L} Y_u u_R \epsilon \phi^* &= (\bar{u}_L \quad \bar{d}_L) Y_u u_R \begin{pmatrix} 0 & 1 \\ -1 & 0 \end{pmatrix} \begin{pmatrix} 0 \\ v + \frac{H}{\sqrt{2}} \end{pmatrix} = \\ &= v \bar{u}_L Y_u u_R + \bar{u}_L \frac{Y_u}{\sqrt{2}} u_R H, \quad (2.9) \end{aligned}$$

again with the Goldstone bosons abstracted from the description of the system. When writing down these terms it is common to use the more compact notation  $\tilde{\phi} \equiv \epsilon \phi^*$ , and the same for the complex-conjugate representation of the fermions,  $\tilde{\ell}_L \equiv \epsilon \ell_L^c$ , with  $\ell_L^c$  defined as usual,  $\ell_L^c \equiv C \bar{\ell}_L^T$ . In conclusion, we have a few more terms to add to our SM Lagrangian, which account for the masses<sup>4</sup> of the fermions and their interactions with the Higgs boson:

$$\mathcal{L}_{\text{Yukawa}} = \bar{\ell}_L Y_e e_R \phi + \bar{\ell}_L Y_\nu \nu_R \tilde{\phi} + \overline{Q_L} Y_u u_R \tilde{\phi} + \overline{Q_L} Y_d d_R \phi.$$

<sup>4</sup> As we said above, for the case of the neutrinos the use of right-handed neutrinos and the Higgs mechanism is not the only option. In fact it is not the most popular one. See section 3.1.1 for more on this matter.

---

A final remark must be noted about these mass terms: both for leptons and quarks there are two mass matrices, one associated to  $e_R$  ( $d_R$ ) and the other to  $\nu_R$  ( $u_R$ ). All four matrices are independent, so in principle the  $Y$ 's are completely general  $3 \times 3$  complex matrices which we must diagonalise in order to find the leptons (quarks) with well-defined masses. The diagonalisation of a general complex matrix can be carried out through two unitary matrices, one acting from the left and the other from the right; for instance, to diagonalise  $Y_e$  one only has to rotate adequately  $e_R$  and  $\ell_L$  in flavour space, that is, one has to express the charged leptons in the basis with well-defined mass. But then something interesting happens when we try to do the same for the neutrinos: we can rotate the  $\nu_R$ 's, but we have already consumed the liberties of  $\ell_L$  by finding the charged leptons with definite mass: if we diagonalise  $Y_\nu$  then we un-diagonalise  $Y_e$  and vice-versa. This issue implies that some of the non-diagonal terms in these matrices are physical quantities that we cannot ignore: there is a mismatch between the charged lepton mass eigenstates and the neutrino mass eigenstates, or as it is usually expressed, there is physical *mixing* between the mass and flavour states of the leptons. This is a direct consequence of  $\ell_L$  taking part in both  $Y_e$  and  $Y_\nu$ , and the same happens for quarks. Of course, there is no problem in working with quarks and leptons with well-defined masses (though that doesn't have to be always convenient): one can diagonalise at the same time  $Y_e$  and  $Y_\nu$  at the expense of transporting the physical off-diagonal quantities to other interactions in the Lagrangian – for the SM, to the weak charged currents. In that place they will behave as mixing terms that may transform flavour-conserving interactions into flavour-changing ones. More on the fundamental topic of the dynamics of flavour can be found in [19] and in chapters 11 and 12 of [26]; on the interesting matter of identifying the physical flavour parameters we recommend [36].

#### 2.1.4 Hypercharge

At this point we might be tempted to think that the task is done: we have, indeed, endowed our gauge theory with massive gauge bosons and we have found the way to construct mass terms for the fermions, and all

these things we've done without breaking any golden rule. Something, however, should make us suspect that the job is not quite finished yet: we know that the weak vector bosons are massive, but the  $W$ 's and the  $Z$  have different masses, and equation (2.7) assigns the same mass to all of them. Furthermore, some significant things happen related to the electric charge: we know that electromagnetism is described by a  $U(1)$  gauge theory; the photon is, as far as we know, exactly massless, so the  $U(1)$  symmetry is not broken. Naively, we may think that this means that the symmetry-breaking Higgs field must be electrically neutral. And that can be done; we can assign  $Q(\phi) = 0$  and let all the electric charge rest on the fermionic fields, either singlets or doublets. But this programme would encounter two problems: first, the doublets must be assigned a charge as a whole, but we know that the neutrino is neutral, while the electron is charged. Second, two of the Goldstone bosons end up as the longitudinal components of the  $W$ 's, which are electrically charged; these particular Goldstones, therefore, must be charged too, and as they are degrees of freedom of the Higgs field, the picture of a neutral  $\phi$  doesn't seem consistent. These two facts suggest some sort of 'coupling' between  $SU(2)$  and electric charge; this idea is reinforced if we note that, for all the doublets in (2.1), there's a difference of 1 between the charge of the up component and the down component.

To fix these issues *hypercharge* is introduced; the idea is to put a new gauge boson into the game in such a way that the photon emerges as a combination of the  $SU(2)$  bosons and this new one. If we get to do so, electric charge will be a combination of the new charge and the  $SU(2)$  charges, and we will have  $SU(2)$  multiplets with different electric charges for each component. As a side effect we will also gain a new gauge coupling which will allow us to have different masses for the  $W$ 's and the  $Z$ . Let us discuss how this happens: first we introduce a gauge phase symmetry "of hypercharge", that we denote as  $U(1)_Y$ ; this symmetry has just one generator and thus one associated gauge boson, that we denote by  $B_\mu$ . The covariant derivative is then modified to

$$D_\mu = \partial_\mu - ig T_a W_\mu^a - ig' Y B_\mu$$

for a general field with  $SU(2)$  structure and hypercharge  $Y$ . Note

that  $Y$  suffers from an ambiguity of definition: as the coupling,  $g'$ , and the charge itself always appear in the form of the product  $g'Y$ , the physics does not change if we rescale  $Y$  by a factor  $\kappa$  and  $g'$  by  $\kappa^{-1}$ .  $g'$  and  $Y$ , so, are ill-defined; this is a common feature to all Abelian gauge symmetries. The degeneracy will be resolved when we choose a well-defined relation between hypercharge,  $SU(2)$  charges and electric charge. To get to that point let us first discuss the spontaneous breaking of this somewhat more involved  $SU(2) \otimes U(1)$  symmetry.

The scheme we follow is the same we have already practiced for plain  $SU(2)$ : all the relevant features emerge from the Higgs field kinetic term, after we insert equation (2.6):

$$(D_\mu\phi)^\dagger D^\mu\phi = \frac{v^2}{4} \left( g^2 W_\mu^a W_a^\mu + 4g'^2 Y_\phi^2 B_\mu B^\mu - 4gg' Y_\phi B_\mu W_3^\mu \right) + v\sqrt{2} \left( g' Y_\phi B_\mu \partial^\mu \theta_3 - \frac{g}{2} W_\mu^a \partial^\mu \theta_a \right) + \dots \quad (2.10)$$

Here  $Y_\phi$  represents the hypercharge assignment of the Higgs field. We have selected two sets of pieces: the second one informs us that the hypercharge gauge boson couples only to the third Goldstone, while the first yields the mass matrix for the vectorial bosons. We note from this mass matrix that all the terms are diagonal save for one mixing between  $W_3$  and  $B$ .  $W_1$  and  $W_2$  are degenerate, and their mass is determined by the  $SU(2)$  coupling constant; of course, any combination of  $W_1$  and  $W_2$  will have the same mass as they have. Indeed, when we recover electric charge we will see that a certain combination has definite electromagnetic properties; we will identify such combination with the weak, charged  $W$  boson.

For the remaining two gauge bosons, some discussion about their masses is in order. It's easy to check that the mass matrix

$$\begin{pmatrix} W_\mu^3 & B_\mu \end{pmatrix} \frac{v^2}{4} \begin{pmatrix} g^2 & -2gg' Y_\phi \\ -2gg' Y_\phi & 4g'^2 Y_\phi^2 \end{pmatrix} \begin{pmatrix} W_3^\mu \\ B^\mu \end{pmatrix} \quad (2.11)$$

possesses a null eigenvalue, which has to correspond to the photon. The rotation

$$\begin{pmatrix} W_\mu^3 \\ B_\mu \end{pmatrix} = \begin{pmatrix} \cos \theta_W & \sin \theta_W \\ -\sin \theta_W & \cos \theta_W \end{pmatrix} \begin{pmatrix} Z_\mu \\ A_\mu \end{pmatrix}$$

with  $\tan \theta_W \equiv 2g'Y_\phi/g$ , identifies the relevant combinations, and defines the important *weak angle*,  $\theta_W$ . The photon is the only massless gauge boson that remains in the theory; it has to be associated with an unbroken, one-generator subgroup of  $SU(2) \otimes U(1)_Y$ . There is only one possibility if the subgroup is to have just one generator: a  $U(1)$  symmetry, which corresponds nicely with the known  $U(1)_{\text{em}}$  of QED. The conserved charge of  $U(1)_{\text{em}}$  is, of course, electric charge; we can identify it by isolating the photon in the  $SU(2) \otimes U(1)_Y$  covariant derivative:

$$\begin{aligned} D_\mu &= \partial_\mu - ig T_a W_\mu^a - ig' Y B_\mu = \\ &= \partial_\mu - ig (T_1 W_\mu^1 + T_2 W_\mu^2) - i(g \cos \theta_W T_3 - g' Y \sin \theta_W) Z_\mu - \\ &\quad - i \frac{gg'}{\sqrt{g^2 + 4g'^2 Y_\phi^2}} (2Y_\phi T_3 + Y) A_\mu, \end{aligned}$$

that allows us to define<sup>5</sup>:

$$e \equiv \frac{gg'}{\sqrt{g^2 + 4g'^2 Y_\phi^2}} \quad Q \equiv 2Y_\phi T_3 + Y. \quad (2.12)$$

These definitions are obscured by the presence of  $Y_\phi$ , which we should fix to its numerical value. But before we must figure it out:  $Y_\phi$ , as we read it in equation (2.12), is related to the charge spacing between the up-components and the down-components of the doublets, which we know to be of one unit. Indeed, if we apply the definition of electric charge to the components of the Higgs field itself, should we write  $\phi^T = (\phi_{\text{up}} \ \phi_{\text{down}})$ , we obtain

$$\begin{aligned} Q(\phi_{\text{up}}) &= 2Y_\phi \\ Q(\phi_{\text{down}}) &= 0. \end{aligned}$$

---

<sup>5</sup> Of course  $U(1)_{\text{em}}$  is Abelian too, and it is also affected by a scaling ambiguity. It can be made apparent by substituting  $Y \rightarrow \kappa Y$  and  $g' \rightarrow g'/\kappa$ , which also relates it to the ambiguity in  $U(1)_Y$ . The definition for  $Q$  in (2.12) is actually a choice, and fixes  $\kappa = 1$ . The reader can check that all the discussion that follows can be carried out with  $\kappa$  explicitly inserted in the expressions and no argument can be found to constrain its value. Another popular choice is  $\kappa = 1/2$ , in analogy to the Gell-Mann-Nishijima formula that relates electric charge and strong isospin.



There are two remarkable discoveries here: first, as we expected, the spacing between the two components depends only on  $Y_\phi$ ; in order to make it of  $+1$  charge units, as we see in the lepton and quark doublets, we require  $Y_\phi = +1/2$ . Second: the down-component has null electric charge, irrespective of the value of  $Y_\phi$ ; there is a good reason for that:  $\phi_{\text{down}}$  is the component of the Higgs field that gets a VEV, as we established in (2.6), and if the photon exists and is massless it's because its associated symmetry is unbroken. The theory ensures  $U(1)_{\text{em}}$  remains exact by assigning  $Q = 0$  to the relevant component of the symmetry-breaking field.

Incidentally, let us digress for a moment to comment, as we promised, on the choice we made in equation (2.6) for the  $SU(2)$  direction of the VEV. The reason is simple to state: electromagnetic interactions do not change flavour. Had the VEV been located in another direction, say  $\langle \phi \rangle^T = (v/\sqrt{2} \quad v/\sqrt{2})$ , the  $B$  boson would have mixed with some combination of the  $W_a$ , and the photon would have been in part  $W_1$  or  $W_2$ ; consequently,  $Q$  would have had components along  $T_1$  or  $T_2$ , which are nondiagonal and provide flavour-changing interactions. This is not acceptable: a photon that matches phenomenology needs  $B$  to mix only with  $W_3$ . This is achieved by a handful of directions, of which the one chosen in (2.6) is the most commonly used.

Returning to our discussion of hypercharge, the result  $Y_\phi = +1/2$  greatly simplifies the expressions that describe the breakdown of the  $SU(2) \otimes U(1)_Y$  symmetry, starting with the coupling and the charge of the electromagnetic interaction, which become

$$e = \frac{gg'}{\sqrt{g^2 + g'^2}} \quad Q = T_3 + Y. \quad (2.13)$$

This final expression for  $Q$  allows us to find the hypercharges for all the fields of the theory; we display them in table 2.1 together with a reminder of their  $SU(2)$  properties. We can also identify the electrically charged  $W$  boson: we know it should appear out of a combination of  $W_1$  and  $W_2$  –as it is a complex field it requires two real fields to be assembled–, and we know that any field that creates a charge  $q$  should verify  $[Q, \psi] = q\psi$ ; as the  $W$  bosons carry no hypercharge, it all reduces to finding a combination of  $W_1$  and  $W_2$

	$\ell_{L\alpha}$	$e_{R\alpha}$	$\nu_{R\alpha}$	$Q_{L\alpha}$	$u_{R\alpha}$	$d_{R\alpha}$	$\phi$
$SU(2)$	$1/2$	$0$	$0$	$1/2$	$0$	$0$	$1/2$
$Y$	$-1/2$	$-1$	$0$	$+1/6$	$+2/3$	$-1/3$	$+1/2$

Tab. 2.1: Electroweak charges of the non-gauge fields in the Standard Model. For  $SU(2)$  the representation is indicated; for hypercharge the convention given in equation (2.13) is assumed. The doublets  $\ell_L$  and  $Q_L$  are detailed in equation (2.1). The greek indices represent components in a flavour vector, as the analogous fields in different families have the same charge assignments.

such that  $[T_3, W^+] = +W^+$ . The  $SU(2)$  matrix which verifies this is  $T_+ \equiv T_1 + iT_2$ , and the associated combination of gauge bosons yields

$$W^\pm \equiv \frac{1}{\sqrt{2}} (W_1 \mp iW_2) .$$

For practical purposes we will work, as usual, with a  $W^\mu$  field and its Hermitian conjugate. Let us define by convention  $W \equiv W^-$  and  $W^\dagger \equiv W^+$ , meaning that the “particle” states –those created by the operator  $a^\dagger$ – will carry charge +1.

### 2.1.5 Concluding remarks

As for other properties of the gauge bosons, we can now write them down clearly. For instance, we can read their masses from equation (2.10) and from the eigenvalues of (2.11):

$$m_W^2 \equiv \frac{v^2}{4} g^2 = \frac{\pi\alpha}{\sin^2 \theta_W} v^2$$

$$m_Z^2 \equiv \frac{v^2}{4} (g^2 + g'^2) = \frac{\pi\alpha}{\sin^2 \theta_W \cos^2 \theta_W} v^2 ,$$

where we have expressed the masses first as a function of fundamental electroweak parameters and then in terms of the somewhat more practical  $\alpha$  (the fine-structure constant) and  $\theta_W$ . We can also write the weak

interaction vertices in terms of the relevant fields after spontaneous symmetry breaking; they arise from the fermion kinetic terms, which are of the form

$$\mathcal{L}_{\text{kin-ferm}} = i \bar{\Psi}_L \gamma_\mu D^\mu \Psi_L + i \bar{\psi}_R \gamma_\mu D^\mu \psi_R,$$

where the covariant derivative acting on the left-handed fields contains  $SU(2)$  structure, while the one acting on  $\psi_R$  carries, if anything, just the hypercharge part. Let us write explicitly the charged-current vertex for a general doublet notated as  $\Psi_L^T = (\Psi_L^{\text{up}} \quad \Psi_L^{\text{down}})$ :

$$g \bar{\Psi}_L \gamma_\mu (T^1 W_1^\mu + T^2 W_2^\mu) \Psi_L = \frac{e}{\sqrt{2} \sin \theta_W} \bar{\Psi}_L^{\text{down}} \gamma_\mu \Psi_L^{\text{up}} W^\mu + \text{H.c.} \quad (2.14)$$

And then the somewhat more cumbersome neutral-current vertices, which get stupendously simplified for the photon:

$$\begin{aligned} & g T_\psi^3 \bar{\psi}_L \gamma_\mu \psi_L W_3^\mu + g' (Q_\psi - T_\psi^3) \bar{\psi}_L \gamma_\mu \psi_L B^\mu + g' Q_\psi \bar{\psi}_R \gamma_\mu \psi_R B^\mu = \\ & = e \bar{\psi} \gamma_\mu \left[ \frac{T_\psi^3}{\sin \theta_W \cos \theta_W} P_L - Q_\psi \tan \theta_W \right] \psi Z^\mu + e Q_\psi \bar{\psi} \gamma_\mu \psi A^\mu, \end{aligned}$$

and where  $\psi_L$  represents either  $\Psi_L^{\text{up}}$  or  $\Psi_L^{\text{down}}$ , with its corresponding isospin assignment being  $T_\psi^3$ .

## 2.2 Effective theories

A second element that will be present throughout the next chapters is the notion of effective theory. Essentially<sup>6</sup>, the idea is that when a system has two very separated scales the dynamics of each scale tends to proceed independently of that of the other. This principle is easy to understand in the specific case of particle physics, where the natural scale difference is *energetic*: there exist light particles and heavy particles; at low energies one sees all the light particles,

<sup>6</sup> The reader interested in a more thorough discussion may look into some of the many references available in the literature. Two classical ones are [37, 38], but also interesting, with different approaches, are [39–43].

but none of the heavy ones; at high energies one can produce the heavy states, but cannot discern the masses of the light ones. One could think, thus, of devising specific theories for working at low or high energies which would be simpler than the complete model; such theories are called “effective” when some of the dynamical degrees of freedom—in the case of particle physics, the fields that describe the particles—are completely erased in the process. For instance one can think of simply eliminating the high-energy fields from the Lagrangian in order to describe the dynamics at low energies; of course, this would be just a first approximation, as the low-energy behaviour is not completely independent of the heavy fields: they can mediate process as virtual particles and generate effects that would not be observed if the light particles were the only ingredient. Therefore, a second step is to incorporate all these effects *without* reintroducing the heavy fields. But one does not need to account for all the effects of the heavy particles, as this would be equivalent to recovering the complete model; part of the beauty of this game is to realise that some effects are more important than others, and to identify the leading and the subleading ones. In this way one can weigh how deep wants to dig into the theory—or, analogously, how much precision one’s calculation requires—and then make an explicit cut, forget about the effects smaller than that. This sequence roughly describes the making of an effective theory.

So, how do these ideas effectively crystallise in the everyday work of a particle physicist? Have a look at figure 2.1a); it represents the transition  $\phi_1\phi_2 \rightarrow \phi_3\phi_4$  mediated by a  $\Phi$  field in the  $s$  channel. Let us now assume that the fields  $\phi_i$  are light and  $\Phi$  is heavy, and that the whole process proceeds with an energy sufficiently low so that a physical  $\Phi$  cannot be produced by any means; this transition, however, is allowed and will happen with some rate, as a  $\Phi$  in an internal leg does not need to be a detectable particle. We can calculate this rate: it only involves the internal propagator of  $\Phi$ , which is just

$$\frac{i}{p^2 - m_\Phi^2}. \quad (2.15)$$

Now, as we want to abstract  $\Phi$  from our description of the dynamics of  $\phi_1, \phi_2, \phi_3$  and  $\phi_4$ , we could forget that (2.15) comes at all from the

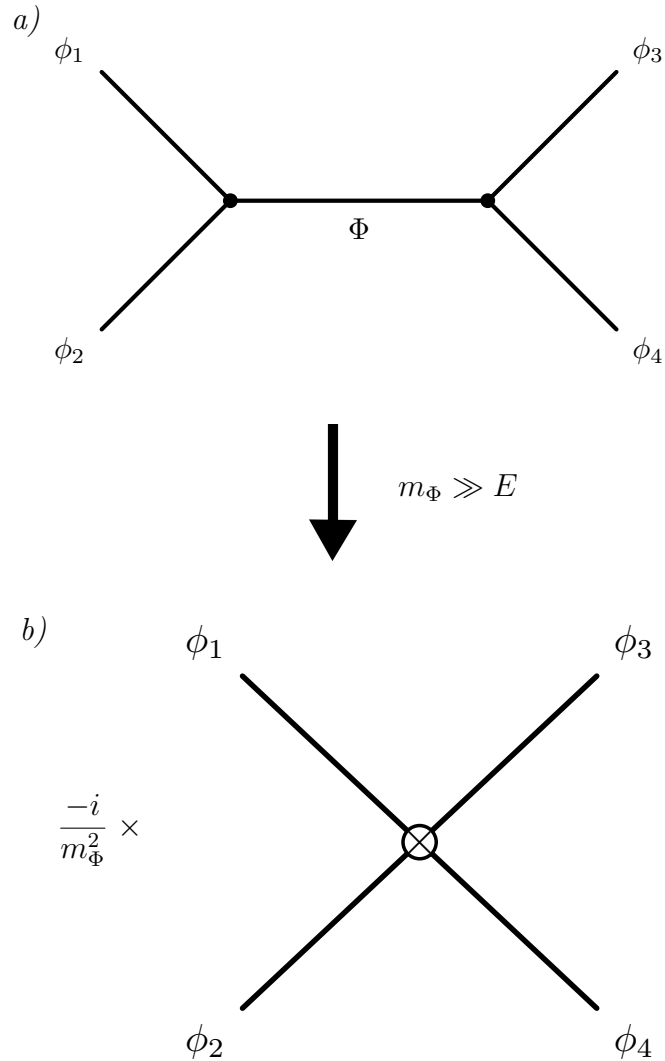


Fig. 2.1: An example of how a heavy field is eliminated from the low-energy description of physics: the four light fields  $\phi_1$ ,  $\phi_2$ ,  $\phi_3$  and  $\phi_4$  scatter with the mediation of a heavy field  $\Phi$ . If the typical energies of the  $\phi_i$  system are much below the mass of  $\Phi$ , it can be reduced to a numerical factor that depends on its mass, and for the light fields there remains a  $\phi_1\phi_2\phi_3\phi_4$  effective vertex.

---

contraction of a field; we could just consider it a sort of ‘form factor’, an addendum necessary for the calculation of  $\phi_1\phi_2 \rightarrow \phi_3\phi_4$ . Moreover, if  $m_\Phi$  is really much heavier than any energy scale we want to consider, we can neglect the internal momentum. By doing this we are left with  $-i/m_\Phi^2$ , a number; a dimensionful quantity too, but in any case not a field nor any kind of operator. What remains then for the calculation of the process? Just four external legs of light fields; we can represent the situation after ‘forgetting’ about  $\Phi$  as the diagram in figure 2.1*b*): the process has reduced to a four-field vertex and a dimensionful factor.

This example is paradigmatic: heavy fields that only act as virtual particles leave behind multi-field vertices that involve the light fields *times* dimensionful factors usually related to their masses. The next step is immediate: if this four-field vertex has appeared as a byproduct of a four-field process, other vertices, with arbitrary number of light fields, will emerge from other, N-field processes. We can learn from here the way to construct our effective theory, even if we know nothing about the underlying heavy physics: we will have to consider every combination of light fields which can take part in a low-energy process; this essentially means any combination of fields that respects all the conserved charges, as any physical process must do. The result will be a list of operators with ever-growing number of fields, each of them representing more and more complicated processes mediated by the heavy fields. Of course, given a certain set of heavy fields not all the operators will be equally important. It may even happen that some of them are not present at all, if the symmetries of the heavy fields forbid the associated processes. But as long as we are ignorant of the heavy physics we must consider all and every one of them.

Let us write these ideas in a more systematic way. We have a quantum field theory for which we know the relevant fields and symmetries, that is, the Lagrangian, up to some energy. The theory shows no hint that further physics is required: the Lagrangian is renormalisable, and so valid up to arbitrarily high energies. At this stage we have simply stripped away the heavy physics from the theory. Then we would like to introduce its virtual effects on the low-energy fields; for that aim, we proceed by adding all the operators that respect Lorentz symmetry and any other symmetry of the low-energy theory,

irrespective of the number of fields. As the original Lagrangian was renormalisable, it contained terms up to dimension four; the effective terms, so, will begin at dimension five:

$$\mathcal{L}_{\text{eff}} = \mathcal{L} + \sum_{n=5}^{\infty} \sum_i \left( \frac{C_i^{(n)}}{\Lambda^{n-4}} \mathcal{O}_i^{(n)} + \text{H.c.} \right). \quad (2.16)$$

In this expression  $n$  indicates the dimensionality of the operator and  $i$  labels the different operators of the same dimension, whose number will depend on the field content of  $\mathcal{L}$ . As a Lagrangian must have dimensions of  $E^4$ , the effective operators must be accompanied by dimensionful couplings with dimensions of inverse mass to an appropriate power; this is a reflection of the fact that these operators are the result of ‘freezing’ one or more internal propagators from a physical process, much in the way we display in figure 2.1. The dimensionality of the effective coupling is carried by the parameter  $\Lambda$ , which has dimensions of mass; the effective coefficients  $C_i^{(n)}$  collect the dimensionless factors of the coupling. The separation between  $\Lambda$  and  $C$  is somewhat arbitrary, and when one knows nothing about the properties of the heavy particles it is customary to take  $C_i^{(n)} = 1$ .

The effective interactions are, by construction, nonrenormalisable. This should not be a surprise, as we know that nonrenormalisable theories are not valid to all energy scales: processes that involve a nonrenormalisable vertex yield unacceptably large amplitudes at high energies, thus violating the unitarity of the  $S$  matrix. This violation occurs generically at energies of the order of  $\Lambda$ , and is considered an indication that the scale of the new particles has been reached; one must then drop the effective theory and replace it by a new, renormalisable QFT that includes the heavy fields. For this reason,  $\Lambda$  is usually termed the *new physics scale*, and for this reason  $\Lambda$  is often considered the most important parameter in the effective theory. When the underlying theory is simple it may coincide precisely with the mass of the new particles, but more commonly it will be a combination, sometimes rather involved, of several dimensionful parameters; if these parameters are not too different, though,  $\Lambda$  will still point in the correct direction, indicating at least the order of magnitude of the heavy masses. It may also happen, if the underlying theory presents several mass scales,

---

that different effective operators show different new physics scales; again, if these are not too different the interpretation of  $\Lambda$  is safe. Moreover, equation (2.16) still holds, even in this case, if we cleverly integrate inside the  $C$ 's the appropriate (dimensionless) combination of parameters so that  $\Lambda$  is replaced, where needed, by another  $\Lambda'$ .

This far we have briefly explained how we construct an effective field theory. But once we have it, how exactly do we use it? Well, it depends on what we know about the underlying heavy physics. If we know nothing about it we must consider the whole set of effective operators and try to measure experimentally their couplings. That may be easier if we select those operators that yield processes forbidden in the low-energy theory – for instance, some effective interactions may break a global symmetry that prevents certain process in the low-energy theory: that would be a good place to start. In the general case we would think that lower-dimensional operators offer the best experimental shot, as they are suppressed by less powers of  $\Lambda$ , which is assumed to be large. As we dig deeper in the details of the low-energy theory we gain access to higher-dimensional operators and also to heavier masses in the lowest-dimensional ones. So, as we said above, details are relevant: the effective contribution may be hidden in the fifth or sixth digit of a measurement, and this is also a way to investigate the physics of heavy particles. When no positive experimental result is found, at least we can place bounds on the new physics scale, which should roughly correspond to the mass of the new particles.

If we know something about the underlying theory –perhaps that it breaks certain global symmetry, or that it only involves scalar particles–, we can probably restrict the spectrum of effective operators: we can know that some of them don't exist at all, or that others are loop-generated and thus suppressed respect to those generated at tree level. These considerations help to focus on the correct operators in order to look for the optimal experimental signatures.

Finally, we may be working in a theoretical framework; if we know absolutely the physics of the heavy particles, our interest can be to deduce their low-energy effects in order to simplify the calculations in that regime. The procedure is to calculate in the underlying theory the full process that generates the effective interaction, and then match



this calculation with the corresponding result in the effective theory. We will do so at several points throughout this work, as it will allow us to compare the sensitivity of direct searches for the new particles with that of precision low-energy measurements.

### 3. NEUTRINOS

All the work presented here revolves around neutrinos and their properties. Due to their extremely light masses neutrinos are ubiquitous in the universe, but their lack of electric charge makes them very difficult to spot and study; as far as we know, they only interact through purely weak interactions, that is, through processes mediated by a  $W$  or a  $Z$ , which are suppressed at low energies by  $m_{W,Z}^{-2}$ ; charged currents, for instance, which are responsible for processes such as  $\nu_e + X \rightarrow e + Y$ , of uttermost experimental importance, are governed by the small Fermi effective coupling,  $G_F \equiv \frac{\sqrt{2}}{8} \frac{g^2}{m_W^2} = (1.16637 \pm 0.00001) \times 10^{-5} \text{ GeV}^{-2}$ . It is, thus, interesting to investigate if neutrinos may feel additional interactions, which would provide new windows into their properties; this investigation is especially relevant if the new interactions shed some light on the neutrino properties that are still poorly known, such as their masses and their flavour structure. In this chapter we review some of these features, focusing on those which will be of interest for the studies that we are to present in the remaining of this work. The reader interested in a more comprehensive review may consult any of the very good texts that already exist in the literature, for instance [44], [45–47] or [48].

#### 3.1 Neutrino masses

The origin and nature of neutrino masses is one of the most enticing puzzles in modern particle physics. Their minute value, their flavour structure –so different from what we observe in the quark sector–, or the intriguing possibility that they open a gateway into the violation of lepton number are just some of the issues that attract our interest in this matter. In this section we review several features

of neutrino masses, focusing on those which will be developed in forthcoming chapters. For a more comprehensive review we refer the reader to [44, 45, 49, 50].

### 3.1.1 Masses and the nature of fermionic particles

One of the tough problems we face when studying neutrino masses is that we don't even know how to write them. We have learnt a lot about their structure, and day after day we lay a better siege to their value, but the fact is that we still ignore their true character, their *nature*. Fermions are known to have two classes of mass terms: the first is derived from Paul Dirac's relativistic quantum equation for the fermion [51, 52]; it describes the mixing of two fields, one of them left-handed under Lorentz transformations and the other one right-handed:

$$m \bar{\chi}_R \psi_L .$$

This Dirac mass term yields fields with *four* internal degrees of freedom, and is suited for particles that carry internal charges such as electric charge, for it can be naturally transmitted from  $\psi_L$  to  $\chi_R$ . The degrees of freedom distribute among two polarisations for an excitation which carries charge  $+Q$  and two for an excitation that carries charge  $-Q$ : an *antiparticle*.

The second option, proposed by Ettore Majorana [53], consists in changing one of the fields for the *charge-conjugate* of the other, for we know that the operation of charge conjugation changes the chirality of the affected field. The mass term is written then as

$$m \bar{\psi}_L^c \psi_L ,$$

and it describes a fermion field with just *two* degrees of freedom; besides, the field  $\psi_L$  can't be assigned an internal charge, for it would be broken by the combination  $\bar{\psi}_L^c \psi_L \sim \psi_L \psi_L$ . The result, thus, resembles quite much a real field: having only the polarisations for one fermionic excitation and being unable of carrying charges, it describes a fermion which is its own antiparticle. The Majorana field is a real fermionic field.

As we see, the matter between Dirac and Majorana fields is more about the available degrees of freedom and the ability to carry charges than the mass term itself, though these properties emerge of course from the symmetries of the mass term. Most of the fundamental fermions in the Standard Model are electrically charged, so they can only be Dirac fermions. And indeed, as we described in section 2.1.3, each left-handed field in the SM has a right-handed counterpart which allows to construct Dirac mass terms. Neutrinos, however, are different: they are neutral and they don't possess any other charge that we know of; they might, therefore, be the only Majorana fermions on the landscape. Well, to be absolutely truthful they *could* actually carry one charge that we know of: lepton number. Lepton number is a global symmetry felt only by the leptonic fields of the theory that causes leptons to be created or annihilated exclusively in pairs lepton-antilepton. It is defined by the transformations

$$\begin{aligned}\ell_{L\alpha} &\rightarrow e^{iL\theta} \ell_{L\alpha} \\ e_{R\alpha} &\rightarrow e^{iL\theta} e_{R\alpha}\end{aligned}\tag{3.1}$$

where the Lagrangian just requires that  $L(\ell_{L\alpha}) = L(e_{R\alpha})$ , but conventionally it is usually assumed that  $L(\ell_{L\alpha}) = L(e_{R\alpha}) = +1$ . If we add right-handed neutrinos to our description of neutrino masses they receive the same lepton number assignment as  $e_{R\alpha}$ . Lepton number would be broken by the presence of a Majorana mass for the neutrinos; its conservation, however, is experimentally established to an astonishing level of precision [32]. It may seem a bit dull even to consider the possibility of neutrino masses being Majorana after this statement, but something comes to the rescue: neutrino masses are unbelievably small<sup>1</sup>. If they were the only source of lepton number violation then it would be only very slightly violated; actually our experiments, being greatly precise, would not have reached the precision required to record it. So, all in all, Majorana masses are still an open possibility for neutrinos, and an exciting one that points to a mass generation mechanism different from that of the other fermions.

Let us follow this thread by reviewing some details about the generation of Dirac or Majorana masses for the neutrinos. We begin

---

<sup>1</sup> See section 3.2.

with the known, more conventional, Dirac masses. By an argument of economy it seems reasonable to think that they are generated by the same Higgs mechanism that yields masses for the other fermions. For this aim we need three –at least– right-handed neutrinos with charges as displayed in table 2.1, and Yukawa couplings of the like of (2.9), which upon SSB provide

$$\bar{\ell}_L Y_\nu \nu_R \tilde{\phi} \longrightarrow \bar{\nu}_L m_\nu \nu_R + \dots, \quad (3.2)$$

where  $m_\nu = v Y_\nu$ . From the theoretical point of view Dirac masses are a simple and consistent choice: they require no further addition to a Standard Model that we know to work fine; besides, they allow naturally for lepton number conservation, as firmly suggested by experiment. However, the same reasons that make Dirac masses acceptable also make them sort of disappointing: in a pure-Dirac scenario Yukawa couplings are the only source for neutrino masses; the same Yukawa couplings that yield a top quark of 173 GeV provide an electron of 511 keV, and then three neutrinos with masses at a fraction of the eV. In the standard Higgs mechanism everything is encoded inside the Yukawa couplings, of whose origin we know nothing. We obtain no explanation, no insight on the hierarchy of the fermion masses, and especially we learn nothing about the enormous gap between the electron and the neutrinos. Is disappointment an argument good enough to drop a physical theory? Probably not. But it is good enough to entice imagination, and that’s also part of what we do.

Can Majorana masses help in our aim to explain the smallness of neutrino masses? Before considering this question we need to find a way to fit them within the Standard Model. Constructing a Majorana mass for the neutrinos won’t be as simple as writing  $m \bar{\nu}_L^c \nu_L$ : although neutrinos are electrically neutral they are not chargeless. Neutrinos belong in the leptonic doublet  $\ell_L$ , which carries  $SU(2)$  charge as well as hypercharge; a combination like  $\bar{\ell}_L \tilde{\ell}_L$  would break all those charges, providing also a disastrous Majorana mass term for the charged leptons. One can check that actually there’s no renormalisable combination of the fields in the Standard Model that can yield a Majorana mass term for the neutrinos. It was Steven Weinberg in [54]<sup>2</sup> who realised

<sup>2</sup> But see also the work by Weldon and Zee a year later, [55].

that one can combine the operator  $\tilde{\phi}^\dagger \ell_L$ , which is hyperchargeless and  $SU(2)$ -singlet, with its complex-conjugate to obtain a dimension-five interaction that upon SSB really provides Majorana neutrino masses. This operator is usually known nowadays as the *Weinberg operator*:

$$\left(\overline{\tilde{\ell}_L \phi}\right) \xi \left(\tilde{\phi}^\dagger \ell_L\right) \longrightarrow \overline{\nu}_L^c m_\nu \nu_L + \dots, \quad (3.3)$$

where we have  $m_\nu = v^2 \xi$  and  $\xi$  is an effective coupling with dimensions of inverse mass, as it corresponds to a dimension-five operator; we can extract the dimensionful part in the form of a new physics scale as we explained in section 2.2, and write  $\xi = C/\Lambda$ , with  $C$  some combination of dimensionless couplings which generate the operator in the underlying high-energy theory.

Other operators of higher dimensionality also provide Majorana neutrino masses, but they are suppressed by higher powers of  $\Lambda$  and their effect is subdominant; the Weinberg operator is the primary source of Majorana masses for the neutrinos in the Standard Model. This fact has two important consequences: first, if the masses of the neutrinos are Majorana then there has to be new physics beyond the Standard Model; this is straightforward, as they cannot be constructed with renormalisable, pure-SM interactions. Second, the resulting Majorana masses have the form  $m_\nu = Cv^2/\Lambda$ , that is, if the new physics is much heavier than the electroweak scale the masses can be strongly suppressed. In this way, Majorana masses offer a twofold explanation: the masses of the neutrinos are very small because they are related to very heavy physics, and we cannot explain their smallness in the framework of the Standard Model because it is actually related to something else. Philosophically speaking this is much more rewarding than “they are very small because this is the way they are”.

Of course, from this starting point a wide world of possibilities has been explored in the past thirty years: some Majorana mass models do not actually need very heavy new physics, some models mix Majorana and Dirac mass terms for the neutrinos, and some others manage to construct naturally small Dirac mass terms – see, just as an instance of the overwhelming variety, [56–63] or the models described in part II of [45]. We won’t review this vast and ever-changing world here, but

---

in section 3.3 we will briefly explain a framework for neutrino mass generation that has become very popular and is taken by itself as a starting point for proposing new ideas: the *seesaw mechanism*. But let us first describe what we know and what we don't about neutrino masses and establish some notation for the forthcoming discussion.

### 3.1.2 Neutrino oscillations

Flavour mixing and oscillation phenomena constituted our initial gateway into neutrino masses. Let us introduce in this section the intuitive notion of oscillation, which will be used in section 3.2 to describe our knowledge of neutrino masses.

As a starting point, note that neutrinos are always produced and detected in association with a charged lepton – actually, what we see in many experiments is indeed the charged lepton, and from it we infer the quality of the unseen neutrino. For decades, the definitory fact for neutrino species was flavour: we had one ‘electron’, one ‘muon’ and one ‘tau’ neutrino according to which lepton they were paired with in the weak interactions. Equation (2.1) essentially follows this line of thought through the vertices in (2.14). However, as early as in the 1960’s we learnt, by means of the Homestake experiment [64, 65], that something odd was happening to these flavoured neutrinos: they seemed to get lost. The disappearance was first noted in solar neutrino experiments: these looked for electron neutrinos produced in the core of the Sun, and found only one third of the neutrino flux expected from the best solar models available at the moment. Of course the first reactions were of astonishment: first the theoretical solar calculations were blamed for the anomaly and then the experiment reliability was put under question; however, independent calculations showed the theoretical expectations to be correct and subsequent solar neutrino searches [66–71] confirmed the deficit. The advent of atmospheric neutrino experiments, though initially brought no disagreement with the total expected flux [72–75], finally led to the identification of an anomaly [76, 77]: these surveys looked for neutrinos produced in the upper atmosphere as a byproduct of cosmic ray collisions; at low energies they expected to find twice as many muon neutrinos as electron neutrinos, but the ratio showed

to be just a little above unity. This result seemed to suggest again that muon neutrinos were getting lost somewhere – or maybe was it electron neutrinos who were appearing out of nowhere?

The situation was puzzling. Several mechanisms were proposed to explain the neutrino deficits, among them neutrino oscillations. The idea behind oscillations was tricky, but it can be expressed in one sentence: if neutrinos do have masses but the states with definite mass don't coincide with the states with definite flavour, then flavour won't be conserved during propagation. In other words: there are three neutrino flavours, and correspondingly one should have three neutrino masses; however, there's no reason for these masses to be assigned to one flavour each. Maybe the quantum-mechanical state with mass  $m_1$  is neither  $\nu_e$  nor  $\nu_\mu$  nor  $\nu_\tau$ , but a combination of all three, and so on with the other two masses. Then the other way around would also be true: a  $\nu_e$  would be a combination of the states with masses  $m_1$ ,  $m_2$  and  $m_3$ . If that were the case, then the components in  $\nu_e$  would propagate independently, for propagation –time-evolution, in the end– in quantum mechanics deals with energies: it is the states with definite energy which propagate unperturbed.  $\nu_e$ , which has no definite energy –no definite mass–, will be perturbed during propagation: its three massive components will dephase and the mixture will change, transforming the  $\nu_e$  a little bit into a  $\nu_\mu$  or a  $\nu_\tau$ . When happening in a vacuum, this transformation will be cyclical: at some point during propagation the mixture will return to  $\nu_e$  and the process will repeat over and over again. That's why this bizarre behaviour got to be called *oscillation*. In the end, the effect is simple: neutrinos change flavour as they move. If we didn't find all the solar neutrinos it was because we only looked for electron neutrinos; the moment the SNO experiment also looked for the other two varieties [78] we found exactly what we expected.

This, unfortunately, is no place to tell the full details about oscillations, even though it is a beautiful and enlightening story. For more information we refer the reader to specific texts on the matter, for instance [50, 79–81]. We will only go on to say that the fight to determine the mechanism behind the several neutrino deficits was a tough one, and oscillations only emerged as a clear winner when the KamLAND



experiment, which studied neutrinos produced in human-made nuclear reactors, allowed us to check that the disappearance probability of neutrinos is energy- and distance-dependent in the way one should expect from oscillations [82] – see the references cited above, or simply check out equation (3.8).

### 3.1.3 Writing masses and mixings

Let us now take a small break in this section in order to establish the notation of neutrino masses and mixings as we will use throughout the rest of the text. We start by writing the fields that describe the flavour eigenstates; in a straightforward notation we call them  $\nu_e, \nu_\mu, \nu_\tau$  as in equation (2.1). Then we denote the fields with definite mass by  $\nu_1, \nu_2, \nu_3$ , and their associated masses by  $m_1, m_2$  and  $m_3$ , in good logic. It is important to note that “1”, “2”, “3” are just conventional labels; they don’t pretend to say anything about the values of the masses and, in particular, they *don’t* imply  $m_1 < m_2 < m_3$ . In the following section –3.2– we will describe what we know and what we don’t about the parameters that we are about to define here.

Given the eigenfields with well-definite mass and flavour, let us now consider the relation between them; as usual in quantum mechanics, it can be described by a linear change of basis:

$$\begin{pmatrix} \nu_e \\ \nu_\mu \\ \nu_\tau \end{pmatrix} = U_{\text{PMNS}} \begin{pmatrix} \nu_1 \\ \nu_2 \\ \nu_3 \end{pmatrix},$$

where  $U_{\text{PMNS}}$  is usually called the Pontecorvo-Maki-Nakagawa-Sakata matrix [83–86]; it contains the observable parameters that describe the mixing between flavour and mass eigenstates [87]. With three neutrino species three of these parameters are ‘mixing angles’, that is, values which control the amount of flavour violation in processes like oscillations or charged-current interactions; one more parameter is a phase, a constant that triggers CP-violating processes. If the neutrinos are Majorana particles, two more phases will be present in the PMNS matrix. The reason for this is that the number and nature of the mixing parameters depends on the structure of the masses and the flavour

symmetries available to the involved fields; initially, any parameter present in the mass matrices would be either a mass, a mixing or a phase, but some of them can be proven to be physically irrelevant. The fields have flavour redundancies, they can be rearranged in flavour space without changing the observable quantities of the theory; if we can find one such rearrangement which eliminates from the Lagrangian a certain parameter, then that parameter was not physical, it could not influence observable results. The process of identifying the physical parameters is described in more detail in [36], but we sketch it here for the case of Dirac and Majorana masses in order to clarify the differences in the PMNS matrix for these two scenarios.

If the masses of the neutrinos are of Dirac type, then the flavour matrix we're interested in is  $Y_\nu$ , as written in equation (3.2). This matrix is initially a completely general  $3 \times 3$  complex matrix, and so it possesses 18 parameters, 9 of which are moduli and the remaining 9 are phases; out of the 9 moduli, 3 describe the masses themselves, and some of the remaining 6 can be physically relevant mixings, but we don't know how many; of the 9 phases we don't know either how many are physical. Then let us look at the relevant fields: the fields with flavour structure in (3.2) are  $\ell_L$  and  $\nu_R$ . We should identify the flavour transformations that we can apply upon them without changing the rest of the physics; that's easy to do by looking at the kinetic terms in (2.2): the weak interactions remain invariant if we apply any unitary transformation in flavour space to  $\ell_{L\alpha}$  and  $\nu_{R\alpha}$ . So, we could think that we have two unitary  $3 \times 3$  matrices to eliminate spurious parameters from  $Y_\nu$ .

However,  $\ell_L$  not only contains neutrinos: it also carries the left-handed components of the charged leptons,  $e_L$ , which in turn are involved in the charged lepton masses, whose flavour structure is given by  $Y_e$ , as seen in equation (2.8). This means that any flavour transformation acting upon  $\ell_L$  affects both  $Y_\nu$  and  $Y_e$ : it might happen that by a transformation on  $\ell_L$  we erase a parameter from  $Y_\nu$  but it is transferred to  $Y_e$  instead of being properly eliminated; such a parameter should count as physical. In consequence, it is not correct to look for the physical parameters just in  $Y_\nu$ ; the right approach is to consider the physical parameters in *both*  $Y_\nu$  and  $Y_e$ . And if  $Y_e$  is

involved then the  $e_{R\alpha}$  are also involved. That makes *two* completely general  $3 \times 3$  complex matrices, composed initially of 18 moduli and 18 phases, and to attack them we have *three* unitary  $3 \times 3$  matrices, which provide 9 moduli and 18 phases.

These are our weapons. Now just one element remains to be unveiled: in the end, we aim to transform  $Y_e$  and  $Y_\nu$  in two diagonal matrices which describe Dirac masses for the charged leptons and the neutrinos. These masses allow for one internal symmetry, as we discussed earlier: lepton number; a global  $U(1)$  symmetry acting simultaneously on  $\ell_L$ ,  $e_R$  and  $\nu_R$ . For our purposes, a global phase in the unitary matrices that remains free, as we can see in equation (3.1). When we carry out our calculation we need to account for this liberty which in the end has to remain.

The rest is arithmetics: we have 18 moduli and 18 phases; we can use the unitary transformations to diagonalise the Yukawa couplings; that means setting 36 equations, one for each degree of freedom in  $Y_e$  and  $Y_\nu$ . All of them will be nonlinear, and many can be difficult even to set, but that doesn't matter for our purposes: all we want to know is how many parameters we can eliminate from the equations by adjusting the unitary matrices to the appropriate values. And that can be known by simple counting: we have 9 free moduli from the unitary matrices, so we can neutralise 9 of the moduli; we have 18 free phases, so we can eliminate 18 phases. But remember that one of the phases in the unitary matrices is to remain free, so we can only absorb 17 of the phases in the Yukawas. Result: a Dirac mass pattern for the leptons yields 9 physical moduli and 1 physical phase. The final arrangement of these physical parameters is somewhat arbitrary, as it is also arbitrary which elements in the initial Yukawa matrices we choose to absorb. However, for a matter of physical significance it is customary to take 6 of the physical parameters to be the masses of the charged leptons and the neutrinos; the remaining 3 are the three mixing angles in the PMNS matrix. The phase has become universally known as the *Dirac phase* of the mixing matrix. The six masses remain of course in the now-diagonal mass matrices, while the mixings and the phase are incorporated into the PMNS matrix. Again there are many possible parametrisations, but it is customary to use the following, in

the form of three Euler angles with an added phase:

$$\begin{aligned}
 U_{\text{PMNS}}^{\text{Dirac}} &= \begin{pmatrix} 1 & 0 & 0 \\ 0 & \cos \theta_{23} & \sin \theta_{23} \\ 0 & -\sin \theta_{23} & \cos \theta_{23} \end{pmatrix} \times \\
 &\times \begin{pmatrix} \cos \theta_{13} & 0 & \sin \theta_{13} e^{-i\delta} \\ 0 & 1 & 0 \\ -\sin \theta_{13} e^{i\delta} & 0 & \cos \theta_{13} \end{pmatrix} \begin{pmatrix} \cos \theta_{12} & \sin \theta_{12} & 0 \\ -\sin \theta_{12} & \cos \theta_{12} & 0 \\ 0 & 0 & 1 \end{pmatrix} \quad (3.4)
 \end{aligned}$$

As for Majorana masses, all the matter is to repeat the same algorithm: now we don't have  $\nu_R$ 's, so we have one less unitary matrix to play with; the neutrino mass matrix is determined by the  $\xi$  couplings appearing in (3.3), which conform a complex *symmetric*  $3 \times 3$  matrix; and the charged leptons' Yukawas are also involved in the diagonalisation process, as they also involve the fields  $\ell_L$ . That makes 15 moduli and 15 phases in  $\xi$  and  $Y_e$ , and 6 free moduli and 12 free phases from the unitary transformations of  $\ell_L$  and  $e_R$ . As lepton number is broken due to the terms in (3.3), none of the free phases has to be preserved this time. The counting then yields 9 physical moduli (again) and 3 physical phases. The custom parametrisation is identical to that for Dirac masses, but incorporating the two new phases as the phases of two of the eigenvalues of the neutrino mass matrix. We call these two phases *Majorana phases* and denote them by  $\alpha_1, \alpha_2$ ; then we write

$$\begin{aligned}
 U_{\text{PMNS}}^{\text{Majorana}} &= \begin{pmatrix} 1 & 0 & 0 \\ 0 & \cos \theta_{23} & \sin \theta_{23} \\ 0 & -\sin \theta_{23} & \cos \theta_{23} \end{pmatrix} \begin{pmatrix} \cos \theta_{13} & 0 & \sin \theta_{13} e^{-i\delta} \\ 0 & 1 & 0 \\ -\sin \theta_{13} e^{i\delta} & 0 & \cos \theta_{13} \end{pmatrix} \times \\
 &\times \begin{pmatrix} \cos \theta_{12} & \sin \theta_{12} & 0 \\ -\sin \theta_{12} & \cos \theta_{12} & 0 \\ 0 & 0 & 1 \end{pmatrix} \begin{pmatrix} e^{i\alpha_1/2} & 0 & 0 \\ 0 & e^{i\alpha_2/2} & 0 \\ 0 & 0 & 1 \end{pmatrix}. \quad (3.5)
 \end{aligned}$$

We conclude this section by indicating an example of mixing pattern that has gained some popularity in the recent years: the so-called tribimaximal mixing. The great deal of data which was released in the late 90's and early 2000's hinted a mixing structure with  $\nu_3$

maximally mixed between  $\nu_\mu$  and  $\nu_\tau$  and  $\nu_2$  maximally mixed among all the flavours. The strict realisation of this pattern was soon dubbed ‘tribimaximal mixing’ [88] due to the maximal ‘bi’-mixing of  $\nu_3$  and the maximal ‘tri’-mixing of  $\nu_2$ ; such realisation implied strong predictions for the angles: the atmospheric angle was bound to be maximal,  $\theta_{23} = 45^\circ$ , the solar angle was to lead to the trimaximal mixing,  $\theta_{12} \simeq 35.3^\circ$ , and the reactor angle was required to vanish. This latter condition carried one further consequence: the mass-mixing system gained an additional liberty and the Dirac phase ended up not being physical; it, this way, disappeared from the parametrisation. The final PMNS matrix of tribimaximal mixing looked like

$$U_{\text{PMNS}}^{\text{tbm}} = \begin{pmatrix} \sqrt{2/3} & 1/\sqrt{3} & 0 \\ -1/\sqrt{6} & 1/\sqrt{3} & 1/\sqrt{2} \\ 1/\sqrt{6} & -1/\sqrt{3} & 1/\sqrt{2} \end{pmatrix}.$$

Nowadays tribimaximal mixing is ruled out as a realistic ‘final-word’ description of the leptonic mixing, as we can appreciate in table 3.1, but it can still be regarded as a fair approximation whose symmetries may hint the symmetries of the underlying flavour physics that generates neutrino masses. As such, it’s still worth to be borne in mind.

### 3.2 Our knowledge of the mass sector

In this section we will review our knowledge about the neutrino mass and mixing parameters. This means, as we discussed in the previous section, finding out the value of no less than 7 different parameters: three masses, three mixing angles and one phase – plus two more phases, were the neutrinos to be Majorana fermions. Needless to say, no single experiment can probe the whole set of parameters; rather, it’s been the patient juxtaposition of different experimental results what has provided our present knowledge about neutrino masses. Neutrino oscillation experiments, for instance, are well-suited for measuring mixing angles and squared-mass differences between the various massive neutrinos; they can also provide information about the Dirac

---

CP-violating phase, but they are not sensitive to the values of the masses themselves or to the Majorana phases. Precise measurements of the  $\beta$ -decay spectrum of certain nuclides can yield information on the absolute scale of neutrino masses, but they only probe a certain *combination* of  $m_1$ ,  $m_2$  and  $m_3$ , not the three of them separately. Cosmological observables are sensitive to a different combination of the masses –their sum– and they offer a fairly good constraint on it, but with the drawback that it depends somewhat on our knowledge of the cosmological parameters. Neutrinoless double beta decay, finally, is an excellent probe of the Majorana/Dirac nature of the neutrinos, but the interpretation of an eventual positive result must be taken with care: while a positive  $0\nu\beta\beta$  signal immediately implies that neutrinos are Majorana particles, the decay amplitude may or may not yield numerical information on neutrino masses, depending on how the decay proceeds internally – if it is triggered by heavy, LNV-ing physics the amplitude will inform about the couplings of such heavy physics, whereas if it’s the active neutrinos who provide the dominant contribution it will measure the  $m_{ee}$  element of the mass matrix. Therefore,  $0\nu\beta\beta$  requires a synergy with other, possibly high-energy experiments in order to establish precisely what kind of information we can extract from it.

As a general statement it can be said that the struggle to measure the absolute masses of the neutrinos is a tough one; when the day arrives it will require to combine the results of several different experiments together with the best knowledge we can gather about mixing angles and phases. Fortunately, the mixing sector is reasonably well-known even today due to the fantastic precision achieved by the oscillation experiments; in fact, at the moment of writing only the Dirac phase and the sign of one mass splitting remain to be measured. Let us begin our review without any further introduction by stating the results we can derive from neutrino oscillations.

### 3.2.1 Oscillation experiments

Oscillation experiments probe, as we explained in section 3.1.2, flavour nonconservation during neutrino free propagation. A review of the oscillation mechanism in full detail can be found for instance in [79, 80];

here, for the purposes we're interested in, let us consider the oscillation in vacuum of two neutrino species:

$$P(\nu_\alpha \rightarrow \nu_\beta) = \sin^2(2\theta_{ij}) \sin^2\left(\frac{\Delta m_{ij}^2 L}{4E}\right). \quad (3.6)$$

This expression describes the probability that a neutrino is detected with flavour  $\beta$  after a flight of length  $L$  if it had flavour  $\alpha$  at the moment of production and it carries an energy  $E$ . We assume two mass eigenstates, labeled as  $i$  and  $j$ , to underlie the two flavour states  $\alpha$  and  $\beta$ ; the expression  $\Delta m_{ij}^2$  refers to the difference of the square of their masses,  $\Delta m_{ij}^2 \equiv m_i^2 - m_j^2$ ; the angle  $\theta_{ij}$  describes the mixing of  $i$  and  $j$  with  $\alpha$  and  $\beta$ :

$$\begin{pmatrix} \nu_\alpha \\ \nu_\beta \end{pmatrix} = \begin{pmatrix} \cos \theta_{ij} & \sin \theta_{ij} \\ -\sin \theta_{ij} & \cos \theta_{ij} \end{pmatrix} \begin{pmatrix} \nu_i \\ \nu_j \end{pmatrix}. \quad (3.7)$$

With these elements, we can read in (3.6) two important properties of oscillations: first, the amount of flavour violation is directly dependent on the mixing angle, in such a way that if  $\theta_{ij} = 0$  a  $\nu_\alpha$  remains  $\nu_\alpha$  all the way long – that is, looking at (3.7): if the flavour and mass eigenstates coincide there are no oscillations. Second, the wavelength of the oscillations depends exclusively on the difference of squared masses and the energy, in such a way that if  $\Delta m_{ij}^2 = 0$  no change in flavour occurs – that is, one can only observe oscillations if  $m_i$  and  $m_j$  are *different*.

Of course, expressions (3.6) and (3.7) do not represent the situation of real neutrinos, of which we have at least three species<sup>3</sup>, but they can help in getting an idea of what is being observed in the experiments. Essentially, oscillation experiments count the number of neutrinos of a certain species –sometimes of several species– coming from a known source, and look for discrepancies with the initial composition of the source. They also measure the energy of the neutrinos, in order to look for an agreement with spectra such as (3.6). There are mainly four relevant sources of neutrinos: the Sun, the atmosphere, man-made nuclear reactors and *ad-hoc* neutrino beams produced in particle

<sup>3</sup> For instance, two-species oscillations conserve CP, and indeed there is no CP-violating phase in (3.6).

accelerator facilities. Each source is sensitive in its own particular way to a subset of the mixing parameters. Let us here sketch what information can be extracted from each family of experiments. A more complete review can be found in [50].

Solar neutrinos [89] originate in the inner core of the Sun as a byproduct of its fusion nuclear reactions [48]; significant processes are the proton-proton reaction,  $p + p \rightarrow d + e^+ + \nu_e$ , which provides most of the solar neutrinos but only with low energies –up to 400 keV–, and the boron-8 process,  ${}^8\text{B} \rightarrow {}^8\text{Be} + e^+ + \nu_e$ , which provides only a small fraction of the total neutrino flux, but with energies above a few MeV’s, that make them easier to detect. The neutrinos produced inside the core travel through the Sun’s plasma and oscillate in this environment. The presence of matter can affect the oscillation process as described by the Mikheyev–Smirnov–Wolfenstein effect – [90–93], see [94] for a review; in the case of the Sun, its density profile marks a change in the quality of oscillations at 1 – 3 MeV: neutrinos with energies below this value –for instance those coming from the  $p$ - $p$  reactions– oscillate as they would do in vacuum, resulting in a conversion of 30% of the electron neutrinos into the other two species. For energies above a few MeV, however, the conversion is enhanced by matter effects and up to 70% of the  $\nu_e$ ’s are transformed. This satisfactorily accounts for the discrepancies between theory and experiment that were recorded during the 20<sup>th</sup> century [64–71]; the advent of the SNO experiment, which was capable of measuring  $\nu_e$ ’s as well as the other two flavours, confirmed this interpretation [78]. Solar neutrino oscillations are mainly due to the mixing between  $\nu_1$  and  $\nu_2$ , and so these experiments allow to measure the angle  $\theta_{12}$  and the squared-mass splitting  $\Delta m_{21}^2$ . However, the uncertainties in our knowledge of the solar properties and the eventful trip of the neutrinos from the Sun –with oscillations in matter along the solar interior, then oscillations in vacuum to reach Earth, and then again oscillations in matter at least during the nighttime– casted some degeneracy on the combination of oscillation parameters that could account for the observations. It was only by bringing together solar, atmospheric and reactor results that the correct regime could be identified (see section 3 of [50] for a more detailed discussion), yielding values of about  $\theta_{12} \simeq 35^\circ$  and  $\Delta m_{21}^2 \simeq 10^{-4} \text{ eV}^2$  – we present



the current best values in table 3.1. Note that we have indicated here a full value for  $\Delta m_{21}^2$ , with a well-defined sign, even though the neutrino oscillation probabilities, like (3.6), are insensitive to the signs of the squared-mass splittings. The reason is that oscillations in matter, whose equations we won't quote here, open up the possibility of distinguishing the sign of the mass splitting; this is an important feature of matter effects and it is expected to allow in the near future to measure the sign of the remaining mass splitting.

Atmospheric neutrinos [95] are produced several kilometers above the ground by the collision of incoming cosmic rays; the first cosmic-ray hit produces pions and kaons, which eventually decay to muons and, as lepton family number demands, muon (anti-)neutrinos; the muons then subsequently decay and give one more muon antineutrino (neutrino) and one electron (anti-)neutrino. We can summarise thus in a nutshell the most relevant processes for the production of atmospheric neutrinos; as a result of this scheme, if all the produced muons get to decay before hitting the ground the flux of atmospheric muon (anti-)neutrinos is expected to be roughly twice the flux of electron (anti-)neutrinos<sup>4</sup>. Experiments to study this source of neutrinos have been carried out since the 1960's, but in these first stages no discrepancy was found between the expected neutrino fluxes and the experimental data [72–75]; later, in the 80's, when the experiments became capable of discriminating between electron-neutrino and muon-neutrino events, it was noticed that even if the total flux was consistent with expectations, the *relative* number of  $\nu_\mu$ 's respect to  $\nu_e$ 's was not in consonance [76, 77]. This was the first hint of oscillations in atmospheric neutrinos. However, the big power of this family of experiments is their capacity to observe neutrinos that have travelled different distances, and so are in different points of the oscillation curve (3.6). The trick is that neutrinos can go through the whole planet without impediment, and so one can select the flight length simply by recording the incidence angle of the neutrino event – downward-going neutrinos are to have been produced in the

---

<sup>4</sup> This happens actually only for low-energy muons. Consequently, neutrinos with  $E_\nu \lesssim 1$  GeV show a ratio  $\phi(\nu_\mu)/\phi(\nu_e) \sim 2$ , but as energy increases and less muons decay during their atmospheric travel, less electron neutrinos are produced and this ratio also increases.

atmosphere directly above the experiment and they will have flown about 15 km until they reach the detector; upward-going neutrino events, however, are to be associated with a neutrino produced at the other side of the Earth, and they store information about a flight of approximately 12800 km. With such a large range of available baselines atmospheric neutrino experiments are very well suited for testing oscillation curves, and indeed the first claim of observation of neutrino oscillations came from Super-Kamiokande [96]; shortly after, other experiments confirmed the discovery [97, 98]. Neutrino telescopes, like ANTARES [99] and IceCube [100], can also measure the parameters of atmospheric oscillation. Due to the hierarchies in the mass splittings and the mixing angles, these experiments probe mainly the angle  $\theta_{23}$  and its associated splitting,  $\Delta m_{32}^2$ ; for them, values around  $\theta_{23} \simeq 45^\circ$  and  $|\Delta m_{32}^2| \simeq 10^{-3}$  eV are found. Note that the sign of  $\Delta m_{32}^2$  is not yet known. To determine it we need experiments sensitive both to the atmospheric parameters and to matter effects, which can discriminate the sign of the splitting. This can be achieved with atmospheric neutrinos, especially if the experiments attain sensitivities in the energy range of 1 – 12 GeV, where oscillations in the mantle and the core of the Earth are enhanced by resonant matter effects [101, 102]. Such searches are already planned and will be carried out in the near future.

Reactor neutrinos [103] are neutrinos produced in nuclear reactors due to  $\beta$  decay processes; they are, therefore, basically electron antineutrinos with energies of the order of the MeV. With such a composition, reactor neutrino fluxes resemble somewhat solar neutrinos, only with a different energy spectrum as they are generated by different nuclear processes. And indeed reactor neutrinos can yield information about the solar oscillation parameters: if we write the 3-species electron antineutrino disappearance probability we can identify two competing terms,

$$P(\bar{\nu}_e \rightarrow \bar{\nu}_{\mu,\tau}) = 4 \sin^2 \theta_{13} \cos^2 \theta_{13} \sin^2 \left( \frac{L}{4E} \Delta m_{31}^2 \right) + \\ + \cos^4 \theta_{13} \sin^2(2\theta_{12}) \sin^2 \left( \frac{L}{4E} \Delta m_{21}^2 \right) + \dots, \quad (3.8)$$

plus other subleading contributions that include the interference of these two terms and matter effects – one can check that given our knowledge of the mass splittings and the possible baselines available on planet Earth those contributions are indeed subdominant. Equation (3.8) displays an interesting situation: the composition of two oscillations with different characteristic lengths; one of them is associated with solar oscillations, and has  $L_{\text{char}} = 4E/\Delta m_{21}^2 \sim 200$  km for the typical energies of reactor neutrinos. The second component is given by the atmospheric scale, as  $\Delta m_{32}^2 \gg \Delta m_{21}^2$  and so  $\Delta m_{31}^2 \simeq \Delta m_{32}^2$ ; then, for the first term in (3.8) we have  $L_{\text{char}} \simeq 4E/\Delta m_{32}^2 \sim 5$  km. Therefore, the hierarchies of the neutrino mass splittings allow to identify two regimes in electron antineutrino oscillations, and that in turn opens up the possibility of designing two kinds of reactor neutrino experiments: long-baseline ( $L \sim 100$  km) ones, which probe the solar parameters,  $\theta_{12}$  and  $\Delta m_{21}^2$ , and short-baseline ( $L \sim 1$  km) facilities, which should be sensitive to the third mixing angle,  $\theta_{13}$ , and the atmospheric scale,  $\Delta m_{31}^2 \simeq \Delta m_{32}^2$ . The fact that  $\theta_{13}$  is small compared to  $\theta_{12}$  further helps to separate the two components in (3.8). The first reactor neutrino experiments were carried out with short or intermediate baselines, and weren't sensitive enough to detect the small antineutrino disappearance induced by  $\theta_{13}$  [104–108]. Then there came KamLAND, which operated with longer baselines and was thus probing the solar neutrino parameters; its achievement was a big one, because it firmly established the scenario of a large  $\theta_{12}$  and  $\Delta m_{12}^2$  above  $10^{-6}$  eV<sup>2</sup> [109]. Moreover, KamLAND provided definitive evidence that the mechanism underlying neutrino flavour transformation was indeed oscillations by noticing that the energy spectrum of the reactor neutrinos was distorted along propagation [82] – as different energies result in different survival probabilities, see (3.8). Finally, a new generation of short-baseline experiments has very recently provided strong proof of a nonzero  $\theta_{13}$  [110–112], opening thus the door to CP violation in the neutrino sector (see section 3.1.3). Due to the sensitivity of reactor experiments to  $\theta_{13}$  it has grown increasingly common to dub it the ‘reactor angle’; its value lies, as of today, around  $\theta_{13} \simeq 10^\circ$ .

Finally, accelerator neutrinos are muon neutrinos produced in an accelerator facility by colliding particles against a fixed target [113].

---

The procedure has a similar effect to the cosmic ray collisions that generate atmospheric neutrinos: pions are produced, and then these decay to muons and muon (anti-)neutrinos. The difference is that for these experiments the muons are stopped as efficiently as possible, so that the electron neutrinos resulting from their decays are emitted in random directions and the final neutrino beam contains mostly neutrinos of the muon family. A detector is then located at some distance in the trajectory of the beam; often the experiments comprise two detectors: one “near” detector close to the collision point whose function is to characterise the initial composition of the beam, and one “far” detector that allows to assess how the beam has changed during its travel. Such good knowledge of the beam properties allows to examine various channels of oscillation: the dominant  $\nu_\mu \rightarrow \nu_\tau$  oscillations are usually searched for in terms of “ $\nu_\mu$  disappearance”, as most beams are not energetic enough to produce a  $\tau$  (but see [114, 115]); these searches, so, investigate the same physical process as atmospheric neutrino experiments and provide independent measurements for the atmospheric oscillation parameters [116, 117]. Another interesting process is the appearance of electron neutrinos out of the muon species,  $\nu_\mu \rightarrow \nu_e$ , a subdominant oscillation that is sensitive to the reactor angle and to the CP phase  $\delta$ ; this channel has also been intensely investigated [118–121], but with less sensitivity than the reactor experiments and with no luck yet in what concerns CP violation. Future accelerator experiments will further probe the  $\nu_\mu \rightarrow \nu_e$  channel and plan to use matter effects in the Earth’s crust to elucidate the sign of the atmospheric mass splitting [122].

Accelerator neutrino beams have been also used to design short-baseline experiments, located at the order of hundred meters away from the collision point; these are sensitive to large mass-squared differences, and have been running to look for exotic oscillations into more massive neutrino species, possibly sterile. The LSND experiment reported a positive result in this direction [123], but subsequent independent searches seem to disfavour this claim [124, 125]. The matter stays controversial as of autumn 2013 [126].

Such a fantastic battery of experiments yields a healthy flux of independent and cross-checkable results which can be combined in order

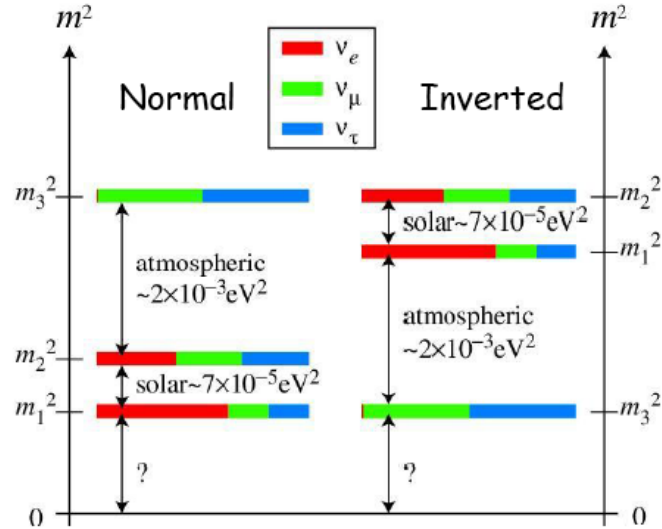


*Fig. 3.1:* This picture displays the two possible mass orderings depending on the sign of the atmospheric mass splitting – either  $\Delta m_{32}^2$  or  $\Delta m_{31}^2$ , for this matter. In normal hierarchy the two mass eigenstates separated by the solar mass splitting are lighter than the third one, whereas in inverted hierarchy it is the other way around. Note that the sign of the solar mass splitting is known, and consequently we know that  $\nu_1$  is lighter than  $\nu_2$ . The colours represent the flavour content of each mass eigenstate; the approximate tribimaximal mixing can be appreciated in  $\nu_2$  and  $\nu_3$ . The figure has been obtained from [127].

to attain better statistical significance. It is actually very common to do so, and the so-called ‘global fits’ have become the standard source of knowledge about neutrino masses and mixings. Table 3.1, which summarises our latest information about neutrino masses and mixings, refers its oscillation data to the global fit in [128]. Some features can be noted from these data: first, they are not anymore compatible with tribimaximal mixing;  $\theta_{13}$  has been measured to be nonzero and  $\theta_{23}$  shows some preference for non-maximal values. The Dirac phase, thus, is physical, and the experiments aiming to measure it now know that there’s something to measure indeed.

One more feature is noticeable from table 3.1: as we already anticipated, we have no clue on the sign of the atmospheric mass splitting,  $\Delta m_{31}^2$  (or  $\Delta m_{32}^2$ , if we prefer). This means that we don't fully know the ordering of the mass eigenstates. The reader may remember that we commented in section 3.1.3 that the numbers in  $m_1, m_2, m_3$  were mere labels and they didn't imply an ordering; knowing the differences between them we know the gaps that separate them, but not knowing the sign of those differences we are left with a handful of possible ways to arrange the masses and the gaps. Fortunately, we do know the sign of  $\Delta m_{21}^2$ , so only a twofold degeneracy remains to be resolved. In figure 3.1 we depict the two possibilities; the configuration in which  $m_1 < m_2 < m_3$  is conventionally called “normal hierarchy”, whereas the second configuration, that yields  $m_3 < m_1 < m_2$  is dubbed “inverted” hierarchy. Note that in table 3.1 some values of the best fit can be different if one or the other hierarchy is assumed.

### 3.2.2 Tritium beta decay and the magnitude of neutrino masses

Oscillation experiments allow to measure mixing angles and mass-squared differences, but offer no information on the absolute scale of the masses. The lightest mass eigenstate could lie anywhere from zero to several tenths of electronvolt<sup>5</sup>. A different experimental approach is needed in order to reveal the absolute magnitude of the masses; unfortunately, we don't know yet of a procedure to probe independently the values of  $m_1, m_2$  and  $m_3$  [133]. Among the several possibilities, direct observation in  $\beta$  decay spectra may be the closest to what we would naively call “measuring a mass”. Its main virtues are the fact that it involves very well-known physics, a reasonable independence from other measurements, and a low level of model-theoretical noise. The idea is simple: in a  $\beta$  decay process, a neutron is transformed into a proton by emission of an electron and an electron antineutrino,  $n \rightarrow p + e^- + \bar{\nu}_e$ . The neutrino is elusive, and only very rarely we would be able to detect it; the electron, however, is easily traceable, and we can measure its energy and momentum. The available energy for the proton-electron-antineutrino system is  $Q = m_n - m_p - m_e - m_\nu$ ,

<sup>5</sup> See section 3.2.3 for the rationale of this upper bound.

<b>Oscillation parameters [128]</b>		
$\Delta m_{21}^2$	$(7.62 \pm 0.19) \times 10^{-5} \text{ eV}^2$	
$ \Delta m_{31}^2 $	$(2.55^{+0.06}_{-0.09}) \times 10^{-3} \text{ eV}^2$	NH
	$(2.43^{+0.07}_{-0.06}) \times 10^{-3} \text{ eV}^2$	IH
$\sin^2 \theta_{12}$	$0.320^{+0.016}_{-0.017}$	
$\sin^2 \theta_{23}$	$0.613^{+0.022}_{-0.040}$	NH
	$0.43 \pm 0.03$	IH
$\sin^2 \theta_{13}$	$0.025 \pm 0.003$	
$\delta$	$0 - 2\pi$	
<b>Tritium <math>\beta</math> decay</b>		
$m_\beta$	$< 2 \text{ eV}$ 95% CL	[129]
<b>Cosmological constraints</b>		
$\sum_i m_i$	$< 0.23 \text{ eV}$ 95% CL	[130]
<b><math>0\nu\beta\beta</math> decay</b>		
$m_{\beta\beta}$	$< 0.14 - 0.38 \text{ eV}$ 90% CL	[131]
$m_{\beta\beta}$	$< 0.2 - 0.4 \text{ eV}$ 90% CL	[132]

Tab. 3.1: A compilation of the present knowledge on the neutrino mass and mixing parameters; each class of measurements is discussed in the corresponding section – see 3.2.1 for oscillations, 3.2.2 for  ${}^3\text{H}$   $\beta$  decay, 3.2.3 for cosmology and 3.2.4 for  $0\nu\beta\beta$ . The displayed uncertainties correspond to the  $1\sigma$  range. Note that the oscillation parameters are extracted from a global fit and in some cases the fit yields slightly different central values for normal and inverted hierarchy. For the case of  $\theta_{23}$  in NH two different minima are obtained with similar statistical significance.

and it has to be shared among the three particles in a way that respects momentum conservation; as this share is not unique there are many energies available to the electron, and when we measure the energy of outgoing electrons from  $\beta$  decay we observe a continuous spectrum. The spectrum has a lower cut at zero –for the electrons emitted at rest– and an upper cut at  $Q/2$  – when it is the proton or the neutrino who have been emitted at rest, and then the electron takes half the available energy and the remaining particle takes the other half. Thus, measuring the upper end point of the  $\beta$  spectrum is as much as measuring  $Q$ , and if we know very accurately the masses of the involved particles, we can measure the neutrino mass.

This far for the basics of the process. Of course a practical realisation of this simple idea requires coping with many details and experimental challenges, as we can read in [133]. We will be here interested in one of these details: the fact that we aim to measure the mass of a  $\bar{\nu}_e$ . As we know, the flavour states don't have a definite mass; they are, rather, a superposition of states with definite mass. For the electron (anti)neutrino, by looking at (3.4), we see that

$$\bar{\nu}_e = \cos \theta_{12} \cos \theta_{13} \bar{\nu}_1 + \sin \theta_{12} \cos \theta_{13} \bar{\nu}_2 + \sin \theta_{13} e^{-i\delta} \bar{\nu}_3.$$

If we could just take a  $\nu_e$  and measure its mass we would obtain as quantum mechanics prescribes: a fraction  $\cos^2 \theta_{12} \cos^2 \theta_{13}$  of the measurements would yield  $m_1$ , a fraction  $\sin^2 \theta_{12} \cos^2 \theta_{13}$  would yield  $m_2$ , and a fraction  $\sin^2 \theta_{13}$ ,  $m_3$ . However, our experimental setups are not yet sensitive enough to resolve  $m_1$ ,  $m_2$  and  $m_3$ , so what we observe in the end is the *average* of these three values, each weighed by its corresponding probability. We can regard this observable as an effective mass; we denote it by  $m_\beta$ , and write

$$m_\beta^2 = \cos^2 \theta_{12} \cos^2 \theta_{13} m_1^2 + \sin^2 \theta_{12} \cos^2 \theta_{13} m_2^2 + \sin^2 \theta_{13} m_3^2.$$

The current best measurement of the effective electron neutrino mass was carried out by the Troitsk experiment [129], not measuring neutron decay –this can be cumbersome, as neutrons are difficult to store and their half-life does not exceed 15 minutes–, but  $\beta$  decay of tritium ( ${}^3\text{H}$ ). Their measurement could not distinguish the mass of the neutrino but provided a bound,  $m_\beta < 2$  eV at 95% CL.



### 3.2.3 Cosmological bounds

Neutrinos are abundant particles in the universe; the cosmic background of neutrinos, though not yet directly observed, is expected to yield a number density of  $339 \text{ neutrinos/cm}^3$ , a figure comparable with that of the photons of the cosmic microwave background. The cosmological observables, such as the temperature anisotropies of the CMB or the matter power spectrum at large scales, have been shaped by a long evolution of billions of years dominated by gravitational interactions; the fact that neutrinos possess a mass is bound to affect these observables, and they provide an independent way to probe their values. The analysis of cosmological observables usually implies assuming a model for the evolution of the cosmos and comparing the observational data with the results of *in silico* simulations of the evolution of the observables. The details of these calculations, as well as the many subtleties that appear while examining each particular observable, fall out of the scope of this work; they can be consulted in specialised texts such as [134, 135].

Two features, however, of this family of constraints are worth being pointed out. The first concerns the way in which cosmology is sensitive to neutrino masses: as the cosmic neutrinos were produced during an epoch when the three leptonic families were identical to a good approximation –the energies were so high that all lepton species could be regarded as massless–, the background neutrinos are evenly distributed among flavours; therefore, there must be also even proportions of each mass species. As a consequence, the cosmological observables cannot distinguish among the various neutrino masses: they are only sensitive to their total gravitational contribution, to the sum of the masses. It is a generic fact that cosmological considerations only yield bounds –or, eventually, a measurement– for  $\sum_i m_i$ .

The second aspect we would like to remark is the unavoidable parameter degeneracy in cosmological arguments. The evolution of the cosmos is a complex phenomenon that involves various mechanisms and is driven by several sources. A certain observable effect of neutrino masses may in many cases be mimicked by a change in other parameters of the cosmological model. Some effects can be provided either by

---

neutrino masses or by some sort of nonstandard physics. The specific figures, finally, of a given bound may change depending on which parameters are allowed to vary and which are kept fixed when fitting the observed data. These degeneracies are due in part to the complexity of cosmic dynamics, but also to the fact that we cannot *experiment* with the cosmos, but only make observations and try to figure out how these observables came to be the way they are. In the end, what we have is observable quantities and parameters, such as neutrino masses, whose values we would like to extract from the observables; some parameters may be derived with reasonable precision from a single observable, but others can only be determined with precision when other parameters have been fixed, so one needs a family of observables to do the job. The sum of the masses of the neutrinos is a good example of this; it can be probed quite satisfactorily just from the cosmic microwave background if it is above 1 eV, but the CMB loses sensitivity below this level and one needs more observables to increase the precision. We can see this effect in the latest CMB data released by the Planck Collaboration [130]: the reunion of a great deal of data about the CMB by several experiments –Planck power spectrum plus polarisation information from WMAP plus information on high CMB multipoles from the Atacama Cosmology Telescope and the South Pole Telescope– yields a bound on the sum of neutrino masses of  $\sum_i m_i < 0.66$  eV at 95% CL; a good limit, which is tightened, however, by a factor of three when we include in the analysis data on baryon acoustic oscillations that allow to constrain the cosmological evolution parameters. The joint bound with CMB and BAO data reported in [130] is  $\sum_i m_i < 0.23$  eV, again at 95% CL. This is considered the state-of-the-art bound as of today, and as such we quote it in table 3.1. Future data releases by Planck, such as information on the CMB polarisation, will probably improve this bound, but it is remarkable that cosmological considerations begin to approach the inverted hierarchy level, which lies around  $\sum_i m_i \sim 0.1$  eV.

### 3.2.4 Neutrinoless double beta decay

Neutrinoless double beta decay is currently the most sensitive probe to the possible Majorana nature of neutrinos. It is a rare nuclear decay process that essentially consists of two simultaneous  $\beta$  decays occurring to the same nuclide with no outgoing neutrinos:

$${}^A_Z\text{X} \longrightarrow {}^A_{Z+2}\text{Y} + 2e^-; \quad (3.9)$$

as such,  $0\nu\beta\beta$  decay violates lepton number conservation by creating two units of lepton number. A related but lepton-number-conserving process,

$${}^A_Z\text{X} \longrightarrow {}^A_{Z+2}\text{Y} + 2e^- + 2\bar{\nu},$$

dubbed simply ‘double beta decay’, or in short  $2\nu\beta\beta$ , occurs with both Dirac and Majorana neutrinos, and it has already been observed in about a dozen of nuclides [136, 137].  $2\nu\beta\beta$  is a decay mode with very long half-life, about  $10^{20}$  years, and so it is only relevant for nuclides which have all other channels closed – the paradigmatic case is that of nuclides whose  $\beta$ -decay daughter has a higher energy than themselves but have an energetically available daughter at two  $\beta$ -decay steps.

$0\nu\beta\beta$  was initially proposed as a means to enhance the lifetimes of  $2\nu\beta\beta$  [138]: as the phase space of two particles is less suppressed than that of four particles,  $0\nu\beta\beta$  was expected to show higher rates. Nowadays we know that the possible sources of lepton number violation –say, neutrino masses– are also very suppressed, and  $0\nu\beta\beta$  is known to present even longer half-lifetimes, were it to occur. But still, it is one of our best probes of lepton number violation, and an independent window into the properties of the neutrino mass sector; as such, it retains a good deal of interest. Let us briefly<sup>6</sup> describe how  $0\nu\beta\beta$  can be used to investigate Majorana neutrino masses.

Neutrinoless double beta decay has been linked to neutrino masses right from its first appearance in the scientific literature. It was initially conceived to be mediated by lepton-number-violating neutrinos through the process depicted in figure 3.2, with two neutrons becoming two protons by means of charged-current interactions. However, it is clear

<sup>6</sup> For more extensive reviews see references [139–142].

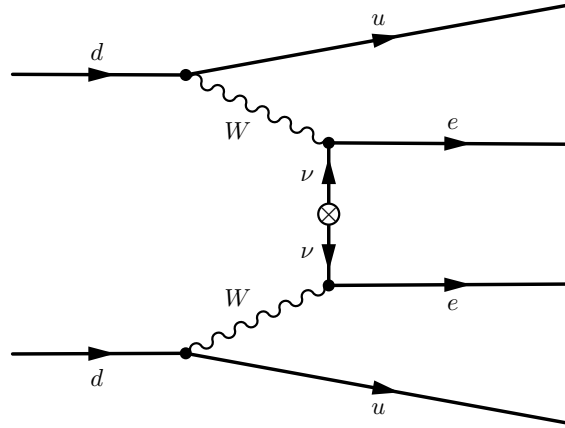
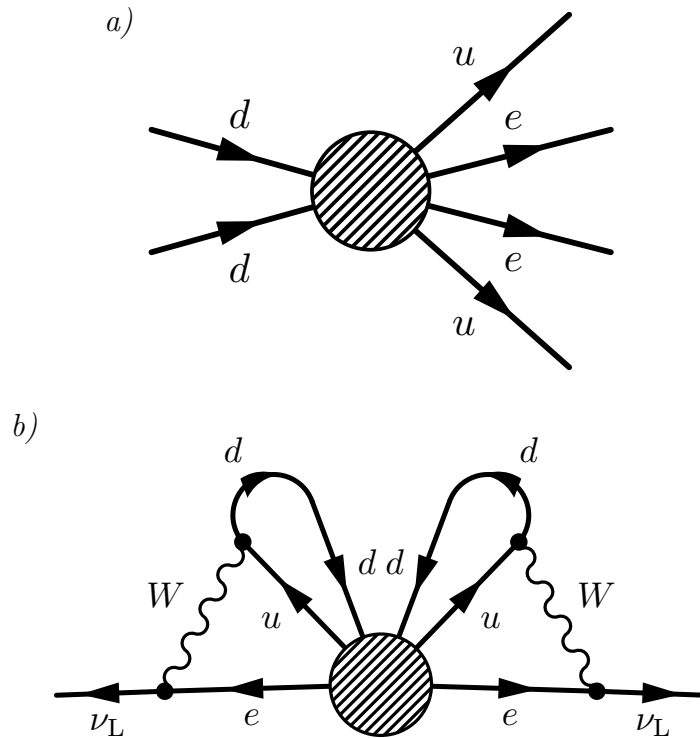


Fig. 3.2:  $0\nu\beta\beta$  mediated by neutrino masses. The diagram displays the process in terms of its fundamental participants – quarks, instead of nucleons or nuclei. The crossed circle represents a Majorana mass insertion necessary to change the helicity of the neutrino and break lepton number.

from (3.9) that it can be mediated by any interaction that transforms two neutrons into protons and yields two electrons; the diagram in figure 3.3a) displays the most general form of the interaction in terms of the fundamental fields of the Standard Model. One would say, then, that  $0\nu\beta\beta$  may or may not be related to neutrino masses: inside the blob of figure 3.3a) there can be Majorana neutrinos and  $W$ 's, but also exotic new scalars, or grand-unifying fields. As far as figure 3.3a) is concerned, the neutrinos might well be Dirac particles and still we could see  $0\nu\beta\beta$  if it's induced by a separate sector of lepton-number-violating new physics.

Wrong. A simple argument shows us so: if the interaction in figure 3.3a) exists, we can always construct a Majorana mass term for the neutrinos –at least for the electron neutrino– by inserting two  $W$ 's and closing the remaining legs in a four-loop diagram; we can see it in figure 3.3b). This diagram will not be calculable in the effective theory, without knowledge of what's inside the blob, but once we provide a renormalisable model that realises the blob it will become a perfectly regular diagram that provides a Majorana component for



*Fig. 3.3:* A diagrammatic representation of the Schechter-Valle theorem. In diagram *a)*, the most general form of generating  $0\nu\beta\beta$  is presented; the blob may be expanded in terms of any lepton-number-violating physics that can accommodate two ingoing  $d$  quarks and two outgoing  $u$  quarks and electrons. In diagram *b)* we show how the blob effective interaction necessarily leads to the generation of a Majorana component for the neutrino mass. This component can be small, as it's suppressed by at least four loops, but the underlying theory may –and in many cases will– produce Majorana neutrino masses through other, less-suppressed processes.

neutrino masses. Indeed it won't be a large Majorana mass – after all, it's at least four-loop suppressed; but from that moment on, electron neutrinos will be Majorana particles and will violate lepton number, if only by a small amount<sup>7</sup>. So, the correct relationship between  $0\nu\beta\beta$  and neutrino masses is: if  $0\nu\beta\beta$  is observed, it may or may not be induced by Majorana neutrino masses, but neutrino masses *will be* Majorana, though the lepton number violation may be small. This result is known as the Schechter-Valle theorem, after the authors who first figured it out [143].

Up to this point we have only discussed qualitative considerations about the implications of  $0\nu\beta\beta$  regarding the nature of neutrinos. Let us now get more quantitative and see how a measurement can inform us about the amount of lepton number violation and about neutrino masses. The calculation of the width of a process like (3.9) is in general complicated, as it involves nuclei, whose dynamics is not absolutely known. For this reason it's usual to separate the width of a  $0\nu\beta\beta$  process in three parts:

$$\left[T_{1/2}^{0\nu}\right]^{-1} = G_{0\nu} |M_{0\nu}|^2 |\varepsilon|^2, \quad (3.10)$$

where  $G_{0\nu}$  is a phase space factor that depends on the energy released in the decay and the atomic number of the parent nucleus,  $M_{0\nu}$  is the nuclear matrix element between the initial and final nuclear states, and  $\varepsilon$  is the parameter or combination of parameters which describe lepton number violation; note, therefore, that “ $\varepsilon$ ” must be understood as something of a symbolic notation, and its concrete form can only be fixed when something about the underlying source of  $0\nu\beta\beta$  is specified.

Of these three elements, the phase space factors are the least problematic: they don't depend on the new physics involved in the process, but just on kinematic considerations and the electric charge distribution of the nucleus; as such, they can be calculated with a reasonable precision and don't introduce much uncertainty in  $T_{1/2}^{0\nu}$ .

---

<sup>7</sup> Actually, in most models with lepton number violation Majorana neutrino masses are generated much before the four-loop level. The diagram in figure 3.3b) will usually be just a renormalisation to the leading tree-level or one-loop contribution, and the masses of the neutrinos may be dominantly lepton-number-violating.

Unfortunately, we cannot say the same about the nuclear matrix elements: their values can't be accessed through experiment –that is, through other than a  $0\nu\beta\beta$  experiment–, and they must be evaluated theoretically; but the calculation involves difficult many-body dynamics, and it can only be attacked by means of models that attempt to capture the nuclear structure and interaction. Popular models include the Interacting Shell Model and the Quasiparticle Random Phase Approximation. The different approaches essentially agree, but only within a range of a factor 2 or 3; thus, the calculation of nuclear matrix elements becomes the main source of uncertainty when interpreting the results of a  $0\nu\beta\beta$  experiment. The interested reader may find more details on nuclear models and the calculation of nuclear matrix elements for instance in [139, 140] and references therein.

As for the third element,  $\varepsilon$ , it is the *raison d'être* of neutrinoless double beta decay experiments. If we see a positive  $0\nu\beta\beta$  signal it means that  $\varepsilon$  is not zero, and thus we have proven that lepton number is violated and, by the Schechter-Valle argument, that neutrinos are Majorana particles. Now the thing is that the most general form of the  $0\nu\beta\beta$  process is that of figure 3.3a), which shows –necessarily– nothing about the internal happenings of the process; a means should be found to classify and parametrise the various possible contributions. We find particularly useful the approach of references [144, 145], where the new physics contributions are classified according to the Lorentz structure of the resulting six-fermion effective vertex. The parameter  $\varepsilon$  is identified, for each different Lorentz arrangement of the three fermionic bilinears, with the coupling of the corresponding effective operator, and bounds are derived for each coupling or for combinations of them. This procedure allows to set bounds on large classes of models: for each particular model one has just to identify the leading six-fermion operators and express its couplings in terms of the model parameters, which allows to translate the general bounds into limits specific for that model.

Let us now discuss in more detail the classic case of  $0\nu\beta\beta$  induced by Majorana neutrino masses. It is depicted in figure 3.2, where we identify the lepton-number-violating element with a fermionic bilinear that couples an electron neutrino with an electron antineutrino, that

is to say, a Majorana mass and in particular the element  $m_{ee}$  of a possible neutrino mass matrix – indeed, observing  $0\nu\beta\beta$  only informs us about violation of lepton number in the electron family, but we do know that  $\nu_e$  is not a mass eigenstate and its mixings are large, so LNV will be right away transmitted to the other families. Going back to equation (3.10), we have just determined that for neutrino-mediated  $0\nu\beta\beta$  we have  $\varepsilon = m_{ee}$ . Let us then examine which knowledge  $m_{ee}$  offers about the neutrino mass and mixing parameters; we have identified in equation (3.5) the physical degrees of freedom of the mixing sector for Majorana neutrinos; by properly convoluting  $U_{\text{PMNS}}$  with the diagonal neutrino mass matrix we can recover the flavour-basis mass matrix:

$$(m_\nu)_{\text{flavour}} = U_{\text{PMNS}} \begin{pmatrix} m_1 & & \\ & m_2 & \\ & & m_3 \end{pmatrix} U_{\text{PMNS}}^T,$$

where we find

$$m_{ee} = \cos^2 \theta_{12} \cos^2 \theta_{13} e^{i\alpha_1} m_1 + \sin^2 \theta_{12} \cos^2 \theta_{13} e^{i\alpha_2} m_2 + \sin^2 \theta_{13} e^{-i2\delta} m_3.$$

Note, however, that for the purpose of neutrinoless double beta decay only the modulus of  $\varepsilon$  matters, so the relevant  $0\nu\beta\beta$  observable is finally defined as:

$$m_{\beta\beta} = \left| \cos^2 \theta_{12} \cos^2 \theta_{13} e^{i(\alpha_1-2\delta)} m_1 + \sin^2 \theta_{12} \cos^2 \theta_{13} e^{i(\alpha_2-2\delta)} m_2 + \sin^2 \theta_{13} m_3 \right|, \quad (3.11)$$

and sometimes dubbed the ‘effective Majorana mass’ of neutrinoless double beta decay.

Several features are worth being noted about this effective Majorana mass: first, it retains much information about the phases; this far it is the only solid observable we have that is sensitive to the Majorana phases, even if it is in the convoluted combination of equation (3.11). Unfortunately, with three neutrino species there are two Majorana phases and just *one* observable, so even in the case we attain a good knowledge of the masses, mixings, Dirac phase and nuclear matrix



elements further experimental input would be needed to determine unambiguously  $\alpha_1$  and  $\alpha_2$ ; clearly, a synergy will be required, possibly with CP-violating observables, if a positive  $0\nu\beta\beta$  signal is observed.

Second, the phase-dependence of  $m_{\beta\beta}$  is good news, but it also opens the door to undesired scenarios: an un-serendipitous combination of the parameters might yield  $m_{\beta\beta} = 0$ , leading to negative  $0\nu\beta\beta$  results even if the neutrinos are Majorana particles. This would require quite an amount of fine tuning and may be regarded as unnatural, but it can be natural in the framework of certain neutrino mass models: in chapter 8 we describe a model which yields a naturally suppressed  $m_{ee}$ . However, even in this case neutrinos are bound not to be the only source of lepton number violation: if Majorana neutrino masses are generated by some high-energy physics these particles are the ultimate source of LNV and may contribute by themselves to  $0\nu\beta\beta$ , as it is the case in the model of chapter 8. All in all, this reminds us that neutrinoless double beta decay results, either positive or null, cannot be taken as the last word about the nature of the neutrino: more investigation is needed in order to determine the origin of neutrino masses and, were the day to arrive, of a possible  $0\nu\beta\beta$  signal.

Third, the combination of parameters in equation (3.11) is a rather complicated one, but we have measurements or strong constraints for many of them and they can be used to evaluate the possible values of  $m_{\beta\beta}$ . All mixings and mass splittings are known with a good level of precision, so the main sources of uncertainty are the absolute scale of the masses, their ordering –either normal or inverse hierarchy, see section 3.2.1–, and the phases, about which we know nothing. This evaluation has been done and is well-known; we present it in figure 3.4. Note the fact that cancellations among the neutrino mass and mixing parameters can only yield  $m_{\beta\beta} = 0$  for normal hierarchy; note also, therefore, that attaining sensitivities below 10 meV without a positive result would mean almost ruling out Majorana neutrinos with inverted hierarchy<sup>8</sup>, but this achievement is very unlikely, even for the

---

<sup>8</sup> The only way out in this scenario would be that some LNV-ing new physics exists whose contribution to  $0\nu\beta\beta$  cancels exactly that of light Majorana neutrinos, but this would require a certain amount of fine tuning and could be regarded as unnatural.

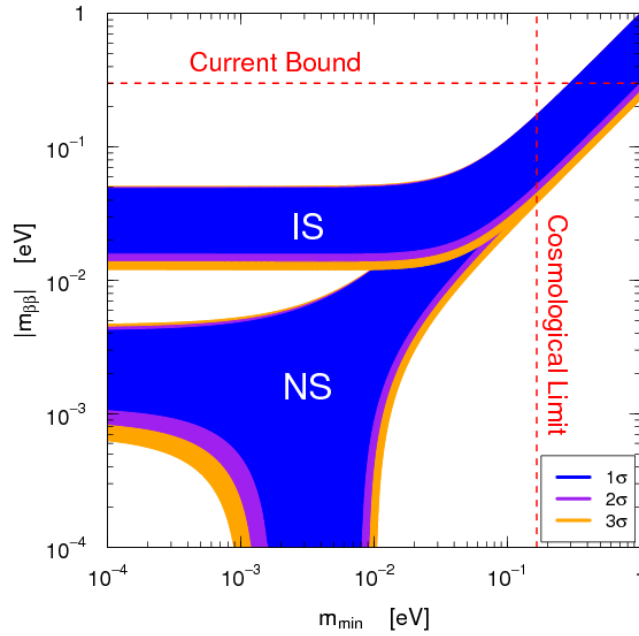


*Fig. 3.4:* A graph that displays the range of allowed values for the effective Majorana mass in terms of the mass of the lightest neutrino – either  $m_1$  for normal hierarchy or  $m_3$  for inverted hierarchy. The variability along the  $m_{\min}$  axis is the result of our lack of knowledge about the absolute scale of neutrino masses, whereas the width of the bands reflects the uncertainties in phases, mixing angles and squared mass splittings. The allowed range is very dependent on the mass hierarchy for small  $m_{\min}$ , yielding two bands, marked here “NS” for “normal spectrum” and “IS” for “inverted spectrum”; as the spectrum grows heavier and the mass splittings become less noticeable the two bands converge. The figure is taken from reference [141].

next generation of experiments [140].

Let us, to conclude, present the most stringent bounds to date on the effective Majorana mass. For more than a decade, the Heidelberg-Moscow experiment stayed as the most sensitive experiment with an upper bound of  $m_{\beta\beta} < 0.35$  eV [146] derived from the search of  $0\nu\beta\beta$  in  ${}^{76}\text{Ge}$ . A subset of the collaboration claimed a detection [147] with  $m_{\beta\beta} = 0.32 \pm 0.03$  eV [148], but this claim stays controversial and the official position of the collaboration is a no-signal result with  $T_{1/2}^{0\nu}({}^{76}\text{Ge}) > 1.9 \times 10^{25}$  yr at 90% confidence level, from where the cited bound on  $m_{\beta\beta}$  is derived. Recently, the EXO collaboration has released the first results of their searches in  ${}^{136}\text{Xe}$ , which offer no evidence of  $0\nu\beta\beta$  and allow to establish  $T_{1/2}^{0\nu}({}^{136}\text{Xe}) > 1.6 \times 10^{25}$  yr; the collaboration derives from there a bound on the effective neutrino Majorana mass of  $m_{\beta\beta} < 0.14 - 0.38$  eV [131], with the interval accounting for the uncertainties in the nuclear matrix elements. Even more recently, the GERDA collaboration has released their first searches of neutrinoless double beta decay [132]; they report a null result with a limit on the half life of  ${}^{76}\text{Ge}$  of  $T_{1/2}^{0\nu}({}^{76}\text{Ge}) > 3.0 \times 10^{25}$  yr at 90% CL, which allows them to bound the effective mass at  $m_{\beta\beta} < 0.2 - 0.4$  eV. Both [131] and [132] clearly disfavour the claim in [147].

As for the near future,  ${}^{136}\text{Xe}$  is expected to draw some attention, with good prospects for EXO, NEXT and KamLAND-Zen; the CUORE experiment, which investigates  ${}^{130}\text{Te}$ , may also attain good levels of sensitivity [140].

### 3.3 Seesaw mechanism

Let us in this section review briefly the seesaw mechanism, one of the most popular ways of explaining the smallness of neutrino masses. The basic idea is simple to grasp: the masses of the neutrinos are very small because they are generated via interactions with very heavy particles; the mass-generating process possesses an internal leg with one of the heavy particles, so the heavier the new particles the lighter the generated masses. The classic picture of the seesaw mechanism provides Majorana masses and generates essentially the Weinberg operator, equation (3.3); this means that these theories are also models

of violation of lepton number, with the violation originating in the heavy sector and being transmitted to the neutrinos. Seesaw-like models are usually classified into three types according to the identity of the heavy particles: in type I seesaw, the neutrino masses are generated through interactions with fermionic  $SU(2)$  singlets, in type II the mediators are scalar  $SU(2)$  triplets, whereas in type III seesaw it is a heavy fermionic triplet who aids to generate neutrino masses.

The mechanism was first proposed at the end of the 1970's by several authors; the community assumes that the general knowledge of the time was ripe and ready to yield this idea and it blossomed in several frameworks: grand-unified theories [149, 150], flavour symmetries [151, 152] and left-right models [153]. From these primeval forms the mechanism evolved and was developed into the three classes mentioned above, inverse seesaw [154–156], Dirac-mass seesaw [59] and many more. We will, in the remaining of this section, discuss the three types of classic seesaw, which are also the simplest realisations of the original idea.

### 3.3.1 Type I Seesaw

Type I seesaw was the first variety of seesaw being developed, back in the end of the 70's [149–153]. In this class of seesaws  $n$  fermion fields, singlets under  $SU(2)$  and with zero hypercharge, are added to the Standard Model; such singlets have the quantum numbers of right-handed neutrinos, so we denote them by  $\nu_{R\alpha}$ . Note that to explain the neutrino data, which require at least two massive neutrinos, a minimum of two extra singlets are needed. Having no charges under the SM, Majorana masses for right-handed neutrinos are allowed by gauge invariance, so the new terms in the Lagrangian are:

$$\mathcal{L}_{\nu_R} = i \bar{\nu}_R \gamma^\mu \partial_\mu \nu_R - \left( \frac{1}{2} \bar{\nu}_R^c M \nu_R + \bar{\ell}_L Y \nu_R \tilde{\phi} + \text{H.c.} \right), \quad (3.12)$$

with  $M$  a  $n \times n$  symmetric matrix in flavour space,  $Y$  a general  $3 \times n$  flavour matrix, and with flavour indices omitted for simplicity. We can recognise in equation (3.12) the necessary interactions to generate the Weinberg operator through the diagram that we display in figure 3.5a). As a  $\nu_R$  is propagated in an internal leg, its mass will suppress the

process, realising the seesaw mechanism. It is also worth noting that the violation of lepton number is also originated in the  $\nu_R$  sector, in particular in their Majorana masses, and is transmitted to the active neutrinos through the Weinberg operator.

The generation of neutrino masses can also be understood non-diagrammatically: the interactions in (3.12) generate, upon spontaneous symmetry breaking –that is, when the Higgs field develops a VEV,  $\langle\phi\rangle = (0 \ v_\phi)^T$ , Dirac mass terms for the neutrinos that can be arranged together with  $M$  in a global ‘neutrino Majorana mass matrix’ as follows:

$$\mathcal{L}_{\nu \text{ mass}} = -\frac{1}{2} \begin{pmatrix} \bar{\nu}_L & \bar{\nu}_R^c \end{pmatrix} \begin{pmatrix} 0 & m_D \\ m_D^T & M \end{pmatrix} \begin{pmatrix} \nu_L^c \\ \nu_R \end{pmatrix} + \text{H.c.}, \quad (3.13)$$

where  $m_D = Yv_\phi$ . The neutrino mass eigenstates will be the eigenvectors of this matrix; unfortunately, if  $m_D$  and  $M$  are arbitrary matrices the diagonalisation is difficult to carry out analytically. However, if one assumes  $M \gg m_D$ , as the diagram in figure 3.5a) requires to obtain small masses for the  $\nu_L$ ’s, (3.13) can be block-diagonalised perturbatively and very approximate eigenvalues and eigenvectors can be obtained. In particular, one finds  $n$  heavy eigenvectors with masses  $\sim M$  which are essentially combinations of the  $\nu_R$ ’s, and three light eigenvectors which are mostly combinations of the  $\nu_L$ ’s with a Majorana mass matrix

$$m_\nu \simeq -m_D M^{-1} m_D^T.$$

This formula is now famous, and it naturally explains the smallness of light neutrino masses as a consequence of the presence of heavy SM singlet fermions.

### 3.3.2 Type II Seesaw

The type II seesaw [57, 87, 157–159] adds to the SM field content only one scalar  $SU(2)$  triplet with hypercharge 1, that we will denote by  $\chi$ . It is useful, in order to deduce the interactions of this triplet with the leptons, to find a notation that displays intuitively the composition of the doublet and triplet representations of  $SU(2)$ . A common way of

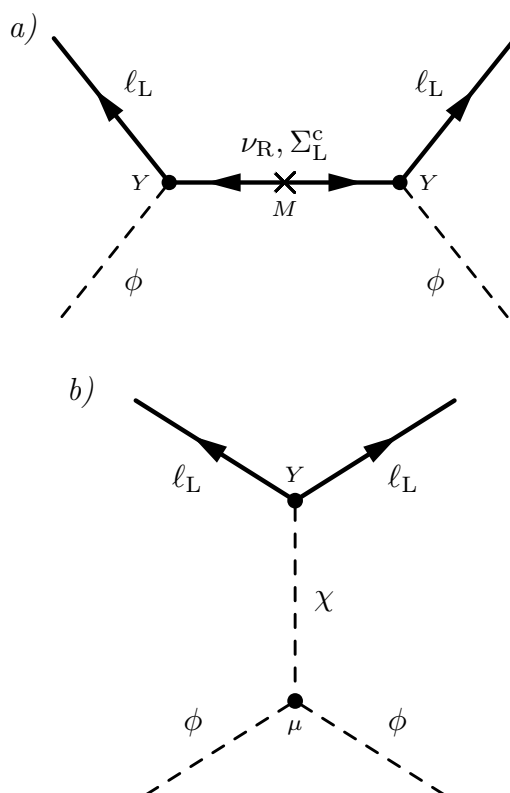


*Fig. 3.5:* Feynman diagrams giving rise to the Weinberg operator (3.3) in the framework of seesaws type I and III (diagram *a*) and seesaw type II (diagram *b*). As emphasised in the text, the presence of heavy particles in an internal propagator suppresses the coefficient of the effective operator, and thus the magnitude of the resulting neutrino masses.

doing so is to write the triplets as  $2 \times 2$  matrices that act on vectors in the doublet representation. For the case of our hypercharge-1  $\chi$  field this matrix reads

$$\chi = \begin{pmatrix} \chi^+/\sqrt{2} & \chi^{++} \\ \chi^0 & -\chi^+/\sqrt{2} \end{pmatrix},$$

where  $\chi^0$ ,  $\chi^+$  and  $\chi^{++}$  are the components of the triplet with definite electric charge. This matrix form of  $\chi$  transforms under  $SU(2)$  gauge transformations as  $\chi \rightarrow U\chi U^\dagger$ . It is easy then to see that gauge invariance allows for just one coupling to the Standard Model fermions: a Yukawa interaction among  $\chi$  and two lepton doublets,

$$\mathcal{L}_{\chi \text{ Yukawas}} = -Y_{\alpha\beta} \bar{\ell}_\alpha \chi \ell_\beta + \text{H.c.}, \quad (3.14)$$

which allows to assign lepton number to the triplet,  $L(\chi) = -2$ . In (3.14) the flavour indices are displayed explicitly, and  $Y$  is a  $3 \times 3$  symmetric matrix.

The terms that need to be added to the SM Lagrangian include these Yukawa vertices together with several pure-scalar interactions, both  $\chi$  self-couplings and interactions with the Higgs doublet. We display here two of them:

$$\mathcal{L}_\chi = \mathcal{L}_{\chi \text{ Yukawas}} - m_\chi^2 \text{Tr}[\chi\chi^\dagger] - (\mu \tilde{\phi}^\dagger \chi^\dagger \phi + \text{H.c.}) + \dots;$$

both are related to lepton number violation:  $m_\chi^2$  would trigger a VEV for  $\chi$ , were it to have the ‘wrong’ sign,  $m_\chi^2 < 0$ . Lepton number would then be spontaneously broken, as  $\chi$  carries lepton number charge, and Majorana neutrino masses should appear. Indeed, (3.14) would immediately induce Majorana masses for the neutrinos, for the VEV of  $\chi$  needs to have the form

$$\langle \chi \rangle = \begin{pmatrix} 0 & 0 \\ v_\chi & 0 \end{pmatrix}$$

in order not to break electric charge. Unfortunately, this program is not phenomenologically viable, because a very small  $|m_\chi^2|$  would be needed, and it would yield light charged scalars which have not been

observed. Besides, it would neither realise the seesaw mechanism nor explain the smallness of neutrino masses.

That's what the  $\mu$  trilinear coupling is useful for. It violates explicitly lepton number and allows to write the diagram in figure 3.5b), with the scalar triplet running in an internal propagator. The  $\mu$  interaction induces a VEV for  $\chi$  through the VEV of  $\phi$ , irrespective of the sign of  $m_\chi^2$ ; in particular, when  $m_\chi^2 > 0$  and  $m_\chi \gg v_\phi$  –as the diagram in figure 3.5b) seems to hint– we obtain

$$v_\chi \simeq \frac{\mu v_\phi^2}{m_\chi^2}.$$

Then the Yukawa couplings in equation (3.14) lead to a Majorana mass matrix for the left-handed neutrinos, with structure

$$m_\nu = 2Yv_\chi \simeq 2\frac{\mu v_\phi^2}{m_\chi^2}Y.$$

Neutrino masses are thus proportional to both  $Y$  and  $\mu$ , and inversely proportional to  $m_\chi^2$ . The seesaw is realised, for the heavier  $\chi$  the lighter the  $\nu_L$ 's, and lepton number is violated by the simultaneous presence of  $Y$ , that assigns lepton number to  $\chi$ , and  $\mu$ , that breaks it.

### 3.3.3 Type III Seesaw

In the seesaw mechanism of type III [160, 161], the Standard Model is extended by fermion  $SU(2)$  triplets,  $\Sigma_{L\alpha}$ , with zero hypercharge. Like in type I, at least two fermion triplets are needed to have two nonvanishing light neutrino masses. As for the case of the type II seesaw (see section 3.3.2), the triplet  $\Sigma_L$  can be written as a  $2 \times 2$  matrix that acts on doublets,

$$\Sigma_L = \begin{pmatrix} \Sigma_L^0/\sqrt{2} & \Sigma_L^+ \\ \Sigma_L^- & -\Sigma_L^0/\sqrt{2} \end{pmatrix},$$



with  $\Sigma_L^0$ ,  $\Sigma_L^+$  and  $\Sigma_L^-$  the components of  $\Sigma_L$  with definite electric charge. The new terms in the Lagrangian are then given by

$$\begin{aligned} \mathcal{L}_{\Sigma_L} = & i \operatorname{Tr} \left[ \overline{\Sigma_L} \gamma^\mu D_\mu \Sigma_L \right] + \\ & + \left( \frac{1}{2} M_{\alpha\beta} \operatorname{Tr} \left[ \overline{\Sigma_{L\alpha}} \tilde{\Sigma}_{L\beta} \right] + \sqrt{2} Y_{\alpha\beta} \overline{\ell_{L\alpha}} \tilde{\Sigma}_{L\beta} \tilde{\phi} + \text{H.c.} \right), \end{aligned} \quad (3.15)$$

where  $\tilde{\Sigma}_L$  is defined analogously to  $\tilde{\ell}_L$ ,  $\tilde{\Sigma}_L \equiv \epsilon \Sigma_L^c \epsilon^\dagger$ , in order to connect the fundamental and complex-conjugate doublet representations of  $SU(2)$ . The coupling content of the model is very similar to that of type I seesaw, see equation (3.12), and so is the diagram that generates the Weinberg operator, figure 3.5a). The difference is that the interactions are richer in content with a triplet: the Yukawas provide mixing between the  $\nu_L$ 's and  $\Sigma_L^0$ , as expected, but also mix the charged leptons with the charged components of  $\Sigma_L$ ; the ‘Majorana’ mass term  $M$  is also richer than it may seem: it indeed yields a Majorana mass for  $\Sigma_L^0$ , but also provides a Dirac mass for a Dirac fermion  $E$  constructed with both  $\Sigma_L^+$  and  $\Sigma_L^-$ ,  $E = \Sigma_L^- + \Sigma_L^{+c}$ . These features endow the model with a more varied phenomenology, though we will not discuss this in detail here.

For what respects the generation of neutrino masses, everything proceeds in a similar fashion as for type I seesaw: the diagram in figure 3.5a) suggests that the heavier  $M$ , the lighter the active neutrino masses. Indeed, if we select from (3.15) the bilinear terms of the neutral leptons we can compose a Majorana mass matrix,

$$\mathcal{L}_{\nu \text{ mass}} = -\frac{1}{2} \begin{pmatrix} \overline{\nu_L} & \overline{\Sigma_L^0} \end{pmatrix} \begin{pmatrix} 0 & m_D \\ m_D^T & M \end{pmatrix} \begin{pmatrix} \nu_L^c \\ \Sigma_L^{0c} \end{pmatrix} + \text{H.c.}$$

with  $m_D = vY$ , which is absolutely equivalent to that of type I seesaw. Therefore, once we assume  $M \gg m_D$  it too provides the classical seesaw formula for the light neutrino masses,

$$m_\nu \simeq -m_D M^{-1} m_D^T.$$

As we already commented, the main difference between type I and type III seesaw is the presence of charged components in  $\Sigma_L$ ; in what

respects neutrino masses, this leads to more stringent constraints upon  $M$ : as the new charged leptons have not been observed one should require  $M_{\alpha\beta} \gtrsim 100$  GeV.

### 3.4 Neutrino magnetic moments

The electromagnetic properties of neutrinos have been a matter of interest for many years. From the experimental point of view neutrinos are known to have very small couplings to photons [32], and indeed in the context of the Standard Model their electric charge is usually assumed to be zero<sup>9</sup>. Other electromagnetic couplings are even more free, and their magnitude depends on the interactions of neutrinos with certain charged particles. In this section we will discuss one such couplings, the magnetic dipole moment; we will motivate its interest and will point out some features of phenomenological interest.

Magnetic and electric dipole moments are dimension-five effective interactions that couple a pair of fermions to a photon, with a characteristic Lorentz structure:

$$\mathcal{L}_{\text{dipole}} = -\frac{1}{2} \overline{\psi_R} (\mu + \epsilon \gamma_5) \sigma^{\alpha\beta} \chi_L F_{\alpha\beta} + \text{H.c.}$$

In this expression  $\chi_L$  and  $\psi_R$  are fermionic fields with left and right chirality, and  $F_{\alpha\beta}$  is the electromagnetic field strength tensor, that involves derivatives of the photon field.  $\mu$  is then called a *magnetic dipole moment* and  $\epsilon$  an *electric dipole moment*. They can be induced by radiative processes which involve charged particles inside a loop, such as those we show in figure 5.1. For the case of the neutrinos, being neutral particles, one can have two types of dipole moments: the fields  $\chi_L$  and  $\psi_R$  can be the left- and right-handed neutrino fields, and

---

<sup>9</sup> Though that is not a fundamental requirement of the theory: they might well have a tiny, but nonzero, electric charge, to the degree allowed by observations. The situation is different in grand unified theories: as they aim to explain the relation between the charges of leptons and quarks they end up quantising electric charge, and neutrinos are neutral by construction – see, for instance, [162] for more on this matter.

then we have the lepton-number-conserving *Dirac dipole moments*,

$$\mathcal{L}_{\text{D-moments}} = -\frac{1}{2} \bar{\nu}_R (\mu_D + \epsilon_D \gamma_5) \sigma^{\alpha\beta} \nu_L F_{\alpha\beta} + \text{H.c.}$$

But we can also construct this same structure with just one neutrino field, say, a left-handed neutrino and its charge-conjugate, which is a right-handed field; we have then *Majorana dipole moments*,

$$\mathcal{L}_{\text{M-moments}} = -\frac{1}{4} \bar{\nu}_L^c (\mu_M + \epsilon_M \gamma_5) \sigma^{\alpha\beta} \nu_L F_{\alpha\beta} + \text{H.c.},$$

which break every charge carried by  $\nu_L$  – in particular, lepton number.

The Dirac or Majorana nature of the dipole moments depends on the nature of the underlying interactions between the neutrinos and the charged particles, and very importantly on the relation of such interactions with lepton number violation. They also depend on whether right-handed neutrinos are allowed or not as standalone fields in the picture of neutrino masses being considered. Actually, often there is a very close relation between, specifically, neutrino magnetic moments and neutrino masses. For instance, in the Standard Model enlarged only with right-handed neutrinos Dirac magnetic moments are generated radiatively if the  $\nu_R$ 's participate in neutrino masses [163, 164]; the converse is also true: if the neutrinos are endowed with Dirac magnetic moments, they immediately acquire a mass through radiative corrections [165, 166]. This intercourse between neutrino magnetic moments and masses makes them a very interesting study case. For instance, the induced magnetic moment in the Standard Model for Dirac neutrinos is tiny due to the smallness of neutrino masses; the exact value is  $\mu_\nu \simeq 3 \times 10^{-19} (m_\nu/1 \text{ eV})$ , far below any foreseeable experimental sensitivity, but it is still interesting to look for them in experiments, because were it to happen that we observe a magnetic moment larger than that predicted by the SM, we would possibly be probing the physics responsible for neutrino masses.

However, neutrino magnetic moments also have interest by themselves; in the past, neutrino magnetic moments were also a matter of interest because if they allowed flavour transitions they might provide an explanation for the solar neutrino puzzle (see section 3.1.2). Today,

---

after the great experiments of the 90's and the 2000's, it is a well-established fact that the solar as well as atmospheric neutrino deficit is due to oscillations induced by mass mixing between the different flavours (see section 3.2.1 and references therein), but the existence of a large neutrino magnetic moment still would be very relevant in a number of scenarios, of which the most important are maybe astrophysical [48, 167]: neutrinos are extremely weakly-interacting particles; this means that they are difficult to trap inside any object, and so they provide a major means for energy to escape from astrophysical bodies. Such energy loss, usually referred to as the *cooling* of the object, is in many cases well-bounded, because a too large energy depletion might compromise the integrity of the body, or drastically change its properties.

A good example is the bound extracted from the luminosity gap between helium-burning stars and hydrogen-burning red giants; it is described in a beautifully simple paper written by Georg Raffelt in 1990 [168]. The idea is the following: the burning of helium requires a temperature roughly 10 times higher than the burning of hydrogen; this temperature can only be achieved by gravitational pressure upon the helium mass. While in its hydrogen-burning phase the star produces huge amounts of helium that cannot be burnt yet, as the temperature inside the star is not high enough; the helium falls toward the center and there it forms an inert core. As the helium accumulates the star keeps burning hydrogen in a shell that surrounds the helium core. The gravity of the core presses the shell, heating it and enhancing the hydrogen burning rate. The star, so, shines brighter and brighter, and meanwhile it undergoes several structural transformations which eventually lead it to the red giant phase. When finally the helium furnace ignites the core expands, alleviating the pressure upon the hydrogen shell, which reduces its burning rate. The helium burning is not energetic enough and cannot compensate for this decrease, so the overall energy emission of the star decreases: a gap in luminosity appears between the stars that have just begun to burn helium and those that are about to.

The interesting thing about this succession of facts is that energy losses in the helium core affect differently helium-burning and not-

---

yet-helium-burning stars: obviously, if the core is losing energy, say by emission of neutrinos, hydrogen-burning red giants will need more massive cores to attain the temperature necessary to ignite helium; as this means more gravitational pressure on the hydrogen shell, the stars will reach greater luminosities before the helium flash; but at the same time, helium-burning stars will inherit more massive cores, so they will also shine brighter. The trick is that our astrophysical models inform us that an additional cooling mechanism enhances *more* the luminosity of hydrogen-burning red giants than that of their helium-burning relatives; consequently, a measurement of the luminosity gap between these two populations constitutes also a measurement of the anomalous cooling mechanisms acting on the stars.

How can we relate this to neutrinos and their magnetic moments? It's simple: neutrinos are accounted for as 'standard' cooling sources when coming from the nuclear reactions occurring inside the core; any additional source of neutrinos is considered 'anomalous'. And magnetic moments provide such an additional source, because photons inside a plasma can decay directly to neutrinos via the process  $\gamma \rightarrow \nu\bar{\nu}$  that would be forbidden in vacuum. This is due to the fact that the electromagnetic interactions of the photons with the charged particles in the plasma dress the photons and endow them with an effective mass; such massive photons are called *plasmons*, and we will denote them by  $\gamma_P$ . The mass of plasmons depends on the temperature of the plasma, and it can vary from roughly 10 keV for red giant cores to several MeV for neutron stars and tens of MeV for supernova cores. Using experimental data on the luminosity gap before and after the helium flash, reference [168] provides a very stringent bound on magnetic moments for neutrino species with masses below 10 keV. We will use this bound in chapter 4.

## 4. RIGHT-HANDED NEUTRINO MAGNETIC MOMENTS

In this chapter we will present and analyse a dimension-five effective operator that provides magnetic moments for the right-handed neutrino degrees of freedom. Right-handed neutrinos are usually regarded as sterile particles, having no gauge couplings at all as they do; an interaction like a magnetic moment may change dramatically the physics of right-handed neutrinos, providing production and decay mechanisms and opening the possibility that they show up in collider experiments and astrophysical systems. We discuss the major constraints that can be derived from the overall nonobservation of right-handed neutrinos, and we also comment on the observation prospects at the LHC and the possible consequences of these magnetic moments in the early universe. Together with this discussion we also consider briefly other dimension-five operators that arise if we consider as low-energy fields the full SM plus right-handed neutrinos; at the dimension-five effective level, the neutrino mass matrix receives additional contributions, and one operator appears that couples the Higgs field to right-handed neutrinos, possibly providing new decay channels for the Higgs boson. This work was carried out together with Arcadi Santamaria, José Wudka and Kyungwook Kim.

### *4.1 An effective theory capable of parametrising all neutrino mass scenarios*

When considering the low-energy effects of new, heavy particles that are not directly probed, one can parametrise their low-energy effects using a series of effective vertices that involve only the light fields [38, 43, 169].

These vertices are constrained only by the gauge invariance of the light theory, irrespective of the new interactions that may appear in the complete model [170]. Assuming that the heavy physics is decoupling, their contributions will be suppressed by powers of the heavy scale  $\Lambda$ , as described in section 2.2.

In this work we aim to study the first-order effective corrections to the Standard Model with a focus on neutrino physics. Some properties of the neutrinos, however, are still poorly understood and this casts some uncertainties on the definition of a proper neutrino-oriented effective theory. Think, for instance, on the identity of the low-energy degrees of freedom: neutrinos have masses, but we don't know yet if they are Dirac-like or Majorana-like. If neutrinos are Dirac particles then their right-handed counterparts exist and must be light – at least two of them, for one of the light neutrinos is still allowed to be massless. If neutrinos are Majorana, then right-handed neutrinos are not necessary, but they are not barred; they might even have masses below the electroweak scale and provide interesting phenomenological features [171, 172]. With all this considered, we think that it is prudent to include right-handed neutrinos among the low-energy degrees of freedom: that allows the effective theory to describe any *a priori* possible pattern of neutrino masses, and can be regarded as a conservative hypothesis. In this chapter we will examine the consequences of retaining the  $\nu_R$ 's among the low-energy fields.

The most general Lagrangian that includes the full Standard Model plus a number of right-handed neutrinos will read

$$\mathcal{L} = \mathcal{L}_{\text{SM}} + \mathcal{L}_{\nu_R} + \mathcal{L}_5 + \dots ,$$

where  $\mathcal{L}_{\text{SM}}$  represents the usual Standard Model with no right-handed neutrinos,

$$\mathcal{L}_{\text{SM}} = i \bar{\ell}_L \gamma_\mu D^\mu \ell_L + i \bar{e}_R \gamma_\mu D^\mu e_R - (\bar{\ell}_L Y_e e_R \phi + \text{H.c.}) + \dots , \quad (4.1)$$

$\mathcal{L}_{\nu_R}$  collects the renormalisable terms that appear when  $\nu_R$ 's are introduced,

$$\mathcal{L}_{\nu_R} = i \bar{\nu}'_R \gamma_\mu \partial^\mu \nu'_R - \left( \frac{1}{2} \bar{\nu}'_R{}^c M \nu'_R + \bar{\ell}_L Y_\nu \nu'_R \tilde{\phi} + \text{H.c.} \right) , \quad (4.2)$$

and  $\mathcal{L}_5$  is the lowest-order –i.e., dimension-five– effective operators that arise in such a theory,

$$\mathcal{L}_5 = \overline{\nu_R}' \zeta \sigma^{\mu\nu} \nu_R' B_{\mu\nu} + \left( \overline{\ell_L} \phi \right) \chi \left( \tilde{\phi}^\dagger \ell_L \right) - \left( \phi^\dagger \phi \right) \overline{\nu_R}' \xi \nu_R' + \text{H.c.} \quad (4.3)$$

Notation in equations (4.1–4.3) follows closely that described in sections 2.1.2 and 2.1.3, with the only difference of a prime ( $\prime$ ) on some of the neutrino fields to denote that these are *not* fields with definite mass; we save the unprimed version for the fields representing light neutrinos with definite mass, equation (4.9). Consequently, the left-handed neutrinos in the flavour doublets also are understood to carry a prime:  $\ell_L \equiv \begin{pmatrix} \nu_L' \\ e_L' \end{pmatrix}$ . Apart from that, the  $SU(2) \otimes U(1)$  charges of the SM fields are the customary ones, see table 2.1; the  $B$  field, remember, represents the gauge boson associated to  $U(1)_Y$ ; and  $\sigma^{\mu\nu}$  is a matrix in spinorial space defined by  $\sigma^{\mu\nu} \equiv \frac{i}{2} [\gamma^\mu, \gamma^\nu]$ , with  $\gamma^\alpha$  the Dirac matrices of the spinorial Clifford algebra. The dots in equation (4.1) indicate that we have omitted the terms involving quarks, and also the kinetic and gauge-fixing terms for the gauge fields, as they will not be used in our discussion.

As for the couplings with structure in generation space, their number and complexity will depend on the number of families of  $\nu_R$ 's that we wish to consider. In the following we will assume that we have three  $\nu_R'$ 's, as that is the minimum number needed to give Dirac masses to the three light  $\nu_L'$  families. With this assumption, the Yukawa couplings  $Y_e$  and  $Y_\nu$  will be completely general  $3 \times 3$  matrices in flavour space;  $M$ ,  $\chi$ , and  $\xi$  are complex symmetric  $3 \times 3$  matrices, while  $\zeta$  is a complex antisymmetric matrix that will ultimately provide magnetic moments for the  $\nu_R$ 's. Without loss of generality,  $Y_e$  and  $M$  can be taken diagonal with real, positive elements.

The term involving  $M$  is the usual right-handed neutrino Majorana mass. The term involving  $\chi$  is known as the Weinberg operator and provides a Majorana mass for the left-handed neutrino fields plus various lepton-number-violating neutrino-Higgs interactions, see section 3.1.1. The term involving  $\zeta$  has been mostly ignored in the literature; it describes electroweak<sup>1</sup> moment couplings for the right-handed neutrinos.

<sup>1</sup> Note that although we stress the generation of magnetic moments, i.e., couplings



We will dedicate a significant part of this chapter to the study of some of the consequences this operator might have on various collider, astrophysical and cosmological observables. Note that Dirac-type neutrino magnetic moments (involving  $\ell_L$  and  $\nu_R'$ ) are generated by operators of dimension  $\geq 6$ , while Majorana-type magnetic moments for left-handed neutrinos (involving only  $\ell_L$ ) require operators of dimension  $\geq 7$ . One can easily see that these effects are subdominant when compared to those produced by the term containing  $\zeta$  in  $\mathcal{L}_5$ .

The couplings  $\chi$ ,  $\xi$ ,  $\zeta$  have dimension of inverse mass, which is associated with the scale of the heavy physics responsible for the corresponding operator. Though we will refer to this scale generically as  $\Lambda$  it must be kept in mind that different types of new physics can be responsible for the various dimension-five operators, and that the corresponding values of  $\Lambda$  might be very different. All these scales, of course, share that they must be much larger than the electroweak scale,  $v \sim 0.25$  TeV, by consistency of the effective-theory approach. In the next section we discuss the possible types of new physics that can generate these operators and the natural size for the corresponding coefficients.

## 4.2 *Heavy physics content of the effective vertices*

In this section we will give a brief account of the combinations of heavy particles that can provide the dimension-five interactions; for each operator we will describe the fields that mediate its generation at the lowest possible order in perturbation theory, and we estimate the size of the effective coupling.

---

to photons, the effective operator actually involves the  $B$  field, and consequently it will generate couplings to both  $A$  and  $Z$  after EWSB. The  $Z$ -moments are suppressed at low energies, but become important as one approaches energies of  $\mathcal{O}(m_Z)$ ; they will thus play a role in collider experiments and cosmological scenarios, as we discuss in the corresponding sections.

$\nu'_L$  Majorana mass term

Using appropriate Fierz transformations we can rewrite the Weinberg operator in (4.3) as follows:

$$\left(\overline{\ell_{L\alpha}}\phi\right)\left(\tilde{\phi}^\dagger\ell_{L\beta}\right)=\frac{1}{2}\left(\overline{\ell_{L\alpha}}\vec{\sigma}\ell_{L\beta}\right)\cdot\left(\tilde{\phi}^\dagger\vec{\sigma}\phi\right)=-\left(\overline{\ell_{L\alpha}}\vec{\sigma}\phi\right)\cdot\left(\tilde{\phi}^\dagger\vec{\sigma}\ell_{L\beta}\right),$$

where  $\alpha$  and  $\beta$  are family indices and  $\vec{\sigma}\equiv(\sigma_1,\sigma_2,\sigma_3)$  is a vector in the adjoint representation of  $SU(2)$  whose components are the  $2\times 2$  Pauli matrices. From these rearrangements we can read the three different processes that generate the operator at tree-level: in the first, a heavy fermion singlet with no hypercharge connects the two  $SU(2)$ -closed pairs; in the second, a hyperchargeless scalar triplet is the mediator; in the third it is a fermion  $SU(2)$  triplet, again with no hypercharge. Of course these are the new physics additions that characterise seesaws of type I, II and III, as we discussed in more detail in section 3.3. If perturbation theory holds for the new physics the effective coupling should read, roughly,

$$\chi\sim\frac{\lambda^2}{\Lambda},\tag{4.4}$$

where  $\Lambda$  in this simple tree-level case denotes the mass of the heavy particle, and  $\lambda$  the coupling constants of the heavy fermions to  $\phi\ell$ , or of the heavy scalar to  $\phi\phi$  and  $\ell\ell$ .

 $\nu'_R$  Majorana mass term

The operator  $\left(\phi^\dagger\phi\right)\overline{\nu'_{R\alpha}{}^c}\nu'_{R\beta}$  can also be generated at tree level. By an argument similar to that in the previous section, the low-energy fields can be grouped into  $\phi\nu_R$  pairs or in a  $\phi^\dagger\phi$  and a  $\nu_R\nu_R$  pair. The first groups can be connected through a heavy fermion isodoublet of hypercharge  $+1/2$ ; the second, via a hyperchargeless scalar singlet. And like in the previous section, if the new physics is perturbative we expect

$$\xi\sim\frac{\lambda^2}{\Lambda},\tag{4.5}$$

where  $\Lambda$  again denotes the mass of the heavy particles, and  $\lambda$  the coupling of the heavy fermion to  $\phi\nu_R$  or the heavy scalar to  $\phi^\dagger\phi$  and  $\nu_R\nu_R$ .

$\nu'_R$  electroweak coupling

The electroweak moment operator, unlike the previous cases, cannot be generated at tree level. The reason is not difficult to grasp; being its form

$$\mathcal{L}_\zeta = \overline{\nu'_{R\alpha}} \sigma^{\mu\nu} \nu'_{R\beta} B_{\mu\nu},$$

it is clear that a charged internal leg is needed in order to insert the  $B$  boson, as the  $\nu'_R$ 's are hyperchargeless. But if the  $\nu'_R$ 's are to be connected to charged particles there must be more than one of them so that their hypercharges cancel. In consequence, the topology of the generating diagram must include a loop of charged particles that closes to yield the external hyperchargeless legs. At the lowest order, that is, at one loop, this can be realised by two different combinations of fields: first, via a scalar-fermion pair  $\{\omega, E\}$  which have opposite, nonzero hypercharges *and* present both interactions  $\omega \overline{E} \nu'_R$  and  $\omega \overline{E} \nu'^c_R$ . Alternatively, the loop can also be provided by a vector-fermion pair  $\{W'_\mu, E\}$ , again with opposite and nonzero hypercharges and again having couplings  $W'_\mu \overline{E} \gamma^\mu \nu'_R$  and  $W'_\mu \overline{E} \gamma^\mu \nu'^c_R$ .

In this class of models we will have, roughly,

$$\zeta \sim \frac{g'y\lambda^2}{16\pi^2} \frac{m_{\text{fermion}}}{\max(m_{\text{fermion}}^2, m_{\text{boson}}^2)} < \frac{g'y\lambda^2}{16\pi^2 m_{\text{fermion}}}, \quad (4.6)$$

where  $\lambda$  denotes the coupling of the two heavy particles to the  $\nu'_R$ , and  $y$  the hypercharge of the heavy boson or fermion. A specific example is provided in chapter 5.

*Perturbativity of the heavy particle couplings*

The reader should note that the estimates (4.4–4.6) rely on the assumption that the heavy physics is connected to the low-energy fields through weak, perturbative interactions. Were this not the case, we would have no reliable way to guess the values of the effective couplings, but we could still obtain estimates of their *natural* values through naive dimensional analysis (NDA) [173, 174]; this would yield

$$\chi, \xi \sim \frac{16\pi^2}{\Lambda} \qquad \zeta \sim \frac{1}{\Lambda}, \quad (4.7)$$

where  $\Lambda$  would be, in this case, the scale of the strong interactions. However, a number of caveats apply even to these naturality estimates: (4.7) assumes that *all* the fields, including the low-energy  $\phi$ ,  $\ell_L$  and  $\nu_R$ , participate in the strong interactions. Mixed scenarios, for instance with the new particles having indeed nonperturbative couplings but being connected to the low-energy fields by weak interactions, could be more complicated. Anyway, it can be useful to have in mind estimates such as (4.7) in order to weigh the influence of possible nonperturbative scenarios. For practical purposes, in the remaining of this chapter we will ignore these details and will label as “ $\Lambda$ ” just the inverse of the effective coupling; as we will discuss extensively the electroweak moment interaction, most of the time it will be understood that

$$\Lambda \equiv \frac{1}{\zeta},$$

but when it has to be interpreted otherwise we will explicitly indicate so. Note that this choice implies that  $\Lambda$  will have an immediate translation in terms of “regime of strong interactions of the heavy particles”; if the reader wants to recover the values associated to a weakly-coupled theory it will be enough to substitute  $\Lambda \rightarrow 16\pi^2 \Lambda$ , as can be seen from equations (4.6) and (4.7).

### 4.3 The Lagrangian in terms of mass eigenfields

In this section we will consider the possible mass structures of the neutrino sector, and we will discuss the changes that allow to express the Lagrangian in terms of the fields with well-definite mass. For the representative case of three very light neutrinos, mostly  $\nu_L'$ 's, and three relatively heavy ones, essentially  $\nu_R'$ 's, we present the effective interactions of our interest in terms of the mass eigenfields.

The first step in this program is to construct the neutrino mass matrix and identify the degrees of freedom with definite mass. From equations (4.1–4.3) it is straightforward to obtain the neutrino and charged lepton mass matrices after SSB. Replacing  $\phi \rightarrow \langle \phi \rangle = v/\sqrt{2} (0, 1)^T$  yields the following mass terms for the leptons

$$\mathcal{L}_m = -\bar{e}_L M_e e_R - \bar{\nu}_L' M_D \nu_R' - \frac{1}{2} \bar{\nu}_L'^c M_L \nu_L' - \frac{1}{2} \bar{\nu}_R'^c M_R \nu_R' + \text{H.c.}, \quad (4.8)$$

where

$$\begin{aligned} M_e &= \frac{v}{\sqrt{2}} Y_e & M_D &= \frac{v}{\sqrt{2}} Y_\nu \\ M_L &= \chi v^2 & M_R &= M + \xi v^2. \end{aligned}$$

It is worth noticing that, up to possible coupling-constant factors,  $M_D \sim v$  while  $M_L \sim v^2/\Lambda$ . Various situations arise depending on the hierarchy between  $M_R$ ,  $M_D$  and  $M_L$ : if we have  $M_R \gg M_D \gg M_L$  the theory describes a standard type I seesaw; seesaws of types II and III would be indistinguishable in our dimension-five Lagrangian, but would leave a footprint of the form  $M_L \gg M_D^2/M_R$  – but beware, many other underlying models could leave the same mark. In these seesaw-like cases there is no conserved or approximately conserved fermion number and the mass eigenstates are Majorana fermions. In contrast, when  $M_D \gg M_R, M_L$  there is an approximately conserved fermion number and the mass eigenstates will be Dirac fermions up to small admixtures – the so-called pseudo-Dirac fermions. Of course, the details of the mass matrix diagonalisation vary tremendously from one scenario to another. Throughout this chapter we will take as an example case the seesaw scenario,  $M_R \gg M_D \gg M_L$ , which can accommodate rather easily our current phenomenological knowledge. In the following we proceed to describe the diagonalisation procedure and the mass eigenstates in this scenario.

First of all, note that, as corresponds to a type I seesaw, when  $M_R \gg M_D \gg M_L$  the neutrino sector splits into two groups: the light neutrinos, which are primarily  $\nu_L'$ 's, and the heavy ones, which are composed mainly of  $\nu_R'$ 's. In such a case the mass matrices can be approximately diagonalised blockwise, leading to two  $3 \times 3$  Majorana mass matrices,

$$\begin{aligned} \text{heavy : } & \mathcal{M}_N \simeq M_R \\ \text{light : } & \mathcal{M}_\nu \simeq M_L - M_D^* M_R^\dagger{}^{-1} M_D^\dagger. \end{aligned}$$

These matrices can subsequently be diagonalised by using unitary

matrices  $U_N$  and  $U_\nu$ , such that

$$\begin{aligned} M_N &\equiv U_N^T \mathcal{M}_N U_N \\ M_\nu &\equiv U_\nu^T \mathcal{M}_\nu U_\nu, \end{aligned}$$

where  $M_N$  and  $M_\nu$  are diagonal matrices with positive elements (if one chooses the  $\nu'_R$  basis so that  $M_R \simeq \mathcal{M}_N$  is diagonal then we have the further simplification that  $U_N = \mathbb{1}$ ). This way the mass Lagrangian (4.8) can be rewritten in terms of mass eigenfields as

$$\mathcal{L}_m = -\bar{e} M_e e - \frac{1}{2} \bar{\nu} M_\nu \nu - \frac{1}{2} \bar{N} M_N N, \quad (4.9)$$

where  $\nu$  and  $N$  are Majorana fields ( $\nu^c = \nu$  and  $N^c = N$ ) that represent, respectively, the light and heavy mass eigenstates, and we assumed that the charged leptons are defined as the fields that diagonalise  $Y_e$ . This is enough to express the ‘‘flavour’’ spectrum of  $\nu'_L$ ’s and  $\nu'_R$ ’s in terms of the mass spectrum of  $\nu$ ’s and  $N$ ’s:

$$\nu'_L = P_L (U_\nu \nu + \varepsilon U_N N + \dots) \quad (4.10)$$

$$\nu'_R = P_R (U_N N - \varepsilon^T U_\nu \nu + \dots), \quad (4.11)$$

where  $P_{L,R} = \frac{1}{2}(\mathbb{1} \mp \gamma_5)$  are the usual chiral projectors, and

$$\varepsilon \simeq M_D M_R^{-1}$$

is a  $3 \times 3$  matrix that characterises the mixing between heavy and light neutrinos. Note that barring cancellations in  $\mathcal{M}_\nu$ , the elements of the mixing matrix  $\varepsilon$  obey in most cases, even when the light masses are not given by the seesaw mechanism, that

$$|\varepsilon_{\alpha\beta}| \lesssim \sqrt{\frac{m_\nu}{m_N}},$$

where  $m_\nu$  represents a mass of the order of the light neutrino masses and  $m_N$  a mass of the order of the heavy neutrino masses. This is due to the fact that even when the seesaw is not the generating

mechanism for the light neutrino masses we need to ensure that seesaw-like pieces don't spoil the mass structure – that is, with too large contributions. Therefore, the mixing is required to be at the level of  $\sqrt{m_\nu/m_N}$  (the seesaw mixing) or below. The only scenario that allows for large  $\varepsilon$  is one where the right-handed degrees of freedom have very light masses, of the order of the eV or below; but this scenario is very constrained phenomenologically and does not seem very appealing – see the discussion in sections 4.4.3 and 4.5.1.

Now we can use these expressions to write the effective operators in equation (4.3) in terms of the mass eigenfields; this will be of use when computing the amplitudes for processes in which the masses are a relevant element. Substituting equation (4.11) into the electroweak moment operator in (4.3) and using the well-know expression for  $B$  in terms of the photon and the  $Z$  fields, we obtain the magnetic and  $Z$  moments in terms of the mass eigenfields:

$$\begin{aligned} \mathcal{L}_\zeta = & \left( \bar{N} U_N^\dagger - \bar{\nu} U_\nu^\dagger \varepsilon^* \right) \sigma^{\mu\nu} \left( \zeta P_R + \zeta^\dagger P_L \right) \times \\ & \times \left( U_N N - \varepsilon^T U_\nu \nu \right) \left( c_W F_{\mu\nu} - s_W Z_{\mu\nu} \right), \end{aligned} \quad (4.12)$$

where  $F_{\mu\nu}$  and  $Z_{\mu\nu}$  are the Abelian field strengths of the photon and the  $Z$ , and  $c_W \equiv \cos \theta_W$ ,  $s_W \equiv \sin \theta_W$ , with  $\theta_W$  the weak mixing angle. We see that the original  $\nu'_R$  electroweak moment operator generates a variety of couplings when expressed in terms of mass eigenstates: both magnetic and  $Z$ -moments appear, and they connect either heavy-heavy, light-heavy or light-light degrees of freedom with increasing suppression. Note also that, as  $\zeta$  is an antisymmetric matrix in flavour space, *all* the moments generated by  $\mathcal{L}_\zeta$  are *transition* moments, even those linking heavy-heavy and light-light fields.

Similarly, if we use equation (4.11) to substitute in the last term of (4.3), we obtain, in addition to a contribution to the  $N$  mass, a Higgs-heavy neutrino interaction:

$$\mathcal{L}_\xi = -v H \bar{N} \left( \xi P_R + \xi^\dagger P_L \right) N + \dots, \quad (4.13)$$

where we took  $U_N = \mathbb{1}$  and the dots represent other interactions generated by this operator:  $HHNN$  vertices, for instance, as well as  $N - \nu$  and  $\nu - \nu$  interactions that are suppressed by the mixing  $\varepsilon$ ;

these vertices are also generated by the neutrino Yukawa coupling in  $\mathcal{L}_{\nu_R}$ , where they're likewise suppressed.

Finally we should mention that when equation (4.10) is introduced into the SM weak interactions  $\bar{\nu}'_L \gamma^\mu \nu'_L Z_\mu$  and  $\bar{e}_L \gamma^\mu \nu'_L W_\mu$ , one obtains  $N - \nu - Z$  and  $N - e - W$  couplings that, although suppressed by  $\varepsilon$ , are important for the decays of the lightest of the heavy neutrinos.

## 4.4 Collider effects

### 4.4.1 General considerations

In this section we discuss the variety of effects that the dimension-five operators can yield in a collider experiment. A first estimation of the importance of such effects can be made as a result of the nonobservation of new particles in LEP-II, Tevatron and the LHC [32]: as the present bound is essentially  $m_{\text{NP}} > 100$  GeV or better for most classes of particles, we can infer that the effective operators have at least  $\Lambda > 100$  GeV. However, the bound affects differently the various effective interactions, and the perturbativity or not of the heavy physics couplings can be an important factor. For instance, for the electroweak moments a weakly-coupled new physics would imply  $\Lambda = 1/\zeta \sim (4\pi)^2 m_{\text{NP}}$ , as seen in equation (4.6), and so  $\Lambda > 15$  TeV; this would most likely suppress its effects beyond our present and near-future experimental sensitivities. A strongly-coupled scenario, though more difficult to study theoretically, might significantly lower the scales of the new interactions, putting them at the reach of the LHC or the future linear collider; in fact, if we have merely  $\zeta = 1/m_{\text{NP}}$  the effects of this interaction would have been observable at LEP, as we consider later in section 4.4.3. In conclusion, a scenario with nonperturbative new physics optimises the possibility of observing the effective interactions in colliders; weakly-coupled new particles are not discarded, but in general direct searches seem a more efficient way to probe their existence.

Apart from the new physics responsible for the effective interaction, our theory considers a number of new fermionic, neutral degrees of freedom associated to the  $\nu'_R$ . Our discussion below essentially focuses on



their production and observability in colliders, which can be achieved either through mixing with the left-handed species or through the effective interactions. It is reasonable then to ask which is the relevant mechanism for their collider phenomenology: would a positive experimental signal be probing just mixing or the new effective interactions? We can easily argue that in most cases it is the effective interactions who are in charge of the collider effects: as we discussed in section 4.3, if the new fermions are heavy the heavy-light mixing is  $\varepsilon \lesssim \sqrt{m_\nu/m_N}$ , a value too small to provide a significant production mechanism unless  $m_N$  is rather small; but even in this case astrophysical considerations (see section 4.5.1) impose very stringent bounds on any production mechanism, rendering any collider effect unobservable. Therefore, mixings can be safely ignored for most purposes in collider phenomenology; a notable exception is the decay of the neutral fermions, which is governed by the effective magnetic moments except for the lightest of the  $N$ 's. In the following section we comment thoroughly on the phenomenology of the neutral fermions' decays.

#### 4.4.2 *Decay mechanisms for the new neutral fermions*

Before discussing the impact of the new interactions in past and future collider experiments, we would like to analyse the dominant decay modes of the new neutral fermions associated to the  $\nu_R'$ 's. These fermions can potentially be produced in colliders through the electroweak moments or Higgs decays, as described in the remaining passages of this section; once produced they will decay, and the decays will provide a means to identify the relevant interactions. Let us here, so, consider such decay mechanisms in some detail. Though in principle we could have three or more right-handed neutrinos, for this discussion it will be enough to consider two of them: the lightest heavy state, that we will label  $N_1$ , and the next-to-lightest, identified as  $N_2$  – of course with  $m_1 < m_2$ . The decays of all the heavier particles will proceed as those of  $N_2$  to  $N_1$ .

The heavy neutrinos have essentially two mechanisms to decay: through mixing, involving the SM weak vertices, and through the

electroweak moment interactions<sup>2</sup>. The latter allows decays from one of the  $N$ 's to another with emission of a photon or  $Z$ , and are suppressed by the unknown new physics scale  $\Lambda$ ; the first link the heavy neutrinos to a gauge boson and a light lepton, and are in turn suppressed by the mixing  $\varepsilon$ . As these mixings are expected to be small, the electroweak moments are expected to dominate the decays of the heavier states, if they are observable at all. The  $N_1$ , however, has no heavy state to decay to, and so its decays probe the heavy-light mixing.

We begin by describing the decay modes mediated by the electroweak moments. If they are strong enough to produce the new neutral fermions<sup>3</sup>, the dominant decay channel for  $N_2$  will be  $N_2 \rightarrow N_1\gamma$ , and also  $N_2 \rightarrow N_1Z$  if  $N_2$  is heavy enough. The most prominent experimental signature of these decays should be the presence of a hard photon, which will appear if  $N_2$  is heavy enough –say,  $m_2 > 10$  GeV– and the mass splitting with  $N_1$  is large enough<sup>4</sup>. The lifetime of the heavy neutrinos will be very short if these modes are available; for instance, we find that for a  $N_2$  produced at center of mass energies ranging from 100 – 1000 GeV the associated decay lengths are well below 10 nm unless  $m_2 \simeq m_1$ . The reader can find the expressions for the decay widths collected in section 4.7 at the end of the chapter.

The decays of the lightest heavy neutrino are richer, as it decays to a variety of SM particles. As discussed above, this means that the  $N_1$  decays will always be suppressed by the mixing parameter  $\varepsilon$ , and the corresponding decay lengths will be much longer. In figure 4.1 we present the dominant decay modes of  $N_1$  for a set of typical values of the parameters. As we can see, the electroweak moments provide a channel suppressed by mixing, whose products are a light neutrino and a photon; the rest of the modes are mediated by SM vertices plus mixing. Since all the decay widths are proportional to  $\varepsilon$ , the branching ratios will depend weakly on the heavy-light mixing parameters; they

<sup>2</sup> A third option, namely  $N_2 \rightarrow N_1H$  through the  $\xi$  operator, will not be considered in this analysis.

<sup>3</sup> See sections 4.4.3 and 4.4.4 for a discussion of the production of heavy neutrinos in colliders.

<sup>4</sup> It could happen that  $N_2$  and  $N_1$  are almost perfectly degenerate; then this sort of decays will be suppressed by kinematics, and other channels to SM particles, like  $N_2 \rightarrow \nu\gamma$ , or  $N_2 \rightarrow \ell W, \nu Z, \nu H$ , although suppressed by  $\varepsilon$ , could be relevant.

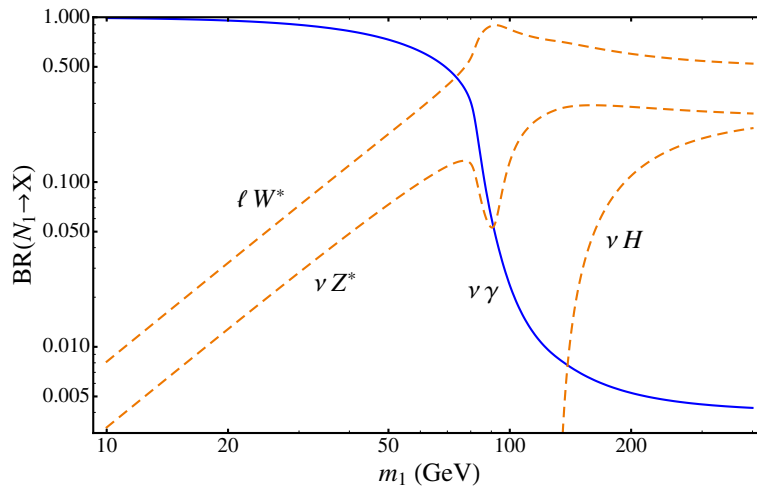


Fig. 4.1: Decay branching ratios for  $N_1$ . The solid line corresponds to the channel mediated by the magnetic moments *and* mixing,  $N_1 \rightarrow \nu\gamma$ , while the dashed lines represent the various decays to SM particles through SM vertices and mixing. For this figure we took  $\varepsilon = 10^{-6}$ ,  $\Lambda = 10$  TeV,  $m_H = 130$  GeV.

will, however, be sensitive to the strength of the new magnetic moment interaction. For light  $N_1$  masses, under the threshold of  $W$ 's and  $Z$ 's, the electroweak moments prevail over the SM modes; the magnitude of this prevaillance depends mainly on the value of  $\Lambda$ , and could serve to measure it. Note, in fact, that the decay width  $\Gamma(N_1 \rightarrow \nu\gamma)$  is suppressed by  $\Lambda^{-2}$ , while the rates to gauge bosons are not; thus, for relatively small  $\Lambda$ , say  $\Lambda \sim 1$  TeV, the mode  $N_1 \rightarrow \nu\gamma$  could also be relevant even above the threshold of production of the weak gauge bosons.

For  $m_1$  above  $m_W$  the decays are dominated by the two-body mode  $N_1 \rightarrow \ell W$  and for masses above  $m_Z$  the decay  $N_1 \rightarrow \nu Z$  is also important. If  $m_1 > m_H$ , the  $N_1$  can also decay into a physical Higgs boson; the main difference with the gauge boson channels is that the Higgs width varies tremendously along its allowed mass range; for light Higgs masses, like the one considered in figure 4.1, the width is very small and therefore virtual production is suppressed and the branching

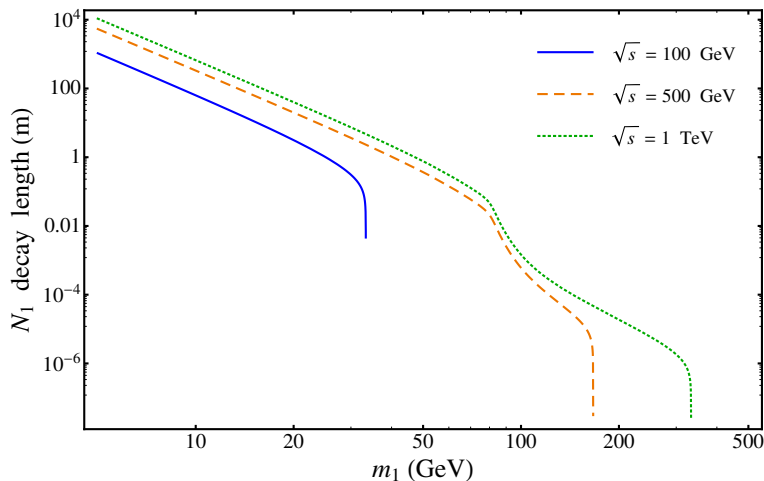


Fig. 4.2:  $N_1$  decay lengths for the case of a pair-production of  $N_1$  and  $N_2$  with several center-of-mass energies. The solid line corresponds to 100 GeV, the dashed line to 500 GeV, and the dotted one to 1 TeV. For this calculation we chose  $m_2 = 2m_1$ ,  $\Lambda = 10$  TeV and  $\varepsilon = 10^{-6}$ .

ratio drops rapidly for  $m_1 \lesssim m_H$ . Notice that for  $m_1 \gg m_H$  the decay widths  $\Gamma(N_1 \rightarrow \nu Z)$  and  $\Gamma(N_1 \rightarrow \nu H)$  converge, and equal one half of  $\Gamma(N_1 \rightarrow \ell W)$ , as required by the equivalence theorem [175, 176]; see also, for more on this, the discussion in section 4.7.

The experimental signatures of the  $N$  decays are very well-defined, but they involve photons that can be differently boosted, or single gauge bosons plus unobservable neutrinos – that is, missing energy. This means that the  $N$  detection will be affected by a significant background of SM processes. It would be nice if we had some other feature that can be easily separated from the standard background. The  $N_1$ 's may provide such a feature, for their decays are suppressed by the mixing factor  $\varepsilon$  which can be very small, and so they might decay away from the collision point and provide a displaced vertex. Such vertices have been considered as the experimental signatures of theories with long-lived neutral particles [177–179], and the same studies might be applicable to right-handed neutrinos endowed with magnetic moments.

In order to know if our theory yields such a feature, we have estimated the decay length for an  $N_1$  produced in an accelerator with present or near-future energies. The results are not conclusive, because the decay length depends on the mixing factor  $\varepsilon$ , which can vary along several orders of magnitude, and on the boost of the  $N_1$ , which in turn depends on the production mechanism and the properties of the collider in which it is produced. Besides, in order to observe a displaced vertex we need the decay length not to be very short, but we need also that the  $N_1$  decays inside the detector; this leaves an experimentally observable range between some tenths of a millimeter and several meters. In figure 4.2 we present some estimates of the  $N_1$  decay lengths as a function of its mass. Several important assumptions have been made: the  $N_1$  is produced through the electroweak moment interaction together with an  $N_2$  (remember that the electroweak moments are all of them transition moments, so they cannot produce a  $N_1$  pair); the  $N_1$  later decays into the allowed decay channels, all suppressed by  $\varepsilon$ . Decay lengths are presented as a function of the  $N_1$  mass for different values of the energy in the center-of-mass frame, and assuming  $m_2 = 2m_1$ ,  $\Lambda = 10$  TeV and  $\varepsilon = 10^{-6}$ . We observe that the decay lengths of the  $N_1$  will be very small for masses above 100 GeV. However, for masses below this value the decay lengths could range from a few millimeters to a few kilometers, depending on the  $N_1$  and the  $N_2$  masses, the heavy-light mixing, the electroweak coupling and the kinematical configuration of the experiment. In conclusion, it is possible that the  $N_1$ 's provide displaced vertices in collider experiments, but a scenario with too short or too long decay lengths is also perfectly plausible.

#### 4.4.3 *Heavy neutrinos in $e^+e^-$ colliders*

The electroweak moments provide an optimal mechanism for the production of the heavy neutrinos, as they couple to photons and  $Z$ 's; pair-production through a photon or a  $Z$  in the  $s$  channel –the so-called Drell-Yan process– has become paradigmatic for charged particles in all sorts of colliders, and thanks to the electroweak moments it would be also applicable to the chargeless heavy neutrinos. But precisely because of this, the nonobservation of heavy neutral leptons in the previous

generation of accelerators must place bounds on the strength of the electroweak interactions and the masses of the heavy neutrinos. In particular they were not observed at a  $Z$  factory such as LEP1 [180–183] and its successor LEP2 [184–186]. The most conservative bounds are obtained by assuming that all the produced neutrinos escape undetected; but remember that the electroweak moments are antisymmetric, and thus the heavy neutrinos are produced in dissimilar pairs. If an  $N_1$  is produced, it is relatively likely that it escapes, because it can only decay through heavy-light mixing and, as discussed above, the corresponding decay length could be very large. The heavier states, however, will decay rapidly into  $N_1$  and  $\gamma$ , with the energetic photon providing a potentially clear signature. For that reason, it should be possible to set bounds stronger than those that merely assume that all neutrinos escape, but these bounds would show some dependence on the neutrino spectrum – for instance, if the  $N_1$  and  $N_2$  are almost degenerate the photon could be too soft to provide a viable signal. Instead of providing an exhaustive description of all possible scenarios we will focus on the more diaphanous bound on the invisible decays of the  $Z$  boson, leaving for the end of the section a brief comment on the bounds derived from visible heavy neutrino decays.

Data from LEP has established with a remarkable precision that  $Z$ 's decay essentially to three species of invisible particles, that we identify with the three families of active neutrinos. The invisible width of the  $Z$  reads [32]

$$\Gamma_{\text{inv}} = 499.0 \pm 1.4 \text{ MeV} ,$$

whereas we can construct the standard contribution of the three active neutrinos by using the experimental  $Z$  width to charged leptons,  $\Gamma_{\ell^+\ell^-} = 83.984 \pm 0.086 \text{ MeV}$ , and the theoretical SM calculation for the corresponding widths,  $\Gamma_{\nu\bar{\nu}}^{\text{th}} / \Gamma_{\ell^+\ell^-}^{\text{th}} = 1.991 \pm 0.001$ . Then

$$\Gamma_{\nu\bar{\nu}}^{\text{SM}} = 3 \left( \frac{\Gamma_{\nu\bar{\nu}}}{\Gamma_{\ell^+\ell^-}} \right)^{\text{th}} \Gamma_{\ell^+\ell^-} = 501.6 \pm 0.6 \text{ MeV} ,$$

which is fairly compatible with the experimental result. A small room, though, remains for other contributions to the invisible width,

provided they are rare enough. If we assume that these nonstandard contributions are entirely given by decays to heavy neutrinos,  $\Gamma_{\text{inv}} = \Gamma_{\nu\bar{\nu}}^{\text{SM}} + \Gamma(Z \rightarrow N_1 N_2)$ , we have

$$\Gamma(Z \rightarrow N_1 N_2) = -2.6 \pm 1.5 \text{ MeV}. \quad (4.14)$$

But of course the width is a positive-definite quantity, and this result has to be interpreted as “ $\Gamma(Z \rightarrow N_1 N_2)$  is compatible with zero”. The question then is how large can  $\Gamma(Z \rightarrow N_1 N_2)$  be, given the statistical significance of (4.14). We calculate this value by using the Feldman & Cousins prescription [187] and obtain

$$\Gamma(Z \rightarrow N_1 N_2) < 0.72 \text{ MeV} \quad 95\% \text{ CL}$$

Now, if we look at the theoretical expression for  $\Gamma(Z \rightarrow N_1 N_2)$ , given in section 4.7, we deduce

$$\Lambda = \frac{1}{|\zeta_{12}|} > 7 \sqrt{f_Z(m_Z, m_1, m_2)} \text{ TeV},$$

where  $f_Z(m_Z, m_1, m_2)$  is a phase space factor defined in equation (4.15) and normalised in such a way that  $f_Z(m_Z, 0, 0) = 1$ . For example,  $\Lambda > 1.9 \text{ TeV}$  if  $m_1 = m_2 = 35 \text{ GeV}$ .

If the right-handed neutrino electroweak moment is large enough to allow significant production of  $N_1, N_2$  pairs at LEP energies, the dominant decay of  $N_2$  will be also mediated by the electroweak moments,  $N_2 \rightarrow N_1 \gamma$ , unless the mass of  $N_1$  is very close to that of  $N_2$ . Then, the resulting photons could be detected and separated from the background if  $E_\gamma > 10 \text{ GeV}$ . In fact, searches for this type of processes –note that some searches for excited neutrinos probe exactly this sort of signal– have been conducted at LEP1 [180–182, 188] and at LEP2 [184–186]. If the mass of the heavy neutrino is  $\lesssim 90 \text{ GeV}$ , one typically obtains upper bounds on the production branching ratio,  $BR(Z \rightarrow N_1 N_2)$ , of the order of  $2 - 8 \times 10^{-6}$  [180, 188] depending on the masses of  $N_1$  and  $N_2$ . These bounds usually rely on several assumptions on the properties and spectrum of the heavy neutrinos; for instance, the limit we just quoted for the branching ratio assumes that  $BR(N_2 \rightarrow N_1 \gamma) = 1$  and that  $m_2 > 5 \text{ GeV}$ . But this procedure allows

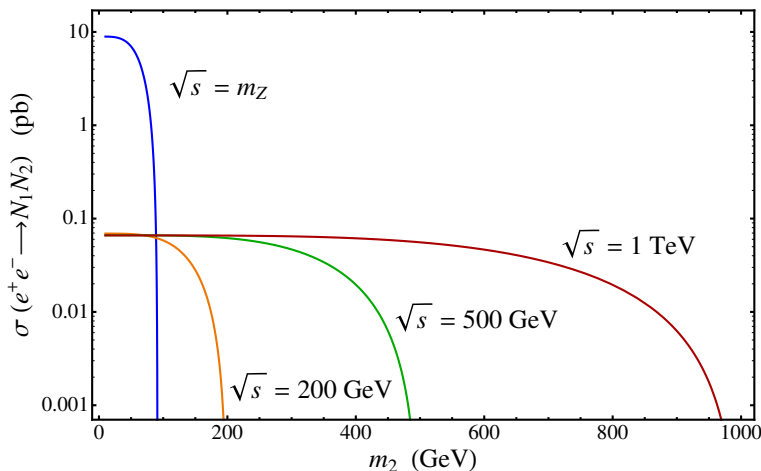


Fig. 4.3:  $e^+e^- \rightarrow N_1N_2$  as a function of the heavy neutrino mass,  $m_2$ , for different center-of-mass energies. For producing this plot we took  $m_1 = 0$  and  $\Lambda = 10$  TeV.

to set much stronger bounds. For instance, assuming that  $m_1 = 0$  and  $m_2$  is relatively light,  $10 \text{ GeV} < m_2 < m_Z$ , we can use the conservative limit  $BR(Z \rightarrow N_1N_2) < 8 \times 10^{-6}$  to obtain  $\Lambda > 40$  TeV. Data from LEP2 can also be used to place limits on the couplings for masses up to 200 GeV [184–186]. For typical values of  $m_1, m_2$  one can set upper bounds on the production cross section of the order of 0.1 pb (this number calculated for  $\sqrt{s} = 207$  GeV), which translate into bounds on  $\Lambda$  of the order of a few TeV. In general these bounds depend strongly on the spectrum of  $N_1$  and  $N_2$  –for instance, they are completely lost if  $m_2 - m_1 \lesssim 10$  GeV–, but they could be important if some signal of this type is seen at the LHC.

Finally, it is a straightforward calculation to obtain the production cross section of the heavy neutrinos in a  $e^+e^-$  collider. We show it in section 4.7, and in figure 4.3 we plot it as a function of  $m_2$  for the center-of-mass energies of LEP1 and LEP2. We also included results for  $\sqrt{s} = 500$  GeV and  $\sqrt{s} = 1000$  TeV, in view of the proposals for future  $e^+e^-$  colliders like the International Linear Collider (ILC). We see that, except for collisions at the  $Z$  peak, which are enhanced by about two orders of magnitude, or close to the threshold of production, which are



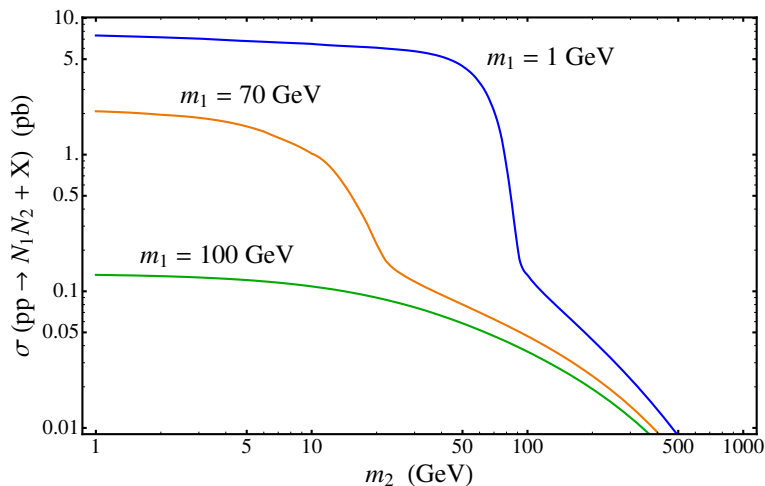


Fig. 4.4:  $pp \rightarrow N_1 N_2 + X$  cross section at the LHC as a function of the mass of  $N_2$  assuming the nominal center-of-mass energy of  $\sqrt{s} = 14$  TeV. For this plot we chose  $\Lambda = 10$  TeV and drew three curves for a few representative values of the mass of  $N_1$ .

suppressed by phase space, the cross sections are quite independent of the center-of-mass energy and are determined essentially by the magnitude of the electroweak moments; for the example value of  $\Lambda = 10$  TeV the cross sections are of the order of 0.1 pb.

#### 4.4.4 Neutral heavy lepton production at the LHC

The right-handed electroweak moment can mediate the production of the heavy neutrinos at hadron colliders. In particular, at the LHC the main production mechanism will be the Drell-Yan mechanism, that is, through an  $s$ -channel  $Z$  or photon. The differential cross section for proton-proton collisions can be computed in terms of the partonic

cross sections as follows<sup>5</sup>:

$$\begin{aligned} d\sigma(pp \rightarrow N_1 N_2 + X) = \sum_q \int_0^1 dx_1 \int_0^1 dx_2 & \left( f_q(x_1, \hat{s}) f_{\bar{q}}(x_2, \hat{s}) + \right. \\ & \left. + (q \leftrightarrow \bar{q}) \right) d\hat{\sigma}(q\bar{q} \rightarrow N_1 N_2, \hat{s}), \end{aligned}$$

where  $\hat{s} = x_1 x_2 s$  is the invariant mass in the partonic center-of-mass reference frame,  $\hat{\sigma}$  is the partonic cross section, and  $f_q(x_1, \hat{s})$ ,  $f_{\bar{q}}(x_2, \hat{s})$  are the parton distribution functions for the proton. Using the partonic cross sections given in section 4.7 and performing the convolution over the parton distribution functions<sup>6</sup> we find the total cross section as a function of the heavy neutrino masses, as displayed in figure 4.4. The cross section depends on the masses and the coupling  $\zeta_{12} = 1/\Lambda$ . In figure 4.4 we represent the total cross section in terms of  $m_2$  and offer several curves for representative values of  $m_1$ . The main conclusion is that large cross sections can be obtained, but mainly for  $m_1 + m_2 \lesssim m_Z$ , where the LEP bound applies. The reason for this enhancement is precisely that for light masses the heavy neutrino pairs can be produced in the decay of a real  $Z$ , whose resonant production dominates the Drell-Yan process. But since the decay  $Z \rightarrow N_1 N_2$  has not been observed at LEP, it seems unlikely that we can observe such enhanced production of heavy neutrinos at the LHC. For larger masses the cross section decreases rapidly, down to still observable but less favourable levels.

Finally, in figure 4.5 we present the differential cross section for the process  $pp \rightarrow N_1 N_2 + X$  for different sets of heavy neutrino masses. For  $m_1 + m_2 \lesssim m_Z$  we observe a peak in transverse momentum for the pairs produced through an on-shell  $Z$ .

#### 4.4.5 Higgs decays into heavy neutrinos

In our discussion of the dimension-five Lagrangian we are focusing mainly on the right-handed neutrino electroweak moments, which are

<sup>5</sup> See [189] for a very clear review on the matter.

<sup>6</sup> We used, in particular, the CTEQ6M parton distribution sets [190], and checked our results against the CompHEP software [191, 192].

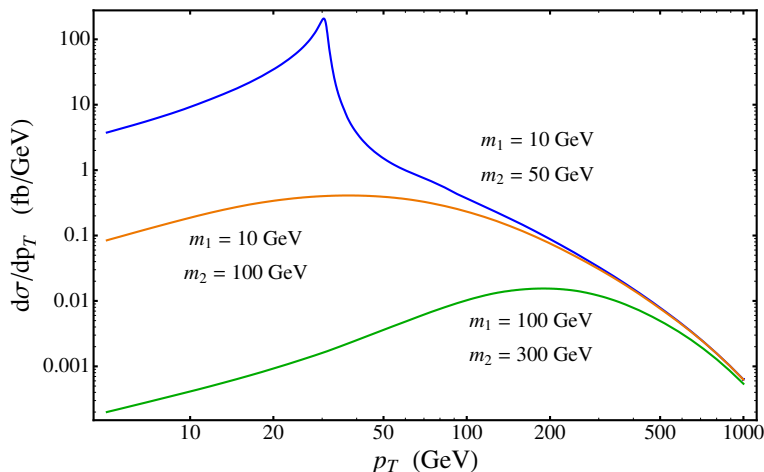


Fig. 4.5: Transverse momentum distribution of the process  $pp \rightarrow N_1 N_2 + X$  for different sets of heavy neutrino masses. When the sum of the masses allows for it, the production process is dominated by a resonant intermediate state with a real  $Z$  which shows up as a peak roughly at  $p_T^{\text{res}} = m_Z - m_1 - m_2$ .

phenomenologically richer than the other two operators. However, there is one scenario in which the effective Majorana mass for the  $\nu'_R$  becomes relevant: as commented in section 4.3, the  $\xi$  operator yields interactions between the physical Higgs boson and the heavy neutrinos which could be relevant for Higgs searches at the LHC/ILC. In particular, it yields a  $HNN$  vertex that induces new additional decays of the Higgs into heavy neutrinos, if allowed by kinematics. Let us briefly discuss the possible effects of this operator.

Equation (4.13) describes the vertex that is relevant for our discussion; several other interactions, involving heavy-light or light-light pairs of neutrinos have been omitted, as they are suppressed by the heavy-light mixing, which is expected to be small. As a first approach we will ignore also here those interactions and will focus on the heavy-heavy vertex, parametrised just by the effective coupling  $\xi$ . From (4.13) we compute the decay width of the Higgs boson into two heavy neutrinos, see equation (4.20). Then we can compare with the usual

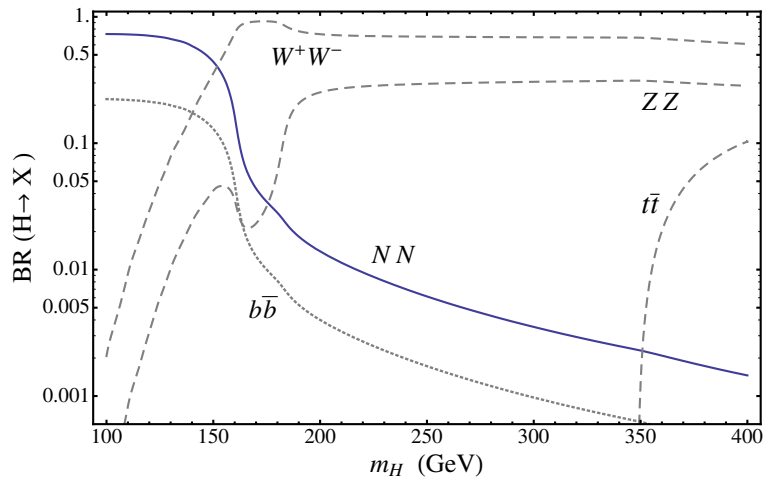


Fig. 4.6: Estimated branching ratios for Higgs decays with a new physics scale of  $1/\xi = 10$  TeV. The solid line corresponds to the new channel to heavy neutrinos, which dominates below the  $WW$  threshold; the usual SM channels are indicated as dashed lines, except for the  $b\bar{b}$  channel, which is displayed as a dotted line. For this calculation we have neglected the masses of the heavy neutrinos with respect to the Higgs boson mass.

SM decay rates of the Higgs boson; in figure 4.6 we represent the decay branching ratios into the different channels for a new physics scale of  $\Lambda \equiv 1/\xi = 10$  TeV, and neglecting the masses of the heavy neutrinos respect to the mass of the Higgs boson. Notice that, as this interaction can be generated at tree level,  $\Lambda$  can be identified roughly with the masses of the new particles that generate the operator – see equation (4.5), but remember that it relies on the new physics being perturbative, and the couplings  $\lambda$  might be small.

Looking at figure 4.6 we see that if  $m_H$  lies below the  $WW$  threshold the heavy neutrinos can dominate the decays of the Higgs. In fact, for low enough  $\Lambda$  these decays could be significant even when the  $WW$  and  $ZZ$  channels are open. This has an immediate consequence: if the heavy neutrinos escape undetected, the detection of the Higgs boson becomes a challenge; other important modes, such as  $H \rightarrow \gamma\gamma$ , become additionally suppressed, and this might even lead to an “invisible Higgs”

scenario [193, 194]. However, the effect of this new interaction needs not be troublesome; once produced, the  $N$ 's have to decay. If the magnetic moment interaction of right-handed neutrinos is also present the heaviest neutrinos can decay into lighter ones and photons, and those photons could be detected. Moreover, the lightest of the heavy neutrinos will decay into light neutrinos and photons. As discussed in section 4.4.2, this is suppressed by the heavy-light mixing, therefore the  $N_1$  could be rather long-lived and produce non-pointing photons which could be detected. If the magnetic moment interaction is not present, the heavy neutrinos will have three-body decays of the type  $N_1 \rightarrow W^*\nu$  or  $N_1 \rightarrow Z^*\nu$ , suppressed by the heavy-light mixing, as well as a one-loop-suppressed  $N_1 \rightarrow \nu\gamma$  decay.

In conclusion, the introduction of the  $\xi$  operator opens new possibilities for the phenomenology of the Higgs boson that can be explored in the near future at the LHC, though the recent discovery of the Higgs boson [33, 34] and the first measurements of its decay branching ratios [195, 196] seem to disfavour that the exotic couplings play a prominent role.

## 4.5 *Astrophysical and cosmological considerations*

In this section we consider several astrophysical and cosmological systems and processes that may be affected by the presence of an extra magnetic coupling of the neutrinos. The potential number is of course vast; we don't pretend here to exhaust the possibilities, but rather we present some of the most interesting scenarios in which the magnetic moment can play a role.

### 4.5.1 *Astrophysical effects*

Among the various astrophysical processes that are affected by neutrino magnetic couplings, the cooling of red giant stars plays a prominent role because it provides a very tight bound on the magnitude of the magnetic moments – provided the masses of the neutrinos involved are sufficiently small. This limit is based on the observation that photons in a plasma acquire a temperature-dependent mass, being then referred

to as *plasmons* ( $\gamma_P$ ); any electromagnetic neutrino coupling will then open a decay channel for the plasmon into a neutrino pair, unless kinematically forbidden. If produced, the neutrinos leave fast the star, resulting in an additional cooling mechanism that is very sensitive to the size of the magnetic moment [168, 197–202]; this can be used to impose a stringent upper limit on this moment.

The electroweak moment affects in principle only the right-handed degrees of freedom; this translates into a preferential coupling to the heavy neutrinos, as we described in section 4.3. From equation (4.12), and taking already  $U_N = \mathbb{1}$ , we write the magnetic coupling to the heavy species as

$$\mathcal{L}_{\zeta\text{-heavy}} = c_W \bar{N} \sigma^{\mu\nu} (\zeta P_R + \zeta^\dagger P_L) N F_{\mu\nu}.$$

In a nonrelativistic nondegenerate plasma the emissivity of neutrinos is dominated by transverse plasmons [48], which have an effective mass equal to the plasma frequency,  $m_P = \omega_P$ . A calculation [48] shows that the decay width of these plasmons into two neutrino species with definite mass, labeled by  $i$  and  $j$  and satisfying  $m_i + m_j < m_P$ , is

$$\Gamma(\gamma_P \rightarrow N_i N_j) = \frac{2c_W^2}{3\pi} \frac{m_P^4}{\omega} |\zeta_{ij}|^2 f_Z(m_P, m_i, m_j),$$

where  $\omega$  is the plasmon energy in the plasma rest frame, and  $f_Z$  has been defined in equation (4.15). The total decay rate is then

$$\Gamma(\gamma_P \rightarrow NN) = \frac{\mu_{\text{eff}}^2}{24\pi} \frac{m_P^4}{\omega},$$

$$\mu_{\text{eff}}^2 = 16c_W^2 \sum_{\text{all}} |\zeta_{ij}|^2 f_Z(m_P, m_i, m_j),$$

where the sum runs over all allowed channels, with  $i > j$  and such that  $m_i + m_j < m_P$ . The observational limits from red giant cooling then imply [48]

$$\mu_{\text{eff}} < 3 \times 10^{-12} \mu_B,$$

where  $\mu_B$  is the Bohr magneton. This translates into a bound on the couplings  $\zeta_{ij}$  *provided* the sum of the associated neutrino masses lies

below  $m_P$ ; for instance, for  $\zeta_{ij}$  real and assuming  $m_i, m_j \ll m_P \simeq 8.6$  keV we have

$$|\zeta_{ij}| < 8.5 \times 10^{-13} \mu_B \quad \iff \quad \Lambda > 4 \times 10^6 \text{ TeV} .$$

This bound is somewhat degraded when the neutrino masses are comparable to  $m_P$ .

This far we have just considered the plasmon decay into the heavy species of neutrino (those which are primarily  $\nu_R'$ ); it is clear from equation (4.12) that the plasmon can also decay into  $N$ - $\nu$  and  $\nu$ - $\nu$  pairs, but with the amplitude suppressed by  $\varepsilon$  and  $\varepsilon^2$ , respectively, which are small numbers unless the  $N$ 's are very light (see the discussion in section 4.3). But this case,  $m_N \sim m_\nu$ , is already covered by our discussion above and the ‘mixed’ vertices offer no new insight. Another option is to consider the case in which the plasmon decay to  $N$ 's is kinematically forbidden,  $m_N > m_P \sim 10$  keV, and then set bounds on the process  $\gamma_P \rightarrow \nu\nu$  that proceeds through mixing; the bound depends in that case on  $m_N$ , and is generally weak. For instance, taking  $\varepsilon$  at its maximum,  $\varepsilon^2 \sim m_\nu/m_N$ , and  $m_N$  at its minimum,  $m_N = 10$  keV, the bound reduces to just  $\Lambda > 40$  TeV for a large value of the light mass,  $m_\nu = 0.1$  eV. With  $m_N$  around several hundreds of keV's the bound drops already below the TeV.

The same line of reasoning can be applied to other astrophysical objects. This might be of interest because the corresponding plasma frequency, and thus  $m_P$ , will be larger in denser objects, and the corresponding limits will apply to heavier neutrino states. Unfortunately, the limits themselves are much poorer. As an example, we consider the case of a neutron star, whose plasma frequency in the crust is  $\omega_P \sim 1$  MeV. This could allow us to extend the magnetic moment bounds to higher neutrino masses; however, the much weaker limit,  $\mu_{\text{eff}} < 5 \times 10^{-7} \mu_B$  [203] implies  $\Lambda \gtrsim 23$  TeV when  $m_i, m_j \lesssim 1$  MeV, which is not competitive with bounds derived below from  $\gamma + \nu \rightarrow N$  in supernovae, which also apply in this range of masses. Limits derived from plasmon decays in the sun and supernovas are also not competitive [48, 204].

The neutrino electromagnetic coupling would also affect other interesting processes. For example, it generates a new supernova cooling

mechanism through  $\gamma + \nu \rightarrow N$ , when kinematically allowed, with the  $N$  escaping. Limits on this anomalous cooling [48] imply that the effective magnetic moment must lie below  $3 \times 10^{-12} \mu_B$  provided the heavy neutrino mass lies below  $\sim 30$  MeV – the order of the maximum energy of the neutrinos in the supernova core. As the process involves a  $\nu - N$  transition, the coupling is suppressed by an  $\varepsilon$  factor; this leads to a bound of the form

$$\Lambda \gtrsim 4 \times 10^6 \times \sqrt{m_\nu/m_N} \text{ TeV}$$

at its best, i.e., using the most constraining value for the mixing. Taking, for example,  $m_\nu \sim 0.1$  eV we obtain  $\Lambda > 1.5 \times 10^4$  TeV for  $m_N = 10$  keV and  $\Lambda > 390$  TeV for  $m_N = 10$  MeV. These limits are interesting in the region  $10 \text{ keV} < m_N < 30 \text{ MeV}$ , where red giant bounds do not apply.

#### 4.5.2 *The electroweak moments as a source of CP asymmetry in the early universe*

The electroweak moments are also of interest because they violate lepton number and may contribute to the baryon asymmetry of the universe. As is well known, the baryonic content of the observable universe is greatly dominated by matter, with only trace amounts of antimatter [205, 206]; Sakharov proposed in the sixties that this matter domination needs not to be an initial condition of the universe, but can be a result of the dynamics of the particle species if certain conditions are satisfied [207]. For this aim, the Standard Model seems to lack some of the necessary ingredients; in particular it cannot provide a strong enough violation of CP so to produce the observed baryon asymmetry [208–210]. The electroweak moments that we are discussing provide several new phases that are potentially CP-violating, therefore it is worth to check if they can help in this matter. As the theory presents a number of heavy neutrinos it is natural to consider a scheme of baryogenesis through leptogenesis [211, 212].

In the leptogenesis scenario<sup>7</sup> the baryon asymmetry is not generated in the quark sector, but rather it originates in the dynamics of

---

<sup>7</sup> It would go beyond the scope of this work to heartily review the intricate



leptons and then it is transferred to the baryons through certain non-perturbative electroweak processes [215]. The way in which the lepton asymmetry is first produced depends on the particular realisation of leptogenesis, but a standard mechanism is the CP-violating decays of heavy neutrinos. These processes are affected by CP-odd phases –in our case, the physical phases that appear in the electroweak moments– and by phases that do not change sign under CP transformations, these ones appearing in the one-loop diagrams of the  $N$  decay as imaginary parts of the loop integral. The interference between the two classes of phases generates in the end different rates for the two CP-conjugated channels,  $N \rightarrow \ell_L \phi$  and  $N \rightarrow \bar{\ell}_L \bar{\phi}$ , and thus a different number of leptons and antileptons. The electroweak moments do not change substantially this panorama: they just provide a new contribution to the one-loop correction, with a  $B$  gauge boson running inside the loop and  $\zeta$  delivering some of the CP-odd phases.

The relevant diagrams are presented in figure 4.7. Note that the one-loop corrections require a second heavy neutrino due to the antisymmetry of the electroweak moments; and as we need these graphs to yield an imaginary part, by the optical theorem the ‘inner’ heavy neutrino must be lighter than the outer one. This scenario is not free of problems: if  $m_1 < m_2$  then the channel  $N_2 \rightarrow N_1 \gamma$  is open, and it will in most cases dominate the decays of  $N_2$ , leaving a negligible number of CP-violating leptonic decays. The only situation in which the  $\zeta$ -mediated mechanism can be relevant is when  $N_2$  and  $N_1$  are nearly degenerate; this scenario is usually referred to as *resonant leptogenesis* [216, 217].

We now go on to calculate the lepton asymmetry emerging from the processes in figure 4.7. We will assume that  $m_N \gg v$  so that we can neglect electroweak symmetry breaking and assume that all gauge bosons, leptons and scalars are massless except for the heavy neutrinos, which have a Majorana mass term. Also, for simplicity, we neglect the Yukawa couplings of the charged leptons; as the electroweak moments provide new sources of CP violation, the Yukawas need not be an essential piece in producing a lepton asymmetry. The relevant

---

details of baryogenesis and leptogenesis. To the interested reader we recommend the good reviews [213, 214].

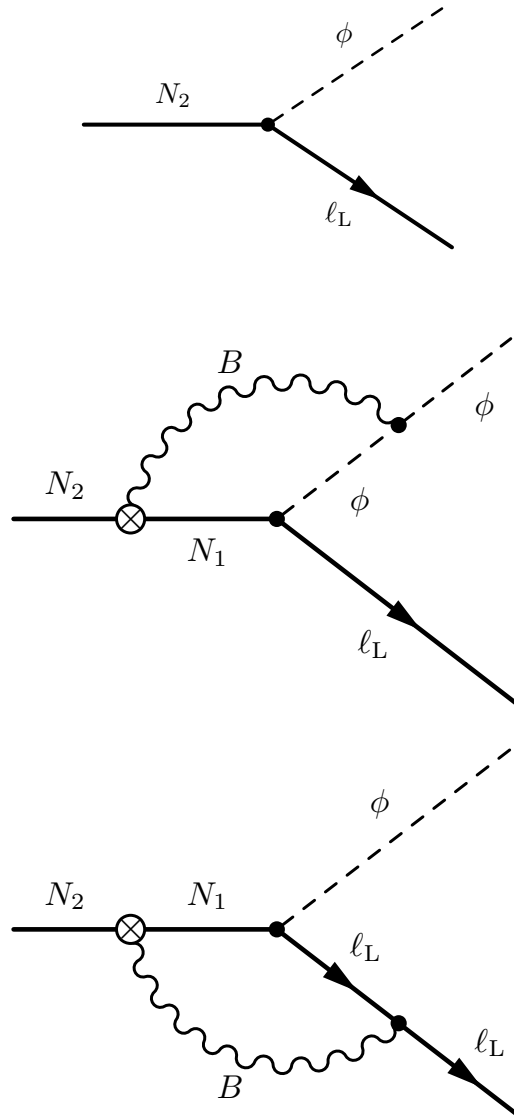


Fig. 4.7: The tree-level and one-loop diagrams that allow to generate a lepton asymmetry through the electroweak moments. The effective vertices are marked as crossed circles.

parts of the Lagrangian are discussed in sections 4.1 and 4.3, but we recapitulate them here:

$$\begin{aligned} \mathcal{L}_N = & \frac{i}{2} \bar{N} \gamma_\mu \partial^\mu N - \frac{1}{2} \bar{N} M_N N - \left( \bar{\ell}_L Y_\nu P_R N \tilde{\phi} + \text{H.c.} \right) + \\ & + \bar{N} \sigma^{\mu\nu} (\zeta P_R + \zeta^\dagger P_L) N B_{\mu\nu}, \end{aligned}$$

where  $N$  are Majorana fields and  $M_N$  is their mass matrix which, without loss of generality, can be taken diagonal. Since we ignore the charged lepton Yukawa couplings we can rotate the doublet fields  $\ell$  so that  $Y_\nu$  is Hermitian; there are no other possible field redefinitions, so  $\zeta$  is, in general, antisymmetric and complex. For  $n$  generations both  $Y_\nu$  and  $\zeta$  contain  $n(n-1)/2$  phases; in particular, for  $n=3$  we will have a total of 6 phases. But even for  $n=2$  we have two phases since both  $Y_{12}$  and  $\zeta_{12}$  can be complex. This is important because  $CP$ -violating observables should depend on those couplings; it also means that we can make our estimates in a model with just two generations, as we will do for simplicity.

Assuming two generations with  $N_2$  the heavier of the heavy neutrinos, we consider the lepton-number-violating decays  $N_2 \rightarrow \ell_e \phi$  and  $N_2 \rightarrow \bar{\ell}_e \bar{\phi}$ . At tree level the amplitudes are simply

$$\mathcal{A}_0(N_2 \rightarrow \ell_e \phi) = Y_{e2} \bar{u}(p_e) P_R u(p_2)$$

$$\mathcal{A}_0(N_2 \rightarrow \bar{\ell}_e \bar{\phi}) = Y_{e2}^* \bar{v}(p_2) P_L v(p_e) = -Y_{e2}^* \bar{u}(p_e) P_L u(p_2),$$

where we used  $v(p) = u^c(p)$ . The one-loop corrections that we show in figure 4.7 require a tedious but otherwise straightforward calculation. Naive application of the optical theorem indicates that the loop should develop an imaginary part if  $m_1 < m_2$ ; this expectation is confirmed, and such  $CP$ -even phase allows the process to yield  $CP$ -dissimilar amplitudes. We compute such asymmetry using the standard  $\epsilon$  parameter,

$$\epsilon \equiv \frac{\Gamma(N_2 \rightarrow \ell_e \phi) - \Gamma(N_2 \rightarrow \bar{\ell}_e \bar{\phi})}{\Gamma(N_2 \rightarrow \ell_e \phi) + \Gamma(N_2 \rightarrow \bar{\ell}_e \bar{\phi})},$$

which in our case results

$$\epsilon = -\frac{g'}{2\pi} (m_2^2 - m_1^2) \frac{m_1}{m_2^3} \text{Im} \left[ \frac{Y_{e2} Y_{e1}^*}{|Y_{e2}|^2} (\zeta_{12}^* m_2 + \zeta_{12} m_1) \right].$$

Now, particularising to  $m_1 \ll m_2$  we obtain

$$\epsilon = -\frac{g'}{2\pi} \frac{m_1}{\Lambda} \operatorname{Im} \left[ \frac{Y_{e2} Y_{e1}^*}{|Y_{e2}|^2} e^{-i\delta_{12}} \right],$$

where we defined the complex  $\zeta_{12}$  as  $\zeta_{12} \equiv e^{i\delta_{12}}/\Lambda$ , with  $\Lambda$  real.

In conclusion, we find that the Majorana electroweak moments do generate additional contributions to CP-violating asymmetries in heavy neutrino decays. These, however, are relevant only for the decays of the heavier neutrinos and could be relevant for leptogenesis only when  $m_1$  and  $m_2$  are relatively close; in this limit the amplitude is suppressed by a factor  $m_2^2 - m_1^2$ . In the following section we estimate the region in parameter space where this source of CP violation can be relevant for leptogenesis.

#### 4.6 Summary of bounds and conclusions

As can be seen from the previous sections, the dimension-five operators involving right-handed neutrinos open up observable effects in several scenarios of interest. The electroweak moment operator provides the richest phenomenology, but there are other interesting possibilities. We review in this section the phenomenology of these operators.

The  $\xi$  operator in equation (4.3) is most of all prominent for its ability to affect Higgs boson decays. After spontaneous symmetry breaking, this operator gives rise to several interaction vertices involving heavy neutrinos and the physical Higgs boson, the strongest being a simple  $H N_i N_j$  trilinear, which provides new decay channels of the Higgs to  $N$ 's, if such a process is kinematically allowed. These decays could dramatically change the branching ratios for the Higgs, see figure 4.6, especially in the region  $100 \text{ GeV} < m_H < 160 \text{ GeV}$ , where the gauge boson channels are still closed. The new decays could result in an invisible Higgs, if the heavy neutrinos cannot be detected, or in new, enhanced detection channels if they can be seen through their own decay channels, for instance  $N_2 \rightarrow N_1 \gamma$ , or  $N_1 \rightarrow \nu \gamma$  and  $N_1 \rightarrow e W$  with a displaced vertex. The first measurements of the Higgs boson branching ratios at the LHC [195, 196] seem to indicate that the decays

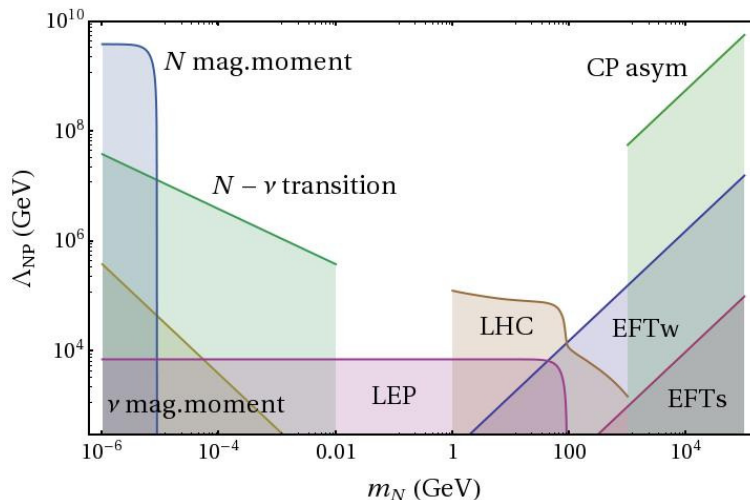


Fig. 4.8: Summary of bounds and prospects for the electroweak moment operator. All the shaded areas represent exclusion regions, except for the ones marked as “LHC” and “CP asym” which are regions of interest. For the construction of this plot we assumed a maximal, seesaw-like mixing,  $\varepsilon \sim \sqrt{m_\nu/m_N}$  with  $m_\nu = 0.1$  eV; for the processes where two heavy neutrinos are in play we assumed  $m_N \equiv m_2$  and neglected  $m_1$ . More details on the interpretation of the several regions can be found in the main text.

to heavy neutrinos are not dominant; a precise determination of the  $b\bar{b}$  branching ratio, which is the main SM decay channel for a Higgs mass of 125 GeV, will reveal if there is room for these exotic decays. Subsequent measurements of the whole set of SM branching ratios will allow to strongly constrain this effective interaction.

Most of this chapter has been devoted to the electroweak moment operator; and indeed it presents a variety of observable effects that make it very interesting from the phenomenological point of view. When expanded in terms of mass eigenstates the unique electroweak moment operator generates  $N - N$ ,  $N - \nu$  and  $\nu - \nu$  magnetic moments, and  $N - N$ ,  $N - \nu$  and  $\nu - \nu$  tensor couplings to the  $Z$ -bosons, as we show in equation (4.12). All the phenomenology of these interactions is controlled essentially by three parameters: the effective

coupling –or, equivalently, the new physics scale–,  $\zeta \equiv 1/\Lambda$ , the heavy-light mixing,  $\varepsilon$ , and the mass of the heavy neutrino,  $m_N$ . In figure 4.8 we summarise, in terms of  $\Lambda$  and  $m_N$ , the constraints discussed in the various sections of this chapter. For that aim, several assumptions are made: first, the mixing is supposed to have a seesaw-like structure,  $\varepsilon \sim \sqrt{m_\nu/m_N}$ ; then the light neutrino masses are assumed to lie at  $m_\nu = 0.1$  eV; as for the heavy neutrino masses, they are identified with  $m_N$  except in the cases where two heavy neutrinos are involved, in which we take  $m_N \equiv m_2$  and we neglect  $m_1$ .

With these assumptions, figure 4.8 shows the regions in the  $\Lambda - m_N$  plane forbidden by the red giant bound on the  $N$  and  $\nu$  magnetic moments, by the supernova bound on the transition magnetic moment  $N - \nu$  and by the LEP bound from the invisible  $Z$  boson decay width. Two more “exclusion” regions are displayed: the areas labeled as “EFTw” and “EFTs” represent the regions where the effective theory would be no longer valid in the weak and strong coupling regime, respectively; inside these regions our calculations make no sense by construction, and particular models should be used to examine the heavy neutrino interactions. We assume that the failure of the effective approach occurs when the low-energy degrees of freedom –the heavy neutrinos, in this case– become heavier than the new physics excitations; this happens in the strong regime for  $m_N > \Lambda$  and in the weak regime for  $m_N > \Lambda/(4\pi)^2$ , see section 4.2. As these are only order-of-magnitude estimations, the EFTw and EFTs regions should be taken with a grain of salt.

Apart from these excluded regions, figure 4.8 presents two more which could be described as “regions of interest”: one in which the electroweak moments can produce observable signals at the LHC, and other where a sizable lepton asymmetry can be generated in the decays of the heavy neutrinos. There is some uncertainty as to how to define the LHC region of interest: to test the new interactions at the LHC one should first produce the heavy neutrinos and after that one should be able to detect them. The analysis of the detection is complicated and depends on the details of the spectrum and the capabilities of the detectors, so we choose to make a conservative requirement: we demand that the heavy neutrinos are produced with rates large enough. In

particular, we plot the region where the cross section of  $pp \rightarrow N_1 N_2 + X$  is at least 100 fb. The area is interrupted below 1 GeV because our calculation, which uses partons and the proton parton distribution functions, becomes unreliable; for low  $N$  masses another approach, maybe involving chiral perturbation theory, should be used.

As for the second region of interest, we have discussed in section 4.5.2 that the electroweak moments contain new sources of CP non-conservation which can modify the standard leptogenesis scenarios. In particular we found that the electroweak moment operator gives additional contributions to the CP asymmetry in heavy neutrino decays. These could be relevant in leptogenesis if  $\epsilon \sim (g'/2\pi) m_N/\Lambda > 10^{-6}$  and  $m_N > 1$  TeV. We represent this region in figure 4.8 and label it as ‘‘CP asym’’.

Figure 4.8 draws the following conclusions about the electroweak moments:

- i)* Red giants cooling imposes very tight bounds for  $m_N \lesssim 10$  keV, strong enough as to require  $\Lambda > 4 \times 10^9$  GeV; in this region of the parameter space, obviously, any effect of the electroweak moment coupling would be totally negligible for any present or planned collider experiment.
- ii)* For  $10$  keV  $\lesssim m_N \lesssim 10$  MeV supernova cooling produced by the magnetic moment transitions  $\gamma + \nu \rightarrow N$  provides strong bounds. These bounds, however, depend on the assumptions made on the heavy-light mixing parameter,  $\epsilon$ . For this mass range there are also limits from red giant cooling, but they are derived from plasmon decay into a  $\nu$  pair, which is proportional to  $\epsilon^2$  and yields less restrictive constraints.
- iii)* For  $m_N \lesssim m_Z$ , the invisible  $Z$  decays require  $\Lambda \gtrsim 7 \times 10^3$  GeV, depending on the details of the heavy neutrino spectrum.
- iv)* For  $m_N \sim 1\text{--}200$  GeV, and roughly  $7$  TeV  $< \Lambda < 100$  TeV, heavy neutrinos could be produced at the LHC with large cross sections. The production mechanism necessarily yields two different mass eigenstates due to the antisymmetry of the Majorana electroweak moments. The heaviest neutrino in the pair would decay rapidly

to hard photons which could be detected. The lightest one is quite long-lived and, in a fraction of the parameter space, would produce non-pointing photons which could be detected.

- v) For masses above the TeV the electroweak moments can potentially interfere with the standard leptogenesis processes, even providing by themselves a significant lepton asymmetry.

A caveat is in order about figure 4.8 and the conclusions drawn above. As commented in section 4.2, throughout this chapter we have defined the new physics scale as  $\Lambda \equiv 1/\zeta$ . Since our operator is a magnetic-moment-like operator, this scale corresponds directly to the mass of new particles only in a nonperturbative context. If the interaction is generated by perturbative physics it arises at one loop and one expects  $\zeta \sim 1/((4\pi)^2 m_{\text{NP}})$ , where  $m_{\text{NP}}$  are the masses of the particles running inside the loop. Thus, for the perturbative case all the constraints discussed above apply, but can be reexpressed in terms of the masses of the new particles using  $m_{\text{NP}} = \Lambda/(4\pi)^2$ . A particularly interesting instance for this change is the region of interest for the LHC; in that case, the relevant range  $\Lambda \sim 10 - 100$  TeV translates into  $m_{\text{NP}} \sim 100 - 1000$  GeV. For such low masses the effective theory cannot be applied at LHC energies and one should use the complete theory that gives rise to the right-handed neutrino electroweak moments. Those models should contain new particles with nonzero hypercharges and masses around 100 – 1000 GeV which should be produced in the LHC via, for instance, Drell-Yan processes. Most likely, weakly-coupled theories providing these electroweak moments will be probed more efficiently by looking for the new particles than they would be by observing the effective interactions.

#### 4.7 *Appendix: Decay rates and cross sections*

In this section we collect the formulas that describe the decay rates and the cross sections referred to in the text. Let us first introduce some notation that will be useful to simplify the presentation of the expressions. As usual,  $s_W \equiv \sin \theta_W$  and  $c_W \equiv \cos \theta_W$  will represent the sine and cosine of the weak mixing angle. We will denote by  $q_f$  the



electric charge of a fermion  $f$ , and its vector and axial couplings will be denoted by  $v_f = t_3(f) (1 - 4|q_f|s_W^2)$  and  $a_f = t_3(f)$ , respectively, with  $t_3(f) = +1/2 (-1/2)$  for up-type (down-type) fermions. When required, we will separate modulus and phase of the effective electroweak coupling as  $\zeta_{ij} \equiv |\zeta_{ij}| e^{i\delta_{ij}}$ . At several moments we will use Källén's lambda function, which reads

$$\lambda(a, b, c) = a^2 + b^2 + c^2 - 2ab - 2ac - 2bc.$$

$$Z \rightarrow N_i N_j$$

The decay width of the  $Z$  boson into heavy neutrinos is

$$\Gamma(Z \rightarrow N_i N_j) = \frac{2}{3\pi} s_W^2 |\zeta_{ij}|^2 m_Z^3 f_Z(m_Z, m_i, m_j),$$

where  $f_Z(m_Z, m_i, m_j)$  is a kinematic factor that reads

$$f_Z(m_Z, m_i, m_j) = \frac{\sqrt{\lambda(m_Z^2, m_i^2, m_j^2)}}{m_Z^6} \left[ m_Z^2 (m_Z^2 + m_i^2 + m_j^2 - 6m_i m_j \cos 2\delta_{ij}) - 2(m_i^2 - m_j^2)^2 \right]. \quad (4.15)$$

Note that  $f_Z$  is defined in such a way that  $f_Z(m_Z, 0, 0) = 1$ .

#### $N_2$ decay rates

If the electroweak interaction is strong enough, the dominant decays of the heavier neutral leptons will proceed to photons or  $Z$ 's plus one of the lighter heavy neutrinos. In our simplified spectrum with just two heavy neutrinos we would have

$$\Gamma(N_2 \rightarrow N_1 \gamma) = \frac{2}{\pi} c_W^2 |\zeta_{12}|^2 m_2^3 (1 - m_1^2/m_2^2)^3$$

$$\Gamma(N_2 \rightarrow N_1 Z) = \frac{2}{\pi} s_W^2 |\zeta_{12}|^2 m_2^3 f_2(m_Z, m_1, m_2),$$

where

$$f_2(m_Z, m_1, m_2) = -\frac{m_Z^6}{2m_2^6} f_Z(m_Z, m_1, m_2),$$

again normalised in such a way that  $f_2(0, 0, m_2) = 1$ .

$N_1$  decay rates

The lightest of the heavy neutrinos,  $N_1$ , can decay only due to mixing with the SM sector. The mixing between left- and right-handed neutrinos induces heavy-light transition interactions in the SM weak vertices, as described at the end of section 4.3. This opens up three SM-like decay channels, whenever kinematically allowed: two of them are neutral, with emission of light neutrino plus a  $Z$  or a Higgs boson, and one charged, involving a charged lepton and a  $W$  in the final state. Actually, these decays are a consequence of the  $\nu'_R$  couplings to the four degrees of freedom of the Higgs doublet; as three of those degrees of freedom end up inside the weak gauge bosons, most of them proceed with a gauge boson in the final state. We will later come back to this point.

Provided  $m_1 > m_W$ , the charged channel is to occur with the following rate:

$$\Gamma(N_1 \rightarrow \ell_\beta W) = \frac{1}{16} |\varepsilon_W^{\beta 1}|^2 \alpha \frac{m_1^3}{s_W^2 m_W^2} \left(1 - \frac{m_W^2}{m_1^2}\right)^2 \left(1 + 2 \frac{m_W^2}{m_1^2}\right), \quad (4.16)$$

where  $\alpha$  is the fine-structure constant and  $\varepsilon_W$  characterizes the mixing of heavy-light neutrinos in  $W$  boson couplings, which is order  $\sqrt{m_\nu/m_N}$  or smaller.

For the first neutral channel, with a  $Z$  in the final state, we obtain

$$\Gamma(N_1 \rightarrow \nu_\beta Z) = \frac{1}{16} |\varepsilon_Z^{\beta 1}|^2 \alpha \frac{m_1^3}{s_W^2 c_W^2 m_Z^2} \left(1 - \frac{m_Z^2}{m_1^2}\right)^2 \left(1 + 2 \frac{m_Z^2}{m_1^2}\right) \quad (4.17)$$

whenever  $m_1 > m_Z$ , with  $\varepsilon_Z$  the mixing factor that corresponds to the  $Z$  couplings. Notice that since  $m_W = c_W m_Z$  the two decay widths are equal up to phase space factors and differences in the mixing factors  $\varepsilon_Z$  and  $\varepsilon_W$ . However, we have two decay channels into  $W$ 's,  $N_1 \rightarrow e^- W^+$  and  $N_1 \rightarrow e^+ W^-$ , and only one into  $Z$ 's. This is an indication that there are two charged degrees of freedom in  $\phi$ , but only one of the neutral ones goes to the  $Z$ .

If  $m_1 > m_H$  the second neutral channel is also open, and its decay

rate is

$$\Gamma(N_1 \rightarrow \nu_\beta H) = \frac{1}{32\pi} |Y_\nu^{\beta 1}|^2 m_1 \left(1 - \frac{m_H^2}{m_1^2}\right)^2. \quad (4.18)$$

This looks at first sight quite different from the other two SM-like channels; however, if we use that  $\varepsilon \simeq M_D M_N^{-1}$ ,  $M_D = Y_\nu v/\sqrt{2}$  and  $\alpha/(s_W^2 m_W^2) = 1/(\pi v^2)$  we can rewrite

$$|\varepsilon|^2 \alpha \frac{m_1^3}{s_W^2 m_W^2} \sim |Y_\nu|^2 \frac{m_1}{2\pi},$$

and so, in the limit  $m_1 \gg m_H, m_W, m_Z$  the three decay widths are identical. This is required by the *equivalence theorem* [175, 176], which states that at energies much above the symmetry breaking scale any calculation can be performed using the unbroken theory; in that theory all the fields except for the  $N$ 's are massless, there is no heavy-light mixing and the  $N$ 's decay into the doublet of leptons and the Higgs scalar doublet through the SM Yukawa couplings. Therefore, the decay rates to all four degrees of freedom in the Higgs doublet must be equal. However, for moderate  $m_1$  the theory begins to ‘perceive’ the broken symmetry, and since  $m_H > m_Z > m_W$  the phase space factors become important. The equivalence of equations (4.16 – 4.18) in the limit  $m_1 \gg m_H, m_W, m_Z$ , which is apparent in figure 4.1, shows that it is the scalar degrees of freedom which are in play in these decays.

Up to this point we have discussed the SM-like decay channels above the kinematical threshold for producing the electroweak bosons. The three of them can also proceed below their threshold through a virtual heavy boson, yielding suppressed three-body decays. These virtual modes, however, are immediately in competition with any other weaker interaction at hand. And indeed, it so happens that the same electroweak moments provide such an interaction: as we see in equation (4.12), with one mixing insertion a channel to photon plus light neutrino is open. This channel is not competitive when the SM-like modes are fully open, but it can be important if  $m_1 < m_W$ . Its decay rate reads

$$\Gamma(N_1 \rightarrow \nu_\beta \gamma) = \frac{2}{\pi} |\varepsilon_\gamma^{\beta 1}|^2 c_W^2 m_1^3,$$

where  $\varepsilon_\gamma$  is a parameter that comprises the effective coupling together with the mixing factors as seen in equation (4.12); it is of

order  $(1/\Lambda) \sqrt{m\nu/m_N}$ . The relevance of this channel for  $N_1$  decays is further discussed in section 4.4.2.

$e^+e^- \rightarrow N_1N_2$  cross section

By neglecting the heavy-light mixing, the LEP and ILC heavy neutrino production is given entirely by the electroweak couplings. The cross section then reads

$$\sigma(e^+e^- \rightarrow N_1N_2) = \frac{2}{3} \alpha |\zeta_{12}|^2 f_Z(\sqrt{s}, m_1, m_2) \eta_e(s),$$

with  $f_Z$  defined in equation (4.15) and  $\eta_e$  carrying information about the involved diagrams. For a general fermion we have

$$\eta_f(s) = 4c_W^2 q_f^2 - 4q_f v_f \operatorname{Re}[\chi(s)] + \frac{v_f^2 + a_f^2}{c_W^2} |\chi(s)|^2, \quad (4.19)$$

where  $\chi(s)$  represents the Lorentzian-like structure generated by the one-loop-corrected  $Z$  propagator,

$$\chi(s) = \frac{s}{s - m_Z^2 + im_Z \Gamma_Z}.$$

Of course, for the case of an  $e^+e^-$  collider it is enough to take  $f = e$ , but these general expressions will be of use shortly.

*Partonic cross sections for  $pp \rightarrow N_1N_2 + X$*

To compute the  $pp \rightarrow N_1N_2 + X$  cross section we proceed by computing the collisions among the partons inside the proton and then convoluting over the parton distribution functions of the proton. So, diagrammatically we just compute the cross section for  $q\bar{q} \rightarrow N_1N_2$  proceeding through a photon or a  $Z$ , which is the main production process that the partons can provide. The cross section reads

$$\begin{aligned} \frac{d\hat{\sigma}}{d\Omega}(q\bar{q} \rightarrow N_1N_2) &= \frac{\alpha}{6\pi} |\zeta_{12}|^2 \eta_q(\hat{s}) \frac{\sqrt{\lambda(\hat{s}, m_1^2, m_2^2)}}{\hat{s}^3} \times \\ &\times \left[ (m_1^2 + m_2^2) (\hat{s} + 2\hat{t}) - 2\hat{t} (\hat{s} + \hat{t}) - m_1^4 - m_2^4 - \right. \\ &\quad \left. - 2\hat{s} m_1 m_2 \cos 2\delta_{12} \right], \end{aligned}$$

with  $\hat{s}$  and  $\hat{t}$  the Mandelstam variables for the partonic collision in the center-of-mass frame of the quarks, and  $\eta_q$  the function defined in equation (4.19) but with the appropriate quantum numbers for the relevant quarks.

*Higgs boson decays into heavy neutrinos,  $H \rightarrow N_i N_j$*

Up to now we have only discussed cross sections and decays induced by the electroweak moment interaction or by SM interactions plus heavy-light mixing. The  $\xi$  term in equation (4.3) also has interesting consequences, in particular if the  $N$ 's are light enough it can induce new decay modes for the Higgs boson. We found

$$\Gamma(H \rightarrow N_i N_j) = \frac{v^2}{2\pi m_H^3} |\xi_{ij}|^2 \sqrt{\lambda(m_H^2, m_i^2, m_j^2)} \times \\ \times \left[ m_H^2 - m_i^2 - m_j^2 - 2 m_i m_j \cos 2\delta'_{ij} \right], \quad (4.20)$$

where  $\xi_{ij} = |\xi_{ij}| e^{i\delta'_{ij}}$ . Note that, as  $\xi$  is a symmetric matrix, there's no need that  $i \neq j$ , as it happened with the electroweak moments. A full discussion of these decays can be found in section 4.4.5.

## 5. A MODEL FOR RIGHT-HANDED NEUTRINO MAGNETIC MOMENTS

In this chapter we present a very simple model that gives rise to right-handed neutrino electroweak moments. In the previous chapter we discussed the phenomenological consequences of such an interaction; maybe the most prominent would be the fact that right-handed neutrinos cease to be ‘sterile’ if the coupling is large enough. We also concluded that if the underlying physics is weakly coupled the observation of the electroweak moments would be more difficult than the observation of the new particles themselves. Motivated by this, we present here an extension of the Standard Model in which the right-handed neutrino electroweak moments can arise, and we analyse part of its phenomenology. The model includes, in addition to the SM fields and the right-handed neutrinos, a charged scalar singlet and a charged,  $SU(2)$ -singlet, vector-like fermion. The electroweak moments are generated at one loop, and their couplings are calculable and well-defined. In the simplest version of the model the new charged particles are stable due to a global symmetry and they can constitute charged dark matter, which is strongly disfavoured by cosmological and astrophysical considerations. To avoid such problems we extend minimally the model by allowing a soft breaking of the symmetries, which is enough to induce CHAMP decays. The resulting decays proceed mainly to leptons of the third family. We conclude that in collider experiments the model should be searched for in a similar fashion as one does with heavy charged leptons. This work was carried out together with Arcadi Santamaria and José Wudka.

## 5.1 The model

As discussed extensively in the previous chapter, the dimension-five interactions in a low-energy scenario consisting of the Standard Model and a number of right-handed neutrinos fall into three classes:

$$\mathcal{L}_5 = \overline{\nu_R^c} \zeta \sigma^{\mu\nu} \nu_R B_{\mu\nu} + \left( \overline{\ell_L \phi} \right) \chi \left( \tilde{\phi}^\dagger \ell_L \right) - \left( \phi^\dagger \phi \right) \overline{\nu_R^c} \xi \nu_R + \text{H.c.}, \quad (5.1)$$

with the notation described in detail in section 4.1. The reader will notice a difference between equation (5.1) and the corresponding expressions in chapter 4; there we used  $\nu_R'$  to denote the flavour-basis right-handed neutrino fields, in order to distinguish them from the mass eigenfields. In this chapter we will omit this notation, as we will not be interested in the details of neutrino mass diagonalisation. The couplings  $\chi$ ,  $\xi$ ,  $\zeta$  in equation (5.1) have dimension of inverse mass, which is associated with the scale of heavy physics responsible for the corresponding operator. The  $\chi$  term is the well-known Weinberg operator [54] that yields Majorana masses for the left-handed neutrinos; the term involving  $\xi$  gives a contribution to the right-handed neutrino Majorana masses, but also provides interactions that could induce invisible Higgs decays, as commented in section 4.4.5; the  $\zeta$  operator was the main character of chapter 4, as it induces magnetic-moment-like interactions for the  $\nu_R$ 's which have many phenomenological consequences – see sections 4.4 and 4.5. Regarding their flavour structure,  $\chi$  and  $\xi$  are in general complex symmetric matrices in flavour space, while  $\zeta$  is complex and antisymmetric. The number of  $\nu_R$ 's is not fixed from first principles; let us consider, throughout this chapter, three right-handed neutrino families, in analogy to the three known lepton families.

In this chapter we will describe a model that gives rise to the electroweak moments  $\zeta$ . As we argued in section 4.2 of the previous chapter, this has to occur at least at the one-loop level, and the models necessarily involve either a scalar-fermion pair with opposite, nonzero hypercharges and having Yukawa couplings to both  $\nu_R$  and  $\nu_R^c$ , or a vector-fermion pair with the same properties. Here we will focus on the first possibility, since a massive vector field suffers from well-known renormalisation problems that are not related to the generation of

electroweak moments. Therefore, we enlarge the SM by adding a negatively charged scalar singlet,  $\omega$ , and one negatively charged vector-like<sup>1</sup> fermion,  $E$ ; formally, we write their charges under  $SU(3)_C \otimes SU(2)_L \otimes U(1)_Y$  as

$$\omega \sim (0, 0, -1), \quad E_L, E_R \sim (0, 0, -1),$$

where it is understood that  $Q = Y + T_3$ .

The Lagrangian of the model contains all the renormalisable terms allowed by gauge invariance. To describe it, let us first separate the standard pieces from the new physics additions:

$$\mathcal{L} = \mathcal{L}_{\text{SM}} + \mathcal{L}_{\text{NP}}.$$

We include in  $\mathcal{L}_{\text{NP}}$  all the terms that involve the new particles, including the right-handed neutrinos.  $\mathcal{L}_{\text{SM}}$ , thus, comprises just the ‘pure’ Standard Model terms; among all of them, we will use throughout our discussions the following:

$$\mathcal{L}_{\text{SM}} = i \bar{\ell}_L \gamma_\mu D^\mu \ell_L + i \bar{e}_R \gamma_\mu D^\mu e_R + (\bar{\ell}_L Y_e e_R \phi + \text{H.c.}) + \dots,$$

with  $Y_e$  the Yukawa couplings of the charged leptons, which are completely general  $3 \times 3$  matrices in flavour space. The omitted terms include the SM gauge boson, Higgs boson and quark kinetic terms, quark Yukawa interactions and the SM Higgs potential.

We now go on to describe the new physics contribution; in order to present the different terms, we split  $\mathcal{L}_{\text{NP}}$  into four parts:

$$\mathcal{L}_{\text{NP}} = \mathcal{L}_{\text{K}} + \mathcal{L}_{\text{Y}} - V_{\text{NP}} + \mathcal{L}_{\text{extra}}.$$

$\mathcal{L}_{\text{K}}$  describes the kinetic and mass terms of the new particles,

$$\begin{aligned} \mathcal{L}_{\text{K}} = & D_\mu \omega^\dagger D^\mu \omega + i \bar{E} \gamma_\mu D^\mu E - m_E \bar{E} E + \\ & + i \bar{\nu}_R \gamma_\mu \partial^\mu \nu_R - \left( \frac{1}{2} \bar{\nu}_R^c M_R \nu_R + \text{H.c.} \right), \end{aligned} \quad (5.2)$$

---

<sup>1</sup> This fermion should contain the two chiralities if it is to couple to  $\nu_R$  and  $\nu_R^c$ . Of course one can imagine more complicated scenarios with two or more fermionic additions, but we will stick to this minimal version of the mechanism.



with  $M_R$  the Majorana mass term of right-handed neutrinos, which is a complex symmetric matrix in flavour space.

$\mathcal{L}_Y$  contains the standard Yukawa interactions of right-handed neutrinos and the new Yukawa couplings needed to generate the electroweak moments:

$$\mathcal{L}_Y = \overline{\ell}_L Y_\nu \nu_R \tilde{\phi} + \overline{\nu}_R^c h' E \omega^\dagger + \overline{\nu}_R h E \omega^\dagger + \text{H.c.} \quad (5.3)$$

$Y_\nu$  is a general  $3 \times 3$  complex matrix and, if there is just one generation of  $E$ 's,  $h$  and  $h'$  are three-component vectors in flavour space. Note that lepton number is explicitly broken in this model even in the absence of a Majorana mass for the  $\nu_R$ 's, due to the joint action of the  $h$  and  $h'$  couplings, that assign opposite lepton number charges to  $E$  or  $\omega$ . Indeed, the lepton-number-violating  $\zeta$  and  $\xi$  interactions will proceed through one  $h$  and one  $h'$  insertion, as seen in figures 5.1 and 5.2.

The SM scalar potential is enlarged with several terms involving  $\omega$ ; we collect them inside  $V_{\text{NP}}$ :

$$V_{\text{NP}} = m'_\omega{}^2 \omega \omega^\dagger + \lambda_\omega (\omega \omega^\dagger)^2 + 2\lambda_{\omega\phi} \omega \omega^\dagger \phi^\dagger \phi.$$

Note that  $m'_\omega$  is *not* the physical mass of the charged scalar; after the breaking of electroweak symmetry, an additional  $\omega \omega^\dagger$  term will emerge from the quartic coupling  $\lambda_{\omega\phi}$ . If we have  $\langle \phi^0 \rangle = v/\sqrt{2}$ , the final physical mass will be  $m_\omega^2 = m'_\omega{}^2 + \lambda_{\omega\phi} v^2$ . To  $V_{\text{NP}}$  we will just demand that it yields a meaningful theory: we need  $\lambda, \lambda_\omega > 0$  and  $\lambda\lambda_\omega > \lambda_{\omega\phi}^2$  in order for the potential to be bounded from below, and  $m_\omega^2 > 0$  so that  $U(1)_{\text{em}}$  remains unbroken. It is important to remark that with only one Higgs doublet there cannot be trilinear couplings between the doublet and the singlet. Therefore, the potential has two independent  $U(1)$  global symmetries, one for the singlet and one for the doublet.

Apart from those already commented, the SM symmetries allow for the following Yukawa couplings and mass terms that involve the new particles:

$$\mathcal{L}_{\text{extra}} = \overline{E}_L \kappa e_R + \overline{\ell}_L Y_E E_R \phi + \overline{\ell}_L f \ell_L \omega^\dagger + \overline{e}_R f' \nu_R^c \omega + \text{H.c.}, \quad (5.4)$$

which can be set to zero by imposing a discrete symmetry that affects only the new particles,

$$E \rightarrow -E \qquad \omega \rightarrow -\omega,$$

in which case *all* low-energy effects of the new particles will be loop-generated. In fact, the resulting Lagrangian will have a larger continuous symmetry,

$$E \rightarrow e^{i\alpha} E \qquad \omega \rightarrow e^{i\alpha} \omega, \qquad (5.5)$$

which is not anomalous, and therefore there will be a charge, carried only by  $E$  and  $\omega$ , which will be exactly conserved. In such case, the lightest of the  $E$  or  $\omega$  will be completely stable becoming a CHAMP, which could create serious problems in the standard cosmology scenarios. We will discuss this issue in section 5.3.2.

## 5.2 Generation of the dimension-five operators

### 5.2.1 The right-handed neutrino electroweak moments

The model is constructed in such a way that the generation of electroweak moments is straightforward: the  $h$  Yukawas allow to open up the  $\nu_R$ 's into a loop of  $E$  and  $\omega$  which violates lepton number if closed through a  $h'$  coupling; then, to obtain electroweak moments one has only to attach a  $B$  to the  $E$  or  $\omega$  legs. The relevant diagrams are presented in figure 5.1. The calculation is somewhat cumbersome, but it can be simplified by assuming  $M_R \ll m_E, m_\omega$  and then neglecting all external momenta and masses. Then we obtain

$$\zeta_{ij} = \frac{g'}{(4\pi)^2} (h'_i h_j^* - h'_j h_i^*) \frac{f(r)}{4m_E},$$

where  $r \equiv (m_\omega/m_E)^2$ , and  $g'$  is, as usual, the  $U(1)_Y$  gauge coupling.  $f(r)$  is a loop function which reads

$$f(r) = \frac{1}{1-r} + \frac{r}{(1-r)^2} \log r \quad \rightarrow \quad \begin{cases} 1, & r \ll 1 \\ 1/2, & r = 1 \\ (\log r - 1)/r, & r \gg 1 \end{cases}. \qquad (5.6)$$

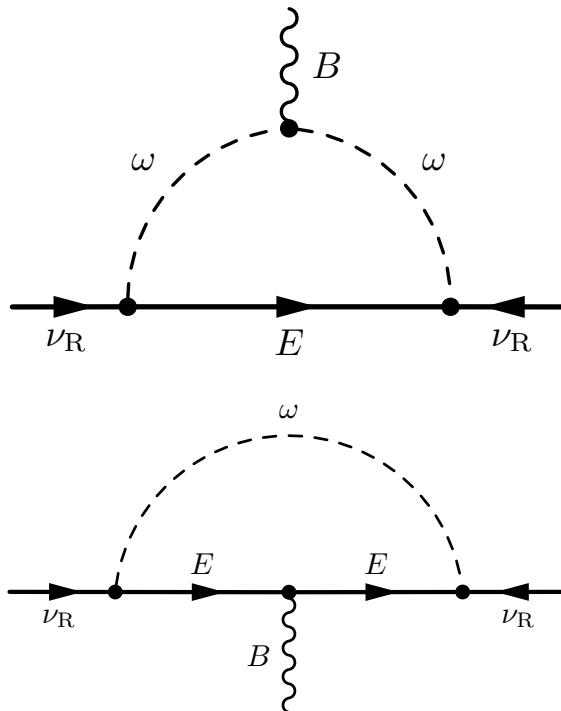


Fig. 5.1: The diagrams that contribute to the right-handed neutrino Majorana electroweak moments at leading order.

Note that only a small subset of all the interactions provided by the model are in play in the generation of electroweak moments. In particular, the moments violate lepton number, but the Majorana mass of the  $\nu_R$ 's is not needed at all; in fact, these sort of one-loop diagrams can give us clues about the natural value for  $M_R$  in this model, see section 5.3.1. Notice, too, that none of the 'rejected' interactions in equation (5.4) participate in the electroweak moments; therefore, the moments offer no clue, at least at leading order, about the stability of the new particles.

We can use these expressions to estimate the magnitude of the generated electroweak moments; take, for instance,  $m_\omega = m_E$ , and  $(h'_i h_j^* - h'_j h_i^*) = 0.5$ , while  $g' = \sqrt{4\pi\alpha}/c_W \simeq 0.35$ ; then  $\zeta \simeq 10^{-4}/m_E$ . In terms of  $\Lambda \equiv 1/\zeta$  we would have  $\Lambda = 10^4 m_E$ , meaning that the

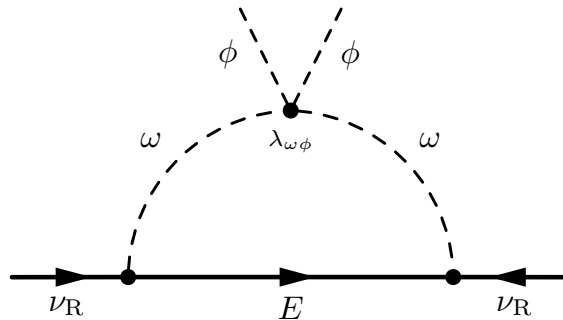


Fig. 5.2: The diagram that yields the  $(\phi^\dagger\phi)\bar{\nu}_R^c\xi\nu_R$  interaction at one loop.

bounds derived for the electroweak moment will be roughly 10,000 times weaker than those derived from direct search of the new charged particles. This is in agreement with our conclusions from chapter 4 for weakly-coupled theories, see for instance section 4.4.1. For this particular example the LEP and Tevatron bound of  $m_E > 100$  GeV translates into  $\Lambda > 10^6$  GeV; as we can see in figure 4.8, this bound is way better than those derived on the electroweak moments from collider experiments. Only in the regime of light  $\nu_R$ 's, where astrophysical bounds apply, we find such stringent limits on the electroweak moments that we can extract stronger bounds on the masses of the new particles. For example, for very light right-handed neutrinos, where the red giant cooling applies, we have  $\Lambda \gtrsim 4 \times 10^9$  GeV and so  $m_E \gtrsim 400$  TeV, a stupendously demanding bound.

### 5.2.2 The effective Higgs boson interaction

In addition to the electroweak moments, this model also provides at one loop the dimension-five operator  $(\phi^\dagger\phi)\bar{\nu}_R^c\xi\nu_R$ , which yields several lepton-number-violating interactions among right-handed neutrinos and the Higgs boson; in section 4.4.5 of the previous chapter we pointed out that some of these interactions could enhance the decays of the Higgs boson to  $\nu_R$ 's, maybe providing a mechanism for invisible Higgs decays. The process that generates the  $\xi$  interaction is very similar to those for the electroweak moment, but with one insertion of the quartic scalar coupling  $\lambda_{\omega\phi}$ ; we present the relevant diagram in figure

5.2. A simple calculation yields

$$\xi_{ij} = \frac{\lambda_{\omega\phi}}{(4\pi)^2} (h'_i h_j^* + h'_j h_i^*) \frac{f_\phi(r)}{4m_E}, \quad (5.7)$$

where we have again  $r \equiv (m_\omega/m_E)^2$ , and  $f_\phi(r)$  can be written in terms of  $f(r)$ , defined in equation (5.6), as follows:  $f_\phi(r) \equiv 4f(1/r)/r$ .

As we did with the electroweak moments, we can use now equation (5.7) to estimate the magnitude of the effective interaction. Take, say,  $\lambda_{\omega\phi} = (h'_i h_j^* + h'_j h_i^*) = 0.5$  and  $m_E = m_\omega$ ; then we will have  $\xi \simeq 10^{-3} m_E$  or, expressed in terms of the new physics scale,  $\Lambda \equiv 1/\xi = 10^3 m_E$ . In section 4.4.5 we showed that a new physics scale of a few tens of TeV might still interfere with the Higgs boson decays. The interaction generated by the model seems, thus, too weak; this is not a surprise, as this is a weakly-coupled model, and the effective interaction has to compete with the nonsuppressed renormalisable Higgs couplings.

### 5.3 Phenomenological analysis

#### 5.3.1 Considerations on the mass of the right-handed neutrinos

In this model, the tree-level Majorana mass for the right-handed neutrinos,  $M_R$ , is in principle arbitrary. However, there are several one-loop processes that interfere with the tree-level Majorana masses; in this short section we describe these mechanisms and discuss the information they provide about the scale of Majorana masses within this model.

The first contribution emerges from the  $\xi$  interaction discussed in section 5.2.2; after the spontaneous breaking of electroweak symmetry this operator generates several terms, and among them there is a Majorana mass for the  $\nu_R$ 's. This mass will be present even if  $M_R$  is set to zero in the Lagrangian, and so it can serve as a sort of 'basal value' for the final Majorana mass in the model; indeed, the only way in which the theory could yield smaller Majorana masses in the end is by finely cancelling this contribution, a possibility that we regard as scarcely natural and we prefer to dismiss. It is important to note that even

though this mass is generated at one loop –see figure 5.2, and replace the Higgs doublets by VEV’s– it does *not* renormalise the tree-level Majorana mass  $M_R$ , as it results from the  $\xi$  operator, which is different in essence from a bare Majorana mass. The effect of renormalisation is different and subtler, and is to be discussed below.

We see, by looking at equations (5.1) and (5.7), that the Majorana mass provided by the  $\xi$  operator reads roughly

$$M_R^{(\xi)} \sim \frac{\lambda_{\omega\phi}}{(4\pi)^2} h' h \frac{v^2}{4m_E}.$$

Therefore we can estimate a lower bound on the final Majorana mass of the  $\nu_R$ ’s as

$$M_R^{(f)} \gtrsim \frac{0.1 \text{ GeV}^2}{m_E} \sim 1 \text{ MeV},$$

where the superindex “(f)” indicates that this is the “final” Majorana mass, resulting from the sum of all the effective contributions. For this estimate we took first  $h' = h = \lambda_{\omega\phi} = 0.1$  and then  $m_E \sim 100 \text{ GeV}$ . Smaller values for the coupling constants, or heavier  $E$  masses would yield milder bounds.

The second consideration about the right-handed neutrino Majorana masses regards the naturality of the renormalisation procedure. The same one-loop diagrams that generate the electroweak moments, see figure 5.1, yield a renormalisation of the  $\nu_R$  Majorana mass if we remove the  $B$  leg. The diagrams, of course, are divergent and their contribution is only meaningful after we regularise the theory and remove the infinities; moreover, their contribution is added to the tree-level Majorana mass and it is only this combination which is physically observable. Therefore, rigorously speaking, we should have nothing to discuss about these one-loop corrections, as they’re not physical; however, if we trust that perturbation theory and quantum field theory are capturing some features of reality, we would be inclined to think that the one-loop corrections should be *corrections* indeed, and so smaller than the tree-level mass. This argument appeals to the naturality and consistency of the theory, and though it is not strictly phenomenological it can provide an intuition of a ‘reasonable’ scale for the parameters. Applied to the Majorana masses, it yields the

following result: the one-loop diagrams are logarithmically divergent, and their corrections will be of order

$$\delta M_R \sim \frac{h'h}{(4\pi)^2} m_E,$$

suppressed by an additional factor  $(m_E/m_\omega)^2$  if the scalar is much heavier than the vector-like fermion. It is then natural to require  $M_R \gtrsim \delta M_R$ , which is estimated to be  $M_R \gtrsim 5$  MeV for  $h = h' = 0.1$  and  $m_E = 100$  GeV.

### 5.3.2 $E$ or $\omega$ as CHAMP's

The model as described so far contains only the couplings necessary to generate the right-handed neutrino Majorana electroweak moments. But it is clear that the trilinear vertices  $\bar{\nu}_R E \omega^\dagger$  and  $\bar{\nu}_R^c E \omega^\dagger$  alone cannot induce decays for both the  $E$  and the  $\omega$ . The lightest of the two will remain stable and could then accumulate in the galaxy clusters, appearing as electrically charged dark matter. The idea that dark matter could be composed mostly of charged massive particles was proposed in [218, 219] and it is strongly constrained from very different arguments [220–224]. One might still consider the possibility of having massive stable  $E$  or  $\omega$  particles within the reach of the LHC, but with a cosmic abundance lower than the one required for dark matter. Unfortunately, such scenario seems also to be excluded, at least under the most usual assumptions: if one considers, as in [218], that the  $E$ 's and  $\omega$ 's were produced in the early universe through the standard freeze-out mechanism [225], the bounds from interstellar calorimetry [224] and terrestrial searches for super-heavy nuclei [221, 222] completely close the window of under-TeV CHAMP abundances.

There is, however, a way to escape all these bounds. A recent paper [226] notes that CHAMP's, if very massive or carrying very small charges, are expelled from the galactic disk by the magnetic fields. That situation prevents any terrestrial or galactic detection and leaves room for CHAMP's to exist. The bound specifically states that particles with  $100 (Q/e)^2 \text{ TeV} \lesssim m \lesssim 10^8 (Q/e) \text{ TeV}$  are depleted from the disk, and in fact our model, if we forbid the terms in equation (5.4),

does not fix the hypercharge of  $E$  and  $\omega$ , so they can be millicharged. Unfortunately, this situation is not interesting for our purposes, for this kind of CHAMP's would give rise to very small neutrino magnetic moments and wouldn't show up in the future accelerators, either due to their heavy masses or to their small couplings.

In conclusion, we need an additional mechanism for  $E$  or  $\omega$  decays. The easiest way to accomplish this is by allowing one or more of the couplings in equation (5.4), which can be taken small, if needed, by arguing that (5.5) is an almost exact symmetry. We discuss one of the possibilities in section 5.3.3. The scenario of decaying CHAMP's has, on its own, a number of advantages and drawbacks. Some recent papers [227, 228] have pointed out that the presence of a massive, charged and colourless particle during the process of primordial nucleosynthesis might lead to an explanation for the cosmic lithium problem. Also, the decay of massive particles during nucleosynthesis could have a dramatic influence in the final abundances of primordial elements, which provides us with bounds on the lifetime and abundance of CHAMP's that could be useful.

### 5.3.3 Allowing for CHAMP decays

If the new particles have to decay the global symmetry (5.5) needs to be broken, and for that aim it is enough to allow some of the terms in equation (5.4). For the sake of simplicity, we will consider only the case in which the symmetry is softly broken by mixings between  $E$  and the charged leptons; that is, we will add to our Lagrangian the term

$$\mathcal{L}_\kappa = \overline{E}_L \kappa e_R + \text{H.c.},$$

where  $\kappa$  is, if there is just one generation of  $E$ 's, a three-component vector in flavour space with dimensions of mass. The choice of a soft breaking is motivated, as usual, by the fact that the model remains closed under the renormalisation group flow; with only  $\mathcal{L}_\kappa$  added, none of the other terms in (5.4) needs to be introduced for the model to remain renormalisable.

The  $\kappa$  term will induce decays of  $E$  into SM particles much like the heavy neutrino decays in seesaw models, since only this mixing links



$E$  to the SM degrees of freedom. After diagonalisation of the charged lepton mass matrix one obtains interactions that connect  $E$  to  $W\nu$ ,  $Z\ell$  and  $H\ell^2$ . As the current bound on heavy charged leptons requires that  $m_E > 100$  GeV, the  $W$  and  $Z$  will be produced on-shell; the Higgs channel may or may not be open depending on the value of  $m_E$ .  $\omega$ , on the other hand, can only decay through the Yukawa  $\bar{E}\nu_R\omega$  vertices, and kinematics can complicate the scenario if the masses of  $\omega$ ,  $E$  and the  $\nu_R$ 's are comparable. For the sake of simplicity, in the following we will consider  $m_\omega > m_E \gg M_R$ , so that the  $\omega$ 's decay rapidly to on-shell  $E$  and  $\nu_R$  and then the  $E$  decays through the channels described above.

In figure 5.3 we offer the widths and branching ratios for the leading decay channels of  $E$ . Several features can be noted, all related to the fact that these are mixing-mediated decays. First, the decay widths are suppressed by powers of  $m_\ell/m_E$ , where  $m_\ell$  is the mass of the charged lepton in the final state; therefore, if the  $\kappa$ 's are all of the same order  $E$  will decay mainly to leptons of the third family. Figure 5.3 reflects this fact and only considers channels with  $\tau$  or  $\nu_\tau$  in the final state. Second, in plot *a*) of figure 5.3 we notice that the rates decrease when  $m_E$  increases, even though the phase space increases with  $m_E$ ; again, this is due to the  $m_\tau/m_E$  factor, which compensates for the increase in phase space. Thirdly, we note in figure 5.3*b*) that the branching ratios of the  $Z\tau$  and  $H\tau$  channels converge as  $m_E$  increases; interestingly, the branching ratio of the  $W\nu_\tau$  channel converges to twice the value of the other two. This is again a mixing effect: the decays are controlled by mass couplings, and the bosons involved are essentially the components of the scalar Higgs doublet; even when the decay proceeds to  $W$  or  $Z$ , it is the longitudinal component which dominates the process. Therefore, and accordingly with the equivalence theorem –see section 4.7 for more on this topic–, as we progress to high energies the channels reproduce the statistics of the decays to components of  $\phi$ , that is: half the decays to  $\phi^\pm\nu_\tau$  ( $W^\pm\nu_\tau$ ), one quarter to  $\phi_p^0\tau$  ( $Z\tau$ ), and one quarter to  $\phi_s^0\tau$  ( $H\tau$ ).

As for the possible cosmological effects of the new particles and

---

<sup>2</sup> The  $\gamma\ell$  channels are subdominant: since  $U(1)_{\text{em}}$  remains unbroken, flavour-changing vertices involving photons are forbidden at tree level; the corresponding processes occur, but proceed necessarily through loops and are thereby suppressed.

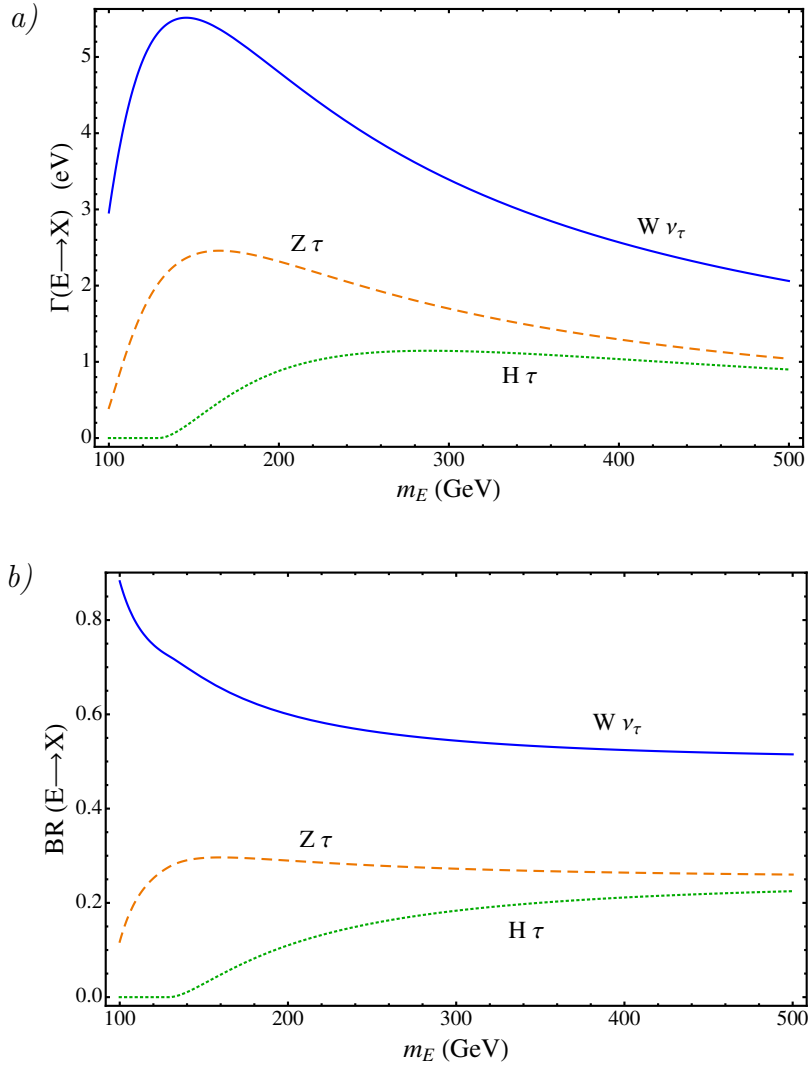


Fig. 5.3: Decay widths and branching ratios for the dominant decay channels of the vector-like fermion  $E$ . The Higgs boson mass has been fixed to  $m_H = 129$  GeV; in  $a)$  we have taken for the mixing  $\kappa_\tau = 1$  GeV.

their decays, for the example value of  $\kappa_\tau = 1$  GeV the decay widths of  $E$  are of the order of the eV. With such lifetimes there will be no  $E$ 's at the epoch of primordial nucleosynthesis and it won't be affected. Note, however, that the decay rates depend upon  $\kappa_\tau^2$ , and  $\kappa_\tau$  is relatively free, so the decay rates can vary in several orders of magnitude depending on the value of  $\kappa_\tau$ . For  $\kappa_\tau < 10^{-7}$  GeV the CHAMP's will affect nucleosynthesis and might help to solve the cosmic lithium problem [227, 228]. They might also affect the CMB by distorting the blackbody spectrum and by modifying the optical depth; these two observables are very sensitive and could impose tight limits on the value of  $\kappa$ . For this discussion we will take a conservative approach and we will just require that the relic CHAMP's have decayed by the present time; this means considering  $\kappa_\tau > 10^{-16}$  GeV.

### 5.3.4 Lepton Flavour Violating processes

For general  $\kappa$ 's and  $Y_e$ 's family lepton flavour is not conserved. It is then mandatory to determine if processes such as  $\mu \rightarrow 3e$ ,  $\mu \rightarrow e\gamma$ , or  $\tau \rightarrow 3\mu$  introduce any restrictions on the parameters of the model. In this section we discuss this possibility.

In order to calculate the amplitudes for these low-energy processes we choose to integrate out the heavy particles that mediate them and use an effective Lagrangian which describes the low-energy interactions of the light leptons. We carry out the integration<sup>3</sup> by using the equations of motion for  $E$  and expanding in powers of  $1/m_E$ . One then obtains

$$\mathcal{L}_{\text{LFV}} = -\frac{i}{m_E^4} \bar{e}_R \kappa \kappa^\dagger (\gamma_\mu D^\mu)^3 e_R + \dots,$$

which, after spontaneous symmetry breaking and using the equations of motion, leads to a lepton-flavour-violating interaction of the  $Z$  with the left-handed component of the charged leptons,

$$\mathcal{L}_{\text{LFV}} = \frac{e}{2 s_W c_W} Z_\mu \bar{e}_L C_{\text{LFV}} \gamma^\mu e_L, \quad C_{\text{LFV}} \simeq \frac{v^2}{2m_E^4} Y_e \kappa \kappa^\dagger Y_e^\dagger. \quad (5.8)$$

<sup>3</sup> For a detailed example of the integration procedure in the case of a singly-charged scalar see [229].

$C_{\text{LFV}}$  is a matrix in flavour space which is not, in general, diagonal; therefore, the interaction (5.8) will induce processes such as  $\mu \rightarrow 3e$  and  $\tau \rightarrow 3\mu$ . Without loss of generality we can take  $Y_e$  diagonal with elements proportional to the charged lepton masses; then we can estimate the branching ratio for  $\mu \rightarrow 3e$  as

$$\text{BR}(\mu \rightarrow 3e) = \frac{\Gamma(\mu \rightarrow 3e)}{\Gamma(\mu \rightarrow e\nu\bar{\nu})} \simeq \frac{|m_e(\kappa\kappa^\dagger)_{e\mu}m_\mu|^2}{m_E^8}.$$

Our effective Lagrangian is an expansion in powers of  $1/m_E$  which could be compensated, in part, by  $\kappa\kappa^\dagger$  factors in the numerator; thus, for consistency, we should require  $\kappa < m_E$ , which allows us to establish an upper bound on the branching ratio. Recalling also that the present limit on the mass of charged heavy leptons is  $m_E > 100$  GeV [32], we obtain

$$\text{BR}(\mu \rightarrow 3e) < \left( \frac{m_\mu m_e}{(100 \text{ GeV})^2} \right)^2 < 10^{-16},$$

to be compared with present bounds, which are of the order of  $10^{-12}$  [32]. As we see, the model contribution to  $\mu \rightarrow 3e$  is still far from being observable, even taking large values of  $\kappa$ .

We can use the same reasoning to calculate the model contribution to  $\tau \rightarrow 3\mu$ ; it is enough to notice that once  $\kappa$  is fixed  $\mu \rightarrow 3e$  and  $\tau \rightarrow 3\mu$  only differ in a kinematical factor of  $(m_\tau/m_\mu)^2$ :

$$\text{R}(\tau \rightarrow 3\mu) \equiv \frac{\Gamma(\tau \rightarrow 3\mu)}{\Gamma(\tau \rightarrow \mu\nu\bar{\nu})} < \left( \frac{m_\tau m_\mu}{(100 \text{ GeV})^2} \right)^2 < 10^{-10},$$

which is, too, under the present sensitivity for this process, fixed at about  $10^{-7}$  [32].

Another very restrictive process is  $\mu \rightarrow e\gamma$ , whose branching ratio is bounded at  $5.7 \times 10^{-13}$  by the MEG experiment [230]. The collaboration expects to improve this limit to roughly  $10^{-13}$  [231]. However, this process only arises in our model at one loop, and therefore we do not expect stringent bounds from it. A further possibility would be the electroweak oblique parameters, but as the new particles are singlets under  $SU(2)$  they only enter in the  $W$  self-energies through mixing,

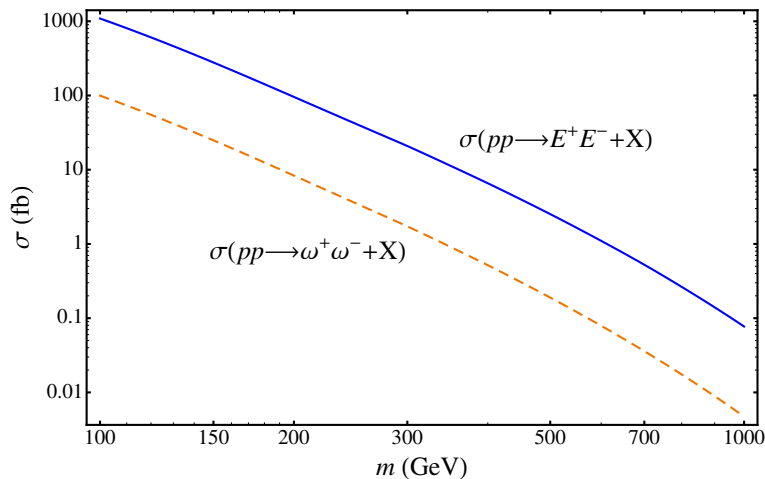


Fig. 5.4: Production cross sections of the charged particles at the LHC, calculated at its nominal center-of-mass energy,  $\sqrt{s} = 14$  TeV.  $m$  represents either  $m_E$  or  $m_\omega$ , as it corresponds for each curve.  $X$  represents that in a proton-proton collider we expect to generate together with the heavy particle pair other hadronic or leptonic products.

suppressed by powers of the masses of the light leptons; therefore, their contributions are too small to be observed at the currently available precision.

Finally there is  $\mu - e$  conversion in nuclei, which also provides strong limits; for instance,  $\mu - e$  conversion in titanium yields  $\sigma(\mu^- \text{Ti} \rightarrow e^- \text{Ti}) / \sigma(\mu^- \text{Ti} \rightarrow \text{capture}) < 4.3 \times 10^{-12}$  [232]. In our model, the process is induced by exactly the same interaction (5.8) that gives  $\mu \rightarrow 3e$ , and we again do not expect, at the present, a strong bound. However, given the future plans to improve the limits in several orders of magnitude [233, 234], then perhaps  $\mu - e$  conversion will provide the best bound for LFV-ing processes in this model. In any case, current data on LFV cannot constrain this mechanism for  $E$  decays.

### 5.3.5 The model at colliders

Despite the fact that the new particles are  $SU(2)$  singlets and only have Yukawa couplings to right-handed neutrinos, they have electric charge and can be copiously produced at the LHC, if light enough, through the Drell-Yan process. In figure 5.4 we show the production cross sections for a proton-proton collision at the LHC. To compute these cross sections we calculated the corresponding quark-antiquark collision and convoluted its cross section with the parton distribution functions of the proton<sup>4</sup>. Since the particles are produced by  $\gamma$  and  $Z$  exchange, there are no unknown free parameters except for the masses of the particles. We see that cross sections from 1 fb to 1 pb are easily obtained for the production of  $E^+E^-$  pairs with  $100 \text{ GeV} < m_E < 700 \text{ GeV}$ . For equal masses the production cross section for  $\omega$  is roughly one order of magnitude smaller.

Once pair-produced, the particles have to be detected and identified. The characteristic signatures for this identification are very different depending on the lifetimes of the particles, mostly because if the  $E$  and  $\omega$  are long-lived they can be tracked directly in the detectors or, at least, be identified through a displaced decay vertex. The relevant parameter for this behavior is  $\kappa$ , the  $E - e$  mixing. For  $\kappa \lesssim 1 \text{ MeV}$ , the  $E$ 's will have decay lengths roughly over 1 centimeter<sup>5</sup>; additionally, for  $\kappa < 0.2 \text{ MeV}$ , they will go through the detector and behave as a heavy ionizing particle. A lot of work has been carried out to analyse the signatures of CHAMP's inside the detectors –see, for instance, [235], and [236] for a recent improvement–, and also displaced vertices have been discussed – see, for example, [237, 238]. If  $\kappa > 1 \text{ MeV}$  the  $E$ 's will decay near the collision point and behave roughly as a fourth-generation charged lepton.

Discovering the  $\omega$ 's can be much harder, because they will be produced at a significantly lower rate and the signatures of their decays

---

<sup>4</sup> See, for a very clear review on the matter, [189]. In our calculation we used the CTEQ6M parton distribution sets [190] and we checked our results against the CompHEP software [191, 192].

<sup>5</sup> Note that there's room in the parameter space for this kind of effects even if one requires that CHAMP's do not affect the primordial nucleosynthesis, for if  $\kappa > 100 \text{ eV}$  all the  $E$ 's will have decayed before nucleosynthesis.

---

depend strongly on the details of the model. In the  $m_\omega > m_E$  scenario, they will decay quickly into an  $E$  and a heavy neutrino –at least if we want  $h$  and  $h'$  large enough to have significant electroweak moments– and then one has to rely again on the detection of  $E$ 's unless the heavy neutrino provides a cleaner signal, which is unlikely. In any case, we think that the  $E$ 's, produced in a much greater number, should be considered the signature of this model, and perhaps the doorway to understand the  $\omega$  and heavy neutrino decays.

## 6. NEUTRINOLESS DOUBLE BETA DECAY AND NEUTRINO MASSES

Neutrino oscillation and tritium  $\beta$ -decay experiments offer us a picture of stupendously small neutrino masses that claim for an explanation. At the same time, the search for neutrinoless double beta decay is our best shot to elucidate the Dirac or Majorana character of neutrino masses. Indeed, in the classic picture of the process  $0\nu\beta\beta$  is induced by neutrino masses – see, for example, figure 6.1. If we interpret the present and near future  $0\nu\beta\beta$  experiments in this terms, then only degenerate mass regime will be explored – it is possible that we enter the inverse hierarchy regime, but probably we won't be able to completely explore it (see section 6.11 in [140]). However, one can imagine other scenarios: maybe  $\nu$  masses are indeed Majorana but they don't constitute the dominant contribution to  $0\nu\beta\beta$ ; were this the case, a signal in  $0\nu\beta\beta$  would not necessarily pin neutrino masses to the degenerate or inverse hierarchies. In this chapter we examine a class of effective operators that provide such sort of a situation; these operators involve at low energies only the leptons and bosons of the Standard Model. Here we will analyse their relevance in a model-independent way by using effective field theory, whereas in chapters 7 and 8 we will discuss particular models that realise the scenarios described here. This work was carried out together with Arcadi Santamaria, José Wudka, Francisco del Águila and Subhaditya Bhattacharya.

### 6.1 *Violating lepton number through leptons and bosons*

The relationship between neutrino masses and neutrinoless double beta decay is a deep and well-known one; we can state for sure that if  $0\nu\beta\beta$  is observed then neutrino masses are of the Majorana kind, as it



was uncovered in 1982 in a celebrated paper by Schechter and Valle [143]. Beyond this, however, we can say nothing, for the mechanisms generating neutrino masses and, were it the case,  $0\nu\beta\beta$ , are unknown. We want to use effective field theory to investigate this relationship in a model-independent way and, in particular, to examine scenarios where  $0\nu\beta\beta$  is enhanced with respect to neutrino masses; EFT is a good choice for this aim, as both  $0\nu\beta\beta$  and  $\nu$  masses occur at low energies and in most scenarios the physics responsible for LNV lies above the TeV scale.

The exploration of  $0\nu\beta\beta$  and neutrino masses through EFT has been carried out in the past [239–242], usually including operators with quark fields but excluding those which involve gauge bosons; the survey by Babu and Leung [239] specifically states “It may be more difficult to generate such operators at tree level from an underlying renormalisable theory, making them perhaps less interesting for the generation of neutrino masses”. We will focus on the converse situation: operators without quarks but explicitly including the SM gauge bosons; we will explore this scenario and will prove that large families of models can generate such operators.

As a first step, let us briefly (and rather naively) consider how this class of operators might provide  $0\nu\beta\beta$  and neutrino masses. Consider first  $0\nu\beta\beta$ ; the ‘traditional’ mechanism, with all LNV accounted for by neutrino Majorana masses, is displayed in figure 6.1. This scenario would fit among the ones we wish to explore, as no quarks are involved in the effective interaction, but just leptons – and scalar Higgs bosons, which get a VEV, see section 3.1.1. However, this mechanism has been extensively discussed and investigated and we won’t stay on it for long; we will rather take it as a sure reference point and maybe a scenario we’d like to avoid, as we will argue later on. Anyway, how else can  $0\nu\beta\beta$  be generated through effective interactions that only involve leptons and gauge bosons? If we want it to be generated at tree level in the effective theory –and that’s desirable, as we would like large rates of  $0\nu\beta\beta$ – we are left with just two more scenarios: in the first one, depicted in figure 6.2a), the effective interaction involves one  $W$  and one electron, and leaves one neutrino which acts as a  $t$ -channel mediator and is absorbed in a common weak interaction vertex. Note that all

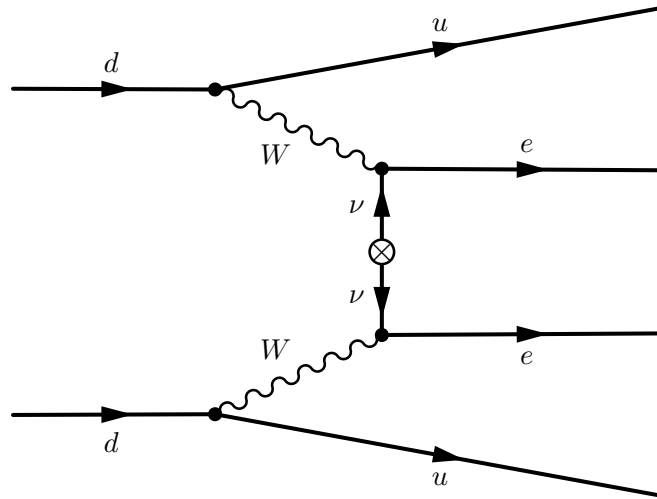


Fig. 6.1: The ‘classical’ mechanism for  $0\nu\beta\beta$ , with a Majorana mass insertion in the internal neutrino propagator; the effective interaction is realised through the well-known Weinberg operator, depicted here as a crossed circle. This can be considered the first and most widely known of three ways of generating  $0\nu\beta\beta$  with effective operators that don’t involve quarks.

the LNV occurs in the effective vertex, and the neutrino does not need to be Majorana to provide  $0\nu\beta\beta$ . This interaction, that we present here in a post-EWSB fashion, can arise from several gauge-invariant nonrenormalisable operators; let us refer from now on to any such kind of vertex as a “ $W\nu e$  interaction”; let us also call “ $W\nu e$  mechanism” to the several processes that yield  $0\nu\beta\beta$  and neutrino masses through the mediation of a  $W\nu e$  vertex.

The second option is displayed in figure 6.2b), and involves a single LNV-ing vertex with two  $W$ ’s and two electrons. There are no more possibilities, as two  $W$ ’s and two electrons are necessarily involved in the process –the first due to the fact that the quarks must transform through the SM weak interaction, and the latter because they’re the observable products of the reaction– and the emission of any other particle in the effective interaction would imply the closing of a loop, which we wish to avoid. We will label from now on this interaction as a

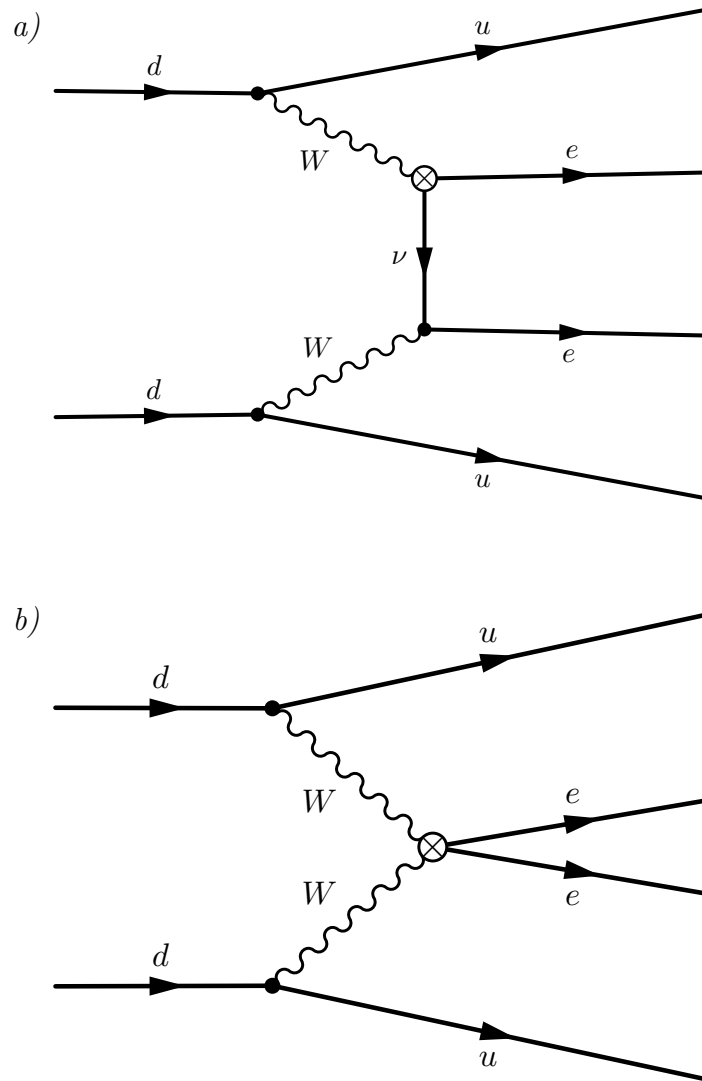


Fig. 6.2: The two ways of generating  $0\nu\beta\beta$  with effective vertices that involve  $W$ 's but not quarks: in *a*), through a  $W\nu e$  vertex; in *b*), through a  $WWee$  interaction.

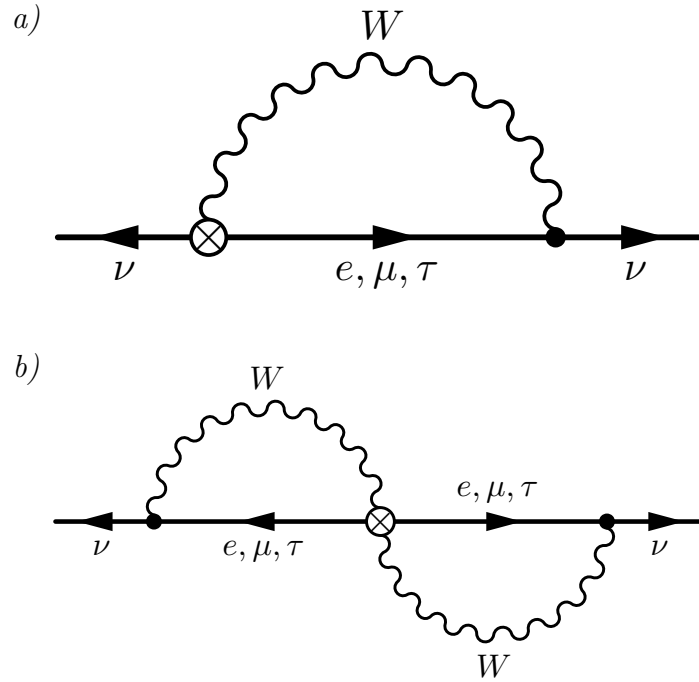


Fig. 6.3: The diagrams that illustrate the generation of neutrino masses a) at one loop, in effective theories with a  $W\nu e$  vertex, and b) at two loops, in effective theories that include a  $WWee$  interaction.

“ $WWee$  vertex”, and the associated processes, the “ $WWee$  mechanism”. Correspondingly, to the Weinberg operator that appears in figure 6.1 we will refer sometimes as a “ $\nu\nu$  interaction”, and to the generation of neutrino masses at tree level and figure 6.1 itself, the “ $\nu\nu$  mechanism”.

On the other hand we have neutrino masses; we want to know what sort of Majorana masses can be associated with the three effective operators we have just described. The first one is trivial: it is already describing a Majorana neutrino mass, which is generated at tree level and that’s all. More interesting are the other two: it is apparent at first sight that every  $W - e$  pair can produce a neutrino by closing a loop. Thus, we would expect the  $W\nu e$  interaction to generate neutrino masses at one loop and the  $WWee$  interaction to generate them at two loops, as seen in figure 6.3. Note, however, that in the effective

theory these radiative neutrino masses are not truly calculable: as the theory is nonrenormalisable, of the loops depicted in figure 6.3 we can only compute the running part; the matching, as is only logical, is lost when we abstract from the underlying, high-energy theory, and cannot be recovered from the low-energy operators. In other words: a complete calculation of the loop-generated neutrino masses requires that we stick with a particular model. In chapters 7 and 8 we offer two such models that allow to specify the loops in figure 6.3 with full detail. In section 6.4 we will comment further on what the effective theory can tell us about neutrino masses.

It's time now, after this somewhat qualitative introduction, to proceed to a formal deduction of these effective operators in an explicitly gauge-invariant form that will allow for practical calculations. In the next section we will work out such a deduction, and in the meantime we will discover a remarkable connection between the chirality of the leptons involved in the effective interaction and the leading mechanism for  $0\nu\beta\beta$ ; this will have consequences for both model-building and radiative generation of neutrino masses.

## 6.2 Identification of the relevant operators. The role of chirality

### 6.2.1 Preliminary remarks

The first step for the design of an effective theory is the choice of the low-energy fields; for this role we will take the whole Standard Model with the usual doublet Higgs field and no further addition, neither new light fermions (in particular we won't consider light right-handed neutrinos) nor any extension of the scalar sector<sup>1</sup>. This election seems reasonable, as the physics responsible for LNV is deemed to lie above the TeV scale. The effective theory will then be constructed by listing all the operators comprised of the SM fields and compatible with the SM local symmetries, including those of dimension greater than four. The effects of new physics, which are necessarily virtual at low energies,

---

<sup>1</sup> But see chapter 7, where we will present a model with a second light Higgs doublet which will simplify our discussion.

are described, or rather parametrised, by the coefficients  $C_i^{(n)}$  which accompany the tower of nonrenormalisable operators. Explicitly, we write

$$\mathcal{L} = \mathcal{L}_{\text{SM}} + \sum_{n=5}^{\infty} \sum_i \left( \frac{C_i^{(n)}}{\Lambda^{n-4}} \mathcal{O}_i^{(n)} + \text{H.c.} \right),$$

where  $n$  denotes the canonical dimension of the operator,  $i$  labels the several independent operators of the same dimension, and  $\Lambda$  represents the NP scale. When the NP contains several scales  $\Lambda > \Lambda' > \dots$  the coefficients  $C$  may contain powers of  $\Lambda/\Lambda'$ . For this analysis we'll be considering all along the new physics to be weakly coupled and decoupling.

Operators contributing to  $0\nu\beta\beta$  decay must involve two leptons of either chirality,  $\ell_L$  or  $e_R$ , and a number of scalar doublets,  $\phi$ , to make the product invariant under  $SU(2)_L \times U(1)_Y$  transformations. Besides, they can have covariant derivative ( $D_\mu$ ) insertions, which do not change the field quantum numbers. It is useful to note that operators differing in an even number of covariant derivatives, say  $\mathcal{O}' \sim D^2\mathcal{O}$ , are generated simultaneously –i.e., at the same loop level– in a given model. This can be understood if we think of the two covariant derivatives as two extra gauge bosons in the effective vertex; if a model can generate  $\mathcal{O}$  at some loop level, then to generate  $\mathcal{O}'$  one only needs to emit a gauge boson at some point in the Feynman diagram and immediately afterwards revert the change with the emission of a second gauge boson. There's a particularly interesting application of this principle for the case we are considering: the no- $W$  operator depicted in figure 6.1 is nothing but a Majorana mass for the neutrinos, and so the Weinberg operator,  $(\bar{\ell}_L\phi)(\tilde{\phi}^\dagger\ell_L)$ . This operator involves two lepton doublets, and so two left-handed leptons, specifically  $\nu_L\nu_L$ ; by this argument, there will be one operator which will be generated along with the Weinberg operator and which only differs from it in two covariant derivatives. This operator will yield an interaction of the form  $WWe_Le_L$ , exactly of the  $WWee$  kind depicted in figure 6.2b). Of course, the  $WWe_Le_L$  interaction will be suppressed with two additional powers of  $\Lambda$  respect to the Weinberg operator and will be subdominant for what  $0\nu\beta\beta$  concerns. But the lesson we must extract from this is that if we want

to model  $0\nu\beta\beta$  according to the  $WWee$  mechanism *we cannot rely on an operator with two left-handed electrons* for it will be generated along with the Weinberg operator, which will take control of the double beta decay. However, if we look for a model generating an operator of the type  $WWe_R e_R$ , which is not directly related to the Weinberg operator, maybe we'll have the option of relegating it to a higher loop level and obtain a  $WWee$ -dominated  $0\nu\beta\beta$ .

We take this idea as an inspirational starting point: in what remains of this section we will prove that chirality can be used to isolate qualitatively different operators that correspond to the three mechanisms described in the previous section. As they *are* qualitatively different, they can be used to devise models in which each of the three mechanisms dominates  $0\nu\beta\beta$  and neutrino masses.

### 6.2.2 Notation

The deduction of effective operators for the SM, and especially this class that includes covariant derivatives, can be a little bit cumbersome due to the need to correctly close Lorentz and  $SU(2)$  indices and to the several Fierz reorderings that can be carried out. In order to simplify the process let us introduce some composite fields with definite lepton number and hypercharge and no  $SU(2)$  charge. As we want to construct operators with just two leptons we will only need a handful of them. First let us present the composite fields with one lepton:

$$\begin{aligned}
 N_\alpha &= \phi^\dagger \tilde{\ell}_{L\alpha} & \Psi_\alpha^\mu &= \phi^\dagger D^\mu \tilde{\ell}_{L\alpha} \\
 Y(N_\alpha) &= 0 & Y(\Psi_\alpha^\mu) &= 0 \\
 L(N_\alpha) &= -1 & L(\Psi_\alpha^\mu) &= -1 \\
 \dim(N_\alpha) &= 5/2 & \dim(\Psi_\alpha^\mu) &= 7/2
 \end{aligned}
 \tag{6.1}$$

where the usual notation has been used for the SM fields – see sections 2.1.2 and 2.1.3. Note that we have selected hyperchargeless combinations of fields in order to make even easier the construction of the effective operators. These fields need not to have a definite physical signification, as they're just artifacts that we are going to use according to their charges and canonical dimension. But anyway, someone might insist; in such a case  $N$  could be regarded as a “left-handed,

$SU(2)$ -singlet lepton”, and  $\Psi$  maybe as a “left-handed, singlet lepton plus a gauge boson”. Indeed, if we let the electroweak symmetry to break spontaneously we obtain

$$\begin{aligned} N_\alpha &= -v \nu_{L\alpha}^c + \dots, \\ \Psi_\alpha^\mu &= -v \left[ \left( \partial^\mu + \frac{i}{2} \frac{g}{\cos \theta_W} Z^\mu \right) \nu_{L\alpha}^c + \frac{ig}{\sqrt{2}} W^\mu e_{L\alpha}^c \right] + \dots, \end{aligned} \quad (6.2)$$

where the ellipsis denote the terms involving the physical Higgs boson, which are not of interest for our study. Note that  $N$  represents in the end just a left-handed neutrino, whereas  $\Psi$  is a more complicated combination of fields. Note also that we have not defined a composite field involving the right-handed  $SU(2)$  singlets; as they only carry hypercharge and lepton number it's not difficult to add them directly to the effective operators when needed.

Let us now go ahead to composite fields with two leptons; as we are interested in two-lepton operators, such composite fields must comprise all the leptonic content in the final operator; and as we want the operators to violate lepton number in two units, so must do the composite field. It so happens that there is only one field combination that fulfils all these conditions and cannot be built from  $N$  or  $\Psi$  through Fierz rearrangements. It is this one here:

$$\begin{aligned} J_{\alpha\beta}^\mu &= \bar{\ell}_{L\alpha} D^\mu \tilde{\ell}_{L\beta} \\ Y(J_{\alpha\beta}^\mu) &= 1 \\ L(J_{\alpha\beta}^\mu) &= -2 \\ \dim(J_{\alpha\beta}^\mu) &= 4, \end{aligned} \quad (6.3)$$

which might be described as a “LNV-ing leptonic current plus a gauge boson”; indeed after SSB it takes the somewhat convoluted form

$$\begin{aligned} J_{\alpha\beta}^\mu &= \bar{\nu}_{L\alpha} \left[ \overleftrightarrow{\partial}^\mu - ig \left( \frac{\cos 2\theta_W}{2 \cos \theta_W} Z^\mu + \sin \theta_W A^\mu \right) \right] e_{L\beta}^c + \\ &+ \frac{ig}{\sqrt{2}} \left( W^{\mu\dagger} \bar{\nu}_{L\alpha} \nu_{L\beta}^c - W^\mu \bar{e}_{L\alpha} e_{L\beta}^c \right) - \frac{ig}{2} \frac{1}{\cos \theta_W} Z^\mu \bar{e}_{L\alpha} \nu_{L\beta}^c. \end{aligned} \quad (6.4)$$



This exhausts the list of leptonic pieces that we are to use. Now only one more element is needed: if we look at (6.3) we see that  $J$  has hypercharge 1; we don't have, however, any other piece that can cancel such hypercharge, were we to use  $J$  at some point:  $N$  and  $\Psi$  are hyperchargeless, the leptonic right-handed singlets would yield too many leptons in the operator, and the combination  $\phi^\dagger \tilde{\phi}$  vanishes with just one scalar doublet. We need, so, one more bosonic composite field; it must be analogous to  $\phi^\dagger \tilde{\phi}$ , but nonzero. The only option is to add a vector boson:

$$\begin{aligned}\mathcal{W}^\mu &= \phi^\dagger D^\mu \tilde{\phi} \\ Y(\mathcal{W}^\mu) &= -1 \\ L(\mathcal{W}^\mu) &= 0 \\ \dim(\mathcal{W}^\mu) &= 3.\end{aligned}\tag{6.5}$$

This  $\mathcal{W}$  operator is a sort of “hidden gauge boson” plus other terms with scalar fields, as we can see by letting  $\phi$  take a VEV:

$$\mathcal{W}^\mu = -i \frac{g}{\sqrt{2}} v^2 W^\mu + \dots\tag{6.6}$$

With all these elements we are ready to begin our task. Just remember a few rules that must be observed while constructing the operators:

- i)* **Only two leptons:** We only want two leptons in our effective operator, in order to generate  $0\nu\beta\beta$  with no loops. This rapidly exhausts the possible combinations of fields; for example, if  $J$  is used there's no room for more leptons.
- ii)* **Right-handed singlets:** The composite fields  $N$ ,  $\Psi$ ,  $J$  and  $\mathcal{W}$  contain only left-handed leptons; the right-handed singlets  $e_{R\alpha}$  must be added by hand whenever convenient. Recall their charge assignments and dimensionality:

$$Y(e_{R\alpha}) = -1 \qquad L(e_{R\alpha}) = 1 \qquad \dim(e_{R\alpha}) = 3/2$$

- iii)* **Watch out for hypercharge:** Hypercharge constrains considerably the possible combinations:  $N$  and  $\Psi$  are hyperchargeless,

and  $J$ ,  $\mathcal{W}$  and  $e_R$  have unit hypercharge (with various signs), but  $J$  and  $e_R$  cannot be combined.

*iv) Close Lorentz indices:*  $\Psi_\mu$ ,  $J_\mu$  and  $\mathcal{W}_\mu$  have a Lorentz four-vector index; they can be closed with one another, but also by using any Dirac matrix, like  $\gamma_\mu$  or  $\sigma_{\mu\nu}$ , or additional derivatives. Derivatives acting upon the composite fields or lepton singlets must be adapted to their charge content; for example,  $N$  and  $\Psi$  are hyperchargeless singlets, so they require just common partial derivatives,  $\partial_\mu$ . All the pieces we are to use are  $SU(2)$  singlets, so these ‘external’ derivatives will never include the  $SU(2)$  generators or gauge bosons.

Finally, remember that  $N$ ,  $\Psi$  and  $e_R$  have spinorial indices that must also be closed in a consistent way.

### 6.2.3 Operators with two left-handed leptons

This class of operators comprises, as we already anticipated, the Weinberg operator and several other higher-order operators. They must be constructed without using the right-handed singlets  $e_{R\alpha}$ , and remember that they must violate lepton number in two units,  $\Delta L = \pm 2$ . The lowest-order operator can be built using only the  $N$  fields; it is of dimension five, and reads

$$\mathcal{O}_{\alpha\beta}^{(5)} = \overline{N}_\alpha N_\beta^c = - \left( \overline{\ell_{L\alpha}} \phi \right) \left( \tilde{\phi}^\dagger \ell_{L\beta} \right) = v^2 \overline{\nu_{L\alpha}^c} \nu_{L\beta}. \quad (6.7)$$

Of course, as expected this operator is nothing but the Weinberg operator, and generates tree-level neutrino masses suppressed by just one power of the new physics scale.

At dimension 6 we don’t find any operator of our interest: all LNV-ing operators at this level involve quarks and also violate baryon number in one unit; they are, thus, not useful for providing  $0\nu\beta\beta$  and neutrino masses without additional new physics. At dimension 7, however, several possibilities appear: first we find an operator which is made of  $\mathcal{O}^{(5)}$  plus a SM-singlet pair of scalar doublets,  $(\phi^\dagger\phi)$ ; but this operator does not provide a new mechanism for  $0\nu\beta\beta$  or neutrino masses, and we will ignore it. The interesting dimension-7 operators

are those which are structurally different from  $\mathcal{O}^{(5)}$ , and it's easy to check that there're only three of them:

$$\begin{aligned}\mathcal{O}_{\alpha\beta}^{(7\text{I})} &= \overline{N_\alpha^c} \partial_\mu \Psi_\beta^\mu = - \left( \overline{\ell_{L\alpha}} \tilde{\phi} \right) \partial_\mu \left( \phi^\dagger D^\mu \tilde{\ell}_{L\beta} \right) \\ \mathcal{O}_{\alpha\beta}^{(7\text{II})} &= \overline{\Psi_{\alpha\mu}^c} \Psi_\beta^\mu = - \left( \overline{D_\mu \ell_{L\alpha}} \tilde{\phi} \right) \left( \phi^\dagger D^\mu \tilde{\ell}_{L\beta} \right) \\ \mathcal{O}_{\alpha\beta}^{(7\text{III})} &= J_{\alpha\beta}^\mu \mathcal{W}_\mu = \left( \overline{\ell_{L\alpha}} D^\mu \tilde{\ell}_{L\beta} \right) \left( \phi^\dagger D_\mu \tilde{\phi} \right)\end{aligned}$$

By looking at (6.2), (6.4) and (6.6) we see that all three operators yield vertices of the type  $W\nu_L e_L$ ; additionally,  $\mathcal{O}^{(7\text{III})}$  also provides a  $WW e_L e_L$  interaction. We could think that these operators can be a source for the mechanisms described in section 6.1, but they are not: they differ from  $\mathcal{O}^{(5)}$  in two covariant derivatives, and so they will be produced always together with it.  $\mathcal{O}^{(5)}$  will yield neutrino masses at tree level and the  $\mathcal{O}^{(7)}$ 's will provide them through loops;  $\mathcal{O}^{(5)}$  will give  $0\nu\beta\beta$  suppressed by  $\Lambda^{-1}$ , whereas the  $\mathcal{O}^{(7)}$ 's will be suppressed by  $\Lambda^{-3}$  – with the  $\Lambda$  scale identical for one and the others, as all of them are generated by the same physics. All effect of these left-left  $\mathcal{O}^{(7)}$ 's, therefore, will be subdominant; they cannot provide leading and observable  $W\nu e$ - and  $WW ee$ -like mechanisms. To produce such mechanisms we need to resort to operators with one or more right-handed lepton. Let us in the next two sections derive such operators.

#### 6.2.4 Operators with one left- and one right-handed lepton

For this class of operators we need the usual two-unit violation of lepton number and one leptonic singlet,  $e_R$ ; the field  $J$  will be therefore forbidden, as its use would yield one lepton too many. If we study the possible combinations of the remaining fields we easily see that there's only one lowest-order operator, and it is of dimension 7:

$$\mathcal{O}_{\alpha\beta}^{(7)} = \overline{e_{R\alpha}} \gamma^\mu N_\beta \mathcal{W}_\mu = \overline{e_{R\alpha}} \gamma^\mu \left( \phi^\dagger \tilde{\ell}_{L\beta} \right) \left( \phi^\dagger D_\mu \tilde{\phi} \right). \quad (6.8)$$

We label it just “ $\mathcal{O}^{(7)}$ ”, as it is the only dimension 7 operator that we will be considering from now on. By looking at (6.2) and (6.6) we identify that this  $\mathcal{O}^{(7)}$  provides a vertex

$$\mathcal{O}_{\alpha\beta}^{(7)} = i \frac{g}{\sqrt{2}} v^3 W_\mu \overline{e_{R\alpha}} \gamma^\mu \nu_{L\beta}^c + \dots, \quad (6.9)$$

plus many others that involve the physical Higgs boson. This vertex will be the starting point for the  $W\nu e$  mechanism. We will not discuss here any other higher-order operator of this class, even if they could eventually prove independent from  $\mathcal{O}^{(7)}$  and thus provide their own sources for the  $W\nu e$  interaction; as  $\mathcal{O}^{(7)}$  is the least suppressed of this family of operators we will concentrate our analysis on it.

### 6.2.5 Operators with two right-handed leptons

For this class of operators all leptons are provided by the  $SU(2)$  singlets  $e_R$ ; hence, of the composite fields only  $\mathcal{W}$  will be available. As happened with the left-right class, we soon realise that with these elements there is only one lowest-order operator violating LN in two units; it appears at dimension 9, and reads

$$\mathcal{O}_{\alpha\beta}^{(9)} = \overline{e_{R\alpha}} e_{R\beta}^c \mathcal{W}^\mu \mathcal{W}_\mu = \overline{e_{R\alpha}} e_{R\beta}^c \left( \phi^\dagger D^\mu \tilde{\phi} \right) \left( \phi^\dagger D_\mu \tilde{\phi} \right). \quad (6.10)$$

As in the previous case, this one will be the only dimension 9 operator we will be considering, so we label it just “ $\mathcal{O}^{(9)}$ ”. By letting electroweak symmetry to break we find this operator to yield an interaction

$$\mathcal{O}_{\alpha\beta}^{(9)} = -\frac{g^2}{2} v^4 W^\mu W_\mu \overline{e_{R\alpha}} e_{R\beta}^c + \dots$$

plus others involving the physical Higgs boson; this interaction will be the basis for the  $WWee$  mechanism. As with the left-right operators we won't consider higher-order interactions of this class, as  $\mathcal{O}^{(9)}$  is the least suppressed of all; such investigation might be interesting if other, higher-order operators can be generated independently of  $\mathcal{O}^{(9)}$ .

### 6.2.6 A note to the model builder

In this section we have derived the gauge-invariant form of the lowest-order effective vertices that generate the  $\nu\nu$ ,  $W\nu e$  and  $WWee$  interactions. We have observed that the chirality of the involved leptons allows to select a set of operators which dominantly contribute to just one of the mechanisms; in other words, chirality helps not to mix the three mechanisms at the effective theory level. But at the level of

the underlying model the situation can be different: if lepton number is broken, all three  $\mathcal{O}^{(5)}$ ,  $\mathcal{O}^{(7)}$  and  $\mathcal{O}^{(9)}$  are to be generated; this is inevitable, and in general the three mechanisms will compete and mix. As model builders, in many cases we will want this not to happen. This issue can be addressed by imposing restrictions on the model, usually in the form of additional symmetries; the point will be to relegate the generation of the unwanted operators to a higher loop level and, equally important, to make sure that they are generated through the same physics as the one we want to focus on.

For instance, consider this rather paradigmatic case: we want to produce a model where  $0\nu\beta\beta$  and the neutrino masses are dominated by the  $WWee$  mechanism. We have a model that generates  $\mathcal{O}^{(9)}$  at tree level, that's all right, but it also generates  $\mathcal{O}^{(5)}$  at tree level. This poses a double trouble: first,  $\mathcal{O}^{(5)}$  is going to compete with  $\mathcal{O}^{(9)}$  for the preeminence in  $0\nu\beta\beta$ , but as  $\mathcal{O}^{(5)}$  is suppressed by  $\Lambda^{-1}$  and  $\mathcal{O}^{(9)}$  by  $\Lambda^{-5}$ , the  $\nu\nu$  mechanism is bound to win. Consequently, we devise a suitable symmetry which forbids some of the couplings that yield  $\mathcal{O}^{(5)}$ ; it's gone, and problem solved. But lepton number is broken, and it reappears at one loop through the mediation of other couplings; it is not anymore a threat to  $0\nu\beta\beta$ , because it's loop-suppressed, but it yields one-loop neutrino masses which compete with the two-loop masses generated by  $\mathcal{O}^{(9)}$ . We apply the same principle again: look for the way to forbid any of the relevant couplings for the one-loop generation of  $\mathcal{O}^{(5)}$ . And again it goes away. But at two loops... here it is once more. But of course it is:  $\mathcal{O}^{(9)}$  generates neutrino masses at two loops; we realise that the diagrams generating  $\mathcal{O}^{(5)}$  are nothing but the same that yield neutrino masses through  $\mathcal{O}^{(9)}$ . So we can just forget about  $\mathcal{O}^{(5)}$ : the  $WWee$  mechanism explains it all, and if we control  $\mathcal{O}^{(9)}$  we control the  $WWee$  mechanism. Moral: the problem is *not* the presence of  $\mathcal{O}^{(5)}$ ; you cannot, in fact, avoid its presence. The problem is, rather, if it arises from some physics independent of the operator you're interested in; then it competes, and it probably spoils some of your plans. If you can control the generation of the unwanted operators to the point that they arise from the operator you want to dominate, then everything will probably be all right. We will find, in chapters 7 and 8, particular examples of how to deal with these issues.

### 6.3 Implications for neutrinoless double beta decay

The fundamental parameter of an effective theory is the new physics scale,  $\Lambda$ . It is easy just by intuition to understand that  $0\nu\beta\beta$  can provide a *lower* bound for it: the higher  $\Lambda$ , the lower the  $0\nu\beta\beta$  rate; we have upper bounds on this rate, so they must translate into lower bounds on  $\Lambda$ . This is the main purpose of this section. For that aim we will use the limits on  $0\nu\beta\beta$  in  $^{76}\text{Ge}$  [243]; as the traditional picture for  $0\nu\beta\beta$  is that mediated by neutrino masses –what we have called the  $\nu\nu$  mechanism–, the limit is usually expressed in such terms, and written

$$m_{\beta\beta} \equiv |m_{ee}| < 0.24 - 0.5 \text{ eV}. \quad (6.11)$$

But we would prefer a more versatile expression, one that can be easily applied to the  $W\nu e$  and  $WWee$  mechanisms, as they do not directly involve neutrino masses. To derive such an expression we first estimate the amplitude of the  $\nu\nu$  process by looking at figure 6.1,

$$|\mathcal{A}_{0\nu\beta\beta}^{(\nu\nu)}| \sim \frac{G_F^2}{p_{\text{eff}}^2} |m_{ee}|. \quad (6.12)$$

Here  $p_{\text{eff}}$  represents the energy scale of  $0\nu\beta\beta$ ,  $p_{\text{eff}} \sim m_\pi$ , which is the dominant scale in the neutrino propagators. From (6.12) we construct a dimensionless quantity that we can bound by using (6.11):

$$\frac{p_{\text{eff}}}{G_F^2} |\mathcal{A}_{0\nu\beta\beta}^{(\nu\nu)}| \sim \frac{|m_{ee}|}{p_{\text{eff}}} < 5 \times 10^{-9}, \quad (6.13)$$

and then we note that the amplitudes for the  $W\nu e$  and  $WWee$  mechanisms have the same dimensionality as  $\mathcal{A}_{0\nu\beta\beta}^{(\nu\nu)}$  (look for example at figures 6.5 and 6.6, and notice that each mechanism removes from the diagram one neutrino propagator but adds a  $v/\Lambda^2$  factor); so, the quantity displayed in (6.13) is also dimensionless for the other mechanisms, and can be used directly to derive bounds for them.

#### *Bounds on $\mathcal{O}^{(5)}$*

The previous discussion essentially gives us all the elements: when the  $\nu\nu$  mechanism is realised by  $\mathcal{O}^{(5)}$ , neutrinoless double beta decay looks

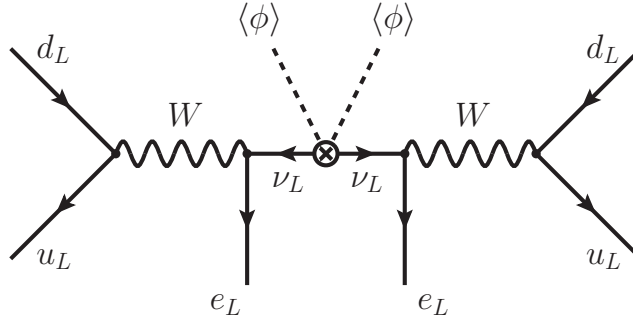


Fig. 6.4: The process of  $0\nu\beta\beta$  through the  $\nu\nu$  mechanism, particularised here to the  $\mathcal{O}^{(5)}$  operator.

as in figure 6.4; then we have

$$|\mathcal{A}_{0\nu\beta\beta}^{(5)}| \sim \frac{G_F^2}{p_{\text{eff}}^2} \frac{v^2}{\Lambda} |C_{ee}^{(5)}|, \quad (6.14)$$

and so, by applying (6.13) we obtain a terrific bound,

$$\frac{\Lambda}{|C_{ee}^{(5)}|} > 10^{11} \text{ TeV}. \quad (6.15)$$

This result would put the particles responsible for the  $\nu\nu$  mechanism way beyond the reach of any present or planned experiment, unless  $C_{ee}^{(5)}$  proves to be extremely small. This is the main reason why we turn to the other two mechanisms, that yield less pessimistic prospects from the experimental point of view.

#### Bounds on $\mathcal{O}^{(7)}$

Figure 6.5 depicts  $0\nu\beta\beta$  mediated by  $\mathcal{O}^{(7)}$ ; from there we can estimate

$$|\mathcal{A}_{0\nu\beta\beta}^{(7)}| \sim \frac{G_F^2}{p_{\text{eff}}^2} \frac{v^3}{\Lambda^3} |C_{ee}^{(7)}|, \quad (6.16)$$

and then from (6.13)

$$\frac{\Lambda}{|C_{ee}^{(7)}|^{1/3}} > 100 \text{ TeV}.$$

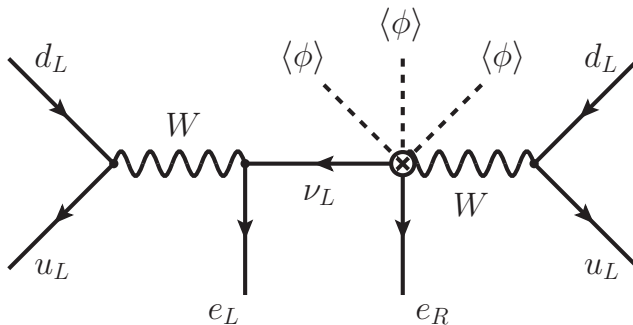


Fig. 6.5: The process of  $0\nu\beta\beta$  as generated by the  $W\nu e$  mechanism, particularised here to the  $\mathcal{O}^{(7)}$  operator.

These are order-of-magnitude estimates, but one can also use detailed nuclear matrix elements available in the literature to derive bounds on new physics providing  $0\nu\beta\beta$  [144, 244]. The  $W\nu e$  interaction induced by the operator  $\mathcal{O}^{(7)}$  can be expressed as a modification of the standard weak interaction,  $W_\mu \bar{e} \gamma^\mu ((1 - \gamma_5) + \eta(1 + \gamma_5)) \nu$ , where  $\nu = \nu_L + \nu_L^c$  is a Majorana field. Then, the strong limit on  $\eta$  derived using detailed nuclear matrix elements calculations,  $|\eta| < 4.4 \times 10^{-9}$  (note that  $\eta$ , in [144]’s notation, reads  $\epsilon_{V-A}^{V+A}$ ), implies in our case

$$|\eta| = \frac{v^3}{\Lambda^3} |C_{ee}^{(7)}| < 4.4 \times 10^{-9},$$

as can be seen by comparing the definition of  $\eta$  with (6.9). This now translates into a bound which is very close to our estimate:

$$\frac{\Lambda}{|C_{ee}^{(7)}|^{1/3}} > 106 \text{ TeV}. \quad (6.17)$$

#### Bounds on $\mathcal{O}^{(9)}$

A first estimate of the bound can be obtained by looking at figure 6.6; we can write then

$$|\mathcal{A}_{0\nu\beta\beta}^{(9)}| \sim G_F^2 \frac{v^4}{\Lambda^5} |C_{ee}^{(9)}|, \quad (6.18)$$



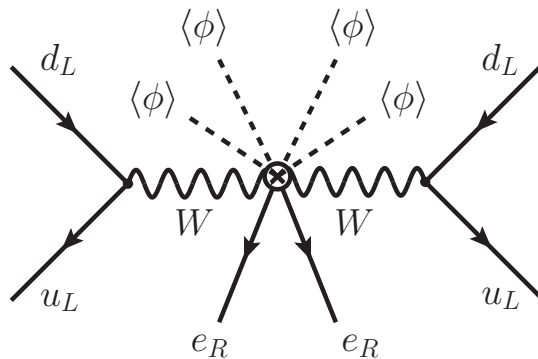


Fig. 6.6: The process of  $0\nu\beta\beta$  as generated by the  $WWee$  mechanism, particularised here to the  $\mathcal{O}^{(9)}$  operator.

and again by comparing with (6.13) we obtain

$$\frac{\Lambda}{|C_{ee}^{(9)}|^{1/5}} > 2 \text{ TeV},$$

which is a rather hopeful bound, suggesting that the physics responsible for the  $WWee$  mechanism might be probed at the LHC. It is thus even more interesting to check the more solid bounds that can be obtained by using detailed nuclear matrix element calculations [145]. In this work the authors derive bounds for the coefficients of effective six-fermion interactions that provide  $0\nu\beta\beta$ ; the six-fermion interaction induced by  $\mathcal{O}^{(9)}$ , with [145]'s notation and normalisation, reads

$$\mathcal{L}_{0\nu\beta\beta} = \frac{G_F^2}{2m_p} \epsilon_3 (\bar{u}\gamma^\mu(1-\gamma_5)d) (\bar{u}\gamma_\mu(1-\gamma_5)d) \bar{e}(1-\gamma_5)e^c,$$

where  $m_p$  denotes the proton mass, and for our case

$$\epsilon_3 = -2m_p \frac{v^4}{\Lambda^5} C_{ee}^{(9)}.$$

Now we read from [145] the bound for this particular type of new physics,  $|\epsilon_3| < 1.4 \times 10^{-8}$  at 90% CL<sup>2</sup>, and from there we derive

$$\frac{\Lambda}{|C_{ee}^{(9)}|^{1/5}} > 2.7 \text{ TeV}, \quad (6.19)$$

which is very close to our estimate, and emphasises the interest of  $\mathcal{O}^{(9)}$  from the experimental point of view, as the new particles that generate it could be at the reach of the LHC; see, for more on this, the model we discuss in chapter 8.

#### 6.4 Implications for neutrino masses

Once the effective theory generates one of the LNV-ing operators that produce  $0\nu\beta\beta$ , neutrinos will get a mass at some loop order, even if there is no other independent source of neutrino masses – see figure 6.3; the three operators  $\mathcal{O}^{(5)}$ ,  $\mathcal{O}^{(7)}$  and  $\mathcal{O}^{(9)}$  not only stand for new physics at quite different mass scales, but also result in different neutrino mass structures. In this section we want to discuss the details and restrictions that arise for neutrino mass generation in each mechanism.

First note that at the effective theory level we can obtain nothing but estimates. The diagrams in figure 6.3 involve one or two loops, and nonrenormalisable theories do not provide unambiguous calculations of divergent diagrams without resorting to matching, that is, without specifying a concrete high-energy model. As our aim in this chapter is to draw general conclusions, we will stick to the estimates; later, in chapters 7 and 8 we will discuss particular realisations of the effective mechanisms and we will check that these estimates indeed yield reasonable results.

Second, we need a quantity that we can impose to the generated neutrino mass matrices, something that more or less captures ‘the correct neutrino mass scale’. Unfortunately, our lack of knowledge about the neutrino mass eigenvalues –see section 3.2.2 for a brief discussion– makes it difficult to state even the order of magnitude of

---

<sup>2</sup> Actually there is a misprint in reference [145]. We are very grateful to the authors for providing us with the correct limit on  $\epsilon_3$ .

particular elements of the mass matrix. However, we can devise an argument that is reasonable at least for the families of models that we are considering now: first note that even if we don't know the absolute scale of neutrino masses, the atmospheric mass splitting –see table 3.1– points to a scale of at least 0.05 eV. Second, note from the diagrams in figure 6.3 that we expect the elements of the generated mass matrices to be suppressed by powers of the corresponding charged lepton mass – as a chirality flip is needed to close the loop, see figures 6.7 and 6.8. Thus, we can expect generically that the electron and muon elements of the neutrino mass matrix are rather small, but still some pieces of the mass matrix must account for a  $\sim 0.05$  eV scale; the natural candidates are the tau elements. In conclusion, we will take as a reasonable assumption for the neutrino mass matrix, sensible at least for these classes of models, that  $|m_{\tau\tau}| \sim 0.1$  eV. From this assumption we will derive order-of-magnitude estimates for the scales of new physics of the effective interactions.

#### *Neutrino masses from $\mathcal{O}^{(5)}$*

In the  $\nu\nu$  mechanism neutrino masses are generated trivially at tree level once the electroweak symmetry breaks spontaneously. To estimate the scale of new physics for this mechanism we just observe from (6.7) that

$$m_{\tau\tau} = -2C_{\tau\tau}^{(5)*} \frac{v^2}{\Lambda}.$$

Then, imposing  $|m_{\tau\tau}| \sim 0.1$  eV we conclude

$$\frac{\Lambda}{|C_{\tau\tau}^{(5)}|} \sim 6 \times 10^{11} \text{ TeV},$$

which is of the same order as the bound we obtained from  $0\nu\beta\beta$  for this mechanism, equation (6.15). Beware, this is by no means an indication that the  $\nu\nu$  mechanism is about to yield a signal in  $0\nu\beta\beta$ . It is just a reflection that both neutrino masses and  $0\nu\beta\beta$  are tree-level processes for this mechanism; thus, since the bound on  $m_{ee}$  from  $0\nu\beta\beta$  and the bound on  $m_{\nu e}$  from direct searches are of the same order, the two estimates yield similar results.

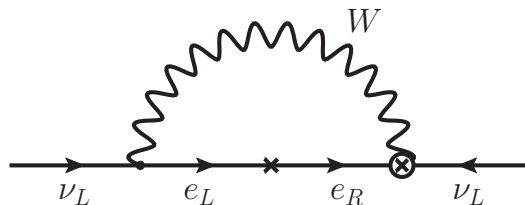


Fig. 6.7: The diagram that generates neutrino masses at one loop with one  $\mathcal{O}^{(7)}$  insertion.

### Neutrino masses from $\mathcal{O}^{(7)}$

In this case the neutrino masses are generated at one loop, as can only be expected given that the effective interaction yields one neutrino and one charged lepton; we need thus to close a loop with the  $W$  and the  $e_R$  to produce a second left-handed neutrino, as we see in figure 6.7. Notice also that as the charged lepton is right-handed a chirality flip, i.e., a mass insertion, is needed; the generated neutrino masses, thus, will be additionally suppressed by one power of the charged lepton masses. When considering particular models this mechanism for providing neutrino masses will happen one loop above the generation of  $\mathcal{O}^{(7)}$ ; in chapter 7 we present a model that realises the least-suppressed scenario:  $\mathcal{O}^{(7)}$  is generated at tree level, and so neutrino masses at one loop.

What can we say about these masses from the EFT point of view? The effective theory can provide logarithmic contributions to the loop depicted in figure 6.7; these contributions are calculable and are obtained in standard effective-field-theoretical fashion using dimensional regularisation and a renormalisable gauge. We obtain for them

$$\delta m_{\alpha\beta} \sim \frac{v^3}{16\pi^2\Lambda^3} \left( m_\alpha C_{\alpha\beta}^{(7)} + m_\beta C_{\beta\alpha}^{(7)} \right) \ln \frac{\Lambda}{v},$$

where the  $m_\alpha$  are understood to be charged lepton masses, whereas  $m_{\alpha\beta}$  represents an element of the neutrino mass matrix. These logarithmic contributions, however, are subleading; the dominant contributions to the loop come from the matching of the effective theory with the

underlying model, which cannot of course be calculated in general. We can nonetheless estimate them using dimensional analysis, and we obtain

$$m_{\alpha\beta} \sim \frac{v}{16\pi^2\Lambda} \left( m_\alpha C_{\alpha\beta}^{(7)} + m_\beta C_{\beta\alpha}^{(7)} \right). \quad (6.20)$$

Notice, however, that even for this estimation it is important to use a renormalisable gauge, for in the unitary gauge spurious positive powers of  $\Lambda$  may appear. Note too that the matching estimate is only suppressed by one power of  $\Lambda$ ; this is logical, as the Weinberg operator, of dimension five, describes the leading contribution to neutrino masses in the absence of  $\nu_R$ . That is to say: the matching estimate is describing a contribution to the Weinberg operator that is generated one loop above  $\mathcal{O}^{(7)}$ ; even if a dimension seven operator is involved, some powers of the heavy masses will be compensated – dimensionally compensated, we mean – by dimensionful couplings or by the loop integrals in such a way that the final result will be effectively suppressed by just one power of heavy scales. Of course, as always, this  $\Lambda$  needs not to be the mass of an actual particle of the theory; if the theory presents several mass scales it can be a combination of them with dimensions of mass. In the model presented in chapter 8 this is in fact the case; look at equation (8.29), where all  $m_\kappa$ ,  $m_\chi$  and  $\mu_\kappa$  are heavy scales of the model.

Now we can use equation (6.20) to estimate the new physics scale for the  $W\nu e$  models. Requiring once more that  $|m_{\tau\tau}| \sim 0.1$  eV we get

$$\frac{\Lambda}{|C_{\tau\tau}^{(7)}|} \sim 4 \times 10^7 \text{ TeV}, \quad (6.21)$$

which is consistent with the bound from  $0\nu\beta\beta$ , equation (6.17), but points to a much heavier scale. Note that equation (6.17) marks the scales that are about to be explored in the forthcoming  $0\nu\beta\beta$  experiments, and it would be nice to obtain a signal there. Equation (6.21) informs us that in the framework of the  $W\nu e$  mechanism only models that provide very suppressed  $C^{(7)}$  coefficients, with  $|C^{(7)}| \sim 10^{-9}$ , can provide a signal in the next round of  $0\nu\beta\beta$  experiments. This is the case of the model we discuss in chapter 7.

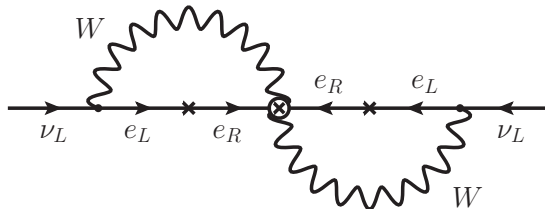


Fig. 6.8: The diagram that generates neutrino masses at one loop with one  $\mathcal{O}^{(9)}$  insertion.

### Neutrino masses from $\mathcal{O}^{(9)}$

The  $\mathcal{O}^{(9)}$  operator provides neutrino masses at two loops, as two charged leptons must be turned into neutrinos; since both leptons are right-handed, two powers of the charged lepton masses will additionally suppress the neutrino masses. The process is shown in figure 6.8. As in the previous section we distinguish between the calculable (logarithmic) contributions,

$$\delta m_{\alpha\beta} \sim \frac{v^4}{(16\pi^2)^2 \Lambda^5} m_\alpha C_{\alpha\beta}^{(9)} m_\beta \ln \frac{\Lambda}{v},$$

which are however subleading, and the dominant contributions from matching, which we cannot but just estimate:

$$m_{\alpha\beta} \sim \frac{1}{(16\pi^2)^2 \Lambda} m_\alpha C_{\alpha\beta}^{(9)} m_\beta. \quad (6.22)$$

Again, by using (6.22) we can estimate the new physics scale for the models that provide the  $WWee$  mechanism. Recalling our reasonable requirement  $|m_{\tau\tau}| \sim 0.1$  eV we obtain

$$\frac{\Lambda}{|C_{\tau\tau}^{(9)}|} \sim 10^3 \text{ TeV}, \quad (6.23)$$

pointing once more to a heavier scale than (6.19), which marks the current limit of observability for the  $0\nu\beta\beta$  effects of  $\mathcal{O}^{(9)}$ . This implies that only models with  $|C^{(9)}| \sim 10^{-4}$  can yield a signal in near-future  $0\nu\beta\beta$  experiments; for models with  $|C_{\tau\tau}^{(9)}| \sim 1$ , the  $WWee$  mechanism

will leave no trace of  $0\nu\beta\beta$ , nor will the new particles show up at the LHC or other planned accelerator experiments. Fortunately, many underlying models can provide small  $C^{(9)}$  coefficients, which would lower the scale in (6.23). In chapter 8 we discuss a model that, although tightly constrained, proves to be able to yield signals in a variety of different experiments while generating acceptable neutrino masses.

### 6.5 Preeminence of the $W\nu e$ and $WWee$ mechanisms in neutrinoless double beta decay

In the previous two sections we described how the  $W\nu e$  and  $WWee$  mechanisms can yield both  $0\nu\beta\beta$  and neutrino masses. Our final aim will be to devise models where these mechanisms lead the generation of these two processes. Neutrino masses, as commented in section 6.2.6, can generally be dealt with by imposing suitable symmetries that forbid the interfering interactions, but  $0\nu\beta\beta$  presents an additional complication: neutrino masses are themselves a source of  $0\nu\beta\beta$ , through the  $\nu\nu$  mechanism. Consequently, it might happen that the new mechanisms generate perfectly acceptable neutrino masses and then these take control of  $0\nu\beta\beta$ . It would be useful to have an indication of under which circumstances our model will be affected by this inconvenience. In this section we will expose a general argument that allows to identify the regime where the new mechanisms overpower their own generated masses in the competition for  $0\nu\beta\beta$ .

First let us consider a theory that provides  $0\nu\beta\beta$  and neutrino masses only through the  $W\nu e$  mechanism. At the model level,  $0\nu\beta\beta$  will be produced by some process and neutrino masses will be generated by other, related process with one additional loop. From the effective theory point of view what we will have is one  $\mathcal{O}^{(7)}$  operator that will yield  $0\nu\beta\beta$  at tree level and one  $\mathcal{O}^{(5)}$  operator that will yield neutrino masses at tree level – remember, the loop diagrams in figure 6.3 are not calculable in the effective theory; the  $\mathcal{O}^{(5)}$  operator accounts at any rate for the loop-generated neutrino masses, with the loop suppression encoded in the coefficient  $C^{(5)}$ . Both  $\mathcal{O}^{(5)}$  and  $\mathcal{O}^{(7)}$  contribute to  $0\nu\beta\beta$ ,

and we can read their contributions from equations (6.14) and (6.16):

$$\begin{aligned}\mathcal{A}_{0\nu\beta\beta}^{(5)} &\sim \frac{G_F^2}{p_{\text{eff}}^2} \frac{v^2}{\Lambda} C_{ee}^{(5)} \\ \mathcal{A}_{0\nu\beta\beta}^{(7)} &\sim \frac{G_F^2}{p_{\text{eff}}} \frac{v^3}{\Lambda^3} C_{ee}^{(7)},\end{aligned}\quad (6.24)$$

where the new physics scale is the same for both contributions, as they all come from the  $W\nu e$  mechanism. The total contribution to  $0\nu\beta\beta$ , then, will be simply  $\mathcal{A}_{0\nu\beta\beta} = \mathcal{A}_{0\nu\beta\beta}^{(5)} + \mathcal{A}_{0\nu\beta\beta}^{(7)}$ , and our question is under which circumstances  $\mathcal{A}_{0\nu\beta\beta}^{(7)}$  is the leading piece. However, the presence of the effective coefficients  $C^{(5)}$  and  $C^{(7)}$  makes it difficult to compare the two terms. We can eliminate them by recalling that neutrino masses connect  $\mathcal{O}^{(7)}$  and  $\mathcal{O}^{(5)}$ ; the neutrino masses in the effective theory emerge from  $\mathcal{O}^{(5)}$ , and they are, by equation (6.7),

$$m_{\alpha\beta} = -2 \frac{v^2}{\Lambda} C_{\alpha\beta}^{(5)*}; \quad (6.25)$$

but at the same time by hypothesis neutrino masses are provided by the  $\mathcal{O}^{(7)}$  interaction, and though we can't calculate them we can estimate them. By equation (6.20):

$$m_{\alpha\beta} \sim \frac{v}{16\pi^2\Lambda} \left( m_\alpha C_{\alpha\beta}^{(7)} + m_\beta C_{\beta\alpha}^{(7)} \right). \quad (6.26)$$

Equations (6.25) and (6.26) can now be used to eliminate  $C_{ee}^{(5)}$  and  $C_{ee}^{(7)}$  in favour of  $m_{ee}$ . Neglecting phases, we have

$$\mathcal{A}_{0\nu\beta\beta} \sim \left( \frac{G_F}{p_{\text{eff}}} \right)^2 \frac{m_{ee}}{2} \left[ 1 + \frac{p_{\text{eff}}}{m_e} (4\pi)^2 \frac{v^2}{\Lambda^2} \right], \quad (6.27)$$

and so the condition for the preeminence of  $\mathcal{O}^{(7)}$  is just

$$\Lambda \lesssim 4\pi v \sqrt{\frac{p_{\text{eff}}}{m_e}} \simeq 35 \text{ TeV}. \quad (6.28)$$

In conclusion: if we want the  $W\nu e$  mechanism to dominate the generation of both neutrino masses and  $0\nu\beta\beta$  we need the new physics



scale to be relatively light. This is good news, for it means that the mechanism can be probed, and eventually ruled out, by direct search of the new particles. Remember, however, that  $\Lambda$  needs not to be the mass of a particle, and so equation (6.28) is only giving us a rough idea of the scale where the generation of  $0\nu\beta\beta$  reverts from one mechanism to the other.

As for the case of the  $WWee$  mechanism, the result is the same as that of the  $W\nu e$  mechanism, equation (6.28). The reason is that by working out equations (6.18) and (6.22) we see that the contribution of  $\mathcal{O}^{(9)}$  to equation (6.27) is the same as for  $\mathcal{O}^{(7)}$  but squared. As we compare with 1, the result is identical. We conclude, so, that we can have preeminence of the  $W\nu e$  and  $WWee$  mechanisms for both neutrino masses and  $0\nu\beta\beta$ , and to achieve that we don't need to renounce the observability of the new particles.

### 6.6 Modeling the lepton-boson mechanisms

In this section we will survey the possible combinations of new particles that can generate the operators  $\mathcal{O}^{(5)}$ ,  $\mathcal{O}^{(7)}$  and  $\mathcal{O}^{(9)}$ . We will do so just by deducing their spin and gauge charges, with no reference to possible new symmetries or interactions, which may be required if one wants to enhance a particular mechanism. So, the listings offered here can be regarded as a first step for the construction of a model. Bear in mind, however, that we will restrict this discussion to sets of particles that generate the relevant operators *at tree level*, in order to obtain large effects in neutrinoless double beta decay. We will assume that the underlying theory is weakly coupled and contains only renormalisable vertices; we also assume the NP respects all the gauge symmetries of the SM. In listing the heavy particles we denote by  $X_T^{(Y)}$ ,  $\Psi_T^{(Y)}$  and  $\Phi_T^{(Y)}$  a heavy vector, fermion or scalar with isospin  $T$  and hypercharge  $Y$ , respectively. When the heavy particles can be either a heavy vector or heavy scalar with the same isospin and hypercharge, we use  $B_T^{(Y)}$  to denote both possibilities.

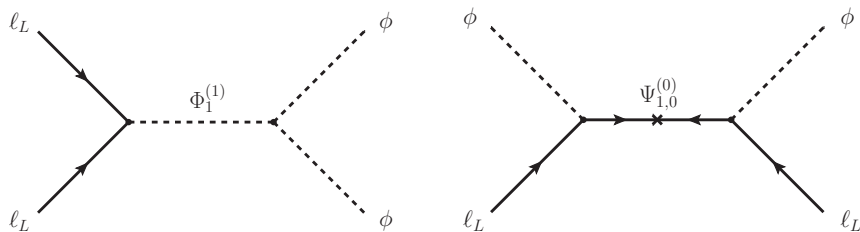


Fig. 6.9: Topologies relevant for the generation of  $\mathcal{O}^{(5)}$ .

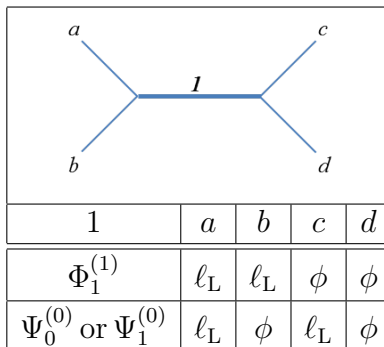
### New physics to generate $\mathcal{O}^{(5)}$

The Weinberg operator,  $\mathcal{O}^{(5)}$ , comprises two leptonic doublets and two scalar doublets; we could represent it by  $\ell_L^2 \phi^2$ , omitting any reference to the closing of spinorial and  $SU(2)$  indices. That essentially means that the Feynman diagram generating  $\mathcal{O}^{(5)}$  must have four external legs, two with  $\ell_L$ 's and two with  $\phi$ 's; there're not so many ways to achieve this. At tree level, and with no nonrenormalisable interactions, there are only two: with two leptons at one side and two scalars at the other, united by a heavy mediator, or with a pair lepton-scalar at each side, united by a heavy mediator. We depict these two possible topologies in figure 6.9; with this in hand, the rest is computing spin and charge sums: in the first case the mediator must be a hypercharge-1,  $SU(2)$ -triplet scalar, and in the second a fermion, either  $SU(2)$  singlet or triplet, with hypercharge 0. We collect these results in table 6.1 in a compact and systematic fashion; this will be useful when considering higher-order operators with more complicated topologies. Note also that the diagrams in figure 6.9 also generate the subleading  $\mathcal{O}^{(7\text{I-III})}$  just by inserting the appropriate number of  $W$ 's into the legs that are not  $SU(2)$  singlets.

To summarise, the new physics additions that can produce  $\mathcal{O}^{(5)}$  are

$$\Psi_0^{(0)} \quad \Phi_1^{(1)} \quad \Psi_1^{(0)}, \quad (6.29)$$

that is to say, exactly the new particle content of so-called seesaws type I, II and III, extensively studied in neutrino mass (i.e. Weinberg operator) generation.



Tab. 6.1: Symbolic representation of the diagrams that can generate  $\mathcal{O}^{(5)}$  at tree level. As we see, roman letters are used to label external (i.e., SM) legs and numbers are used to label internal (i.e., new physics) legs.

### New physics to generate $\mathcal{O}^{(7)}$

The presence of a covariant derivative makes the generation of  $\mathcal{O}^{(7)}$  somewhat more involved, as it consists of several pieces with different gauge boson species. In order to simplify the process it is enough to consider the term of  $\mathcal{O}^{(7)}$  with no gauge bosons:

$$\mathcal{O}^{(7)} = \bar{e}_R \gamma^\mu \left( \phi^\dagger \tilde{\ell}_L \right) \left( \phi^\dagger \partial_\mu \tilde{\phi} \right) + \dots, \quad (6.30)$$

as any model which generates this interaction will necessarily, by gauge invariance, generate also the complete operator. This can be diagrammatically understood by taking a graph that generates (6.30) and attaching the appropriate number of light gauge bosons to the internal heavy propagators, wherever allowed by the quantum numbers. The relevant interaction, so, consists of one  $\ell_L$ , one  $e_R$  and three  $\phi$ 's<sup>3</sup>; this means five external legs in our generating diagram, which can be realised only with one topology: that depicted in table 6.2. A second topology with all three  $\phi$ 's in one vertex and the two leptons at the

<sup>3</sup> Actually, as we see in (6.30),  $\mathcal{O}^{(7)}$  comprises the *charge conjugates* of all these fields, but we prefer not to increase the cumbersomeness of our notation. After all, the physics that generates  $\mathcal{O}^{(7)}$  is the same that generates  $\mathcal{O}^{(7)\dagger}$  but charge-conjugated, so our conclusions remain intact.

1	2	$a$	$b$	$c$	$d$	$e$
$X_{1/2}^{(3/2)}$	$X_0^{(1)}$ or $X_1^{(1)}$	$\ell_L$	$e_R$	$\phi$	$\phi$	$\phi$
$X_{1/2}^{(3/2)}$	$\Phi_1^{(1)}$	$\ell_L$	$e_R$	$\phi$	$\phi$	$\phi$
$\Psi_1^{(0)}$	$X_1^{(1)}$	$\ell_L$	$\phi$	$e_R$	$\phi$	$\phi$
$\Psi_1^{(0)}$	$\Phi_1^{(1)}$	$\ell_L$	$\phi$	$e_R$	$\phi$	$\phi$
$\Psi_0^{(0)}$	$X_0^{(1)}$	$\ell_L$	$\phi$	$e_R$	$\phi$	$\phi$
$\Psi_{1/2}^{(1/2)}$	$X_0^{(1)}$ or $X_1^{(1)}$	$e_R$	$\phi$	$\ell_L$	$\phi$	$\phi$
$\Psi_{1/2}^{(1/2)}$	$\Phi_1^{(1)}$	$e_R$	$\phi$	$\ell_L$	$\phi$	$\phi$
$\Psi_{1/2}^{(1/2)}$	$\Psi_0^{(0)}$ or $\Psi_1^{(0)}$	$e_R$	$\phi$	$\phi$	$\phi$	$\ell_L$

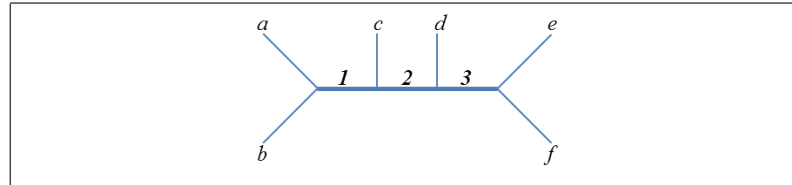
Tab. 6.2: Representation of the diagrams generating  $\mathcal{O}^{(7)}$  at tree level, together with the new physics additions that can realise them.

other side is forbidden at tree level, for a scalar alone cannot couple to the combination  $\bar{\ell}_L \gamma^\mu e_R$  and a vector cannot couple to  $\phi^3$  if the vertex is to be of dimension 4 or lower.

In summary, the new physics we may be interested in is necessarily grouped in pairs, and the possible couples are:

$$\begin{aligned}
& \left\{ X_{1/2}^{(3/2)}, X_{0,1}^{(1)} \right\} & & \left\{ X_{1/2}^{(3/2)}, \Phi_1^{(1)} \right\} \\
& \left\{ \Psi_{1/2}^{(1/2)}, X_{0,1}^{(1)} \right\} & \left\{ \Psi_{1/2}^{(1/2)}, \Phi_1^{(1)} \right\} & \left\{ \Psi_{1/2}^{(1/2)}, \Psi_{0,1}^{(0)} \right\} \\
& \left\{ \Psi_0^{(0)}, X_0^{(1)} \right\} & & \left\{ \Psi_1^{(0)}, B_1^{(1)} \right\}.
\end{aligned} \tag{6.31}$$

It is worth noting that in the last two possibilities the heavy fermions  $\Psi_{0,1}^{(0)}$  necessarily have couplings that would also generate  $\mathcal{O}^{(5)}$  at tree level. In contrast, models containing  $\Phi_{0,1}^{(1)}$  may or may not generate them, depending on whether the heavy scalars couple to  $\bar{\ell}_L \tilde{\ell}_L$ , which



1	2	3	$a$	$b$	$c$	$d$	$e$	$f$
$\Phi_0^{(2)}$	$B_{1/2}^{(3/2)}$	$\Phi_1^{(1)}$	$e_R$	$e_R$	$\phi$	$\phi$	$\phi$	$\phi$
$\Phi_0^{(2)}$	$B_{1/2}^{(3/2)}$	$X_1^{(1)}$ or $X_0^{(1)}$	$e_R$	$e_R$	$\phi$	$\phi$	$\phi$	$\phi$
$\Psi_{1/2}^{(1/2)}$	$B_{1/2}^{(3/2)}$	$\Phi_1^{(1)}$	$e_R$	$\phi$	$e_R$	$\phi$	$\phi$	$\phi$
$\Psi_{1/2}^{(1/2)}$	$B_{1/2}^{(3/2)}$	$X_1^{(1)}$ or $X_0^{(1)}$	$e_R$	$\phi$	$e_R$	$\phi$	$\phi$	$\phi$
$\Psi_{1/2}^{(1/2)}$	$\Psi_1^{(0)}$	$\Phi_1^{(1)}$	$e_R$	$\phi$	$\phi$	$e_R$	$\phi$	$\phi$
$\Psi_{1/2}^{(1/2)}$	$\Psi_1^{(0)}$	$X_1^{(1)}$	$e_R$	$\phi$	$\phi$	$e_R$	$\phi$	$\phi$
$\Psi_{1/2}^{(1/2)}$	$\Psi_0^{(0)}$	$X_0^{(1)}$	$e_R$	$\phi$	$\phi$	$e_R$	$\phi$	$\phi$
$\Psi_{1/2}^{(1/2)}$	$\Psi_0^{(0)}$ or $\Psi_1^{(0)}$	$\Psi_{1/2}^{(1/2)}$	$e_R$	$\phi$	$\phi$	$e_R$	$\phi$	$\phi$
$B_1^{(1)}$	$\Psi_1^{(0)}$	$\Phi_1^{(1)}$	$\phi$	$\phi$	$e_R$	$e_R$	$\phi$	$\phi$
$X_1^{(1)}$	$\Psi_1^{(0)}$	$X_1^{(1)}$	$\phi$	$\phi$	$e_R$	$e_R$	$\phi$	$\phi$
$X_0^{(1)}$	$\Psi_0^{(0)}$	$X_0^{(1)}$	$\phi$	$\phi$	$e_R$	$e_R$	$\phi$	$\phi$

Tab. 6.3: The first topology that can generate  $\mathcal{O}^{(9)}$  at tree level, with a detailed list of the new heavy particles that must run in the internal propagators.

may be forbidden by the symmetries of the underlying theory. From this brute-force list, so, one can select classes of models more or less adequate to enhance the  $W\nu e$  mechanism. In chapter 7 we consider a model that realises one of these possibilities; as we discuss there, for the model to be realistic several other additions are needed, including a second light scalar doublet.

1	2	3	$a$	$b$	$c$	$d$	$e$	$f$
$\Phi_0^{(2)}$	$\Phi_1^{(1)}$	$\Phi_1^{(1)}$	$e_R$	$e_R$	$\phi$	$\phi$	$\phi$	$\phi$
$\Phi_0^{(2)}$	$\Phi_1^{(1)}$	$X_1^{(1)}$	$e_R$	$e_R$	$\phi$	$\phi$	$\phi$	$\phi$
$\Phi_0^{(2)}$	$X_1^{(1)}$	$X_1^{(1)}$	$e_R$	$e_R$	$\phi$	$\phi$	$\phi$	$\phi$
$\Phi_0^{(2)}$	$X_0^{(1)}$	$X_0^{(1)}$	$e_R$	$e_R$	$\phi$	$\phi$	$\phi$	$\phi$
$\Psi_{1/2}^{(1/2)}$	$\Phi_1^{(1)}$	$\Psi_{1/2}^{(1/2)}$	$e_R$	$\phi$	$\phi$	$\phi$	$\phi$	$e_R$
$\Psi_{1/2}^{(1/2)}$	$X_1^{(1)}$ or $X_0^{(1)}$	$\Psi_{1/2}^{(1/2)}$	$e_R$	$\phi$	$\phi$	$\phi$	$\phi$	$e_R$

Tab. 6.4: The second diagram topology to generate  $\mathcal{O}^{(9)}$  at tree level.

### New physics to generate $\mathcal{O}^{(9)}$

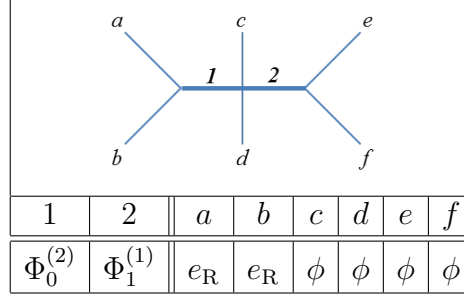
As in the previous case, we will discuss here the new physics additions that can generate the piece of  $\mathcal{O}^{(9)}$  with no gauge bosons; by gauge invariance, those same models will also provide the complete operator. In this case the relevant piece is

$$\mathcal{O}^{(9)} = \bar{e}_R e_R^c \left( \phi^\dagger \partial_\mu \tilde{\phi} \right) \left( \phi^\dagger \partial^\mu \tilde{\phi} \right) + \dots,$$

which comprises two  $e_R$ 's and four  $\phi$ 's<sup>4</sup>. There are three different topologies that can provide the corresponding six-legged diagram; we depict them in tables 6.3, 6.4 and 6.5, together with the various combinations of new particles required for their consistent generation.

Summarising all these possible additions we conclude we can generate  $\mathcal{O}^{(9)}$  whenever our model provides at least one of the following

<sup>4</sup> As in the previous discussion, for simplicity we omit here the complex-conjugates that should be in order for the component fields.



Tab. 6.5: An analysis of the third topology that provides  $\mathcal{O}^{(9)}$  at tree level.

combinations:

$$\begin{aligned}
 & \left\{ B_1^{(1)}, \Phi_0^{(2)} \right\} & \left\{ B_1^{(1)}, \Psi_1^{(0)} \right\} & \left\{ B_1^{(1)}, \Psi_{1/2}^{(1/2)} \right\} \\
 & \left\{ X_0^{(1)}, \Phi_0^{(2)} \right\} & \left\{ X_0^{(1)}, \Psi_0^{(0)} \right\} & \left\{ X_0^{(1)}, \Psi_{1/2}^{(1/2)} \right\} \\
 & & \left\{ \Psi_{1/2}^{(1/2)}, \Psi_{0,1}^{(0)} \right\} & \\
 & \left\{ B_{1/2}^{(3/2)}, \Phi_0^{(2)}, B_1^{(1)} \right\} & & \left\{ B_{1/2}^{(3/2)}, \Phi_0^{(2)}, X_0^{(1)} \right\} \\
 & \left\{ B_{1/2}^{(3/2)}, \Psi_{1/2}^{(1/2)}, B_1^{(1)} \right\} & & \left\{ B_{1/2}^{(3/2)}, \Psi_{1/2}^{(1/2)}, X_0^{(1)} \right\}
 \end{aligned} \tag{6.32}$$

Despite the presence of  $\Phi_1^{(1)}$  and  $\Psi_{0,1}^{(0)}$  in some of these options, these heavy particles need not have the same vertices as the ones leading to  $\mathcal{O}^{(5)}$ . If they do,  $\mathcal{O}^{(9)}$  would have only subdominant effects; but this is in general not the case. In chapter 8 we discuss a model that includes essentially a doubly-charged isosinglet  $\Phi_0^{(2)}$  and a scalar triplet of type  $\Phi_1^{(1)}$ ; imposing additional symmetries the couplings of this model can be selected in a way that suppresses  $\mathcal{O}^{(5)}$ .

## 7. A MODEL REALISING THE $W\nu e$ MECHANISM

In this chapter we will present a short account of a model that realises the  $W\nu e$  mechanism. The model will be presented and its main features will be discussed only briefly; we have not yet developed a full analysis of this model, but it should come about in the near future. As we will see, the model presents a deviation from the plan described in section 6.2.1: it contains a second light scalar doublet with the same quantum numbers as the Higgs doublet. This variation is convenient in order to have neutrino masses dominantly produced by the  $W\nu e$  mechanism while retaining tree-level  $0\nu\beta\beta$ . Thus, we could regard this model as an extension of the popular Two Higgs Doublet Model [245, 246]. As we will see, LNV in this model can be originated either in spontaneous breaking of lepton number or in explicit breaking in the scalar potential; these two ‘paths to LNV’ lead in fact to different effective operators, either involving the usual Higgs doublet or the second scalar doublet. In our discussion we try to determine which is the dominant mechanism and how this dominance depends on the parameters of the model. From our analysis we deduce bounds on the VEV of the second doublet, which lies around the electroweak scale, and on the VEV of the triplet, which is forced to be very small unless compensated by very heavy particles or very small Yukawas. Lepton flavour violation is not directly addressed in our discussion, but the model can accommodate flavour symmetries that effectively suppress all LFV-ing effects. All in all, the model succeeds in realising the  $W\nu e$  mechanism, and the parameters can be arranged in such a way that both  $0\nu\beta\beta$  and neutrino masses are dominated by this mechanism, with some of the new particles at the reach of the LHC. More investigation is still needed, but the model seems promising and its most interesting version will be probed in the next round of high- and low-energy experiments. The work presented



in this chapter was carried out together with Arcadi Santamaria, José Wudka, Francisco del Águila and Subhaditya Bhattacharya.

### 7.1 A model with spontaneous and explicit breaking of lepton number

We begin the construction of our model by considering the couple  $\{\Psi_{1/2}^{(1/2)}, \Phi_1^{(1)}\}$  as read in equation (6.31). Table 6.2 informs us that a Yukawa interaction connecting the heavy and light fermion doublets will be needed,  $\overline{\Psi}_{1/2}^{(1/2)} \Phi_1^{(1)} \ell_L$ , as well as a cubic coupling between the scalars,  $\phi^\dagger \Phi_1^{(1)} \tilde{\phi}$ , that will induce a VEV for  $\Phi_1^{(1)}$ ; the hypercharge assignments ensure that such terms are present. Unfortunately, plain hypercharge enforcement also provides a type-II-seesaw-like coupling,  $\overline{\tilde{\ell}}_L \Phi_1^{(1)} \ell_L$ , which yields masses for the neutrinos at tree level independently of the  $W\nu e$  mechanism. That is inconvenient. To forbid this coupling we call for a  $Z_2$  discrete symmetry under which the heavy fields are odd and the usual SM fields are even. This of course eliminates the unwanted Yukawas, but also forbids the necessary cubic scalar coupling. In order to overcome this difficulty we introduce a new scalar doublet,  $\phi'$ , with the same  $SU(2) \otimes U(1)$  assignments as the Higgs doublet but odd under  $Z_2$ ; then the vertex  $\phi^\dagger \Phi_1^{(1)} \tilde{\phi}'$  is allowed. But by looking at the diagram in table 6.2 we see that the  $\phi'$  occupies an external leg, therefore it cannot be a heavy field. Our setup, thus, requires a second *light* scalar doublet that might show up at the LHC in the near future.

We summarise the new physics additions of our model in table 7.1, where we also introduce a simpler notation to ease the discussion; essentially we will write  $\Phi_1^{(1)} \equiv \chi$  and  $\Psi_{1/2}^{(1/2)} \equiv L_L^c$ , so that  $L_L$  has the same hypercharge as the SM doublets  $\ell_L$ . In order to guarantee the decoupling of the heavy fields we take the  $L$  fermions to be vector-like, and therefore we introduce a right-handed counterpart with the same quantum numbers. We will also allow for several families of the heavy fermions; this is not strictly necessary *a priori*, but can be greatly helpful when dealing with LFV constraints. With all these considerations accounted for, we are ready to write the Lagrangian of

		$T$	$Y$	$Z_2$
$\Phi_1^{(1)}$	$\chi$	1	1	–
$\Psi_{1/2}^{(1/2)c}$	$L_L$	1/2	–1/2	–
	$L_R$	1/2	–1/2	–
	$\phi'$	1/2	1/2	–

Tab. 7.1: The new fields of the model and their charge assignments. The leftmost column presents the fields in the notation of section 6.6; a new, more wieldy naming is introduced in the next column. The  $\phi'$  doublet is not a heavy field, but a second doublet with a mass of the order of the electroweak scale.

the model; the pieces involving the heavy fermions read

$$\mathcal{L}_L = \overline{L}_\alpha (i \not{D} - m_{L_\alpha}) L_\alpha + \left[ y_{\alpha\beta}^e \overline{L}_{L\alpha} e_{R\beta} \phi' + y_{\alpha\beta}^\nu \overline{L}_{L\alpha} \chi \ell_{L\beta} + \text{H.c.} \right], \quad (7.1)$$

where it is understood that  $L_\alpha = L_{L\alpha} + L_{R\alpha}$  and the usual notation –see sections 2.1.2 and 2.1.3– is used for the SM fields. The mass matrix  $m_L$  can be assumed diagonal without loss of generality; the Yukawas  $y^e$  and  $y^\nu$ , however, are general matrices whose number of physical parameters depends on the number of heavy families. Let's say there are three of them,  $\alpha = 1, 2, 3$ ; then  $y^e$  and  $y^\nu$  are  $3 \times 3$  general matrices from which six phases can be removed – overall from the two of them; if it's convenient we can choose to take six phases from one Yukawa matrix and none from the other.

As for the pure-scalar part of the Lagrangian, we can write it as a

scalar potential:

$$\begin{aligned}
V = & -m_\phi^2 \phi^\dagger \phi - m_\phi'^2 \phi'^\dagger \phi' + m_\chi^2 \text{Tr} \{ \chi^\dagger \chi \} + \lambda_\phi (\phi^\dagger \phi)^2 + \\
& + \lambda_\phi' (\phi'^\dagger \phi')^2 + \lambda_\chi (\text{Tr} \{ \chi^\dagger \chi \})^2 + \bar{\lambda}_\chi \text{Tr} \{ (\chi^\dagger \chi)^2 \} + \\
& + \lambda_{\phi\phi} (\phi^\dagger \phi')^2 + \lambda_{\phi\chi} \phi^\dagger \phi \text{Tr} \{ \chi^\dagger \chi \} + \bar{\lambda}_{\phi\chi} \phi^\dagger \chi^\dagger \chi \phi + \quad (7.2) \\
& + \lambda'_{\phi\chi} \phi'^\dagger \phi' \text{Tr} \{ \chi^\dagger \chi \} + \bar{\lambda}'_{\phi\chi} \phi'^\dagger \chi^\dagger \chi \phi' + \\
& + [\mu \phi^\dagger \chi \tilde{\phi}' + \text{H.c.}] .
\end{aligned}$$

Note that in this expression we already disposed the signs so that  $m_\phi^2, m_\phi'^2 < 0$  and  $m_\chi^2 > 0$ . The reason for this election is straightforward: the triplet VEV is phenomenologically forced to be small (see section 8.2.2 in the next chapter), but the physical scalars associated to the triplet must be heavier than 100 GeV; if the triplet VEV is to be induced by its mass term, then it should be small too. A simple way to reconcile these two conditions is to allow for a large, positive  $m_\chi^2$  and let the triplet VEV to be induced by the VEV's of the doublets plus the trilinear interaction  $\phi^\dagger \chi \tilde{\phi}'$ . Then, if we write  $\langle \phi \rangle \equiv v_\phi$  and  $\langle \phi' \rangle \equiv v_\phi'$  we will have

$$\langle \chi \rangle \equiv v_\chi \simeq -\mu^* \frac{v_\phi v_\phi'}{m_\chi^2},$$

which can be small either if  $\mu$  is small or if  $m_\chi$  is large. As for other features of the scalar potential, we note that a sufficient condition for it to be bounded from below, and so allowing for a meaningful vacuum, is that all the quartic couplings are real and positive; no more elaboration on this matter will be needed for our purposes.

Consider now the situation of lepton number in this model; from equations (7.1) and (7.2) we see that it's explicitly broken. LN is transmitted by the Yukawas to the  $\phi'$  and  $\chi$  scalars, and this assignment is honored by the trilinear term  $\mu$ ; but then we have the quartic term  $\lambda_{\phi\phi}$ , and the usual Higgs doublet,  $\phi$ , carries no lepton number because it couples to quarks. Consequently, lepton number is not a

good symmetry for this model, due to the joint action of the  $y^\nu$ ,  $y^e$ ,  $\mu$  and  $\lambda_{\phi\phi}$  interactions. One might therefore think that any LNV-ing amplitude should contain all these couplings, but in the model there is an additional source of lepton number violation: the vacuum; even if some of the couplings needed to violate lepton number were set to zero, lepton number would be broken spontaneously when  $\chi$  and  $\phi'$  take a VEV. And indeed, the interactions of the model are arranged in such a way that a curious competition between explicit and spontaneous breaking arises: when we examine a LNV-ing process we find contributions which require spontaneous violation through the VEV of  $\phi'$ , and others that involve the VEV of  $\phi$  and explicit violation. It so happens that in this model the latter contributions appear suppressed by one loop with respect to the former ones; one might think that they are subdominant, but the first involve  $\langle\phi'\rangle$ , which may be small. An interesting contest, thus, is taking place between the two sources of LNV. In sections 7.2 and 7.3 we present examples of this feature for the processes we are interested in.

## 7.2 Generation of $\mathcal{O}^{(7)}$

The model that we are discussing has two light scalar doublets, and this fact affects the analysis carried out in section 6.6: new effective operators have to be considered that involve the second doublet. As  $\phi$  and  $\phi'$  have the same  $SU(2) \otimes U(1)$  quantum numbers, these operators are mainly versions of those already discussed but with some  $\phi$ 's replaced by  $\phi'$ 's, as long as  $Z_2$  is respected; one important addition is introduced: that the  $Y = -1$  combination  $\phi^\dagger \tilde{\phi}'$  is nonzero with more than one doublet, but this won't be very relevant for the processes we want to analyse. Following our aim of examining the  $W\nu e$  mechanism, we will focus in this section on the generation of the  $\mathcal{O}^{(7)}$  operator, as seen in equation (6.8). But as we just commented, the presence of  $\phi'$  increases the number of  $\mathcal{O}^{(7)}$ -like operators; in fact, the  $Z_2$  symmetry reduces the possibilities to two: one with three  $\phi$  doublets and another with two  $\phi'$ 's and one  $\phi$ . The gauge-invariant form of these operators

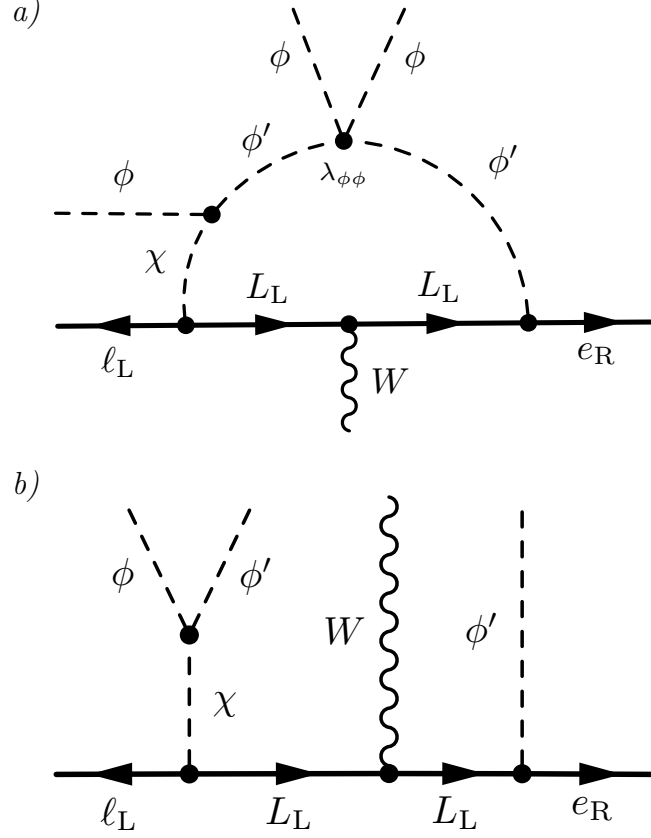


Fig. 7.1: The two main diagrams generating the  $\mathcal{O}^{(7)}$  and  $\mathcal{O}^{(7)'}$  operators seen in equation (7.3).

reads

$$\begin{aligned}\mathcal{O}_{\alpha\beta}^{(7)} &= \overline{e_{R\alpha}}\gamma^\mu \left(\phi^\dagger \tilde{\ell}_{L\beta}\right) \left(\phi^\dagger D_\mu \tilde{\phi}\right) \\ \mathcal{O}_{\alpha\beta}^{(7)'} &= \overline{e_{R\alpha}}\gamma^\mu \left(\phi'^\dagger \tilde{\ell}_{L\beta}\right) \left(\phi^\dagger D_\mu \tilde{\phi}'\right).\end{aligned}\quad (7.3)$$

We present the diagrams that yield the main contributions to the operators in figure 7.1. As we commented in the previous section, the operator with two  $\phi'$  legs is generated at tree level, and becomes LNV-ing once these  $\phi'$  acquire a VEV. The pure- $\phi$  operator is generated at one loop and requires the LNV-ing interaction  $\lambda_{\phi\phi}$ , as  $\phi$  carries no

lepton number. In principle it seems reasonable to think that  $\mathcal{O}^{(7)'}$  is responsible for the leading contribution to the  $W\nu e$  mechanism, as the  $W\nu e$  vertex generated by  $\mathcal{O}^{(7)}$  is suppressed by a factor that is roughly  $\frac{\lambda_{\phi\phi}}{(4\pi)^2} \frac{v_\phi^2}{v_\phi'^2}$ . However, it's necessary to point out that the value of  $v_\phi'$  is not known, and it could be forced to be small by phenomenological constraints; the preeminence of either  $\mathcal{O}^{(7)}$  or  $\mathcal{O}^{(7)'}$  is therefore not firmly decided. In the following we will focus our discussion on the effects of  $\mathcal{O}^{(7)'}$  and related processes, and we will check that a first phenomenological inspection allows for a reasonably large value of  $v_\phi'$  that ensures that it dominates the  $W\nu e$  mechanism.

The calculation of the effective coupling can be carried out just by inspection of the diagram in figure 7.1*b*). The further assumption that all the masses in the  $\chi$  multiplet are equal allows to write the result in terms of the triplet VEV:

$$\frac{C_{\alpha\beta}^{(7)'}}{\Lambda^3} \simeq -i\mu \sum_{\eta} \frac{(y_{\eta\alpha}^e)^* (y_{\eta\beta}^\nu)^*}{m_\chi^2 m_{L_\eta}^2} \simeq -i \frac{v_\chi}{v_\phi v_\phi'} \sum_{\eta} \frac{(y_{\eta\alpha}^e)^* (y_{\eta\beta}^\nu)^*}{m_{L_\eta}^2}. \quad (7.4)$$

The presence of  $v_\chi$  –or, equivalently, the trilinear coupling  $\mu$ –, together with the Yukawas  $y^e$  and  $y^\nu$ , pinpoints the violation of lepton number in the model. We will find this same combination in the expressions for the neutrino masses that we derive in the next section, and we can find it too in the processes that involve explicit violation of LN through the  $\lambda_{\phi\phi}$  interaction. In fact, the relation between  $v_\chi$  and LNV can be used to derive bounds on  $v_\chi$  from the limits on  $0\nu\beta\beta$  and neutrino masses; these bounds, that we discuss in section 7.4, can be very stringent, especially if we don't want the new particles to be very heavy. And there are good reasons not to want them to, as we discuss in the next section.

### 7.3 Neutrino masses and neutrinoless double beta decay

At this point, the generation of  $0\nu\beta\beta$  is straightforward: it suffices to insert either  $\mathcal{O}^{(7)}$  or  $\mathcal{O}^{(7)'}$  into the appropriate combination of tree-level SM processes as seen in figure 6.2*a*). Consequently, the corresponding bounds on the parameters of the model can be simply adapted from

(6.17) by using equation (7.4); we leave this discussion to the next section, where we will gather all phenomenological constraints together. In this section our concern will be, rather, which is the mechanism that actually mediates  $0\nu\beta\beta$ ; as we discussed in section 6.5 of the previous chapter, the  $W\nu e$  mechanism contributes to  $0\nu\beta\beta$ , but it also yields masses for the neutrinos which can take over the generation of  $0\nu\beta\beta$ . In that section we obtained a generic bound on the new physics scale of  $\Lambda \lesssim 35$  TeV; in order to see how that bound applies to this particular model, let us examine the generation of neutrino masses.

Analogously to the case of the  $\mathcal{O}^{(7)}$  operator discussed in the previous section, the neutrino masses in this model can arise either through spontaneous or explicit violation of lepton number. These two possibilities correspond to the two dimension-five operators that we find in the effective theory with a light  $\phi'$ :

$$\begin{aligned}\mathcal{O}_{\alpha\beta}^{(5)} &= -\left(\overline{\tilde{\ell}_{L\alpha}}\phi\right)\left(\tilde{\phi}^\dagger\ell_{L\beta}\right) \\ \mathcal{O}_{\alpha\beta}^{(5)'} &= -\left(\overline{\tilde{\ell}_{L\alpha}}\phi'\right)\left(\tilde{\phi}'^\dagger\ell_{L\beta}\right).\end{aligned}$$

The leading diagrams contributing to these operators are depicted in figure 7.2. In the same way as in the previous section, the masses generated by  $\mathcal{O}^{(5)}$  are suppressed by a factor of roughly  $\frac{\lambda_{\phi\phi}}{(4\pi)^2}\frac{v_\phi^2}{v'^2}$  with respect to those generated by  $\mathcal{O}^{(5)'}$ . This means that, barring other cancellations from the loop functions or the Yukawas, the spontaneous breaking of lepton number is the main source for neutrino masses unless  $v'_\phi$  is small.

Proceeding with our idea of considering spontaneous breaking as the main source of LNV, the neutrino masses are generated by one-loop processes among which the one presented in figure 7.2b) is the leading contribution. From this diagram we estimate the neutrino masses to be

$$(m_\nu)_{\alpha\beta} \simeq \frac{v_\phi'^2\mu}{2(4\pi)^2v}\sum_\eta\frac{m_\alpha(y_{\eta\alpha}^e)^*(y_{\eta\beta}^\nu)^*+m_\beta(y_{\eta\beta}^e)^*(y_{\eta\alpha}^\nu)^*}{m_{L_\eta}^2-m_\chi^2}\log\frac{m_{L_\eta}^2}{m_\chi^2},\quad (7.5)$$

where we have assumed that  $m_{L_\eta}$  and  $m_\chi$  are much greater than all other masses. This expression is very detailed, even a bit too much for

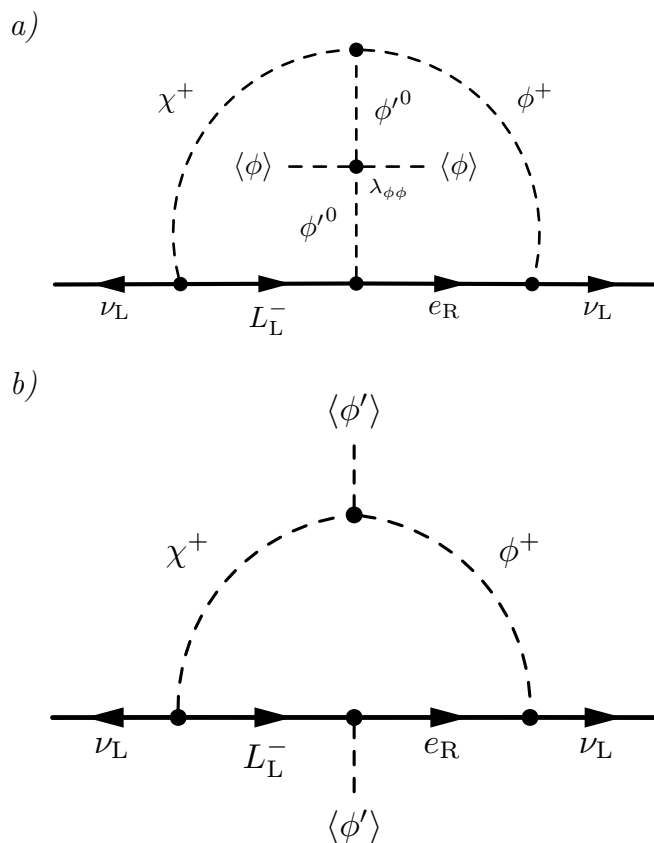


Fig. 7.2: The two leading diagrams that yield neutrino masses, a) through the  $\mathcal{O}^{(5)}$  operator, and b) through the  $\mathcal{O}^{(5) \prime}$  operator.

our purposes; a more handy form can be obtained if we assume the masses in the heavy multiplets to blend into one common heavy scale,  $m_{L_\eta} \sim m_\chi \sim M$ , and thus  $\log \sim 1$ :

$$(m_\nu)_{\alpha\beta} \sim \frac{v'_\phi v_\chi}{(4\pi)^2 v_\phi^2} \sum_\eta \left[ m_\alpha (y_{\eta\alpha}^e)^* (y_{\eta\beta}^\nu)^* + m_\beta (y_{\eta\beta}^e)^* (y_{\eta\alpha}^\nu)^* \right] \quad (7.6)$$

We are now prepared to estimate the contributions of neutrino masses and the  $W\nu e$  vertex to  $0\nu\beta\beta$ . Proceeding as in equation (6.24),



and using (7.6) and (7.4):

$$\begin{aligned}\mathcal{A}_{0\nu\beta\beta}^{(5)} &\sim \frac{G_F^2}{p_{\text{eff}}^2} \frac{(m_\nu)_{ee}}{2} \sim \frac{G_F^2}{p_{\text{eff}}^2} \frac{v'_\phi v_\chi}{(4\pi)^2 v_\phi^2} m_e \sum_\eta (y_{\eta e}^e)^* (y_{\eta e}^\nu)^* \\ \mathcal{A}_{0\nu\beta\beta}^{(7)} &\sim \frac{G_F^2}{p_{\text{eff}}^2} \frac{v'_\phi v_\chi}{M^2} \sum_\eta (y_{\eta e}^e)^* (y_{\eta e}^\nu)^* ,\end{aligned}$$

where we dropped all phases and assumed again that  $m_{L_\eta} \sim m_\chi \sim M$ . The full  $0\nu\beta\beta$  amplitude is the coherent sum of these two contributions,

$$\mathcal{A}_{0\nu\beta\beta} \sim \frac{G_F^2}{p_{\text{eff}}^2} v'_\phi v_\chi \sum_\eta (y_{\eta e}^e)^* (y_{\eta e}^\nu)^* \left[ \frac{m_e}{(4\pi)^2 v_\phi^2} + \frac{p_{\text{eff}}}{M^2} \right] ,$$

and so the  $W\nu e$  vertex dominates if

$$\frac{p_{\text{eff}}}{M^2} > \frac{m_e}{(4\pi)^2 v_\phi^2} \quad \implies \quad M < 35 \text{ TeV} .$$

So, for the case of this model, the requirement that  $0\nu\beta\beta$  is mediated by the heavy particles has a simple meaning: it is not a bound on a complicated combination of scales, but merely on the masses of the  $L$  fermions and the  $\chi$  scalars, which should be at the level of the TeV or at most a few tens of TeV. This will be a useful constraint for the next section, where we analyse the allowed values for the parameters of the model.

#### 7.4 Phenomenological constraints on the model parameters

For the processes we are interested in, the model presents four groups of relevant parameters: the masses of the heavy particles, the Yukawa couplings  $y^e$  and  $y^\nu$ , the VEV of the second doublet,  $v'_\phi$ , and the trilinear coupling  $\mu$ . The aim of this section is to characterise a set of viable values for these parameters from a first inspection focused mainly on LNV-ing observables. For this purpose we will prefer to write the  $\mu$  coupling in terms of the somewhat more physical triplet VEV,  $v_\chi$ ; throughout this section, too, we will omit the details of the

heavy particles' spectrum, and we will assimilate all heavy masses to a common heavy scale,  $m_{L_\eta} \sim m_\chi \sim M$ .

The Yukawas are a source for family-number-violating processes: once  $\phi'$  and  $\chi$  acquire VEV's, the light  $e_R$  and  $\ell_L$  leptons mix with the  $L_\eta$ ; the low-energy effects of such mixings will be proportional to  $y_{\alpha\beta}^e v_\phi'/m_{L_\alpha}$  or  $y_{\alpha\beta}^\nu v_\chi/m_{L_\alpha}$ , and can be made as small as experimentally required either by increasing the heavy masses  $m_{L_\alpha}$  or by reducing the Yukawas  $y_{\alpha\beta}^{e,\nu}$  or the VEV's. The first option doesn't seem convenient, since by the argument exposed in section 7.3 increasing  $m_{L_\alpha}$  would lead to  $0\nu\beta\beta$  dominated by the light neutrino masses; lowering the VEV's is also troublesome, for it would significantly suppress the neutrino masses and possibly the  $0\nu\beta\beta$  rate. As it seems, the only option appears to be to choose small Yukawas. However, we may note that the number of heavy fermion families is not fixed in this model, and if there happened to be three or more we could choose the Yukawas to be aligned with those of the light leptons. And in fact we have an argument in favour of more than one  $L$  family: the light neutrino masses; by looking at (7.5) we see that with only one generation of  $L$ 's  $m_\nu$  will have at most rank two, that is to say, the lightest neutrino will be forced to be massless. This would lead to a tight neutrino mass spectrum that would further constrain the model parameters. Two  $L$  generations allow for three massive light neutrinos, but, for a slightly higher prize, three  $L$  families, mimicking those of the chiral light leptons, open the possibility of imposing a flavour symmetry that would efficiently suppress all LFV-ing effects. Of course this could be sort of arbitrary in a model like this one, not concerned with lepton family hierarchies, but it may be natural in a larger model. In conclusion, increasing the number of heavy lepton families allows us not to worry with the LFV constraints, with the  $y^e$  and  $y^\nu$  possibly being of order 1 as long as they are almost-diagonal in the same basis in which  $Y_e$  is diagonal<sup>1</sup>.

<sup>1</sup> For an estimation of how much alignment we would need to fulfill the LFV constraints we can use the results obtained for other models with a similar lepton mixing structure. For instance, several analyses focused on Littlest Higgs models with T-parity [247–250] yield that the heavy flavours must be aligned with the light charged leptons with a precision better than 1 – 10 % for heavy masses of  $\mathcal{O}(\text{TeV})$ .

With this idea in mind, we move to LNV-ing observables: from equation (6.17) we learn what  $0\nu\beta\beta$  imposes, and in section 6.4 we establish  $(m_\nu)_{\tau\tau} \sim 0.1$  eV as a reasonable requirement for neutrino masses. Looking at equation (7.4) we see that we can identify  $C_{\alpha\beta}^{(7)'} \equiv -i \sum_\eta (y_{\eta\alpha}^e)^* (y_{\eta\beta}^\nu)^*$  and  $\Lambda^3 \equiv v_\phi v_\phi' M^2 / v_\chi$ ; if we assume  $y^e, y^\nu \sim 1$ , (6.17) translates into

$$\frac{v_\phi v_\phi' M^2}{v_\chi} > 10^6 \text{ TeV}^3. \quad (7.7)$$

On the other hand, if we demand  $(m_\nu)_{\tau\tau} \sim 0.1$  eV to (7.6) under the same assumptions we obtain

$$\frac{v_\phi'}{v_\phi} \frac{v_\chi}{v_\phi} \sim 10^{-8}, \quad (7.8)$$

which we can use to eliminate  $v_\phi'/v_\phi$  from (7.7) and then we get

$$\frac{v_\chi}{v_\phi} \lesssim 3 \times 10^{-8} \frac{M}{\text{TeV}}. \quad (7.9)$$

Finally, using (7.9) in return on (7.8) we obtain for  $v_\phi'$ :

$$\frac{v_\phi'}{v_\phi} \gtrsim 0.3 \frac{\text{TeV}}{M}. \quad (7.10)$$

From these constraints we learn that  $0\nu\beta\beta$  demands a very small VEV for the triplet, unless we consent that the new particles are very heavy, thus losing the  $W\nu e$  contribution to  $0\nu\beta\beta$ . With the new particles around the TeV scale,  $v_\chi$  shouldn't be much above the keV scale; this is quite a significant suppression, that we may think calls for further justification. We can, for example, invoke a global symmetry in this fashion:

$$\begin{aligned} L_L &\rightarrow e^{i\alpha} L_L & \phi' &\rightarrow e^{i\alpha} \phi' \\ L_R &\rightarrow e^{i\alpha} L_R & \chi &\rightarrow e^{-i\alpha} \chi \end{aligned}$$

which is broken by the trilinear coupling  $\mu$ ; if this symmetry is just approximate then we can understand that  $\mu$  is small, and in turn

so  $v_\chi$  is. We note, additionally, that this symmetry would also suppress the  $\lambda_{\phi\phi}$  coupling that violates LN explicitly; noticing that both  $\mu$  and  $\lambda_{\phi\phi}$  are involved in the processes with explicit LNV, we may conclude that spontaneous breaking dominates more easily in this scenario.

As for  $\phi'$ , equation (7.10) yields an interesting conclusion: the second doublet is light, but it cannot be *too* light – at least it cannot if its masses and VEV are to be of the same order, as naturality would require. If the new particles have masses around the TeV, then the two doublets lie roughly at the electroweak scale; this is consistent with the fact that no fundamental charged scalars have been observed yet. Of course we could make the new particles heavier and we would have room for lighter  $v'_\phi$ , but at the expense of losing some of the features of the model, and possibly creating a conflict between naturality and direct searches. This situation should be studied with care, considering all contributions to the masses of the charged scalars. Whichever the case,  $\phi'$  appears to live between two somewhat close boundaries: not too light as required by  $0\nu\beta\beta$  and neutrino masses, and not too heavy if it is to remain as a low-energy excitation of the theory.

In a different line of thought, (7.10) also informs us about the preeminent mechanism of LNV: with  $v'_\phi/v_\phi \sim 0.3$ , lepton number would be mainly violated by spontaneous breaking, but taking a slightly heavier  $M$  would set a draw which could be decided by the value of the coupling  $\lambda_{\phi\phi}$ . Explicit breaking may even dominate if the heavy mass scale goes farther towards higher tens of TeV or maybe  $\mathcal{O}(100 \text{ TeV})$ , with the relevant  $W\nu e$  diagrams gradually losing importance for the generation of  $0\nu\beta\beta$ . All in all, dominance of spontaneous breaking seems to be favoured, but a mixed scenario with a significant contribution of explicit breaking cannot be excluded, at least from our present analysis.

Remember, to conclude, that the present discussion relies on several simplifications and order-of-magnitude assumptions; we have not considered, for instance, the role of the Yukawas, which can be large if family symmetries are invoked, but they can also be suppressed for different reasons. Additional suppression from  $y^e$  or  $y^\nu$  would generally result in looser bounds for  $v_\chi$  and  $v'_\phi$ . We think that a good conclusion to draw from this analysis is that the model is consistent

with (i)  $0\nu\beta\beta$  generated through the  $W\nu e$  vertex, possibly with large rates observable in the next round of experiments; (ii) new particles at the reach of the LHC, especially charged scalars from the  $\phi'$  doublet; (iii) a variety of new LFV-ing signals mediated by the heavy leptons and possibly observable in near future experiments.

### 7.5 Collider effects

This model contains, besides the scalar triplet of unit hypercharge  $\chi$ , a second scalar isodoublet and several vector-like lepton doublets. Direct evidence for the  $W\nu e$  mechanism in an accelerator experiment would require the discovery of the new particles together with a demonstration of the presence of LNV-ing interactions. This latter goal seems difficult; as we have seen throughout the discussion, violation of LN in this model involves several couplings –typically expected to be small–, which yields small LNV-ing production and decay rates. In general, the dominant production mechanisms are standard and LN-conserving, or otherwise the production itself is suppressed. As for decays, not all the decay channels of the new particles produce LNV-ing signals, though in some cases they might be dominant. Generally, the idea is to look first for the new resonances in the most sensitive channels and only afterwards to address the observation of LNV-ing events.

The scalars of the theory offer maybe the most promising detection prospects. The triplet, for instance, includes a doubly-charged scalar that has fixed couplings to photons and is produced at colliders with known cross sections. As for the decays, the triplet couples to a light and a heavy lepton, and the latter decays into a light lepton and a  $W$ , a  $Z$ , or a Higgs boson; this may result in a four-lepton decay. Similarly, the extra scalar isodoublet can also undergo decays with four fermions in the final state. Instances of these processes can be

$$pp \rightarrow \chi^{++} + X \rightarrow \ell_\alpha^+ L_\beta^+ \rightarrow \ell_\alpha^+ \ell_\eta^+ Z \rightarrow \ell_\alpha^+ \ell_\eta^+ \ell_\lambda^+ \ell_\lambda^-$$

$$pp \rightarrow \phi'^0 + X \rightarrow \ell_\alpha^+ L_\beta^{-*} \rightarrow \ell_\alpha^+ \ell_\eta^- Z \rightarrow \ell_\alpha^+ \ell_\eta^- \ell_\lambda^+ \ell_\lambda^-$$

Moreover, the new particles can also be pair-produced via the Drell-Yan

---

mechanism, resulting in final states with four charged leptons + jets, or even eight leptons or more. The signal can be striking due to the large number of charged leptons, but there are many open channels and it may be difficult to resolve the different samples.

The heavy vector-like lepton doublets are also mainly produced in pairs. They violate the Glashow-Iliopoulos-Maiani mechanism [251], and can decay through a flavour-changing neutral current into a light lepton and a  $Z$  or Higgs boson [252]; as for the case of sequential fermions, they can also decay into a lepton and a  $W$  boson through the usual charged current interaction. In these cases the final states have at least six fermions, so that the heavy leptons will be relatively easy to find if light enough,  $m_{L_\eta} \lesssim \text{TeV}$  for a center-of-mass energy of 14 TeV and an integrated luminosity of  $100 \text{ fb}^{-1}$  [252–254].

## 8. A MODEL REALISING THE $WW_{ee}$ MECHANISM

This chapter is dedicated to the study of a model that realises the  $WW_{ee}$  mechanism for  $0\nu\beta\beta$  and neutrino masses. It is but one of a family of models that give rise to the operator  $\mathcal{O}^{(9)}$  while suppressing the generation of  $\mathcal{O}^{(5)}$  and  $\mathcal{O}^{(7)}$  – for more information on these operators and the mechanisms they induce see chapter 6, or, more plainly, equations (6.7), (6.8) and (6.10). The  $WW_{ee}$  mechanism is particularly interesting, as it can provide observable signals in a variety of experiments, ranging from  $0\nu\beta\beta$  to high-energy accelerators; we will give here an account of the several points of phenomenological interest and evaluate their importance for the viability of the model. As we will see, the model is tightly constrained from various directions: not only phenomenology, but also our desire to produce a signal in the next round of  $0\nu\beta\beta$  experiments, and even the perturbative consistence of the theory, tend to push the new particles to a rather narrow region in the mass plane; all in all, though, there still seems to be room for them. Another interesting aspect of this model is the structure of the generated neutrino mass matrix, which shows a remarkable suppression in several elements; as a consequence, the model predicts a nonzero value for the reactor mixing angle,  $\theta_{13}$ , and a definite correlation between this value and that of the CP-violating Dirac phase,  $\delta$ . The allowed range for  $\theta_{13}$  is consistent with the recent Daya Bay, RENO and Double Chooz measurements. This work was carried out in collaboration with Arcadi Santamaria, José Wudka, Francisco del Águila and Subhaditya Bhattacharya.

		$T$	$Y$	$Z_2$
$\Phi_0^{(2)}$	$\kappa$	0	2	+
$\Phi_1^{(1)}$	$\chi$	1	1	−
	$\sigma$	0	0	−

Tab. 8.1: The new scalars of the model and their charge assignments. The leftmost column presents the fields in the notation of section 6.6; a new, more wieldy naming is introduced in the next column. The  $\sigma$  field is taken as real to avoid the creation of a Majoron when it develops a VEV.

### 8.1 A model with lepton number softly broken

For the construction of this model we will elaborate upon the  $\{\Phi_0^{(2)}, \Phi_1^{(1)}\}$  combination found in (6.32). This combination includes two scalars: a doubly-charged singlet and a unit-hypercharge triplet, and is, by itself, sufficient to generate the  $\mathcal{O}^{(9)}$  operator. However, in order to have a viable and interesting model we need some extra work: to begin with, if we want the  $WWee$  mechanism to be dominant we need to suppress the competing operators  $\mathcal{O}^{(5)}$  and  $\mathcal{O}^{(7)}$ , both of lower dimensionality and generating neutrino masses at lower loop order. Note, for instance –see (6.29)–, that the presence of  $\Phi_1^{(1)}$  alone is enough to provide  $\mathcal{O}^{(5)}$  at tree level; but by looking at table 6.1 we also see that the coupling  $\bar{\ell}_L \Phi_1^{(1)} \ell_L$  is fundamental to realise the generation of  $\mathcal{O}^{(5)}$ ; if we are clever enough to suppress this coupling we could relegate  $\mathcal{O}^{(5)}$  to a subdominant role. This can be simply achieved by imposing a discrete symmetry, for example a  $Z_2$  under which all SM fields are even and  $\Phi_1^{(1)}$  is odd. We could then ask which can be the  $Z_2$  assignment for  $\Phi_0^{(2)}$ ; by looking at tables 6.4 and 6.5, which describe the topologies that generate  $\mathcal{O}^{(9)}$ , we see that a  $\bar{e}_R^c e_R \Phi_0^{(2)}$  coupling is needed.  $\Phi_0^{(2)}$ , thus, must be  $Z_2$ -even. But then, again looking at tables 6.4 and 6.5, we see that a  $\phi^\dagger \Phi_1^{(1)} \tilde{\phi}$  coupling is needed, and it is forbidden by our  $Z_2$  assignments! There are two options at this point: either we introduce this interaction by hand, explicitly breaking the  $Z_2$  symmetry, or we



introduce a new scalar field that breaks spontaneously  $Z_2$  and allows for this vertex to exist. We choose to follow the second path, but look at section 8.9, for the first one can be convenient on its own merits. The new scalar field must be a hyperchargeless singlet, odd under  $Z_2$ ; we will take it real, for reasons that will become clear in a moment.

The properties of the new scalars are summarised in table 8.1, where a new, simpler notation is defined for the fields. The most general scalar potential compatible with these assignments is

$$\begin{aligned}
V = & -m_\phi^2 \phi^\dagger \phi - m_\sigma^2 \sigma^2 + m_\chi^2 \text{Tr} \{ \chi^\dagger \chi \} + m_\kappa^2 \kappa^\dagger \kappa + \\
& + \lambda_\phi (\phi^\dagger \phi)^2 + \lambda_\sigma \sigma^4 + \lambda_\kappa (\kappa^\dagger \kappa)^2 + \lambda_\chi (\text{Tr} \{ \chi^\dagger \chi \})^2 + \\
& + \lambda'_\chi \text{Tr} \{ (\chi^\dagger \chi)^2 \} + \lambda_{\phi\sigma} \phi^\dagger \phi \sigma^2 + \lambda_{\phi\kappa} \phi^\dagger \phi \kappa^\dagger \kappa + \quad (8.1) \\
& + \lambda_{\phi\chi} \phi^\dagger \phi \text{Tr} \{ \chi^\dagger \chi \} + \lambda'_{\phi\chi} \phi^\dagger \chi^\dagger \chi \phi + \lambda_{\sigma\kappa} \sigma^2 \kappa^\dagger \kappa + \\
& + \lambda_{\kappa\chi} \kappa^\dagger \kappa \text{Tr} \{ \chi^\dagger \chi \} + \lambda_{\sigma\chi} \sigma^2 \text{Tr} \{ \chi^\dagger \chi \} + \\
& + [ \mu_\kappa \kappa \text{Tr} \{ \chi^\dagger \chi^\dagger \} - \lambda_6 \sigma \phi^\dagger \chi \tilde{\phi} + \text{H.c.} ] ;
\end{aligned}$$

among all these interactions<sup>1</sup>, the most important ones for our purposes are the latter two. Note that by an appropriate rephasing of the fields we can always choose  $\mu_\kappa$  and  $\lambda_6$  to be real of either sign; for simplicity, we will take in the following  $\mu_\kappa > 0$  and  $\lambda_6 > 0$ . Notice, however, the minus sign assigned to the  $\lambda_6$  term, whose purpose is to ensure that the VEV of  $\chi$  is positive; indeed, precision electroweak measurements such as the  $\rho$  parameter constrain the VEV of any triplet scalar to be small. This could be accomplished by taking a (negative) small  $m_\chi^2$ , but that would result in very light charged scalars that have not been observed. Therefore, our strategy will be to let  $\phi$  and  $\sigma$  to take a VEV on their own and transmit it to  $\chi$  via the  $\lambda_6$  interaction, thus resulting

---

<sup>1</sup> The reader may notice that (8.1) lacks terms such as  $\text{Tr} \{ \chi^2 \} \text{Tr} \{ \chi^{\dagger 2} \}$ ,  $\text{Tr} \{ \chi^2 \chi^{\dagger 2} \}$  and  $\phi^\dagger \chi \chi^\dagger \phi$ . These terms are not independent from the ones presented and can be related to them by using the fact that any two traceless  $2 \times 2$  matrices  $A$  and  $B$  verify  $\{A, B\} = \text{Tr} \{AB\} \mathbb{1}$ .

in a naturally small  $v_\chi$ . Note that the sign assignments for the mass terms in (8.1) already prefigure this program, allowing us to consider all  $m^2 > 0$ . A complete discussion on the breakdown of electroweak symmetry in this model can be found in section 8.2.2.

Also of interest are the Yukawa couplings allowed in the Lagrangian,

$$\mathcal{L}_Y = \bar{\ell}_L Y_e e_R \phi + \bar{e}_R^c g e_R \kappa + \text{H.c.}, \quad (8.2)$$

where  $Y_e$  is a  $3 \times 3$  matrix that can be taken diagonal with positive eigenvalues without loss of generality;  $g$  is a complex symmetric  $3 \times 3$  matrix with only three physical phases.

Note from (8.1) and (8.2) the intricate situation of lepton number in this model: considering that  $L(\ell_L) = L(e_R) = -1$ ,  $\kappa$  is assigned  $L(\kappa) = +2$  by the  $g$  Yukawas. Were  $\sigma$  to be a complex field,  $\chi$  would be assigned  $L(\chi) = +1$  by the  $\mu_\kappa$  coupling in (8.1) and transmit this charge to  $\sigma$  via the  $\lambda_6$  coupling, with  $L(\sigma) = -1$ . But then, as  $\sigma$  takes a VEV a Majoron would be created that would additionally constrain the model; even though these constraints wouldn't possibly be very tight, as the Majoron would be mainly a singlet with small couplings to matter, we prefer to choose  $\sigma$  to be real, and therefore unable to carry charges – but see section 8.9 for more comments on the possibility of a complex  $\sigma$ . With  $\sigma$  real,  $\chi$  suffers from opposed LN assignments: the  $\mu_\kappa$  interaction would allot  $L(\chi) = +1$ , but the  $\lambda_6$  vertex requires  $L(\chi) = 0$ ; lepton number is, so, explicitly broken if  $\sigma$  is real. Moreover, as  $\mu_\kappa$  is dimensionful it is *softly* broken and the model will not suffer from infinity sickness in radiative corrections. Notice also that none of the LN assignments for  $\chi$  is  $+2$ , which is the one associated to the  $\bar{\ell}_L \chi \ell_L$  coupling that we wish to suppress: that interaction is correctly forbidden by the  $Z_2$  symmetry and when it is loop-generated, after the  $\sigma$  VEV breaks  $Z_2$ , the resulting neutrino masses will be finite and calculable.

To finish this section, a further remark on lepton number and its role on the processes we are interested in: note that in the limit of vanishing  $Y_e$  one can define two different “lepton numbers”, one associated to the doublets  $\ell_L$  and the other to the singlets  $e_R$ . The first, for  $Y_e \rightarrow 0$ , is uncommunicated to the scalar sector, and thus conserved; as a consequence, any sort of  $0\nu\beta\beta$  to left-handed leptons is forbidden, and

Majorana neutrino masses are barred too. The second is transmitted to the scalars via the  $g$  Yukawas, and then broken in the scalar potential by the  $\mu_\kappa$  and  $\lambda_6$  couplings. Therefore,  $0\nu\beta\beta$  to right-handed leptons is allowed in any case, and will be proportional to  $g_{\alpha\beta}$ ,  $\mu_\kappa$  and  $\lambda_6$ , whereas neutrino masses require these three elements together with  $Y_e$ . We will find both results in the corresponding sections, 8.3 and 8.6.

## 8.2 *The scalars of the theory*

The model includes three new scalar fields that yield nine degrees of freedom, to sum to the four provided by the usual SM doublet. Their properties are profoundly intertwined as a consequence of the interactions in the scalar potential and the nontrivial breakdown of electroweak symmetry, which involves three vacuum expectation values. The final physical scalars, with definite masses and electric charges, are combinations of these pre-EWSB building blocks. In this section we present a possible pattern of symmetry breaking that simplifies this potentially intricate panorama and fulfills all phenomenological constraints; we also describe the final spectrum of physical scalars and remark on some couplings that will be of use in the following sections.

### 8.2.1 *Boundedness of the potential*

A necessary condition for any QFT to make sense is that the scalar potential is bounded from below; this is what allows masses to be defined properly and in turn leads to the notion of vacuum expectation value. The scalar potential presented in equation (8.1) is a complicated one and involves many different interactions. Even though most of them will not be of interest for our forthcoming discussion let us briefly analyse the conditions under which the model will present a potential bounded from below, if only to satisfy a drive of professional zeal.

The condition of below-boundedness can be translated essentially –for a regular potential, with no poles– to the requirement that the potential tends to  $+\infty$  in all directions when the fields, taken as C-numbers, diverge. As it is a condition at infinity, it suffices to consider the highest-degree part of the potential, that will be dominant in that

regime – in our case, we just need the quartic terms. Specifically, let us call

$$\begin{aligned}
V^{(4)} \equiv & \lambda_\phi (\phi^\dagger \phi)^2 + \lambda_\sigma \sigma^4 + \lambda_\kappa (\kappa^\dagger \kappa)^2 + \lambda_\chi (\text{Tr} \{ \chi^\dagger \chi \})^2 + \\
& + \lambda'_\chi \text{Tr} \{ (\chi^\dagger \chi)^2 \} + \lambda_{\phi\sigma} \phi^\dagger \phi \sigma^2 + \lambda_{\phi\kappa} \phi^\dagger \phi \kappa^\dagger \kappa + \\
& + \lambda_{\phi\chi} \phi^\dagger \phi \text{Tr} \{ \chi^\dagger \chi \} + \lambda'_{\phi\chi} \phi^\dagger \chi^\dagger \chi \phi + \lambda_{\sigma\kappa} \sigma^2 \kappa^\dagger \kappa + \quad (8.3) \\
& + \lambda_{\kappa\chi} \kappa^\dagger \kappa \text{Tr} \{ \chi^\dagger \chi \} + \lambda_{\sigma\chi} \sigma^2 \text{Tr} \{ \chi^\dagger \chi \} - \\
& - \lambda_6 (\sigma \phi^\dagger \chi \tilde{\phi} + \sigma \tilde{\phi}^\dagger \chi^\dagger \phi) ;
\end{aligned}$$

note that most terms are biquadratic, meaning that the the field combinations always yield a positive C-number, and the only negative contributions may come from a possibly negative coefficient. Were  $V^{(4)}$  strictly biquadratic, a sufficient condition for below-boundedness would be that all the coefficients are positive. Unfortunately, we have also the  $\lambda_6$  term, which we want to be negative and is linear in  $\chi$  and  $\sigma$ . This term forces us into a more convoluted discussion.

To our knowledge, there is no general method for finding the conditions of below-boundedness in a quartic form. We do know, however, of a very straightforward procedure to do so in a *quadratic* form, and we can adapt it to our case here; it is a well-known method, consisting in diagonalising the quadratic polynomial and requiring that the coefficients of the diagonalised form –which only accompany perfect-squared variables, and so positive quantities– are positive. Those coefficients are the eigenvalues of the matrix associated to the quadratic form. Therefore, we will proceed to express our quartic form as a quadratic polynomial, making use of its almost-biquadratic form and implementing variable changes of the form  $\phi^2 \rightarrow x$ . The rest will be to properly collect the matrix of the ‘new’ quadratic polynomial and imposing positive eigenvalues for it.

The components of the quartic form we’re interested in are the scalar fields of our model or, more specifically, the degrees of freedom contained inside them. This adds up to thirteen elements, but not all of them are relevant for the present discussion. In order to identify the

relevant degrees of freedom let us express the involved fields in a new notation. Begin first with the triplet, which as we know encloses three complex fields with definite electric charge – see for instance section 3.3.2 and references therein. That makes six degrees of freedom, but as any piece of the potential is  $SU(2) \otimes U(1)$  gauge-invariant we can work in an  $SU(2)$  gauge which eliminates three of them – remember,  $SU(2)$  is a three-parameter Lie group. Let us then choose the gauge that shapes the triplet, in the doublet representation, as

$$\chi = \begin{pmatrix} 0 & \sqrt{b} e^{-i\mu} \\ \sqrt{a} e^{i\mu} & 0 \end{pmatrix},$$

with  $a$  and  $b$  positive real C-numbers and  $\mu$  an ordinary phase that, we will check, can be abstracted from this discussion. The doublet, in that same gauge, will present its most general form,

$$\phi = \begin{pmatrix} \sqrt{p} e^{i\alpha} \\ \sqrt{q} e^{i\beta} \end{pmatrix},$$

with again  $p$  and  $q$  real positive C-numbers and  $\alpha, \beta$  irrelevant phases. As for the singlets, notice that the pieces in (8.3) only involve the hyperchargeless combination  $\kappa^\dagger \kappa$ , and so a ‘phase’ of  $\kappa$  can also be ignored here; let us define

$$\kappa^\dagger \kappa \equiv c,$$

and  $\sigma$ , for ‘dimensional consistency’,

$$\sigma^2 \equiv d,$$

with both  $c$  and  $d$  real positive C-numbers.

Expressing (8.3) in this new notation yields

$$V^{(4)} = X^T \mathcal{V} X - 2\lambda_6 \left[ q\sqrt{ad} \cos(\mu - 2\beta) - p\sqrt{bd} \cos(\mu - 2\alpha) \right],$$

where  $X^T \mathcal{V} X$  is already a quadratic form with

$$\mathcal{V} = \begin{pmatrix} \lambda_\chi + \lambda'_\chi & \lambda_\chi & \lambda_{\kappa\chi}/2 & \lambda_{\sigma\chi}/2 & (\lambda_{\phi\chi} + \lambda'_{\phi\chi})/2 & \lambda_{\phi\chi}/2 \\ \lambda_\chi & \lambda_\chi + \lambda'_\chi & \lambda_{\kappa\chi}/2 & \lambda_{\sigma\chi}/2 & \lambda_{\phi\chi}/2 & (\lambda_{\phi\chi} + \lambda'_{\phi\chi})/2 \\ \lambda_{\kappa\chi}/2 & \lambda_{\kappa\chi}/2 & \lambda_\kappa & \lambda_{\sigma\kappa}/2 & \lambda_{\phi\kappa}/2 & \lambda_{\phi\kappa}/2 \\ \lambda_{\sigma\chi}/2 & \lambda_{\sigma\chi}/2 & \lambda_{\sigma\kappa}/2 & \lambda_\sigma & \lambda_{\phi\sigma}/2 & \lambda_{\phi\sigma}/2 \\ (\lambda_{\phi\chi} + \lambda'_{\phi\chi})/2 & \lambda_{\phi\chi}/2 & \lambda_{\phi\kappa}/2 & \lambda_{\phi\sigma}/2 & \lambda_\phi & \lambda_\phi \\ \lambda_{\phi\chi}/2 & (\lambda_{\phi\chi} + \lambda'_{\phi\chi})/2 & \lambda_{\phi\kappa}/2 & \lambda_{\phi\sigma}/2 & \lambda_\phi & \lambda_\phi \end{pmatrix}$$

and

$$X^T = (a \ b \ c \ d \ p \ q) ,$$

and the  $\lambda_6$  terms break this structure, as we already knew. The goal is now to integrate these terms into the quadratic form in a way that preserves the significant information about below-boundedness. That can happen; observe that the sign of these terms is not fixed, as they contain cosines of in principle arbitrary phases. Note too that these terms are a problem for below-boundedness as far as they *subtract* from the quadratic polynomial, and so pull to  $-\infty$  two of the directions. Let us now place ourselves in the *worst* of such situations: that where the phases conspire to yield

$$\begin{aligned} -2\lambda_6 [q\sqrt{ad} \cos(\mu - 2\beta) - p\sqrt{bd} \cos(\mu - 2\alpha)] = \\ = -2\lambda_6 [q\sqrt{ad} + p\sqrt{bd}] . \end{aligned}$$

Then consider the general inequality  $\sqrt{xy} \leq (x + y)/2$ ; by using it we can obtain quadratic-like terms that are always *worse* than the original ones,

$$-2\lambda_6 [q\sqrt{ad} + p\sqrt{bd}] \geq -\lambda_6 [q(a + d) + p(b + d)] .$$

Then we can construct a new quadratic form

$$\bar{V}^{(4)} \equiv X^T \bar{\mathcal{V}} X - \lambda_6 [q(a + d) + p(b + d)] \equiv X^T \bar{\mathcal{V}} X$$

with a slightly modified matrix

$$\bar{\mathcal{V}} = \begin{pmatrix} \lambda_\chi + \lambda'_\chi & \lambda_\chi & \lambda_{\kappa\chi}/2 & \lambda_{\sigma\chi}/2 & (\lambda_{\phi\chi} + \lambda'_{\phi\chi})/2 & \bar{\lambda}_{\phi\chi}/2 \\ \lambda_\chi & \lambda_\chi + \lambda'_\chi & \lambda_{\kappa\chi}/2 & \lambda_{\sigma\chi}/2 & \bar{\lambda}_{\phi\chi}/2 & (\lambda_{\phi\chi} + \lambda'_{\phi\chi})/2 \\ \lambda_{\kappa\chi}/2 & \lambda_{\kappa\chi}/2 & \lambda_\kappa & \lambda_{\sigma\kappa}/2 & \lambda_{\phi\kappa}/2 & \lambda_{\phi\kappa}/2 \\ \lambda_{\sigma\chi}/2 & \lambda_{\sigma\chi}/2 & \lambda_{\sigma\kappa}/2 & \lambda_\sigma & \bar{\lambda}_{\phi\sigma}/2 & \bar{\lambda}_{\phi\sigma}/2 \\ (\lambda_{\phi\chi} + \lambda'_{\phi\chi})/2 & \bar{\lambda}_{\phi\chi}/2 & \lambda_{\phi\kappa}/2 & \bar{\lambda}_{\phi\sigma}/2 & \lambda_\phi & \lambda_\phi \\ \bar{\lambda}_{\phi\chi}/2 & (\lambda_{\phi\chi} + \lambda'_{\phi\chi})/2 & \lambda_{\phi\kappa}/2 & \bar{\lambda}_{\phi\sigma}/2 & \lambda_\phi & \lambda_\phi \end{pmatrix} ,$$

where  $\bar{\lambda}_{\phi\chi, \phi\sigma} \equiv \lambda_{\phi\chi, \phi\sigma} - \lambda_6$ . It is sufficient condition for  $V^{(4)}$  to be bounded from below that  $\bar{V}^{(4)}$  is; so, below-boundedness holds if the eigenvalues of  $\bar{\mathcal{V}}$  are all positive.

As we anticipated, this long discussion ends with a not-so-spectacular conclusion: essentially, we learn that we can proceed to the analysis

of the model under assumptions usually considered ‘reasonable’; we don’t really need to calculate the eigenvalues of  $\bar{\mathcal{V}}$ , involving as they do many parameters that are not of interest to our discussion. It is enough to take all the  $\lambda$ ’s positive, including  $\lambda_6$  –that we need–, as far as we keep positive –or at least balanced– the values of  $\lambda_{\phi\chi, \phi\sigma} - \lambda_6$ .

### 8.2.2 Vacuum expectation values

The model possesses three neutral scalars susceptible of developing a VEV: one comes from the doublet, one from the triplet and the third from the neutral singlet  $\sigma$ . We need at least the doublet to acquire a VEV, in order to break electroweak symmetry.  $0\nu\beta\beta$  and neutrino masses need lepton number to be broken, but as it is explicitly violated in the potential (see section 8.1 for more details) the triplet and the singlet can remain VEV-less at the price of having  $0\nu\beta\beta$  at one loop –instead of tree-level– and neutrino masses at three loops – instead of two. As we want to enhance the rate of  $0\nu\beta\beta$  we prefer the scenario with three VEV’s, which presents additional difficulties.

The VEV of the triplet is problematic because we have very strong bounds from electroweak observables. In particular, the  $\rho$  parameter is highly sensitive to the  $SU(2)$  charge of the fields that break the electroweak symmetry, and it is consistent with “breaking by a doublet” to a good degree of precision; specifically, a global fit to electroweak precision data [32] yields

$$\rho = 1.0004^{+0.0023}_{-0.0011} \quad (8.4)$$

at  $2\sigma$ , very close to  $\rho = 1$ , which would indicate pure doublet-mediated electroweak symmetry breaking. This means that any triplet VEV must be small enough not to compete with the standard Higgs doublet for the dominant role in EWSB. We can calculate to which extent (8.4) constrains the triplet VEV. The theoretical expression for  $\rho$  at tree level is

$$\rho = \frac{\sum_j v_j^2 [T_j(T_j + 1) - Y_j^2]}{\sum_j 2v_j^2 Y_j^2},$$

where the sums run over all the scalars of the theory,  $T_j$  represents their isospin,  $Y_j$  their hypercharge and  $v_j$  their VEV<sup>2</sup>. For the case under consideration we obtain a simple expression that can be simplified even further if we assume that  $v_\chi \ll v_\phi$ :

$$\rho = \frac{v_\phi^2 + 2v_\chi^2}{v_\phi^2 + 4v_\chi^2} \simeq 1 - \frac{2v_\chi^2}{v_\phi^2}. \quad (8.5)$$

As we see, the VEV of the triplet contributes negatively to the  $\rho$  parameter, while (8.4) presents a value slightly greater than 1. We can thus derive an upper bound on the value of  $v_\chi$ , that reads

$$v_\chi < 3 \text{ GeV} \quad 95\% \text{ CL}$$

for  $v_\phi = 174 \text{ GeV}$ . This bound is similar to those obtained from more comprehensive surveys, for example a global fit including explicitly the scalar triplet effects [255] which yields  $v_\chi < 2 \text{ GeV}$  at 90% CL.

However, a more complete analysis should also include the radiative corrections to the  $\rho$  parameter induced by the scalar triplet itself, which can be positive [256]. For instance, in the triplet Majoron model loop corrections provide a positive contribution that cancels partially the tree-level one,  $\Delta\rho = \frac{1-\ln 2}{2\pi^2\sqrt{2}} G_F m_{\chi^{++}}^2$ , with  $m_{\chi^{++}}$  the mass of the doubly-charged scalar [257]. Since these contributions depend on the mass splitting of the triplet components, which in our model is not fixed, when we want to consider a conservative bound on  $v_\chi$  we will take

$$v_\chi < 5 \text{ GeV}, \quad (8.6)$$

which is in the line of another recent work [258] that, including one-loop corrections, points to a relaxation of the bound of up to  $v_\chi < 6 \text{ GeV}$  at 95% CL.

As for the VEV of the singlet, it is essentially unconstrained, as it does not contribute to EWSB. The issues with this VEV are more related to its qualitative consequences, such as the creation of domain walls due to the breaking of  $Z_2$ , which we address in section 8.9, or the

<sup>2</sup> Throughout this section we are already implementing the notation presented in equation (8.10) in the next section.



necessary induction of a VEV for the triplet, irrespective of the sign of  $m_\chi^2$ . Indeed, once  $\phi$  and  $\sigma$  take a VEV the  $\lambda_6$  interaction drives  $\chi$  into a nontrivial minimum, bringing to the focus the restrictions on  $v_\chi$  that we just described. We could think of dropping the singlet VEV, but as commented before that would mean relegating  $0\nu\beta\beta$  to the one-loop level, which would spoil part of the interest of the model. Let us, so, examine this nontrivial minimum that involves the three neutral fields and see if it can accommodate the phenomenological restrictions on  $\chi$ .

The minimisation of  $V$  can be carried out in a simple way: just substituting in (8.1) the neutral components  $\phi^0$ ,  $\chi^0$  and  $\sigma$  by  $v_\phi$ ,  $v_\chi$  and  $v_\sigma$  while putting zeros in place of the charged components, and then looking for a minimum of this three-variable function. To simplify the procedure, we will just look for an extremum (the point where the three partial derivatives vanish) and later we will check that it is indeed a minimum; for that aim it is enough to require that the resulting scalar masses are physical, i.e.,  $m^2 \geq 0$ . See section 8.2.3 for a discussion on this matter.

Several solutions are obtained by following this program; most of them present vanishing VEV's for either the doublet or the singlet. We select the solution that yields nonzero values for all three VEV's, and further simplify it by assuming  $v_\chi \ll v_\phi$ ; this is not a very grave loss of generality: given the bound (8.6) this condition is merely factual and must be imposed at some point. Already in this approximation, the VEV's at the minimum read

$$v_\phi^2 \simeq \frac{2\lambda_\sigma m_\phi^2 - \lambda_{\phi\sigma} m_\sigma^2}{4\lambda_\sigma \lambda_\phi - \lambda_{\phi\sigma}^2} \quad v_\sigma^2 \simeq \frac{2\lambda_\phi m_\sigma^2 - \lambda_{\phi\sigma} m_\phi^2}{4\lambda_\sigma \lambda_\phi - \lambda_{\phi\sigma}^2}$$

$$v_\chi \simeq \frac{\lambda_6 v_\sigma v_\phi^2}{m_\chi^2 + \lambda_{\phi\chi} v_\phi^2 + \lambda_{\sigma\chi} v_\sigma^2}. \quad (8.7)$$

Notice that  $v_\phi$  and  $v_\sigma$  are real and positive for all  $\lambda_\phi, \lambda_\sigma, \lambda_{\phi\sigma} > 0$ , in consistency with the conditions derived in section 8.2.1 for the potential to be bounded from below. As for  $v_\chi$ , note that with the present sign assignment  $\lambda_6 > 0$  is the right phase choice to make  $v_\chi$  real and positive; note also that the condition  $v_\chi \ll v_\phi$  somehow suggests that  $m_\chi \gg v_\phi, v_\sigma$ , which looks convenient, as the new charged

scalars provided by the triplet have not yet been observed. Anyway, we will make no assumptions about  $m_\chi$ ; the phenomenological constraints themselves will yield the appropriate restrictions for it – see section 8.7.

### 8.2.3 Physical scalar spectrum

In this section we describe the final spectrum of physical scalars of the model. As we have already mentioned, the theory possesses thirteen scalar degrees of freedom that are arranged into two complex fields with electric charge  $Q = 2$ , two more complex fields but with unit electric charge, and five neutral real fields, of which three are proper scalars and the remaining two are pseudoscalars. Let us establish some notation: we will label the fields provided by the triplet as

$$\chi = \begin{pmatrix} \chi^+/\sqrt{2} & \chi^{++} \\ \chi^0 & -\chi^+/\sqrt{2} \end{pmatrix}, \quad (8.8)$$

whereas those present in the doublet we will call

$$\phi = \begin{pmatrix} \phi^+ \\ \phi^0 \end{pmatrix}. \quad (8.9)$$

In addition, for the purposes of this section we will display explicitly the electric charge of the singlet  $\kappa$ , namely by writing  $\kappa^{++}$ . The neutral components of the various fields, moreover, are separated into their scalar and pseudoscalar components; besides, they are allowed to take VEV's. We define all these elements as follows:

$$\phi^0 = v_\phi + \frac{1}{\sqrt{2}} (\phi_s + i\phi_p), \quad \chi^0 = v_\chi + \frac{1}{\sqrt{2}} (\chi_s + i\chi_p), \quad \sigma = v_\sigma + \sigma_s, \quad (8.10)$$

with an “ $s$ ” subscript representing “scalar” and a “ $p$ ” subscript representing “pseudoscalar”.

After electroweak symmetry breaking fields with equal electric charge and parity mix among themselves; this happens irrespective of their  $SU(2)$  lineage and so the scalars are sorted into four groups,

each of them endowed with its own mass and mixing matrix. These matrices can easily be obtained by substituting equations (8.8), (8.9) and (8.10) into (8.1). If we arrange the fields as

$$\begin{aligned} \mathcal{L}_{\text{mass}} = & - \begin{pmatrix} \kappa^{--} & \chi^{--} \end{pmatrix} M_{++}^2 \begin{pmatrix} \kappa^{++} \\ \chi^{++} \end{pmatrix} - \begin{pmatrix} \phi^- & \chi^- \end{pmatrix} M_+^2 \begin{pmatrix} \phi^+ \\ \chi^+ \end{pmatrix} - \\ & - \frac{1}{2} \begin{pmatrix} \phi_s & \chi_s & \sigma_s \end{pmatrix} M_s^2 \begin{pmatrix} \phi_s \\ \chi_s \\ \sigma_s \end{pmatrix} - \frac{1}{2} \begin{pmatrix} \phi_p & \chi_p \end{pmatrix} M_p^2 \begin{pmatrix} \phi_p \\ \chi_p \end{pmatrix}, \end{aligned}$$

then the mass and mixing matrices<sup>3</sup> take the following form:

$$M_{++}^2 = \begin{pmatrix} \bar{m}_\kappa^2 & 0 \\ 0 & \bar{m}_\chi^2 + \lambda'_{\phi\chi} v_\phi^2 \end{pmatrix} + \frac{v_\chi}{v_\phi} \begin{pmatrix} 0 & 2\mu_\kappa v_\phi \\ 2\mu_\kappa v_\phi & 0 \end{pmatrix} + \mathcal{O}(v_\chi^2/v_\phi^2), \quad (8.11)$$

$$M_+^2 \simeq \begin{pmatrix} 0 & 0 \\ 0 & \bar{m}_\chi^2 \end{pmatrix} + \frac{v_\chi}{v_\phi} \begin{pmatrix} 0 & -\sqrt{2} \bar{m}_\chi^2 \\ -\sqrt{2} \bar{m}_\chi^2 & 0 \end{pmatrix} + \mathcal{O}(v_\chi^2/v_\phi^2), \quad (8.12)$$

$$M_s^2 = \begin{pmatrix} 4\lambda_\phi v_\phi^2 & 0 & 2\sqrt{2} \lambda_{\phi\sigma} v_\phi v_\sigma \\ 0 & \bar{m}_\chi^2 & -\sqrt{2} \lambda_6 v_\phi^2 \\ 2\sqrt{2} \lambda_{\phi\sigma} v_\phi v_\sigma & -\sqrt{2} \lambda_6 v_\phi^2 & 8\lambda_\sigma v_\sigma^2 \end{pmatrix} + \mathcal{O}(v_\chi/v_\phi), \quad (8.13)$$

$$M_p^2 = \begin{pmatrix} 0 & 0 \\ 0 & \bar{m}_\chi^2 \end{pmatrix} + \frac{v_\chi}{v_\phi} \begin{pmatrix} 0 & -2\bar{m}_\chi^2 \\ -2\bar{m}_\chi^2 & 0 \end{pmatrix} + \mathcal{O}(v_\chi^2/v_\phi^2), \quad (8.14)$$

where we used the notation  $\bar{m}_j^2 \equiv m_j^2 + \lambda_{\phi j} v_\phi^2 + \lambda_{\sigma j} v_\sigma^2$  bearing in mind that in the most interesting regions of the parameter space  $m_j^2$  will be the dominant term in such expressions. We have simplified the output by using (8.7) to eliminate the doublet and singlet squared masses in favour of the somewhat more physical  $v_\phi$  and  $v_\sigma$ . We have also separated explicitly the order-0 and order-1 terms in powers of  $v_\chi/v_\phi$ , the small parameter of the model; this separation is significant as far

---

<sup>3</sup> Beware that the “2” superindex is part of the ‘proper name’ of the matrix, and does not at all represent a matricial product. The  $M^2$  matrices are not “mass matrices”, but “squared-mass matrices”.

as the various  $\lambda$ 's are of the same order and don't introduce a new low scale in the model. Finally, we have neglected in the expression of  $M_+^2$  several terms of order  $v_\phi^2/\bar{m}_\chi^2$ .

By looking at the mass matrices (8.11 – 8.14) we note several important features: first, the mixing of the two doubly-charged scalars, dominated by the cubic dimensionful coupling  $\mu_\kappa$ : unless  $\mu_\kappa$  is much above  $m_\kappa$  and  $m_\chi$  –and this may not be natural, see section 8.5–, the mixing is bound to be small, and so one of the physical doubly-charged states will be mainly  $\kappa$ , and the other mainly  $\chi^{++}$ . Secondly, the somewhat seesaw-like structure of  $M_+^2$  and  $M_p^2$ , particularly realised if  $m_\chi \gg v_\phi, v_\sigma$ ; this is consistent with the fact that these two matrices must yield one zero eigenvalue each, for to those eigenvalues will correspond the two would-be Goldstone states that have to provide the longitudinal degree of freedom for the  $W$  and  $Z$  bosons. Actually, as we anticipated in section 8.2.2, to (8.11 – 8.14) we still have to require that they only yield nonnegative eigenvalues, in order for (8.7) to represent a true minimum of the potential. These conditions can be easily implemented in the mass matrices, and we note that they are particularly easy to implement in the limit of large  $m_\chi$ . Indeed, this limit seems especially convenient: it both ensures a phenomenologically viable triplet VEV (see the discussion at the end of section 8.2.2) and greatly simplifies the scalar spectrum, by fixing one definite-mass state in each group to an almost-triplet condition. As we have already stated, we will not restrict our discussion to this scenario –for it would be appealing to have the triplet scalars at the reach of the LHC–, but we will keep it in mind for the sake of having at hand a simple picture of the scalar panorama.

Moving on to a more detailed discussion, let us fix some notation for the definite-mass scalar states. We will call  $\kappa_1$  and  $\kappa_2$  the two massive doubly-charged states; they are the result of a certain mixture of  $\kappa$  and  $\chi^{++}$ ,

$$\begin{aligned}\kappa_1 &= \cos\theta_{++} \kappa^{++} + \sin\theta_{++} \chi^{++} \\ \kappa_2 &= -\sin\theta_{++} \kappa^{++} + \cos\theta_{++} \chi^{++},\end{aligned}\tag{8.15}$$

with  $\theta_{++}$  given by

$$\tan 2\theta_{++} \simeq \frac{4\mu_\kappa v_\chi}{m_\chi^2 - m_\kappa^2 + \lambda'_{\phi\chi} v_\phi^2}.$$

Note that this mixing is small for almost the entire parameter space: the denominator is at least of the order of the electroweak scale squared, while the numerator contains  $v_\chi$ , which is smaller by a factor 100, and  $\mu_\kappa$ , that can be large, but if it's much heavier than  $m_\chi$  or  $m_\kappa$  causes the theory to lose naturalness in loop corrections (see section 8.5 for more on this matter). In conclusion,  $\kappa_1$  is mainly composed of  $\kappa$  for most of the interesting scenarios, whereas  $\kappa_2$  is essentially  $\chi^{++}$ ; consequently,  $\kappa_1$  will prefer singlet-like couplings and will have small triplet-like couplings, while the opposite will be true for  $\kappa_2$ . See section 8.2.4 for specific examples of this feature.

We turn now to the pseudoscalar sector. The matrix (8.14) describes the masses and mixings for two real pseudoscalar fields; one of them must be massless, as the would-be Goldstone boson that provides the longitudinal part of the  $Z$  is a pseudoscalar. One can check<sup>4</sup> that this immediately happens if the fields are shifted to the minimum of the potential, given by (8.7). Moreover, the would-be Goldstone must be mainly a doublet, as argued in section 8.2.2, and indeed this is the case: let us define the definite-mass pseudoscalar fields as

$$\begin{aligned} G^0 &= \cos \theta_p \phi_p + \sin \theta_p \chi_p \\ A &= -\sin \theta_p \phi_p + \cos \theta_p \chi_p, \end{aligned}$$

where  $G^0$  is the would-be Goldstone,  $A$  the remaining physical pseudoscalar, and  $\theta_p$  the mixing angle between the doublet contribution,  $\phi_p$ , and the triplet one,  $\chi_p$ . This angle has to be small, as the electroweak symmetry is broken mainly by the doublet and  $G^0$  must be mainly  $\phi_p$ . And that's what happens, as can be seen rather easily from (8.14):

$$\tan 2\theta_p \simeq -4 \frac{v_\chi}{v_\phi}.$$

---

<sup>4</sup> This check requires the pieces of  $\mathcal{O}(v_\chi^2/v_\phi^2)$  in (8.14), as that is the order of the independent term in the characteristic equation of  $M_p^2$ .

It is sort of elegant that everything can be rewritten in a form that involves only symmetry-breaking-related parameters: as soon as  $v_\chi$  is small compared to  $v_\phi$ ,  $G^0$  will be indeed mainly doublet.

If we look at the singly-charged scalars we find a similar situation to that of the pseudoscalars: the matrix (8.12) must have one zero eigenvalue corresponding to the would-be Goldstone that provides the longitudinal part of  $W$  – note that this time the would-be Goldstone is a complex field, as  $W$  is. The would-be Goldstone, again, has to be essentially a doublet, and we can check that this is precisely the case. Expressing the definite-mass fields as

$$\begin{aligned} G^+ &= \cos \theta_+ \phi^+ + \sin \theta_+ \chi^+ \\ \omega^+ &= -\sin \theta_+ \phi^+ + \cos \theta_+ \chi^+, \end{aligned} \quad (8.16)$$

where  $G^+$  is the would-be Goldstone and  $\omega^+$  is the remaining physical singly-charged scalar, the mixing angle can be calculated as

$$\tan 2\theta_+ \simeq -2\sqrt{2} \frac{v_\chi}{v_\phi},$$

and we observe again that in the limit of  $v_\chi \ll v_\phi$  the Goldstone will be mainly a doublet, as expected.

As for the neutral scalar sector of the model, their mass matrix is not so constrained. One could obtain a few more constraints from requiring that all three eigenvalues are positive, but as our main goal is not to thoroughly characterise the scalar parameters we will avoid that discussion. We will just say that by looking at (8.13) we see that in the limit of large  $m_\chi$  one of the physical states is mainly a triplet, as expected, with mass approximately  $m_\chi$ . The other two neutral scalars depend greatly on the balance of the relevant parameters:  $v_\phi$ ,  $v_\sigma$  and the quartic couplings involved. If  $v_\phi$  and  $v_\sigma$  are of the same order and  $\lambda_{\phi\sigma}$  is not very small, we can expect  $\phi_s$  and  $\sigma_s$  to be pretty much mixed as part of at least two of the physical neutral scalars of the model.

#### 8.2.4 Some couplings of phenomenological interest

In this section we list some couplings that will be of interest during the remainder of our discussion. To begin with, it can be instructive

to express the  $\kappa$  Yukawas to right-handed electrons in terms of the mass eigenfields:

$$\overline{e_R^c} g e_R \kappa = \overline{e_R^c} g e_R (\cos \theta_{++} \kappa_1 - \sin \theta_{++} \kappa_2) , \quad (8.17)$$

checking indeed that  $\kappa_1$  –mainly singlet– retains most of the coupling, while  $\kappa_2$ , mainly triplet, has this interaction suppressed by the sine of the small angle  $\theta_{++}$ .

Also important for  $0\nu\beta\beta$  and neutrino masses will be the gauge interaction of the doubly-charged component of the triplet with two  $W$ 's, namely

$$g^2 W_\mu W^\mu \chi^{0\dagger} \chi^{++} = g^2 v_\chi W_\mu W^\mu (\sin \theta_{++} \kappa_1 + \cos \theta_{++} \kappa_2) + \dots , \quad (8.18)$$

which presents the opposite feature:  $\kappa_1$ , mainly singlet, has this triplet-like interaction suppressed by  $\sin \theta_{++}$ . The dots above represent the terms that involve  $\chi_s$  and  $\chi_p$ , which we will not use.

We present also explicitly here some trilinear couplings that we will use at some point:

$$-\mu_\kappa \kappa^{++} \chi^- \chi^- - 2\mu_\kappa \kappa^{++} \chi^{--} \chi^{0\dagger} + \lambda_6 \sigma \chi^{++} \phi^- \phi^- + \text{H.c.} ;$$

of course, these couplings can also be expressed in terms of VEV's and mass eigenfields by using equations (8.10), (8.15) and (8.16).

Finally, let us write explicitly the Yukawas that change charge and chirality:

$$\overline{\nu_L} Y_e e_R \phi^+ = \overline{\nu_L} Y_e e_R (\cos \theta_+ G^+ - \sin \theta_+ \omega^+) .$$

### 8.3 Neutrinoless double beta decay

$0\nu\beta\beta$  through the  $WWee$  mechanism requires couplings to right-handed electrons and to  $W$  bosons; in this model, the first are provided by the singlet  $\kappa$  and the second by the doubly-charged component of the triplet. As the two of them mix new massive states arise,  $\kappa_1$  and  $\kappa_2$ , which participate of both kinds of interactions, as described in sections 8.2.3 and 8.2.4. These particles are the necessary mediators

for  $0\nu\beta\beta$ . In this section we calculate their contribution to the process of double beta decay and set the appropriate constraints upon the involved parameters to fit the current experimental bounds; we also deduce the range in which the relevant parameters should lie if  $0\nu\beta\beta$  is to be observed in the next round of experimental searches.

We can deduce the model contribution to  $0\nu\beta\beta$  even before thinking about the particular physical process that generates it. Assuming that  $m_\kappa, m_\chi \gg v_\phi, v_\sigma$  and integrating out the heavy  $\kappa$  and  $\chi$  modes we find, after a straightforward calculation, that the effective Lagrangian contains the term

$$\mathcal{L}_9 = 4 \frac{(\lambda_6 v_\sigma)^2 \mu_\kappa}{m_\kappa^2 m_\chi^6} \left( \overline{e_{R\alpha}} g_{\alpha\beta}^* e_{R\beta}^c \right) \left( \phi^\dagger D^\mu \tilde{\phi} \right) \left( \phi^\dagger D_\mu \tilde{\phi} \right) + \text{H.c.}, \quad (8.19)$$

as expected, because the model contains the necessary ingredients to generate the  $\mathcal{O}^{(9)}$  operator (see section 8.1 for more details). The explicit  $WWee$  vertex is revealed once the electroweak symmetry breaks spontaneously and looks

$$\mathcal{L}_9 = -2g^2 \frac{\mu_\kappa v_\chi^2}{m_\kappa^2 m_\chi^2} \overline{e_{R\alpha}} g_{\alpha\beta}^* e_{R\beta}^c W^\mu W_\mu + \text{H.c.} + \dots, \quad (8.20)$$

where we have used the expression for  $v_\chi$  in the limit of large  $m_\chi$ ,  $v_\chi \simeq \lambda_6 v_\sigma v_\phi^2 / m_\chi^2$ , derived from (8.7). It must be emphasised that in this model the interactions violating LN in two units, equation (8.19), happen to be proportional to  $v_\chi^2$ ; this is qualitatively different from other models –for example, seesaw type II– where the LNV-ing interactions are linear in  $v_\chi$ , indicating that a different mechanism is in action here. This is a consequence of having chosen carefully our fundamental vertices so that  $\chi$  cannot be assigned lepton number 2, thus qualitatively separating our model from those that generate  $\mathcal{O}^{(5)}$  at tree level.

One can better understand the form of (8.19) by considering the physical process that gives rise to it. The dominant diagram is shown in figure 8.1, where the different couplings and VEV's involved are displayed explicitly. We note the importance of the mixing between  $\kappa$  and  $\chi^{++}$ , represented by the presence of  $\mu_\kappa$ ; we also note that two VEV's of  $\chi$  are present, but they can be expressed either as such, like



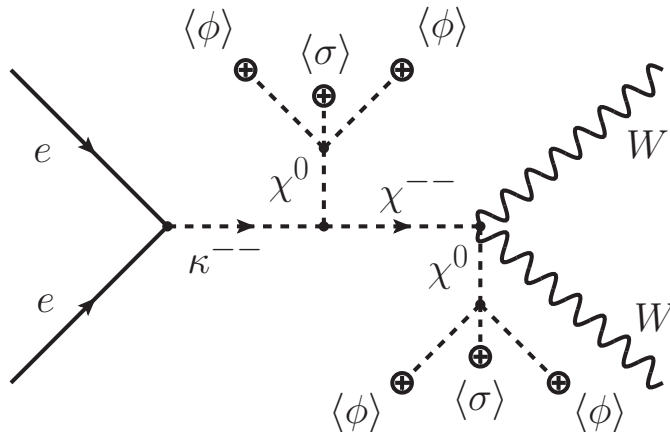


Fig. 8.1: Dominant tree-level diagram contributing to the effective neutrinoless double beta decay operator.

in (8.20), or as combinations of  $v_\phi$  and  $v_\sigma$  with  $\lambda_6$  insertions, as in (8.19). This same process could be displayed in terms of the physical massive states  $\kappa_1$  and  $\kappa_2$  by using their couplings (8.17) and (8.18); we would see then an apparently much cleaner diagram, with just  $\kappa_1$  or  $\kappa_2$  mediating between the pair of electrons and the pair of  $W$ 's. In this view many of the couplings and VEV's that we see in (8.19) would be codified inside the  $\theta_{++}$  mixing; to avoid this 'hiding' we prefer the pre-EWSB vision of figure 8.1, to which we will refer when necessary.

Let us now derive bounds on the model parameters from the experimental limits on  $0\nu\beta\beta$ . For that aim we will use the very general analysis carried out in [145], where the authors used detailed nuclear matrix element calculations to set bounds on all the six-fermion interactions that can provide  $0\nu\beta\beta$ . In our model, the interaction (8.20) leads to a six-fermion vertex of the form

$$\mathcal{L}_{0\nu\beta\beta} = \frac{G_F^2}{2m_p} \epsilon_3 [\bar{u}\gamma^\mu(1 - \gamma_5)d] [\bar{u}\gamma_\mu(1 - \gamma_5)d] \bar{e}(1 - \gamma_5)e^c, \quad (8.21)$$

where  $m_p$  denotes the proton mass and  $\epsilon_3$ , which corresponds to [145]'s notation, reads

$$\epsilon_3 = -8 \frac{m_p \mu_\kappa v_\chi^2}{m_\kappa^2 m_\chi^2} g_{ee}^*.$$

All that is left, so, is to read from [145] the bound that applies to operators like (8.21); it is just  $\epsilon_3 < 1.4 \times 10^{-8}$  at 90% CL<sup>5</sup>. But we will want something else: we would like the model to yield a signal in the next round of  $0\nu\beta\beta$  experiments. In order to implement this requirement we turn again to [145] and see that their bounds are derived from the Heidelberg-Moscow limit<sup>6</sup>,  $T_{1/2} > 1.9 \times 10^{25}$  years for  $^{76}\text{Ge}$  [146]. These numbers are reported to be improved in the next years up to lifetimes of  $6 \times 10^{27}$  years [243], that is to say, an increase in a factor of 20 in sensitivity. Gathering together all these ideas we obtain the following requirement for the parameters of our model:

$$8.75 \times 10^{-11} \stackrel{\text{Next}}{<} \frac{m_p \mu_\kappa v_\chi^2}{m_\kappa^2 m_\chi^2} |g_{ee}| < 1.75 \times 10^{-9} \quad (90\% \text{ CL}), \quad (8.22)$$

where the upper bound corresponds to the Heidelberg-Moscow experimental limit, whereas the ‘‘Next’’ superindex in the lower bound indicates that it’s not an experimental requirement, but only the limit in sensitivity to be attained by the next round of experiments. These conditions will prove to be rather restrictive because their range of variation is relatively narrow; see section 8.7 for a discussion of the constraints that this and other phenomenological requirements set on the new particles of the model.

#### 8.4 Lepton flavour violation constraints

Lepton flavour violation constitutes a very relevant probe to test the phenomenological viability of the model. The  $g$  Yukawas introduce a new flavour hierarchy, independent of that of the Higgs Yukawas  $Y_e$ , and so they can induce all sorts of LFV-ing processes. Here we will look into the most restrictive of them: the tree-level-mediated three-body decays of the form  $\ell_\alpha^- \rightarrow \ell_\beta^+ \ell_\gamma^- \ell_\eta^-$ . Other LFV-ing processes

<sup>5</sup> Actually there is a misprint in [145]. We are very grateful to the authors for providing us with the correct result.

<sup>6</sup> This experiment remained for more than a decade the most sensitive one to the effective neutrino Majorana mass,  $m_{\beta\beta}$ , but has been recently superseded by the EXO bound for  $^{136}\text{Xe}$  [131] and the GERDA bound for  $^{76}\text{Ge}$  [132]. We, nevertheless, stick to the numbers in [145].

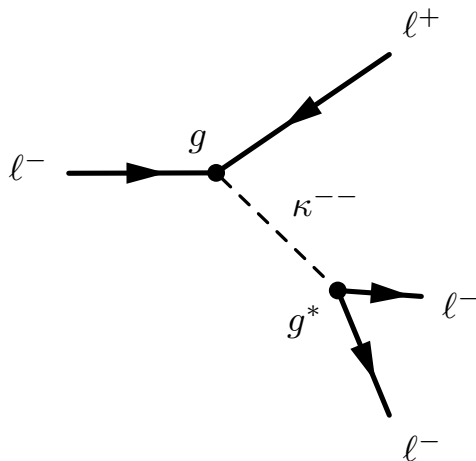


Fig. 8.2: The tree-level diagram that yields LFV-ing three-body decays through the  $g$  Yukawas.

yield milder constraints:  $\ell_\alpha^- \rightarrow \ell_\beta^- \gamma$  proceeds at one loop and the bound on the model parameters is weaker due to the loop factor; similarly happens for  $\mu - e$  conversion in nuclei; the bounds for  $\mu^+ e^- \leftrightarrow \mu^- e^+$  (muonium-antimuonium conversion), though tree-level, are also less restrictive<sup>7</sup>.

So, let us consider the three-body leptonic decays  $\ell_\alpha^- \rightarrow \ell_\beta^+ \ell_\gamma^- \ell_\eta^-$ ; in our model these are mediated by the doubly-charged singlet  $\kappa$ , as depicted in figure 8.2. Of course, in the mass-eigenstate basis the  $\kappa$  couplings get split between the two massive eigenfields  $\kappa_1$  and  $\kappa_2$ , as seen in (8.17), and this is reflected in the expression for the branching ratio of the process,

$$\text{BR}(\ell_\alpha^- \rightarrow \ell_\beta^+ \ell_\gamma^- \ell_\eta^-) = \frac{1}{2(1 + \delta_{\gamma\eta})} \left| \frac{g_{\alpha\beta} g_{\gamma\eta}^*}{G_F \tilde{m}_\kappa^2} \right|^2 \text{BR}(\ell_\alpha^- \rightarrow \ell_\beta^- \nu \bar{\nu}), \quad (8.23)$$

where  $\tilde{m}_\kappa$  is a compact way of representing the contribution of the two

<sup>7</sup> For a more comprehensive discussion of LFV mediated by doubly-charged scalar singlets the reader might find interesting [259, 260], where models with similar features are considered.

mass eigenstates:

$$\frac{1}{\tilde{m}_\kappa^2} \equiv \frac{\cos^2 \theta_{++}}{m_{\kappa_1}^2} + \frac{\sin^2 \theta_{++}}{m_{\kappa_2}^2},$$

and  $\delta_{\gamma\eta}$  accounts for the statistics of identical particles, were it the case that  $\gamma = \eta$ . Note –see the details in sections 8.2.3 and 8.5– that if naturality is required then  $\theta_{++}$  is rather small, and we will have  $\tilde{m}_\kappa \simeq m_{\kappa_1}$ , recovering the case in which only the singlet –or its direct offspring,  $\kappa_1$ – mediates the process.

Let us now adapt the expression (8.23) to the cases that will be more important for our description of the model. The most constrained decay of the type  $\ell \rightarrow 3\ell$  is  $\mu \rightarrow 3e$ ; for it we have the upper bound  $\text{BR}(\mu^- \rightarrow e^+e^-e^-) < 1.0 \times 10^{-12}$  [32], which translates into

$$|g_{\mu e} g_{ee}^*| < 2.3 \times 10^{-5} (\tilde{m}_\kappa/\text{TeV})^2. \quad (8.24)$$

As we will see, for our purposes this constitutes mainly a constraint on  $g_{\mu e}$  because we want  $g_{ee}$  as large as possible in order to enhance  $0\nu\beta\beta$ .

As it couldn't be but expected, the LFV bounds essentially favour small  $g$  couplings and large scalar masses. This sets a conflict with other phenomenological features of the model, and especially with neutrino masses, which are rather suppressed and would prefer *large* values of the  $g$  Yukawas. Amidst this discussion –see sections 8.6 and 8.7 for more details–, one particular LFV-ing process happens to cast a special tension: it's  $\tau^- \rightarrow e^+\mu^-\mu^-$ , whose experimental branching ratio is bounded to be  $\text{BR}(\tau^- \rightarrow e^+\mu^-\mu^-) < 1.7 \times 10^{-8}$  [32]. This means that for our model we must impose

$$|g_{e\tau} g_{\mu\mu}^*| < 0.007 (\tilde{m}_\kappa/\text{TeV})^2. \quad (8.25)$$

As for other three-body decays, most add interesting constraints or suggest that the model could be just one step beyond the current experimental sensitivity, at least if it is to fulfill requirements such as “yield a signal in the next round of  $0\nu\beta\beta$  experiments” or “leave the new particles at the reach of the LHC”. As a general statement we can say that the  $g$  couplings involving only heavy leptons, such as  $g_{\mu\mu}$  or  $g_{\mu\tau}$ , are required not to be very small due to constraints on the neutrino mass matrix; were the new particles not very heavy, these processes could be a good probe of the interactions of the model.

### 8.5 Constraints from naturality and perturbative unitarity

In the discussion of  $0\nu\beta\beta$  carried out in section 8.3 we found that its rate in this model is proportional to the combination of parameters  $\mu_\kappa v_\chi^2 g_{ee}$ ; that happened somehow as expected, for all these couplings are needed in order to violate lepton number, as argued at the end of section 8.1. We will find equally –see section 8.6– that neutrino masses depend on the same combination of parameters. And in both cases we would like it to be large: for  $0\nu\beta\beta$  we want to know if the rate can be large enough to yield a signal in near-future experiments; for neutrino masses, we want to overcome the suppression introduced by the charged-lepton Yukawas. Therefore, at this point the question of how large some couplings can be becomes relevant. It is well known that very large couplings make a quantum field theory unaccessible to perturbative exploration – and so most of our calculations meaningless. It is also generally acknowledged that a theory requiring fine tuning in the process of renormalisation cannot be considered natural; this happens, for example, if two mass scales related by loop corrections are largely dissimilar. In this section we will use these considerations to set upper bounds on the values of the couplings of the model.

Let us first discuss perturbative unitarity. As we know, the scattering matrix that we commonly use to evaluate physical processes is nothing but a reexpression of the time-evolution operator, and the unitary character of this operator can be used to set bounds on the elements of the S-matrix – see, for example [261]. But to calculate such elements we use perturbation theory, so these bounds can be better expressed as “unitarity bounds as long as perturbation theory is valid”. We can use those bounds for our case. Consider the electron-electron scattering mediated by the doubly-charged singlet  $\kappa$  – or more precisely by the massive states that participate from it,  $\kappa_1$  and  $\kappa_2$ . At high-energy, tree-level unitarity requires  $|g_{ee}| < \sqrt{4\pi}$  [175, 262, 263]. Exactly the same is obtained for the analogous processes involving other leptons. In conclusion, we won’t be considering values of the  $g$  Yukawas above  $\sqrt{4\pi}$ ,

$$|g_{\alpha\beta}| \stackrel{\text{Unit}}{<} \sqrt{4\pi}. \quad (8.26)$$

Tree-level unitarity at high energy does not give useful information on dimensionful parameters like  $\mu_\kappa$  because amplitudes involving these couplings decrease with energy. To bound this scale we turn to naturalness arguments, noting that the one-loop self-energies of  $\kappa$  and  $\chi$  involve loops with two powers of  $\mu_\kappa$  which correct  $m_\kappa^2$  and  $m_\chi^2$ . These diagrams are of course divergent, but after renormalisation yield corrections that roughly read  $\delta m_{\kappa,\chi}^2 \sim \mu_\kappa^2/(4\pi)^2$ . For the theory not to be fine-tuned it is enough to require that the one-loop corrections are below the tree-level contribution, that is,

$$\mu_\kappa^{\text{Nat}} < 4\pi \min(m_{\kappa_1}, m_{\kappa_2}), \quad (8.27)$$

where we bound with respect to  $m_{\kappa_1}, m_{\kappa_2}$  rather than  $m_\kappa, m_\chi$ , as those are the physical masses of the theory. Note that other alternative requirements for naturalness, such as the width of the new particles  $\kappa_1$  and  $\kappa_2$  not being larger than their masses, are also met if (8.26) and (8.27) hold.

One must be aware, however, that all these limits are estimates which depend on what is our idea of a ‘natural theory’. Thus, although at the price of fine tuning, one might decide to fix the model parameters outside the range defined by these limits; moreover, there can be model extensions where those values are natural. At any rate, we use equations (8.26) and (8.27) in the text to illustrate that the allowed regions in parameter space are at a large extent bounded if the perturbative theory must stay natural.

### 8.6 A very constrained neutrino spectrum

Lepton number is violated in this model through the conjoint action of the  $g$  Yukawas and the  $\mu_\kappa$  and  $\lambda_6$  scalar interactions; the violation affects at this level the leptonic right-handed singlets, and that’s why  $0\nu\beta\beta$  proceeds mainly to two  $e_R$ ’s. But the breaking is right away transmitted to the left-handed doublets through the charged-lepton Yukawas  $Y_e$ , and once this happens nothing can help the left-handed neutrinos from developing Majorana masses. This occurs at the two-loop level, as was expected for the  $WWee$  mechanism (see section 6.1 for

more on the rationale of the mechanism), and the generated masses are finite and calculable, as none of the mass-generating interactions appear at lower orders. The complete picture of neutrino mass generation, however, is complicated: many interactions are involved, and the nontrivial vacuum structure of the model yields a variety of vertices that connect the several degrees of freedom of the theory. In order to illustrate this situation we present in figure 8.3 three of the diagrams that provide neutrino masses; they are presented in the mass insertion picture so that the role played by the vacuum expectation values can be explicitly identified. As we see, the VEV's enter the diagrams in a variety of ways, and the  $SU(2)$  charges of the involved degrees of freedom are widely dissimilar. It would appear, at first glance, that these processes represent very different contributions to neutrino masses. To make the situation even more convoluted, figure 8.3 hardly represents a small fraction of the total amount of contributing diagrams: the several mixing terms between  $W$ ,  $\phi^+$  and  $\chi^+$  yield a fauna of mixed graphs with varying coupling content and suppression factors. All in all, diagrams *a)* and *b)* represent the leading contributions in this approach, but it's hard to estimate the importance of the remaining graphs, surely subdominant but also much more numerous.

Fortunately, there's more than differences between the graphs presented in figure 8.3; a number of common features can be observed that will prove to be revealing: the loop topology, for instance, is the same for all of them; the electric charge of the particles in each line remains the same; and most important: after maybe some reworking by using equations (8.7), *all* the diagrams are shown to be proportional to  $\mu_\kappa v_\chi^2 Y_e^2 g$  – where  $g$  represents not the weak gauge coupling but one of the  $\kappa$  Yukawas. All these are features which suggest that a simpler picture must exist for the generation of neutrino masses. Most likely one can find a basis for the bosons of the theory where this complicated set of interactions and mixings is encoded inside the couplings of just a few relevant degrees of freedom. A way to explore the possible rearrangements of the bosonic sector is by choosing a particular gauge. One could think initially that the unitary gauge is a good candidate: after all, all the fields there represent physical excitations with definite mass, and only two singly-charged bosons

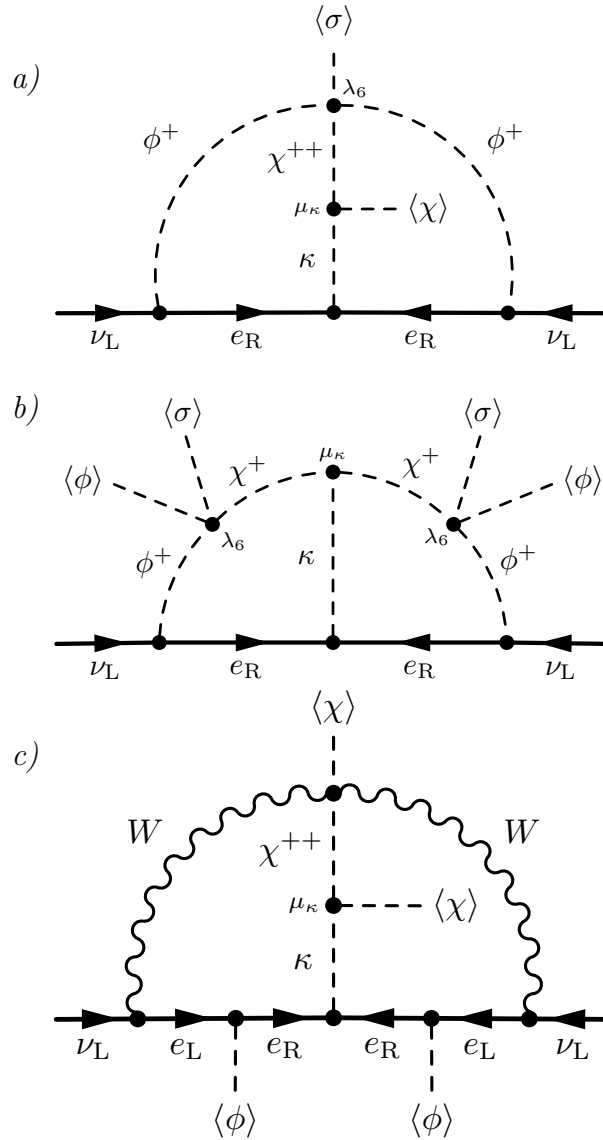


Fig. 8.3: Three of the two-loop processes that provide neutrino masses in this model, displayed in the mass insertion approach. The reader can check that the complete list includes many more, mainly combining several sorts of  $W - \phi^+$ ,  $W - \chi^+$  or  $\phi^+ - \chi^+$  mixing in the scalar legs. However, among all of them, a) and b) represent the dominant contributions.



are present: the massive  $W$  and the scalar  $\omega$ . However, in this gauge other type of difficulties arise: the  $W$  propagators happen to render some quadratically-divergent pieces in the loops, and we know they must cancel because the neutrino masses are finite, but this makes the actual calculation sort of tricky and cumbersome. This is why we looked for a different gauge which succeeds in simplifying the mass generation picture without yielding further complications. Fortunately, such a gauge does indeed exist.

### 8.6.1 Calculation of the two-loop neutrino masses

The difficulty that we want to address with the gauge choice is the large number of mass-generating diagrams, which is mainly due to the extensive mixing between the bosonic fields, both the scalars and the gauge bosons. Therefore, we seek a gauge which cancels most of the mixings between the various singly-charged degrees of freedom; that can be achieved by a gauge fixing of the form

$$\mathcal{L}_{\text{g.f.}} = a \left( \partial^\mu W_\mu^\dagger + b \chi^+ + c \phi^+ \right) \left( \partial^\mu W_\mu^\dagger + b \chi^+ + c \phi^+ \right)^\dagger,$$

where the constants  $a, b, c$  represent

$$a = -\frac{m_W^2}{m_\omega^2} \quad b = -i \frac{m_\omega^2}{m_W^2} \sqrt{1 - \rho} \quad c = -i \frac{m_\omega^2}{m_W^2},$$

with  $m_\omega$  the combination of parameters

$$m_\omega^2 \equiv m_\chi^2 + \lambda_{\sigma\chi} v_\sigma^2 + \left( \lambda_{\phi\chi} + \frac{1}{2} \lambda'_{\phi\chi} \right) v_\phi^2, \quad (8.28)$$

which roughly corresponds to the mass of the physical singly-charged scalar of the theory, and  $\rho$  the electroweak  $\rho$  parameter yielded by the model, equation (8.5). The reader can check that in this gauge there are no  $W\chi^+$ ,  $W\phi^+$  or  $\phi^+\chi^-$  mixing terms; this means that there are just two mass-generating diagrams: one with  $W$ 's and one with  $\phi^+$ 's, which we display in figure 8.4. Without mixing no other two-loop diagram can be closed, because  $\chi^+$  doesn't couple to fermions and there is no mixed  $W\phi^+\kappa_{1,2}$  vertex – not just in this gauge, there is no

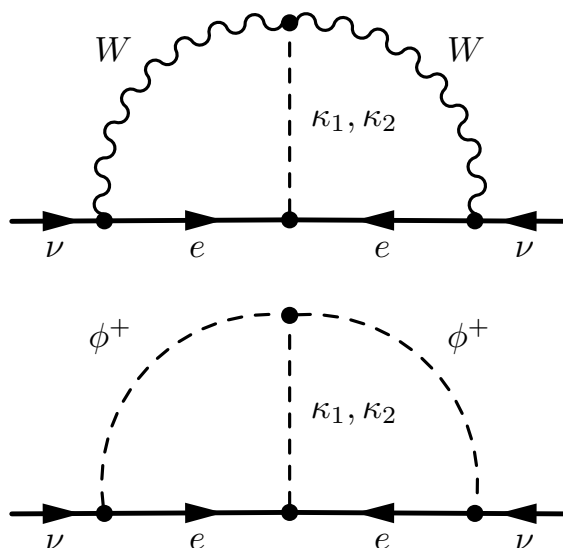


Fig. 8.4: The two diagrams that yield neutrino masses at two loops in the gauge with no  $W - \phi$ ,  $W - \chi$  and  $\chi - \phi$  mixing.

such an interaction in this model. Other relevant features of this gauge include the fact that  $\phi^+$  is massive with mass  $m_\omega$ , and a modified propagator for the  $W$  bosons,

$$iD_{\mu\nu}(k) = \frac{-i}{k^2 - m_W^2} \left[ \eta_{\mu\nu} - \left( 1 - \frac{m_\omega^2}{m_W^2} \right) \frac{k_\mu k_\nu}{k^2 - m_\omega^2} \right],$$

which has no quadratic terms, and so does not yield divergent pieces in the loop integrals.

With all these ingredients at hand, we are now prepared to calculate the neutrino masses. Let us define the neutrino mass matrix as

$$\mathcal{L}_{\text{mass}} = -\frac{1}{2} \bar{\nu}_L m \nu_L^c + \text{H.c.},$$

and note that in the following we will use  $m_{\alpha\beta}$  to denote the elements of the neutrino mass matrix and  $m_\alpha$  to represent the mass of the charged lepton of the family  $\alpha$ . By working out the diagrams in figure 8.4 we obtain

$$m_{\alpha\beta} = \frac{1}{2(2\pi)^4} \frac{\mu_\kappa v_\chi^2}{v_\phi^4} m_\alpha g_{\alpha\beta}^* m_\beta I_\nu, \quad (8.29)$$

where it is worth noting the dependence on the combination of parameters  $\mu_\kappa v_\chi^2$ , which we already found while calculating the post-SSB form of the  $WWee$  interaction, equation (8.20); its presence here is just an indication that this is again the relevant physics in play for neutrino mass generation. In contrast, models which rely on the triplet Yukawas  $\overline{\ell}_L \chi \ell_L$  to yield neutrino masses, like for instance type-II seesaw, show a linear dependence in  $v_\chi$ . In our model the  $Z_2$  symmetry forbids the triplet Yukawas and neutrino masses arise from the  $WWee$  mechanism.

Some discussion is also in order concerning the function  $I_\nu$  which appears in (8.29).  $I_\nu$  is a factor provided by the loop integrals, and as such it is a function of the parameters of the model, especially of the masses running inside the loops. For the case of the gauge we are considering,  $I_\nu$  comprises two contributions, one from each of the diagrams in figure 8.4. We will write  $I_\nu = I_W + I_\phi$ , and we will have, after appropriate rescaling to fit the factors in equation (8.29),

$$\begin{aligned}
I_W &= -2(4\pi)^4 m_W^4 \cos^4 \theta_+ \times \\
&\times \int \frac{d^4 k d^4 q}{k^2 (k^2 - m_W^2) q^2 (q^2 - m_W^2) [(k-q)^2 - m_{\kappa_1}^2] [(k-q)^2 - m_{\kappa_2}^2]} \times \\
&\quad \times \left[ 4 - \left(1 - \frac{m_\omega^2}{m_W^2}\right) \left(\frac{k^2}{k^2 - m_\omega^2} + \frac{q^2}{q^2 - m_\omega^2}\right) + \right. \\
&\quad \left. + \left(1 - \frac{m_\omega^2}{m_W^2}\right)^2 \frac{(k \cdot q)^2}{(k^2 - m_\omega^2)(q^2 - m_\omega^2)} \right], \quad (8.30)
\end{aligned}$$

$$\begin{aligned}
I_\phi &= (4\pi)^4 \left(m_\omega^2 - \frac{1}{2} \lambda'_{\phi\chi} v_\phi^2\right) \times \\
&\times \int \frac{d^4 k d^4 q k \cdot q}{k^2 (k^2 - m_\omega^2) q^2 (q^2 - m_\omega^2) [(k-q)^2 - m_{\kappa_1}^2] [(k-q)^2 - m_{\kappa_2}^2]}, \quad (8.31)
\end{aligned}$$

where we have used  $m_\omega$  as defined in equation (8.28). Note that each of the two diagrams in figure 8.4 represents in turn two processes: one with  $\kappa_1$  and other with  $\kappa_2$  running inside the loop. Some reworking,

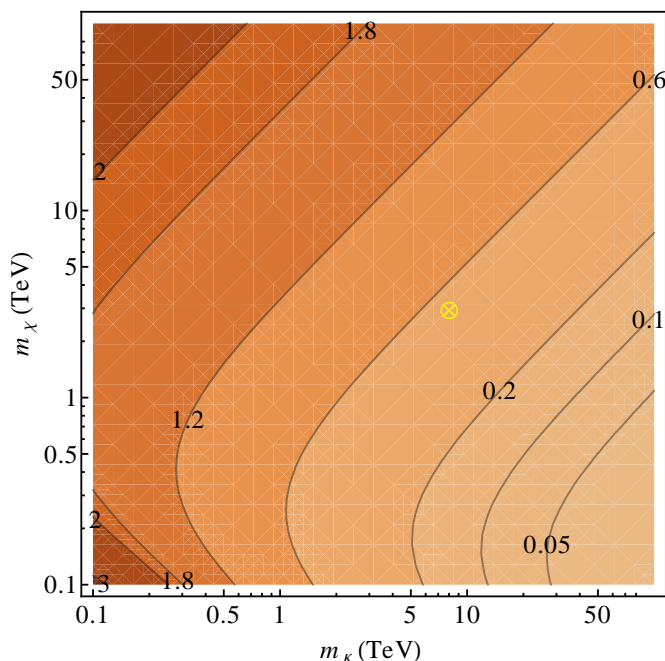


Fig. 8.5: Contour plot for the loop integral  $I_\nu$  in the limit  $v_\chi \ll v_\phi$ , as a function of the masses  $m_\kappa \simeq m_{\kappa_1}$  and  $m_\chi \simeq m_{\kappa_2}$ , and assuming  $m_\omega = m_\chi$  and  $m_W = 80$  GeV. The cross marks the reference point presented in equation (8.38).

which involves the doubly-charged mixing  $\theta_{++}$ , is needed in order to express the total result as seen in equations (8.29 – 8.31); essentially, the unitarity of the doubly-charged mixing matrix is used to join the  $\kappa_1$  and  $\kappa_2$  contributions into one single integral that contains both  $m_{\kappa_1}$  and  $m_{\kappa_2}$  and which is manifestly finite.

In general,  $I_\nu$  is a complicated function of  $m_W, m_{\kappa_1}, m_{\kappa_2}, m_\omega$  and the ratio  $v_\chi/v_\phi$ , which enters into the mixing angles. However, a few reasonable assumptions can be made that very much simplify the scenario: first, it is a phenomenological requirement that  $v_\chi \ll v_\phi$ , which ensures that  $\kappa_1$  and  $\kappa_2$  are not very much mixed; this means that  $m_{\kappa_1} \simeq \bar{m}_\kappa$  and  $m_{\kappa_2} \simeq \bar{m}_\chi$ , in the notation used for equation (8.11). Second, we assume that  $\bar{m}_\kappa \simeq m_\kappa$  and  $\bar{m}_\chi, m_\omega \simeq m_\chi$ , which is true either if  $m_\kappa, m_\chi \gg v_\phi, v_\sigma$  or if the  $\lambda$  couplings involved are small. With

these assumptions,  $I_\nu$  becomes a function only of  $m_\kappa^2/m_W^2$  and  $m_\chi^2/m_W^2$ , which we compute numerically. In figure 8.5 we plot the contours of constant  $I_\nu$  as a function of the masses  $m_{\kappa_1} \simeq m_\kappa$  and  $m_{\kappa_2} \simeq m_\chi$ , with the  $W$  mass fixed to  $m_W = 80$  GeV. From the figure we appreciate that  $I_\nu$  is  $\mathcal{O}(1)$  for a large region of the parameter space, only producing small values when  $m_\kappa \gg m_\chi$ . We conclude, so, that for most cases  $I_\nu$  can be ignored in equation (8.29) for order-of-magnitude estimates, with the remaining involved parameters adequately capturing the physics of neutrino mass generation.

### 8.6.2 The structure of the neutrino mass matrix

Equation (8.29) presents a neutrino mass matrix highly influenced by the charged leptons' masses. The factor  $m_\alpha m_\beta / v_\phi^2$  poses an extra suppression which is element-dependent, and so induces a well-definite hierarchy in the mass matrix that is only modulated by the Yukawas  $g_{\alpha\beta}$  and by global factors. From our present knowledge of neutrino parameters the mass matrix is by no means arbitrary, so it is natural to wonder whether this induced hierarchy is admissible or if it dooms the model to exclusion. In this section we discuss the range of variation of the most tightly pressed elements, while in the next one we examine if this hierarchy can accommodate a phenomenologically viable pattern of neutrino masses.

Let us begin with the matrix element  $m_{ee}$ ; being proportional to  $m_e^2$ , it is most surely forced to be small. How quantitative can we make this assertion? If we take  $\mu_\kappa \sim 10$  TeV,  $v_\chi \sim 2$  GeV, and  $I_\nu, |g_{ee}| \sim 1$ , equation (8.29) yields  $|m_{ee}| \sim 3.7 \times 10^{-6}$  eV, a certainly small value – compare with the other known neutrino mass scales: the atmospheric scale,  $\sqrt{\Delta m_{\text{atm}}^2} = 0.05$  eV, and the solar scale,  $\sqrt{\Delta m_{\odot}^2} = 0.009$  eV. How much can  $m_{ee}$  vary? Making it smaller would only require to take smaller  $|g_{ee}|$ ,  $\mu_\kappa$  or  $v_\chi$  – of course at the prize of reducing the  $0\nu\beta\beta$  rate, which we do not desire, but in this way we could easily have  $|m_{ee}| \rightarrow 0$ . However, how *large* can it be? How much can we push the limit to the more interesting ‘heavy’ scenario? In cooking a large  $|m_{ee}|$  we will end up facing the upper limit on  $v_\chi$ , the unitarity limit on  $|g_{ee}|$  and the naturalness limit for  $\mu_\kappa$  (see equations

(8.6), (8.26) and (8.27), respectively, and the discussion upon them). None of these is a strict and inescapable bound, but rather they're order-of-magnitude estimates that could be stretched, or might change when detailed radiative corrections are considered. We implement them in (8.29) in order to get an estimate of the upper bound on  $|m_{ee}|$ ; for  $v_\chi$  we prefer the 2 GeV bound that does not require loop corrections. With all this considered, we obtain

$$|m_{ee}| < 1.6 \times 10^{-5} \left( \frac{\min(m_{\kappa_1}, m_{\kappa_2})}{\text{TeV}} \right) \text{ eV}.$$

Now we would like an upper bound on the lightest of  $m_{\kappa_1}$  and  $m_{\kappa_2}$ ; as larger masses imply less observable effects, this cannot be obtained from an experimental limit. Rather, we turn to the requirement that a signal is observed in the next round of  $0\nu\beta\beta$  experiments, equation (8.22), which naturally disfavors very heavy masses; from there we find that  $\min(m_{\kappa_1}, m_{\kappa_2}) \sim 10 \text{ TeV}$ , and this translates into

$$|m_{ee}| < 1.6 \times 10^{-4} \text{ eV}. \quad (8.32)$$

Alternatively, we could also translate the experimental limits on  $0\nu\beta\beta$  into bounds on  $|m_{ee}|$ , but for large scalar masses this limit is less stringent than (8.32). In either case, one can say that  $|m_{ee}|$  is typically less than  $10^{-4}$ .

Another very constrained matrix element is  $m_{e\mu}$ ; this one is proportional to  $g_{e\mu}$ , which is tightly bounded by  $\mu \rightarrow 3e$ —see equation (8.24)—, especially if one desires to have large  $0\nu\beta\beta$  rates, and so large values of  $|g_{ee}|$ . By substituting (8.24) into (8.29), one gets

$$|m_{e\mu}| < 2.3 \times 10^{-5} \left( \frac{m_\kappa}{\text{TeV}} \right)^2 \frac{\mu_\kappa v_\chi^2}{2(2\pi)^4 v_\phi^4} \frac{m_e m_\mu}{|g_{ee}|} I_\nu,$$

from where we can eliminate  $|g_{ee}|$  by imposing the observation of  $0\nu\beta\beta$  in the next generation of experiments, and then again pushing the parameters to their maximum values:

$$|m_{e\mu}| < 4.3 \frac{\mu_\kappa^2}{m_\chi^2} \frac{v_\chi^4}{v_\phi^4} I_\nu \text{ eV} < 1.2 \times 10^{-5} \text{ eV},$$

where we took again  $I_\nu \sim 1$  and  $v_\chi \sim 2$  GeV, and used the naturalness bound on  $\mu_\kappa$  together with the observability of  $0\nu\beta\beta$ .

In conclusion, the neutrino mass matrix generated by this model must have tiny  $ee$  and  $e\mu$  elements; more precisely,  $|m_{ee}|, |m_{e\mu}| \lesssim 10^{-4}$  eV. This follows from two assumptions: (i) that  $0\nu\beta\beta$  is at the reach of the next round of experiments, and (ii) that the theory is perturbative and free of unnatural fine tuning up to several tens of TeV. These limits could be somewhat relaxed: in the  $|m_{ee}|$  case by making doubly-charged scalar masses larger, and for  $|m_{e\mu}|$  by allowing a smaller  $|g_{ee}|$ . In both cases the model would lose some interesting feature, and we prefer to stick with these requirements and see if the general picture can make sense anyway. The next section addresses this question.

### 8.6.3 Consequences for the neutrino mass spectrum

In the previous section we discussed that the neutrino spectrum generated by this model must present very small  $m_{ee}$  and  $m_{e\mu}$ . The question now becomes whether it is possible to accommodate the observed pattern of neutrino masses and mixings into this particular structure. To answer this question we need to construct the neutrino mass matrix, because experiments don't probe directly mass matrix elements but rather magnitudes such as mixing angles, phases and squared-mass splittings. Let us use the parametrisation of neutrino masses described in section 3.1.3,

$$m_\nu = U D_\nu U^T, \quad \text{with } D_\nu = \text{diag}(m_1, m_2, m_3) \quad (8.33)$$

and  $U$  the PMNS matrix as seen in equation (3.5). The current best values for the neutrino mass and mixing parameters can be consulted in table 3.1; remember that the phases, the sign of  $\Delta m_{31}^2$  and the absolute scale of neutrino masses are not yet known (see section 3.2 for more details).

The values in table 3.1 can be used, together with equations (8.33) and (3.5), to obtain the elements of the neutrino mass matrix in the flavour basis. First thing to note is the importance of the hierarchy choice; indeed, it is easy to check that for inverted hierarchy the

experimental values of the parameters require  $|m_{ee}| > 10^{-2}$  eV, which is incompatible with the texture generated by our model. Normal hierarchy, however, allows for small  $m_{ee}$  and  $m_{e\mu}$ . Therefore, a first conclusion is that this class of models, if phenomenologically viable at all, yields neutrino masses in normal hierarchy, that is, with  $\Delta m_{31}^2 > 0$ .

The next step should be to explore the neutrino parameter space and see if one can find phenomenologically allowed matrices that agree with the structure provided by (8.29). A possible course of action would be to generate *in silico* sets of random values for the neutrino parameters within their  $1\sigma$  allowed ranges, as read in table 3.1, and obtain the corresponding neutrino mass matrix elements  $m_{\alpha\beta}$ . Then one can use equation (8.29) to solve for  $g_{\alpha\beta}$  in terms of  $\mu_\kappa v_\chi^2 I_\nu$  and check if the phenomenologically allowed values for  $\mu_\kappa, v_\chi, m_\kappa, m_\chi$  –as described in sections 8.3, 8.4 and 8.5– yield phenomenologically allowed values for  $g_{\alpha\beta}$ . One would find tensions between the various phenomenological requirements: while neutrino masses could favour large values for  $g_{\alpha\beta}$ , lepton flavour violation constraints would prefer small values;  $v_\chi$  is bounded to be small, but the largest possible values would favour the observability of  $0\nu\beta\beta$ ; and so on. But let us as a first approach to face a simplified version of the problem: roughly, what we are wondering is whether  $|m_{ee}|, |m_{e\mu}| \sim 0$  is consistent with neutrino oscillation data. We can try and explore this question independently of our model: the task will be just to look if there is room in the *neutrino* parameter space for a mass matrix with exactly vanishing  $m_{ee}$  and  $m_{e\mu}$ . If the answer is yes, then we will know that the model is viable, and we can turn to the other interesting question of in which way small  $m_{ee}$ 's and  $m_{e\mu}$ 's constrain the parameters of the model.

This new, simpler task can be carried out analytically. In order to see how this comes about it is useful to go through a straightforward parameter-counting exercise:  $m$  is a  $3 \times 3$  complex and symmetric matrix specified by 12 real numbers: 3 of these are unphysical and can be absorbed by rephasing the neutrino fields, and 5 of the remaining 9 are measured – 2 mass differences and 3 mixing angles, including  $\theta_{13}$ . If we now impose  $m_{ee} = m_{e\mu} = 0$ , meaning 4 additional (real) constraints, only a discrete set of points will be consistent. In fact, there might be no allowed values at all! Fortunately, we checked that



this is not the case: for most of the neutrino parameter space at least one solution exists and thus the model is viable, although possibly confined to a narrow region of neutrino parameters. Which is not bad news; that, rather, means that the  $WWee$  mechanism yields very sharp predictions for neutrino masses that can be tested experimentally.

Let us now give an example of neutrino parameters that realise the simplified conditions: using the central values of the global fit in [264] we have obtained the following for the unmeasured parameters:

$$\begin{aligned} \alpha_1 &= 0.65 \text{ rad} & \alpha_2 &= -2.32 \text{ rad} \\ \delta &= -0.78 \text{ rad} & m_1 &= 0.0036 \text{ eV}. \end{aligned} \quad (8.34)$$

These values, when substituted in (8.33) and (3.5) produce the following mass matrix:

$$m \simeq \begin{pmatrix} 0 & 0 & 0.59 + 0.58i \\ 0 & 2.47 - 0.2i & 2.64 + 0.2i \\ 0.59 + 0.58i & 2.64 + 0.2i & 2.12 - 0.21i \end{pmatrix} \times 10^{-2} \text{ eV}, \quad (8.35)$$

which presents a recognisable texture. In our model we would interpret this hierarchy as the effect of the charged lepton masses, but note that (8.35) has had no interaction with the model; the texture appears as a consequence of the requirement that  $m_{ee} = m_{e\mu} = 0$ , but the result is consistent with the structure suggested by equation (8.29).

The main source of uncertainty in calculations such as (8.34) is the value of  $\theta_{13}$ , which was only hinted at the time of this analysis<sup>8</sup>. If we repeat the exercise for different values of  $\sin^2 \theta_{13}$  –away from the central point in [264]–, we find a surprising result:  $m_{ee} = m_{e\mu} = 0$  only has solution for  $0.012 < \sin^2 \theta_{13} < 0.024$ , at least for  $s_{12}, s_{23}, \Delta m_{21}^2, \Delta m_{31}^2$  fixed to their central values. It would seem, so, that the texture induced by the charged lepton masses forces  $\theta_{13}$  to be nonzero in this class of models. How much does this result depend on the values of the measured neutrino parameters? Is it robust if we vary  $s_{12}, s_{23}, \Delta m_{21}^2, \Delta m_{31}^2$  within their allowed ranges? We calculated the values of  $\theta_{13}$  and  $\delta$

<sup>8</sup> Barely a few months before the first Daya Bay data were released... We consider, however, that this discussion is still useful and it can be interpreted in the light of the new measurements, as we do below.

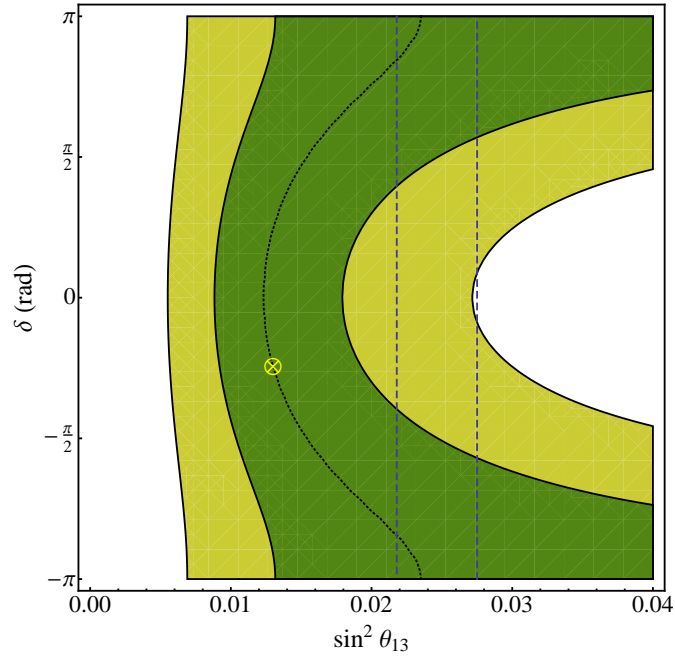


Fig. 8.6: Allowed  $\sin^2 \theta_{13} - \delta$  region if  $m_{ee} = m_{e\mu} = 0$  is to have solution. The green, darker region represents the positive  $\theta_{13} - \delta$  values when  $s_{12}, s_{23}, \Delta m_{21}^2, \Delta m_{31}^2$  are allowed to vary within their  $1\sigma$  range; the yellow, lighter zone is obtained when the neutrino parameters vary throughout their  $3\sigma$  band. The middle dotted curve corresponds to the central values of the neutrino masses and mixings in the global fit performed in [264]. For comparison, we draw (vertical dashed lines) the  $1\sigma$  band for  $\sin^2 \theta_{13}$  from the global fit in [128], which incorporates the recent measurements by Daya Bay, RENO and Double Chooz. The cross stands for the reference point presented in equation (8.38).

that allow for a solution to  $m_{ee} = m_{e\mu} = 0$  letting the rest of neutrino parameters take values in their  $1\sigma$  and  $3\sigma$  bands, and we display the results in figure 8.6. As we can see, the lower bound on  $\theta_{13}$  is robust, and interesting correlations are observed with the allowed values of the phase  $\delta$ : large values of  $\theta_{13}$  tend to prefer  $\delta$ 's around  $\pi$ , while  $\delta$ 's around 0 roughly imply  $\theta_{13}$  near the minimum of its allowed range. Actually, now that we have strong evidence for a nonzero  $\theta_{13}$  [110–112] we can interpret this evidence in the framework of our model: in figure 8.6 we draw two vertical lines representing the  $1\sigma$  band for  $\sin^2\theta_{13}$  from the global fit in [128], which includes the new measurements. From the correlations between  $\theta_{13}$  and  $\delta$  we would deduce that our model prefers a Dirac phase around  $\pi$ , rather than around 0.

Once checked that the model is viable and indeed can yield interesting predictions, it's compulsory to examine the full case with  $|m_{ee}|, |m_{e\mu}| \lesssim 10^{-4}$  eV. In figure 8.7 we present two plots that illustrate the situation: in *a*) we display the values of  $|m_{e\mu}|$  in terms of  $\sin^2\theta_{13}$  if we let the remaining neutrino parameters vary within their  $1\sigma$  band. The green, light area which extends to the whole panel informs us that for a given value of  $\theta_{13}$  one can obtain *any* value for  $|m_{e\mu}|$  by correctly selecting the rest of the parameters. But in plotting this we're not constraining  $|m_{ee}|$ , and it could be large for some of such combinations of parameters. The red, darker region attempts to constrain  $|m_{e\mu}|$  and  $|m_{ee}|$  simultaneously: it represents the values of  $|m_{e\mu}|$  in terms of  $\sin^2\theta_{13}$  wherever it is fulfilled that  $|m_{e\mu}| > |m_{ee}|$ . Therefore, in the red area we can be sure that we are keeping both elements under control; and we see that, as we obtained for the  $|m_{ee}| = |m_{e\mu}| = 0$  case, small values of  $\theta_{13}$  are forbidden, meaning that we cannot produce both  $|m_{ee}|$  and  $|m_{e\mu}|$  small with small  $\theta_{13}$ <sup>9</sup>. Quantitatively, we see that in this realistic case the upper bound for  $\theta_{13}$  disappears, whereas the lower bound is somewhat relaxed, but still clear; we could write that

$$\sin^2\theta_{13} \gtrsim 0.008 \tag{8.36}$$

---

<sup>9</sup> One could worry about the possibility that  $|m_{ee}|$  is greater than  $|m_{e\mu}|$  but still under the  $10^{-4}$  eV bound – say,  $|m_{e\mu}| \sim 10^{-6}$  eV and  $|m_{ee}| \sim 10^{-5}$  eV. But it's possible to check, for instance with a plot of  $|m_{ee}|$  against  $\sin^2\theta_{13}$  –not shown here–, that such configurations cannot be achieved with small  $\theta_{13}$  within  $1\sigma$  variation of the neutrino parameters.

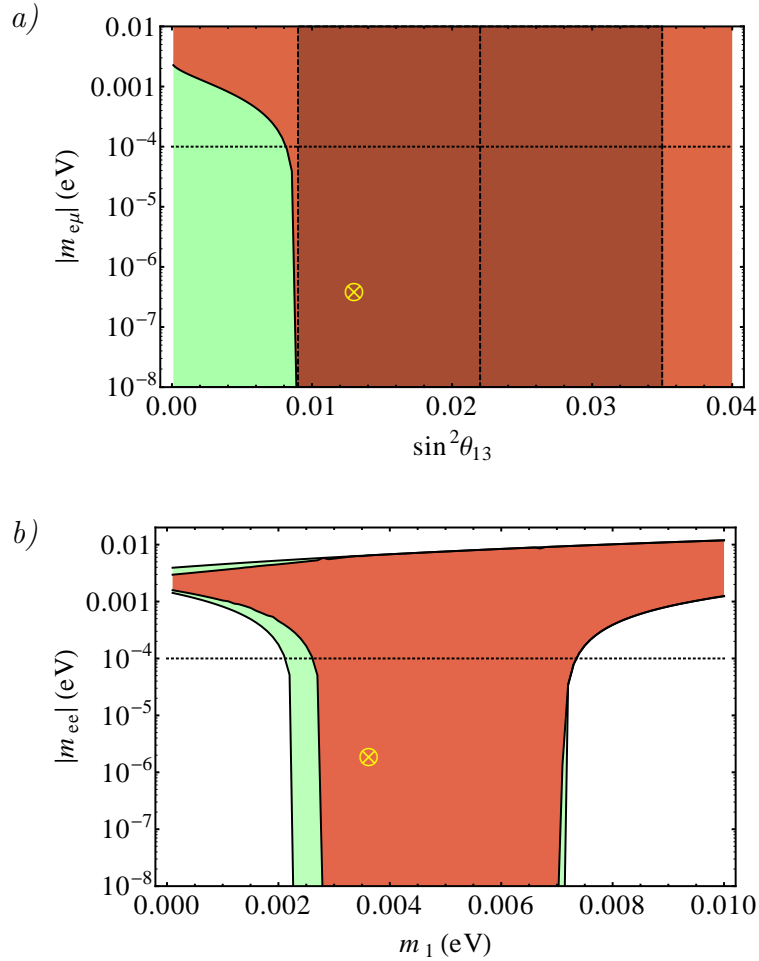


*Fig. 8.7:* These plots show in green the allowed values for  $|m_{e\mu}|$  (up) and  $|m_{ee}|$  (down) if we let the neutrino parameters vary within their  $1\sigma$  experimental band.  $|m_{e\mu}|$  is shown in terms of  $\sin^2\theta_{13}$ , with the red region displaying the additional constraint that  $|m_{e\mu}| > |m_{ee}|$  (see the main text for an explanation).  $|m_{ee}|$  is shown in terms of  $m_1$ , and this time the red area displays the opposite condition,  $|m_{ee}| > |m_{e\mu}|$ . In both graphs we have drawn the estimate upper bound on these two matrix elements,  $10^{-4}$  eV. The yellow crosses represent the reference point presented in equation (8.38).

if the upper bound on  $|m_{ee,e\mu}|$  is fixed in  $10^{-4}$  eV. We observe that if we relax this upper bound to  $10^{-3}$  the lower bound upon  $\theta_{13}$  also decreases, until it completely disappears a little bit above  $10^{-3}$  eV.

Figure 8.7b) is similar to a), but illustrates the bounds that the neutrino mass texture renders upon  $m_1$ , the lightest neutrino mass. Here we represent the element  $|m_{ee}|$  in terms of  $m_1$ . We could expect, from the well-known plots of  $0\nu\beta\beta$  sensitivity (see figure 3.4) that if we are to have very small  $m_{ee}$  we should be lying in the ‘elephant leg’ of  $10^{-3}$  eV  $\lesssim m_1 \lesssim 10^{-2}$  eV. And indeed that is what we find in figure 8.7b): the green, lighter region shows just  $|m_{ee}|$  in terms of  $m_1$  varying the rest of the neutrino parameters within their  $1\sigma$  range, and the red, darker area verifies the additional condition that  $|m_{ee}| > |m_{e\mu}|$ . Both regions show a clear upper and lower bound for  $m_1$ , which is constrained to be  $\mathcal{O}(10^{-3}$  eV), or, more precisely,

$$0.002 \text{ eV} \lesssim m_1 \lesssim 0.007 \text{ eV}. \quad (8.37)$$

The model, so, by virtue of the texture induced in the neutrino mass matrix by the charged lepton masses, yields very definite predictions about some still unmeasured neutrino parameters. These predictions, summarised in equations (8.36) and (8.37), can be used to probe the model and eventually falsify it, particularly in the light of the recent measurements of  $\theta_{13}$ .

### 8.7 Constraints on the parameters of the model

In the previous sections we have listed a number of theoretical and phenomenological features that constrain in several ways the parameters of the model. Not all of them are equally critical: the experimental bounds on  $0\nu\beta\beta$  and LFV-ing processes, sections 8.3 and 8.4, and also the requirement that the neutrino mass matrix fits with the known neutrino parameters, section 8.6.3, are inescapable demands; the unitarity and naturality bounds, section 8.5, and the bound on the triplet VEV, equation (8.6), are to be fulfilled, but might be stretched a bit if the appropriate conditions are met; finally, the requirement that  $0\nu\beta\beta$  is observed in the next round of experiments is something that

we would like to happen, and we impose it in order to find out if that's possible. In this section we will consider all these constraints together and see how much room they leave for the model; as we will see, it is possible to fulfill all of them, but not without tensions and a little bit of high-wire walking.

Let us express the coalescence of the constraints in terms of the scalar masses  $m_\kappa$  and  $m_\chi$ , which are relevant for the appearance of the new particles in collider experiments. Throughout this section we will be assuming that the doubly-charged mixing is small and thus  $m_{\kappa_1} \simeq m_\kappa$  and  $m_{\kappa_2} \simeq m_\chi$ . Equation (8.22) can be our starting point, as it imposes both an upper and a lower bound. Note first that as  $v_\chi$  is small,  $m_\kappa$  and  $m_\chi$  are rather large, and  $g_{ee}$  can be made small without disturbing neutrino masses, the upper bound is easy to satisfy. The lower bound, however, poses more problems: the product  $\mu_\kappa v_\chi^2 |g_{ee}|$  is upper-bounded by unitarity, naturality and the  $\rho$  parameter as seen in equations (8.26), (8.27) and (8.6); this presses the scalar masses to light values, potentially leaving the new scalars at the reach of the LHC. In figure 8.8a) we depict the allowed region in the  $m_\kappa - m_\chi$  plane with all the constraints considered. The blue area represents the allowed region if the triplet VEV is forced to be  $v_\chi < 2$  GeV, and the orange zone corresponds to the more conservative bound  $v_\chi < 5$  GeV.

As we see, the permitted region is rather narrow, and the prospects are not utterly optimistic about a potential LHC discovery. The issue in the 'light' region is an undesirable interaction between neutrino masses, naturality and LFV constraints which comes about as follows: as we see for instance in equation (8.25), if the scalar masses are light LFV forces the  $g$  Yukawas to be smaller. Then we turn to neutrino masses; see the mass matrix (8.35): if the  $m_{ee}$  and  $m_{e\mu}$  elements are to be small, some other elements must carry the weight of the 'heavy' eigenvalue:  $m_{\mu\mu}$ , for instance, has to be  $\mathcal{O}(10^{-2}$  eV). But look at equation (8.29): if the  $g$ 's are small and the  $m$ 's must be large, there is only one way to move: make  $\mu_\kappa$  larger. But this cannot happen, for  $\mu_\kappa$  is forced by (8.27) not to be much larger than  $m_\kappa$  and  $m_\chi$ , which are light. Conclusion: the whole 'light' region for  $m_\kappa$  and  $m_\chi$  is forbidden.

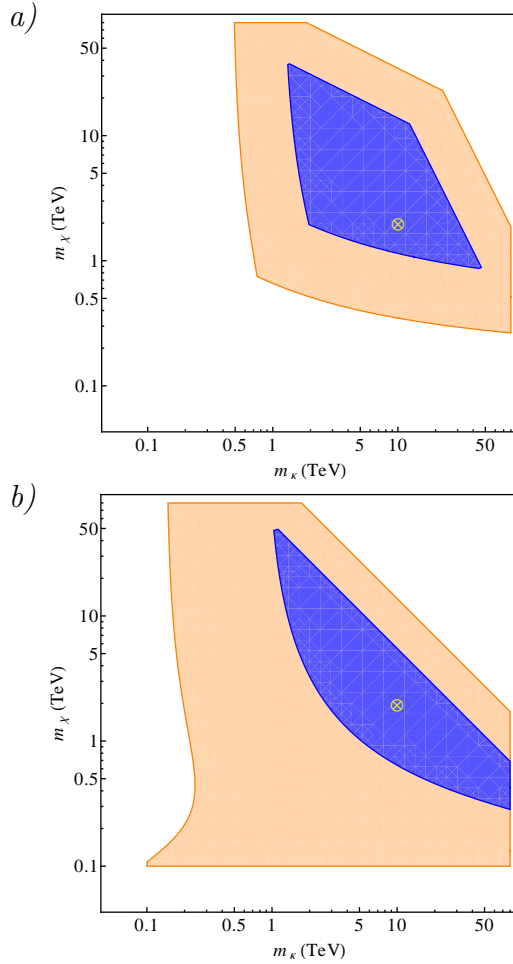


*Fig. 8.8:* Two plots for the allowed region in the  $m_\kappa - m_\chi$  plane. The regions are displayed after applying all the constraints. As the doubly-charged mixing angle is mainly small, we have implemented the approximation  $m_{\kappa_1} \simeq m_\kappa, m_{\kappa_2} \simeq m_\chi$ . The blue areas represent the allowed region if the triplet VEV is forced to be  $v_\chi < 2$  GeV; the orange areas display the allowed region if the bound is relaxed to  $v_\chi < 5$  GeV. The plot labeled as *a)* implements the naturalness limit for  $\mu_\kappa$ , equation (8.27), whereas *b)* implements just an upper bound on the LN-breaking scale,  $\mu_\kappa < 20$  TeV. The reference point described in equation (8.38) is presented in both plots as a yellow crossed circle.

Let us work out this situation numerically: from (8.29) we obtain that

$$|g_{e\tau}g_{\mu\mu}| = \frac{(2(2\pi)^4 v_\phi^4)^2}{m_e m_\tau m_\mu^2} \frac{|m_{e\tau}| |m_{\mu\mu}|}{\mu_\kappa^2 v_\chi^4 I_\nu^2} > \frac{0.065}{I_\nu^2} \left( \frac{\text{TeV}}{\min(m_{\kappa_1}, m_{\kappa_2})} \right)^2,$$

where in the last step we used the upper limits on  $\mu_\kappa$  and  $v_\chi$  (2 GeV in this case) and we made  $|m_{e\tau}| \sim 10^{-3}$  eV and  $|m_{\mu\mu}| \sim 10^{-2}$  eV, according to equation (8.35). Then, combining this result with the bound for  $\tau^- \rightarrow e^+ \mu^- \mu^-$ , equation (8.25), we obtain  $m_\kappa > 1.2$  TeV, limit that can be also observed in figure 8.8a).

Of the three constraints that close the light scalar region, two of them –neutrino masses and LFV bounds– are not negotiable; the naturality bound on  $\mu_\kappa$ , however, is an estimate based on what is considered to be ‘natural’ for a theory. We can relax this latter constraint and see if the light scalar region remains closed; what we will do is to fix a maximum scale for lepton number violation, that is to say, an upper bound on  $\mu_\kappa$  irrespective of the masses of  $\kappa_1$  and  $\kappa_2$ . In figure 8.8b) we depict the allowed region substituting the naturality bound for  $\mu_\kappa < 20$  TeV, and indeed we observe that most of the light scalar region is now open. As a conclusion we might say that a detection of the new scalars at the LHC is not definitely ruled out, but it appears that the phenomenological constraints rather favour a scenario with the scalars at the order of several TeV.

Something to note about the graphs in figure 8.8 is that all observables violating LN are proportional to  $\mu_\kappa v_\chi^2$ ; hence, an increase in  $v_\chi$  can be traded by the corresponding increase in  $\mu_\kappa$ , and vice versa. So, the orange areas in the plots can be also interpreted as the allowed regions for  $v_\chi = 2$  GeV and  $\mu_\kappa < 25\pi \min(m_{\kappa_1}, m_{\kappa_2})$  –in a)– or  $\mu_\kappa < 125$  TeV –in b)–. At the same time, one may wonder why we chose 20 TeV for the bound on  $\mu_\kappa$  in b) or, equivalently, what is the effect of varying such a value. The answer is simple: the blue,  $v_\chi < 2$  GeV region in figure 8.8b) disappears for  $\mu_\kappa \lesssim 8$  TeV, which is a reflection of the narrowness of the range allowed by equation (8.22), as required by our main working assumption that  $0\nu\beta\beta$  should be observed in the next round of experiments. The allowed regions in figure 8.8 are appreciably enlarged by reducing the lower limit in



this equation. This can also be achieved by dropping the issues with naturalness and further increasing  $\mu_\kappa$ .

Finally, we provide in figure 8.8 a ‘benchmark point’, denoted by a cross in the figures, where all constraints are satisfied, including the observation of  $0\nu\beta\beta$  and a VEV triplet under 2 GeV. The coordinates of this point in the parameter space of the model are

$$\begin{aligned}
 m_\kappa = m_{\kappa_1} &= 10 \text{ TeV} & m_\chi = m_{\kappa_2} &= 2 \text{ TeV} \\
 v_\chi &= 2 \text{ GeV} & \mu_\kappa &= 15 \text{ TeV} \\
 g_{ee} &= 1 & g_{e\mu} &= 0.001.
 \end{aligned}
 \tag{8.38}$$

The point is used in the plots throughout this chapter to show that, although under tight pressure, the model can accommodate all the phenomenological and theoretical considerations that we have exposed. It also helps to follow the track of the predictions of the model along their various relevant phenomenological aspects.

## 8.8 The model at colliders

Direct evidence for this type of models would be the discovery of the new scalars at a large collider together with a demonstration of the presence of LNV-ing interactions. This latter goal seems difficult; as we have seen throughout the discussion, violation of LN in this model involves several couplings –typically expected to be small–, which yields small LNV-ing production and decay rates. In general, the dominant production mechanisms are standard and LN-conserving, or otherwise they are suppressed. As for decays, not all the decay channels of the new particles produce LNV-ing signals, though in some cases they might be dominant. Generally, the idea is to look first for the new resonances in the most sensitive channels and only afterwards to address the observation of LNV-ing events. Doubly-charged scalars, for example, have fixed couplings to photons and are produced at colliders with known cross sections. In addition, their decay into leptons offers a very clean signal, which is particularly important at hadronic machines. Therefore, doubly-charged scalars seem a priori the best signal to look for, if they are light enough to be produced.

Studies to search for doubly-charged scalars at colliders have been performed in the past, in many cases motivated by mass-generating mechanisms like seesaw type II, which are different from the one we discussed in this chapter but can have a similar particle content [265–271]; model-independent studies have also been carried out in the literature, like for example [272, 273]. The general conclusion is that the LHC discovery limit reaches masses over 600 GeV for a center of mass energy of 14 TeV and an integrated luminosity of  $30 \text{ fb}^{-1}$  [270, 274]; however, the actual limits achieved may be way better given the outstanding LHC performance, which almost matches the most favourable expectations for a center-of-mass energy of 7 TeV [275]. See, for instance, for a review [276].

Recently, the first results from CMS have been presented at a CM energy of 7 TeV with an integrated luminosity of  $0.89 \text{ fb}^{-1}$  [277]. The analysis assumed a scalar triplet coupled to leptons, with 100% branching ratio to each leptonic channel. No excess over the background was observed, leading to a lower bound on the mass of the doubly-charged scalar of about 250 GeV if the main decay involves  $\tau$  leptons, of about 300 GeV if the main decay product is electrons and muons, and extending up to 375 GeV if only muons are produced. Weaker limits were obtained previously by LEP and the Tevatron; the absence at LEP of a pair-production signal of the type  $e^+e^- \rightarrow \gamma^*, Z^* \rightarrow \kappa^{++}\kappa^{--}$  yields the constraint  $m_\kappa > 100 \text{ GeV}$  [278–280]. Single production via  $e^+e^- \rightarrow \kappa ee$ , as well as the  $u$ -channel contribution of  $\kappa$  to Bhabha scattering have also been studied at LEP [280, 281], but the corresponding bounds depend on the unknown values of the Yukawa couplings and are not much informative. Limits on this sort of scalars have been also derived using Tevatron data [282–284], leading to a limit  $m_\kappa > 100 - 150 \text{ GeV}$ , depending on the details of the model.

In our model the triplet does not directly couple to fermions, while the doubly-charged singlet does not couple to  $W$  pairs; however, triplet and singlet mix. Of the resulting mass eigenstates,  $\kappa_1$  is mainly a singlet and decays dominantly to lepton pairs, while the other,  $\kappa_2$ , is mainly a triplet and will decay to gauge bosons if kinematically allowed. Both of them can be produced at LHC via the Drell-Yan mechanism,  $q\bar{q} \rightarrow \gamma^*, Z^* \rightarrow \kappa^{++}\kappa^{--}$ , with full strength. Since this is the main

production process considered by CMS, the former limits apply directly to  $\kappa_1$  if the mixing can be safely neglected:  $m_{\kappa_1} > 300$  GeV. Limits on  $m_{\kappa_2}$  will be more difficult to obtain because the process  $q\bar{q} \rightarrow \gamma^*, Z^* \rightarrow \kappa_2^{++}\kappa_2^{--} \rightarrow W^+W^+W^-W^-$  is much more complicated to deal with, due to its large backgrounds and the generally difficult reconstruction of several leptonic  $W$  decays.

Notice that there are other production processes that are more specific of our model; in particular, the process that yields  $0\nu\beta\beta$ , shown in figure 8.1, can be reverted and act as a  $WW$ -fusion production channel for  $\kappa_1$  and  $\kappa_2$ .  $\kappa_2$  will be the main product of such processes, as it is mostly a triplet, and it will decay again to  $W$ 's which are difficult to spot. However, a number of  $\kappa_1$ 's could be produced, depending on the value of the doubly-charged mixing angle; the production amplitude will in general be suppressed by the triplet VEV,  $v_\chi$ , and by  $\sin\theta_{++}$ . Nonetheless, this could prove to be the dominant production channel at LHC if  $v_\chi > 1$  GeV and  $m_{\kappa_{1,2}} > 500$  GeV [266]. This is especially relevant for our model since the various constraints, as discussed in section 8.7, favour a relatively large  $v_\chi$  as well as large scalar masses, unlike other triplet models with tree-level neutrino masses, like type II seesaw. A thorough study of the various possibilities is somewhat involved [285], but might deserve future investigation.

## 8.9 Domain walls and alternatives

The model that we have discussed in this chapter is an example of how to obtain  $0\nu\beta\beta$  and neutrino masses through the  $WWee$  mechanism. It is, however, not unique: it belongs to a class of models that share many features, and in particular the suppression of neutrino masses with respect to  $0\nu\beta\beta$ . It is also not speckless: containing as it does a scalar that breaks spontaneously a discrete symmetry, it may trigger the creation of domain walls in the early universe, which is forbidden by cosmological observations [286–288]. Essentially, the problem is that domain walls have their own energy density and should exhibit gravitational effects which have not been detected; if the appropriate circumstances meet they could also yield other effects that have likewise not been observed. The model, therefore, can be regarded as it stands

as problematic; we have preferred however to discuss in detail this particular version because we find that the particle physics motivation is neater here, but in this section we proceed to describe two possible variations that would tackle the domain wall problem.

A first way to avoid the creation of domain walls is to promote the  $\sigma$  field to a complex field, as already commented in section 8.1. In this version of the model lepton number is not explicitly broken, as it can be transmitted from  $\kappa$  to  $\chi$  through the  $\mu_\kappa$  interaction and then again to  $\sigma$  in the  $\lambda_6$  vertex. Specifically, we would have

$$L(\kappa) = +2 \qquad L(\chi) = +1 \qquad L(\sigma) = -1.$$

Within this extension no discrete symmetry is needed: the enforcement of lepton number suffices to forbid the terms that generate neutrino masses at tree level; in fact, one can view the  $Z_2$  symmetry in the model with  $\sigma$  real as a remnant of LN from an extended, high-energy theory which broke spontaneously somehow. The complex- $\sigma$  extension, however, is not free of complications either: lepton number is now a good global symmetry of the theory, and as  $\sigma$  acquires a VEV –and it must happen in order to have tree-level  $0\nu\beta\beta$ – a Majoron is created which requires extra phenomenological considerations. Fortunately, the Majoron will be mainly a singlet and the constraints won't be very severe: its couplings to ordinary matter will be small and its coupling to the Higgs field is essentially free [289]. Even in these favorable circumstances, however, some constraints would need to be considered: the Majorons can be produced inside a supernova and then escape, yielding a new source of supernova cooling that can be bounded [290]; they can provide a mechanism for neutrino decay or annihilation that would affect the neutrino relic abundance [291, 292]. One can choose to compute all these restrictions and then consider the region of parameter space where the model is still viable. Another possibility is to gauge the lepton number symmetry – or rather baryon minus lepton number,  $B - L$ , as  $B + L$  is broken in the SM by nonperturbative effects [215]. This would be an interesting possibility, and with renewed experimental interest (see, for instance, [293] for a review), but it requires the addition of right-handed neutrinos, which provide new sources of neutrino masses and somewhat complicate the scenario. Thus, we

consider that it's not so appealing for the pure investigation of the  $WWee$  mechanism.

A second option to evade the domain wall problem would be to keep the real  $\sigma$  field but engineer the model so that  $v_\sigma$  is very heavy. The domain walls are created during a phase transition in the early universe that occurs roughly at a temperature  $T_c \simeq v_\sigma$ ; if we manage to place this temperature before the inflationary epoch it is reasonable to think that the domain walls exist but are beyond our observable universe. This requires, of course, *huge* values for  $v_\sigma$ , but the phenomenology of the model can be kept more or less the same just by choosing very small values for  $\lambda_6$  – so small, actually, that some might consider that a hierarchy issue is in order. We do not pursue this discussion because within this class of models there is an even simpler one, with the same neutrino physics at low energy and none of these potential drawbacks: it is the same model presented throughout this chapter but without the  $\sigma$  field; instead, we replace it by its vacuum expectation value,  $\sigma \rightarrow v_\sigma$ . Up to coupling constant redefinition this yields the same potential as equation (8.1) but without the terms containing  $\sigma$ , *except* for the  $\lambda_6$  term, which becomes

$$\mu_\chi \phi^\dagger \chi \tilde{\phi}, \quad \text{with} \quad \mu_\chi = \lambda_6 v_\sigma. \quad (8.39)$$

This term is nothing but an explicit breaking of the  $Z_2$  symmetry, and could be regarded as a remnant of a high-energy model with a very heavy  $\sigma$ . The  $\mu_\chi$  coupling can be taken as  $\mathcal{O}(\text{TeV})$ , and then the resulting renormalizable Lagrangian has the same quantum behaviour than ours; in particular, neutrino masses are finite and generated at two loops, and can be obtained from our results by eliminating  $\lambda_6$  using (8.39). Note that within this variation lepton number is still explicitly broken, by the  $\mu_\kappa$  and  $\mu_\chi$  interactions, but none of them allows to assign  $L(\chi) = 2$ . The vertex  $\overline{\tilde{\ell}}_L \chi \ell_L$  is no longer forbidden, because  $Z_2$  is broken, but it can be absent from the Lagrangian –if the model is so devised–, and it will be finitely generated by loops – by the analogous of the diagrams in figure 8.4, and we could check that the resulting neutrino masses will be proportional to  $v_\chi^2$ , thus ensuring that the  $WWee$  mechanism is in action, and not a type-II-seesaw-like one.

## 9. CONCLUSIONS

In this doctoral dissertation we have presented our research on nonstandard properties of neutrinos through the interplay between effective operators and models. The two approaches offer a different set of advantages and drawbacks: effective theories are very general and allow the study of wide classes of models, but have a limited predictive ability; for some time the community stressed this feature and disregarded effective theories as not very powerful tools, but the attitude has changed in the past two decades and now effective operators are actively utilised in theoretical particle physics, including in the exploration of the boundaries of known physics. Models, on the other hand, are complete frameworks which aim to full predictivity; if renormalisable they can yield results up to arbitrary energies and they include all the new particles, whose properties can be investigated with no theoretical impediment. However, precisely because of this, models need to include all the details that make them phenomenologically viable, and these details can be complicated, even to the point of obscuring the relevant mechanism and yielding too specific predictions. Our philosophy is that it is in the combination of these two approaches that we can benefit from the advantages of both while buffering their drawbacks. In our investigation we have applied this principle to the study of new properties of the neutrinos.

This work can be naturally divided into two distinct parts. The first covers chapters 4 and 5, and it is centered on effective operators involving right-handed neutrinos, and especially right-handed neutrino magnetic moments. It is rather unusual that the  $\nu_R$ 's are considered among the low-energy fields when constructing an effective theory; this is motivated by the fact that their role in neutrino mass generation is most diaphanously understood when they are heavy and implement a

seesaw mechanism to yield small masses for the  $\nu_L$ 's. However, this is not the only possibility: for instance, neutrinos could be Dirac particles; or, being Majorana, some of the  $\nu_R$  degrees of freedom might be lighter than the electroweak scale. Including right-handed neutrinos in an effective theory as low-energy fields allows to explore their relation to high-energy particles, to use them as a window to new physics. With this aim in mind, we examined in chapter 4 the lowest-order effective operators that involved Standard Model fields and right-handed neutrinos, and we found, as soon as at dimension five, two operators that have not been previously discussed in the literature.

Both of them were lepton-number-violating operators. The first,

$$\overline{\nu_R^c} \nu_R \phi^\dagger \phi, \quad (9.1)$$

connects a pair of  $\nu_R$ 's to a pair of Higgs fields, and it provides an additional contribution to the Majorana mass of right-handed neutrinos once electroweak symmetry breaks spontaneously. It also yields a Yukawa-like interaction  $\overline{\nu_R^c} \nu_R H$  which triggers decays of the Higgs boson to two right-handed neutrinos; in section 4.4.5 we discuss the issues related to these decays, which may include invisible Higgs boson decays in certain zones of the parameter space.

The second operator is a magnetic-moment-like interaction between a pair of right-handed neutrinos and the hypercharge gauge boson,

$$\overline{\nu_R^c} \sigma^{\mu\nu} \nu_R B_{\mu\nu}, \quad (9.2)$$

which in turn yields proper magnetic moments for the  $\nu_R$ 's plus similar interactions with the  $Z$  boson. The consequences of this set of interactions would be remarkable: right-handed neutrinos, often regarded as 'sterile', could be produced anywhere a photon is present – that is, everywhere. As we have not gathered –yet– evidence of the existence of  $\nu_R$ 's we can only conclude that either they are rather heavy or the effective interactions are very suppressed – of course, given the optimistic assumption that they both exist. Throughout chapter 4 we discuss the phenomenology of these electroweak-moment interactions; in section 4.6 we summarise the constraints and prospects. Some basic conclusions include that if the  $\nu_R$ 's are very light astrophysical bounds

push the new physics responsible for the electroweak moments to very high energies; if the right-handed neutrinos are heavier than 100 MeV the best constraint is provided by LEP and the new particles cannot be lighter than some TeV's, but there's still room to be explored by the LHC.

If the new physics responsible for the right-handed neutrino effective operators is weakly coupled it is pretty likely that the new particles are easier to detect than the effective interactions. This is an additional reason to explore models that realise the operators (9.1) and (9.2). In chapter 5 we provide such a model. It is devised as a minimal extension and contains two new  $SU(2)$  singlets: a scalar,  $\omega$ , and a vector-like fermion,  $E$ , both of which need to be charged so that the  $B$  field couples to them while generating the electroweak moments. The new particles must be endowed at least with two trilinear couplings,  $\overline{\nu}_R E \omega^\dagger$  and  $\overline{\nu}_R^c E \omega^\dagger$ , which combined break lepton number and thus allow to generate the operators we are interested in.  $\omega$  and  $E$  can also have a variety of couplings to the Standard Model fields, but in order to simplify the model we only allow a mixing term between  $E$  and the light right-handed charged leptons. This mixing induces the decay of the heavy charged particles and avoids the problem of  $E$  and  $\omega$  accumulating as charged dark matter, which occurs if we only allow for the trilinear terms. We then discuss the phenomenology of the production and decay of the new particles in collider experiments, and the constraints that can be set on the mixing of the heavy fermions. The model is altogether phenomenologically viable, but from a wider view it may appear as an *ad hoc* mechanism. It would be interesting to consider in future works whether this class of additions, and their LNV-ing trilinear couplings, can be embedded in a more complex framework where their features are more deeply understood.

The second part of the thesis comprises chapters 6, 7 and 8, and in them we discuss the relation between neutrinoless double beta decay and neutrino masses for a certain class of effective operators. The idea that even effective pictures of  $0\nu\beta\beta$  offer information about the generation of neutrino masses is far from new; the same Schechter-Valle theorem –that we depict in figure 3.3– is an example of this sort of argument. In chapter 6 we consider a family of effective interactions



that yield  $0\nu\beta\beta$ : those that provide two charged leptons with violation of lepton number and with no quarks. We realised that the effective lepton-number-violating interactions involving  $W$ 's and leptons had not received much attention in the literature; two such interactions yield  $0\nu\beta\beta$  at tree level in the effective theory, as we see in figure 6.2: the first with one  $W$ , one electron and one neutrino ( $W\nu e$  vertex) and the second with two  $W$ 's and two electrons ( $WWee$  vertex). The effective theory also suggests that the  $W\nu e$  interaction generates neutrino masses suppressed by one loop with respect to  $0\nu\beta\beta$  and the  $WWee$  vertex yields neutrino masses suppressed by two loops (figure 6.3); however, this hierarchy will only be realised if neutrino masses are not independently generated at tree level – that is, if the Weinberg operator is suppressed with respect to the  $W\nu e$  and  $WWee$  interactions. In order to isolate the various mass-generating operators we notice that the chirality of the leptons involved in the effective interaction allows some sort of selection on the dominant mechanism: indeed, the lowest-order operator in this class with one left-handed and one right-handed lepton is the dimension-seven

$$\bar{e}_R \gamma^\mu \left( \phi^\dagger \tilde{\ell}_L \right) \left( \phi^\dagger D_\mu \tilde{\phi} \right), \quad (9.3)$$

which upon spontaneous symmetry breaking realises the  $W\nu e$  interaction. Similarly, the lowest-order operator with two right-handed leptons is the dimension-nine

$$\bar{e}_R e_R^c \left( \phi^\dagger D^\mu \tilde{\phi} \right) \left( \phi^\dagger D_\mu \tilde{\phi} \right), \quad (9.4)$$

which yields a  $WWee$ -like interaction. Chirality, thus, may be used in model-building for favouring the desired mechanism.

Still in chapter 6, we take the operators (9.3) and (9.4) as paradigmatic of the  $W\nu e$  and  $WWee$  mechanisms and discuss the implications of the current  $0\nu\beta\beta$  bounds on the mass of the required new particles. We obtain for the operator (9.3) that the new physics scale should lie roughly above 100 TeV, with some dependence on the effective coefficient – see equation (6.17); essentially, if the coefficient is small the scale may be lowered to energies at the reach of present or planned experiments. For the operator (9.4) we obtain a lower bound on the new

physics scale of just 3 TeV, which can be further lowered if the effective coefficient is small – see equation (6.19). In section 6.5 we also address the question of the dominant contribution to neutrinoless double beta decay: the operators (9.3) and (9.4) induce  $0\nu\beta\beta$ , but so do the neutrino masses that they generate through loops. Which one and under which circumstances will dominate? The effective theory allows us to estimate that if the new particles are relatively light – in particular, if the new physics scale is below 30 TeV – the effective operators will dominate; however, if the new physics is heavy  $0\nu\beta\beta$  will be dominated by neutrino masses.

The possibility of inducing a hierarchy between  $0\nu\beta\beta$  and neutrino masses that enhances the former and suppresses the latter is our main concern when considering the  $W\nu e$  and  $WWee$  interactions. However, the mass-generating loop diagrams in figure 6.3, which are the source of our argument, are actually not calculable in the effective theory, as it is not renormalisable. In order to see if the argument can be realised we must turn to concrete models, and that is what we do in chapters 7 and 8. Chapter 7 presents a rapid examination of a model that realises the  $W\nu e$  mechanism and chapter 8 reports more extensively on a model that yields the  $WWee$  mechanism and has prospects of observability in several near future experiments. In both cases a main concern is to suppress any alternative mass-generating mechanism so that neutrino masses are indeed induced by the  $W\nu e$  and  $WWee$  interactions; this is achieved by invoking discrete symmetries that forbid the undesired terms in the Lagrangian. In both cases we check that  $0\nu\beta\beta$  can be induced at tree level and suppressed neutrino masses are generated, at one loop for the  $W\nu e$  mechanism and at two loops for the  $WWee$  mechanism.

Chapter 7 proposes a realisation of the  $W\nu e$  mechanism. For that aim, we extend the Standard Model with a heavy scalar triplet, a heavy vector-like fermion doublet and a light scalar doublet; therefore, the model resembles an extended two-Higgs-doublet model. The operator (9.3) can be generated either at tree level, by spontaneous breaking of lepton number, or at one loop, by explicit breaking. Neutrino masses, as we expect from the  $W\nu e$  mechanism, can be generated either at one loop by spontaneous breaking or at two loops by explicit breaking. The

---

preeminence of spontaneous or explicit breaking depends on the balance of several parameters, but especially the magnitude of a quartic scalar coupling –the one that breaks explicitly lepton number– and the VEV of the second Higgs doublet, which should be of the order of  $v_\phi$  to ensure the dominance of spontaneous breaking. Our phenomenological analysis yields that explicit breaking should dominate if the masses of the heavy particles lie roughly above 100 TeV, whereas spontaneous breaking is the leading mechanism for light masses at the reach of present or near future experiments. All in all, we have verified that the  $W\nu e$  mechanism can be realised, and  $0\nu\beta\beta$  dominated by the operator (9.3) with one-loop suppressed neutrino masses is feasible, especially if the masses of the heavy particles are below 35 TeV. However, our analysis has not been exhaustive and many issues remain to be addressed; to cite just a few, the violation of lepton family numbers should be examined in detail, and variants of the model should be considered in order to determine if the second Higgs doublet is a necessary ingredient of this class of models.

In chapter 8 we discuss a model that realises the  $WWee$  mechanism and has the ability to produce signals in several ongoing or near-future experiments. The model requires the addition of a heavy scalar triplet and a heavy doubly-charged singlet; several variants of this setup are possible, and we choose also to add a heavy real scalar singlet. The model yields  $0\nu\beta\beta$  at tree level and neutrino masses at two loops. It also induces lepton-flavour-violating processes such as  $\mu \rightarrow 3e$  or  $\tau \rightarrow e + 2\mu$ . The generated neutrino masses are not only suppressed by loop factors, but also by factors of the masses of the charged leptons, which induce a very definite texture on the mass matrix; as a consequence, the model predicts a nonzero  $\theta_{13}$  compatible with the recent measurement of the Daya Bay experiment. The rate of  $0\nu\beta\beta$ , the rate of LFV-ing processes and the elements of the mass matrix are all controlled by the same set of couplings, which induces tensions among the various phenomenological and theoretical constraints; in particular, if one demands that the model provides a positive signal in the present or near-future  $0\nu\beta\beta$  experiments, the allowed range for the parameters gets drastically narrowed, though it remains open. The constraints are discussed in detail in section 8.7; we may conclude from them

---

that the model is definitely viable from the phenomenological point of view. It can comply with the experimental limits, it can provide signals in  $0\nu\beta\beta$  searches and lepton flavour violation experiments, and the heavy particles can have masses around the TeV or even lighter – but if we demand all these features at the same time the situation gets tight. Relaxing the requirement of an imminent  $0\nu\beta\beta$  signal helps to get more space in the heavy-mass range, and relaxing the theoretical constraint of naturalness yields more room for light new particles. All in all, this model and its cognates form a family with a rich phenomenology and realise satisfactorily the  $WWee$  mechanism, providing rather suppressed neutrino masses while keeping the  $0\nu\beta\beta$  rate near observable levels. These models will be tested in the next years by the forthcoming round of searches for lepton number and lepton flavour violation.

To end up, along this work we have explored several ways in which effective field theories may yield insight about neutrino properties and provide fruitful ideas for model building. We hope that the next years provide us with new experimental data to tune up our aims, separate the promising ideas from those that were just fun to explore and inspire new directions of research. It's been a long way, but the road goes ever on.

## 10. EN LA LENGUA DE CERVANTES

El trabajo doctoral que acabamos de exponer presenta nuestras –modestas– contribuciones a la física de los neutrinos. En este capítulo ofrecemos un resumen en castellano, como la legislación requiere; aprovecharemos este obligado *impasse* para enmarcar nuestros trabajos con un lenguaje no técnico, pensando en el público no experto. En el trayecto cometeré, no lo dudo, alguna imprecisión; espero que esos defectos, imposibles de subsanar en un texto breve como éste, se vean compensados por algún otro acierto, y que al final el lector termine con la impresión de que sabe algo más que al principio.

### 10.1 *El título*

Parece lógico empezar por el principio, o sea, por explicar el título de este trabajo: *Exotic properties of neutrinos using effective Lagrangians and specific models*, o lo que es lo mismo: “Propiedades exóticas de los neutrinos a través de lagrangianos efectivos y modelos concretos”. Esta tesis tiene un protagonista absoluto: el neutrino; de él daré alguna cuenta en la sección 10.2 de este mismo capítulo. Nuestro trabajo ha consistido en estudiar propiedades *exóticas* de esta partícula, es decir, propiedades que uno *no* esperaría encontrar en los neutrinos; punto número uno, pues: nuestra investigación se centra en propiedades hipotéticas, que nunca han sido observadas. Si el lector se está preguntando “¿y cómo se estudia algo que nadie ha visto?”, la respuesta es simple: con lápiz, papel y ordenadores. Aún nos quedan muchas cosas que aprender sobre los neutrinos, pero una que hemos aprendido es que su comportamiento viene excelentemente descrito por la teoría cuántica de campos, un fabuloso conjunto de herramientas matemáticas que nos permiten predecir cómo se comportan las partículas. Los

neutrinos, junto con el resto de partículas conocidas, se encuadran en una gran teoría llamada Modelo Estándar, que básicamente plantea las reglas del juego –las masas, las cargas, las relaciones entre las diferentes partículas– que luego vamos a usar cuando pongamos en marcha la máquina de la teoría cuántica de campos. Pero el Modelo Estándar no son las únicas reglas posibles; son unas que funcionan muy bien, pero que probablemente necesiten alguna corrección o algún añadido.

En ese punto entramos nosotros, y lo que hacemos es proponer *extensiones* del Modelo Estándar, añadidos que ayuden a entender las cosas que el Modelo Estándar “puro” no deja del todo claras –alguno de estos “defectos” lo comentamos en la sección 10.2 de este mismo capítulo. Estas extensiones, sin embargo, no salen gratis: aparte de resolver tus problemas pueden crear algunos nuevos (!). Nuestro trabajo es estudiar esas propuestas, comprobar cuáles son sus consecuencias y asegurarnos de que todas están bajo control; por ejemplo, asegurarnos de que cierta extensión que ayuda a entender la masa de los neutrinos no destruye todos los átomos del universo. Por el camino, estas extensiones dan lugar a fenómenos exóticos: cosas que no esperaríamos encontrar ahí y que, si llegásemos a observar, supondrían un punto a favor de esa extensión en concreto, y quizá el primer paso hacia el descubrimiento de algo nuevo. Esos fenómenos exóticos pueden ser muy variados: desde lo más escandaloso, como que se observe una partícula desconocida en un acelerador, hasta lo más sutil, como que la probabilidad de cierta desintegración nuclear sea un poco mayor o un poco menor de lo esperado.

Así pues, ya tenemos las *Exotic properties of neutrinos*; el resto del título sólo explica el *cómo*: en ocasiones hemos usado lagrangianos efectivos y en ocasiones hemos usado modelos. ¿Cuál es la diferencia? Pues hay una diferencia de profundidad y de generalidad. Cuando uno dice que usa una teoría *efectiva* lo que está haciendo es admitir que sólo aspira a describir el nuevo fenómeno, pero no a explicarlo. Explicar un fenómeno implica decir qué nuevas partículas hacen falta, cuáles son exactamente sus propiedades, cómo se relacionan con las partículas que ya conocemos. . . especificar todos estos detalles es construir un *modelo*. Por ejemplo, digamos que el fenómeno que queremos estudiar es que

los neutrinos forman cuerpos sólidos del tamaño de una persona<sup>1</sup>; estudiarlo de manera efectiva consistiría en estudiar estos cuerpos sólidos, su dureza, su estabilidad, cómo interaccionan con la luz, pero nunca plantearse qué es lo que los mantiene unidos. Estudiar este fenómeno mediante un modelo sería describir por qué los neutrinos se unen, cómo sucede esto exactamente, qué nuevas partículas harían falta para ello. . .

Los lagrangianos efectivos son una estupenda manera de centrarse en el fenómeno relevante; cualquier conclusión que uno extrae de un análisis efectivo debe ser válida para todos los modelos que aspiren a explicar el fenómeno, así que el enfoque efectivo es también muy general. Por contra, es incompleto; tal vez una versión realista de tu fenómeno requiere condiciones que tu teoría efectiva no llega a ver. Por eso es útil construir un modelo: para ver en qué medida te encuentras con dificultades en el momento en que quieres hacer algo realista y consistente. Ambos enfoques se complementan, y ésa, la de buscar esa complementariedad, es la filosofía que hemos seguido en este trabajo.

## 10.2 Neutrinos

En esta sección queremos explicar qué es exactamente un neutrino y por qué nos interesa lo suficiente como para que cada año centenares de personas en todo el mundo escriban sus tesis sobre ellos. Para decirlo en una sola frase, los neutrinos son un tipo de partícula elemental que se caracteriza muy especialmente por sus débiles interacciones. Aunque se conocen decenas de partículas diferentes<sup>2</sup>, sólo unas pocas son *elementales*, esto es, indivisibles; la física moderna lista por centenares las partículas *compuestas*, formadas por asociación de otras partículas, como pequeños enjambres o sistemas planetarios, pero apenas un puñado –una veintena– parecen estar formadas sólo por ellas mismas: son elementales. Los neutrinos son tres de los miembros de ese selecto club, caracterizados por interaccionar de manera muy limitada con el

---

<sup>1</sup> Esto es completamente ciencia ficción. Prueba de ello es que Stanisław Lem, uno de los maestros del género, se plantea este fenómeno en su novela *Solaris* [294].

<sup>2</sup> El lector interesado puede consultar las listas que aparecen en Wikipedia [295], o mejor, las exhaustivas tablas del Particle Data Group [32, 296].

resto de las especies; esta propiedad las hace únicas entre las partículas conocidas: sean elementales o compuestas, todas las demás partículas interaccionan más que los protagonistas de este trabajo.

¿Pero qué significa exactamente “interaccionar débilmente”? En pocas palabras, que los neutrinos son capaces de atravesar ingentes cantidades de materia sin darse cuenta de que está ahí. Un cálculo sencillo nos arroja rápidamente que para tener buenas chances de frenar un neutrino de baja energía es necesario interponerle *un año-luz* de plomo. Lo repetiré: si a un neutrino le pones delante “sólo” medio año-luz de plomo es bien probable que lo atraviere sin inmutarse. Este dato es sólo un dato, una anécdota, pero extendámoslo al quehacer científico: imaginemos lo difícil que es estudiar un objeto, el que sea, cuando para estudiarlo hace falta que deje alguna información en nuestras máquinas. . . y para el 99,999. . . % de los neutrinos nuestras máquinas son tan transparentes como el aire.

Las razones para este comportamiento están codificadas en las reglas del juego que nos da el Modelo Estándar: los neutrinos no tienen carga eléctrica, así que no interaccionan con los fotones, las partículas que forman la luz. Sí pueden interaccionar con los electrones, protones y neutrones que hay en los átomos, pero siempre con la ayuda de terceras partículas mucho más pesadas, como los bosones *W* y *Z*; la mediación necesaria de estas partículas pesadas hace, por las reglas de la teoría cuántica de campos, que la interacción con electrones, protones y neutrones sea muy improbable, y de ahí el carácter “fantasmal” de los neutrinos. Sin embargo, todo esto es conocimiento asentado: lo entendemos y lo tenemos controlado desde hace varias décadas. ¿Qué es, pues, lo que hace que los neutrinos sigan siendo interesantes para la comunidad científica *hoy*?

Hay varias respuestas a esta pregunta: la más sencilla quizá sea que debido a su carácter huidizo aún son relativamente desconocidos; otra posible respuesta es que este carácter permite que los neutrinos tengan comportamientos curiosos, como la oscilación, que hace los tres tipos de neutrino cambien de una variedad a otra sólo por el hecho de moverse. Pero la que nos interesa aquí es una tercera razón: su *masa*. Desde que, allá por el año 2000, quedó claro que los neutrinos que se producen en el Sol no desaparecen a medio camino, sino que se transforman en otro



tipo de neutrino –*oscilan* entre las tres variedades–, las ecuaciones nos exigían admitir que los neutrinos habían de tener masa. Hasta entonces no habíamos tenido una sola prueba fehaciente de que no fueran partículas sin masa, como los fotones: se movían a altas velocidades, muy cercanas a la de la luz, y cuando intervenían en reacciones nucleares no dejaban constancia de su carácter masivo. Todas las evidencias previas apuntaban a que, si tenían masa realmente, había de ser muy pequeña, tan pequeña que quedaba eclipsada por su energía cinética, la energía de su movimiento<sup>3</sup>. A día de hoy seguimos intentando observar neutrinos más y más lentos, con la esperanza de distinguir en su comportamiento alguna pista sobre su pequeñísima masa, pero hasta ahora seguimos a ciegas.

Así pues, aquí está el quid de la cuestión: sabemos que los neutrinos tienen masa, y sabemos que es muy muy pequeña – es, al menos, un millón de veces menor que la masa del electrón, que ya de por sí tiene una masa pequeña entre todas las demás partículas. Es más, los neutrinos están solos como partículas con masas ridículamente pequeñas: las demás se mueven entre los 500 keV del electrón y los 175 GeV del quark top, una horquilla de un factor un millón; por debajo del electrón hay otra horquilla de un factor un millón aparentemente *vacía*, sin ninguna partícula conocida; y debajo de ésta, en el sótano de las masas, los tres neutrinos, haciendo gala de su singularidad. Pues bien, esa singularidad es la que los hace interesantes: sabemos que las masas del resto de partículas se pueden explicar gracias al mecanismo de Higgs –ahora ya podemos decirlo, *¡al fin!*, después de que en 2012

---

<sup>3</sup> Es un hecho poco conocido que éste es un principio general: la masa es una forma de energía y el movimiento, otra. En el mundo en que vivimos los objetos tienen mucha más energía acumulada en su masa que en su movimiento, y sería un poco tonto decir que tenemos dudas de si un sofá tiene masa o no: es evidente que la tiene. En el mundo de las partículas, sin embargo, a veces sucede lo contrario: el movimiento aporta mucha más energía que su masa. Entonces se da el caso contrario: es evidente que está en movimiento, pero ¿tiene masa? Las partículas con mucha más energía cinética que masa son prácticamente indistinguibles de una partícula sin masa, y sólo cuando las frenamos empezamos a “darnos cuenta” de que son masivas. Los neutrinos, sin embargo, con su dificultad para interactuar con la materia también son difíciles de frenar, así que la faena está servida: ¿cómo medimos sus masas?

descubriéramos al deseado bosón–, pero a nadie se le escapa que tres individuos un factor un millón por debajo resultan sospechosos: toda la comunidad piensa que lo lógico es que sus masas vengan de otro sitio, de otro mecanismo.

¿Cuál es ese mecanismo? Bueno, ésa es la cosa; hay decenas de propuestas, decenas de candidaturas para explicar que los neutrinos funcionan de otra manera y por qué su manera de funcionar les da masas tan pequeñas – podría ser que los neutrinos se relacionen con una nueva clase de partícula, hasta ahora desconocida, que de alguna manera les “obligue” a tener masas pequeñas; podría ser que alguna nueva ley de la física exija que sus masas, y no otras, tienen que ser pequeñas. Pero más allá de esa lista de candidaturas no tenemos nada: no hemos podido medir aún el valor de las masas, y los experimentos en los que esperábamos ver alguna pista sobre el origen de la masa de los neutrinos han dado resultados negativos. En este contexto se inscribe mi tesis; hay toda una comunidad de físicos teóricos pensando en maneras para que los neutrinos tengan masas pequeñas y, sobre todo, tratando de relacionar esos nuevos mecanismos con experimentos actuales, para que podamos ponerlos a prueba. En esa dirección transitan los trabajos que aquí hemos presentado, y que ahora describiremos brevemente.

### 10.3 Momentos magnéticos de neutrinos dextrógiros

Todos los mecanismos que buscan explicar la pequeñez de la masa de los neutrinos pasan por añadir partículas nuevas al elenco que conocemos actualmente. Una de las incorporaciones más populares es añadir, por cada uno de los neutrinos que tenemos<sup>4</sup>, una nueva partícula, similar a éstos pero con una interacción todavía más débil con el resto de la fauna subatómica. Esas nuevas partículas reciben el nombre de *neutrinos dextrógiros* –aunque a muchos les sonará más la terminología inglesa: right-handed neutrinos–, o, a veces, neutrinos *estériles*, donde esta desagradable palabra hace referencia precisamente a que nuestros

---

<sup>4</sup> O sea, en principio tres, pero luego se pueden hacer variaciones: añadir más, añadir menos, hacer que las nuevas partículas se fusionen con los neutrinos convencionales. . . toda esa zoología modelística requeriría mucho más espacio del que disponemos hoy aquí.

nuevos inquilinos parecen sentir cierta aversión a relacionarse con el resto de partículas. El carácter estéril de los neutrinos dextrógiros, sin embargo, no contribuye particularmente a explicar las masas de los neutrinos “normales” – la verdadera utilidad de los recién llegados reside en otras de sus propiedades, que no corresponde comentar aquí.

Así que fue hasta cierto punto una sorpresa descubrir, mientras estudiábamos algo ligeramente diferente, que nadie había considerado que los neutrinos dextrógiros pudieran tener un momento magnético. El momento magnético es una interacción entre una pareja de partículas y un fotón pero, a diferencia del acoplamiento “habitual” de los fotones –vectorial y gauge–, el momento magnético involucra necesariamente a terceras partículas. Con el acoplamiento vectorial gauge, las partículas que interactúan con el fotón han de tener necesariamente carga eléctrica; con el momento magnético basta con que las terceras partículas implicadas la tengan<sup>5</sup>. Conclusión: los neutrinos dextrógiros, paradigmáticamente estériles y sin carga eléctrica, pueden interactuar con los fotones siempre que, además, interactúen con otras partículas que sí tengan carga.

Como digo, esto es conocimiento estándar, nada nuevo hasta aquí. Lo que fue sorprendente fue darnos cuenta, mientras estudiábamos posibles interacciones exóticas de los neutrinos dextrógiros, que nadie había estudiado una relativamente poco exótica: los momentos magnéticos. Esto es lo que nos proponemos en las referencias [1] y [2]. Hay que decir por adelantado que a día de hoy no tenemos una sola evidencia de la existencia de neutrinos dextrógiros, y por ende tampoco de sus momentos magnéticos; es más, si los fotones andaran por ahí produciendo neutrinos deberíamos habernos dado cuenta ya. El hecho de que no lo hayamos observado señala, genéricamente hablando, que o bien la interacción no existe, o bien es muy débil, o bien los neutrinos dextrógiros tienen masas muy grandes y requieren de fenómenos muy

---

<sup>5</sup> El ejemplo paradigmático es un átomo. Los átomos son neutros porque tienen el mismo número de protones y de electrones. Como tales objetos neutros no deberían interactuar con fotones, pero como en su interior hay electrones y protones que sí tienen carga, los átomos como conjunto pueden interactuar con los fotones a través de un momento magnético – que, en última instancia, involucra a los electrones y protones de su interior.

energéticos para manifestarse.

En la referencia [1] ponemos números a toda esta casuística. En ella estudiamos los momentos magnéticos de neutrinos dextrógiros desde un punto de vista efectivo, es decir, olvidándonos de cómo se origina la interacción –quiénes son las partículas cargadas con las que el neutrino se relaciona– y concentrándonos simplemente en cuáles serían las consecuencias de que los fotones se relacionaran con neutrinos dextrógiros a través de un momento magnético. Y de estas consecuencias hay un buen puñado: el universo está lleno de fotones, y nuestros experimentos están llenos de fotones; las estrellas producen ingentes cantidades de fotones, los aceleradores de partículas también; si este momento magnético fuese un hecho, los neutrinos dextrógiros deberían haber dejado su huella en todos estos sitios. Como no hemos encontrado esa huella, nuestro corpus de observaciones debería decirnos cómo *no es* el momento magnético: si es muy débil, cuán débil ha de ser para que no lo hayamos visto; si los neutrinos han de ser pesados, cuán pesados. En la sección 4.4 analizamos las consecuencias que los momentos magnéticos tendrían en aceleradores de partículas; en la sección 4.5 analizamos cómo los neutrinos dextrógiros afectarían a diversos escenarios astrofísicos y cosmológicos. La figura 4.8 resume las conclusiones del estudio: en el eje de abscisas representamos la masa de los neutrinos dextrógiros y en el de ordenadas la “escala de nueva física”, que básicamente debería corresponderse con la masa de las nuevas partículas que generan los momentos magnéticos. Las regiones sombreadas marcadas como “ $N$  magnetic moment”, “ $N - \nu$  transition” y “LEP” representan regiones excluidas: valores de las masas que entrarían en contradicción con lo que hemos observado.

Por ejemplo, para masas pequeñas, por debajo de 10 keV, la región sombreada azul sitúa las nuevas partículas por encima de  $10^9$  GeV, lo que implica un momento magnético pequeñísimo, prácticamente inobservable. Esta cota proviene de la física de estrellas gigantes rojas, cuya evolución y propiedades en cada etapa de su existencia depende, entre otras cosas, de cuán rápido se enfrían; si los fotones que hay dentro de la estrella pudieran transformarse en neutrinos dextrógiros, éstos escaparían de la estrella llevándose parte de su energía, y por tanto enfriándola. Nuestras observaciones de este tipo de estrella nos

dan información sobre cuán rápido se enfrían, y nos permiten deducir que la práctica totalidad de su enfriamiento procede por los cauces usuales – fotones y neutrinos convencionales; por tanto, se deduce que los momentos magnéticos, de existir, han de ser muy pequeños para que el número de neutrinos dextrógiros que se produzca sea muy limitado.

En la referencia [2] analizamos un modelo muy simple que proporciona momentos magnéticos a los neutrinos dextrógiros. El modelo requiere dos partículas nuevas: un fermión pesado, que sería similar a un electrón pero con una masa mucho mayor, y un escalar cargado – digamos, una suerte de bosón de Higgs, pero a diferencia de éste, con carga eléctrica. El modelo es viable fenomenológicamente, y arrojaría señales en experimentos tales como el LHC de Ginebra, aunque en el tiempo que lleva funcionando no ha encontrado rastro de partículas exóticas como éstas. Por lo demás, el modelo demuestra que es relativamente sencillo generar los momentos magnéticos de neutrinos dextrógiros sin necesidad de extensiones complicadas del Modelo Estándar, y las predicciones del modelo coinciden esencialmente con las que se obtienen de la teoría efectiva en la referencia [1].

#### 10.4 Desintegración doble beta sin neutrinos

La desintegración doble beta es un tipo muy raro de desintegración nuclear, en la que dos neutrones del núcleo atómico se transforman en dos protones y emiten dos electrones. Este proceso ha sido observado en una decena de núcleos, y en todos los casos se ha producido con la emisión de dos antineutrinos; por ejemplo, el núcleo de  $^{136}\text{Xe}$  se desintegra a  $^{136}\text{Ba}$ ,

$$^{136}\text{Xe} \longrightarrow ^{136}\text{Ba} + 2e^- + 2\bar{\nu}_e, \quad (10.1)$$

con una vida media de  $2,4 \times 10^{21}$  años<sup>6</sup>. La emisión de los dos antineutrinos no es baladí: las ecuaciones del Modelo Estándar nos

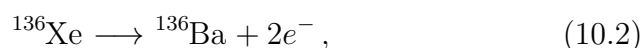
<sup>6</sup> Hemos dicho que estos procesos son en extremo raros: efectivamente, la vida media del  $^{136}\text{Xe}$  es billones de veces más larga que la vida del universo. Para poder observar esta desintegración en un experimento hay que reunir grandes cantidades de xenón radiactivo, y aun entonces apenas se observa la desintegración de un puñado de núcleos.

dan unas cuantas normas sobre cómo puede o no puede producirse una partícula. Los electrones pertenecen a una familia llamada *leptones*, y una de las normas del Modelo Estándar es que el número total de leptones se mantiene constante en todos los procesos físicos usuales (hay unos pocos en los que no, pero sólo se dan a altísimas temperaturas); esta constancia del número de leptones se conoce como *conservación del número leptónico*. Aplicado a la desintegración doble beta, esto quiere decir que si se han producido dos electrones (leptones) hay que producir dos *antileptones* para compensar; esos dos antileptones son los dos antineutrinos. La desintegración del  $^{136}\text{Xe}$  que hemos escrito en (10.1) respeta la conservación del número leptónico, como es de esperar.

Ahora bien, volviendo por un instante a nuestra cruzada por explicar la pequeñez de las masas de los neutrinos, resulta que la gran mayoría de las propuestas exige que el número leptónico no se conserve. O, dicho con un poco más de precisión, resulta que hay muchas maneras de justificar que la masa del neutrino sea pequeña si éste es su propia antipartícula. Si esto confunde al lector, que piense lo siguiente: con un electrón es fácil distinguir entre partícula y antipartícula; el electrón tiene carga  $-1$  y el positrón, su antipartícula, la contraria,  $+1$ . Pero con el neutrino, que no tiene carga eléctrica, ¿cómo aplicamos ese criterio? Hay que diseñar pruebas más sutiles, que pasan por separar el supuesto neutrino del supuesto antineutrino y ver si se comportan de manera diferente; pero dado que los neutrinos se resisten tan tozudamente a ser detectados y manipulados esas pruebas no son factibles. El hecho, a día de hoy, es que no sabemos si cuando hablamos de “neutrinos” y “antineutrinos” estamos hablando de dos partículas diferentes, ambas fantasmales, ambas sin carga eléctrica, o de la misma, que pasa por delante de nuestros ojos travestida de una guisa o de otra sin que nosotros nos demos cuenta.

Hay, sin embargo, una manera de poner a prueba este “carácter” del neutrino: si el neutrino es su propia antipartícula querría decir que es leptón y antileptón al mismo tiempo. Tal cosa no es posible, es un sinsentido; lo es hasta el punto de que hace que el número leptónico deje también de tener sentido: ¿cómo vamos a contar el número de leptones que hay en una habitación si hay unas cuantas

partículas que son, a la vez, un  $+1$  y un  $-1$ ? Si el neutrino es su propia antipartícula inmediatamente el número leptónico deja de ser una vara de medir válida; inmediatamente deja de ser constante; e inmediatamente procesos como (10.1) pueden ocurrir de otras maneras. Los detalles en cuanto a de qué maneras se pueden producir y cuán probable es cada camino pueden llenar –y llenan– monografías enteras y hoy no los comentaremos, pero sí vamos a señalar una alternativa: la desintegración del  $^{136}\text{Xe}$  podría también producirse de la siguiente manera:



es decir, con producción de dos electrones sin ningún antileptón para compensar, en franca violación de la conservación de número leptónico. Si los neutrinos fuesen su propia antipartícula, procesos como (10.2) deberían ocurrir; pero es más: un célebre artículo del año 1982 [143] demostró que también lo contrario es verdad: si se observa un proceso como (10.2), entonces el neutrino es su propia antipartícula.

Procesos como (10.2) reciben el nombre de *desintegración doble beta sin neutrinos* (abreviado,  $0\nu\beta\beta$ ) y, como confío que el lector comprenda ahora, son de la máxima relevancia para todos los que investigamos las propiedades de estas partículas<sup>7</sup>. Nuestra contribución a este campo ha sido analizar una familia de interacciones que violan la conservación del número leptónico, centrándonos en cómo dan lugar a  $0\nu\beta\beta$  y cómo nos pueden ayudar a entender las masas de los neutrinos.

Las interacciones que hemos estudiado se dividen en dos clases: las que involucran a un electrón, un neutrino y un bosón  $W$ , a las que llamamos “tipo  $W\nu e$ ”, y las que involucran a dos electrones y dos bosones  $W$ , que llamaremos “de tipo  $WWee$ ”. En la referencia [5] y el capítulo 6 las analizamos desde un punto de vista estrictamente efectivo, es decir, olvidándonos de qué las origina y pensando únicamente en sus consecuencias para  $0\nu\beta\beta$  y masas de neutrinos. La primera cuestión que nos ocupa es cómo evaluar si nuestras interacciones constituyen la principal contribución a la desintegración doble beta; habitualmente, incluso en modelos sencillos, uno va a tener más de un proceso físico

<sup>7</sup> Resulta irónico: para aprender sobre las propiedades del neutrino debemos diseñar complejos experimentos buscando una desintegración en la que el neutrino no aparece.

que dé lugar a  $0\nu\beta\beta$ , pero nosotros queremos construir modelos en los que la contribución más importante venga de las interacciones  $W\nu e$  o  $WWee$ . A lo largo de nuestro análisis desarrollamos un criterio para separar las interacciones que nos interesan de otras que a menudo las acompañan y que también producen  $0\nu\beta\beta$ ; de esta manera el físico que está construyendo un modelo sabe dónde tiene que mirar y en qué puntos ha de ser cuidadoso si quiere que las interacciones  $W\nu e$  y  $WWee$  sean las más relevantes. Este análisis culmina con una estimación de que las partículas que generan las nuevas interacciones deberían tener masas por debajo de 35 TeV para que las interacciones  $W\nu e$  y  $WWee$  sean las dominantes en  $0\nu\beta\beta$ .

Seguidamente analizamos, siempre desde el punto de vista efectivo, qué información nos da acerca de las nuevas interacciones lo que sabemos sobre desintegración doble beta y masas de neutrinos.  $0\nu\beta\beta$  nos da cotas bastante definidas sobre las masas de las partículas que generan las nuevas interacciones: las responsables de la interacción  $W\nu e$  deberían tener masas por encima de 100 TeV, y las asociadas con la interacción  $WWee$  deberían estar por encima de los 2 TeV, aunque en ambos casos las masas podrían ser algo más ligeras dependiendo de los detalles del modelo subyacente. El caso de la interacción  $WWee$ , pues, nos ofrece una perspectiva bastante optimista, pues partículas de 2 TeV o algo más ligeras podrían ser vistas en el LHC. Las masas de neutrinos nos ofrecen una información en principio menos fiable: no es posible, desde la teoría efectiva, calcular las masas de los neutrinos sin comprometerse con un modelo concreto – cosa que no queremos hacer, porque parte del poder de la teoría efectiva es estar por encima de los modelos. Además, nuestro conocimiento de las masas de los neutrinos es muy incompleto, y es difícil usarlas para obtener información sobre las nuevas interacciones. En cualquier caso, sí es posible hacer estimaciones, aunque éstas están necesariamente sometidas a mucha incertidumbre; tales estimaciones arrojan que las masas de las nuevas partículas deberían estar, para la interacción  $W\nu e$ , alrededor de 40 millones de TeV, una cifra estratosférica que las haría imposible de descubrir en cualquier experimento presente o del futuro cercano. La misma estimación ligada a masas de neutrinos sitúa las partículas asociadas con la interacción  $WWee$  en masas de 1000 TeV, más razonables pero



aún demasiado altas para cualquier experimento que podamos imaginar. Estas estimaciones, pues, enfrían un poco el optimismo de las cifras anteriores, aunque sabemos que sólo son estimaciones. Para dilucidar la cuestión lo mejor es usar los criterios que antes hemos descrito para construir modelos concretos de las interacciones  $W\nu e$  y  $WWee$ ; puesto que los modelos contienen toda la información, éstos sí nos darán información fiable sobre las masas de los neutrinos y sobre cuán ligeras pueden ser las nuevas partículas.

En el capítulo 7 describimos brevemente un modelo que da lugar a la interacción  $W\nu e$ . Este modelo requiere numerosas nuevas partículas, incluyendo nuevos fermiones pesados, que se comportarían de manera similar a electrones y neutrinos pero con masas mucho mayores, y nuevos escalares pesados, en particular uno con carga  $+2$  que podría ser fácil de detectar en un acelerador. El modelo es complicado y ofrece varias maneras de generar la interacción  $W\nu e$  pero, a cambio, es más optimista de lo que cabría esperar del análisis efectivo: las nuevas partículas podrían ser relativamente ligeras y producir alguna señal en el LHC o en otros experimentos que exploran nueva física en las cercanías del TeV. Sin embargo, nuestro análisis de este modelo ha tenido que ser somero por cuestiones de tiempo, y sería deseable volver sobre él para estudiar otros aspectos de su fenomenología, como sus contribuciones a procesos con violación de sabor leptónico.

En el capítulo 8 y la referencia [4] analizamos con detalle un modelo que da lugar a la interacción  $WWee$ . El modelo requiere una cantidad de nuevos escalares – partículas similares al bosón de Higgs, en este caso con cargas eléctricas 0, 1 y 2. Se trata de un modelo bastante prometedor, porque permite generar un espectro de masas de neutrinos compatible con lo observado y, a la vez, podría dar señales en una variedad de experimentos, desde el LHC a experimentos de  $0\nu\beta\beta$ . Nuestra discusión se centra en si es posible obtener el pleno total: proporcionar masa a los neutrinos, ser compatible con las observaciones que tenemos a día de hoy y arrojar también una señal en la nueva generación de experimentos de desintegración doble beta que está empezando a tomar datos actualmente. La respuesta es sí, aunque al exigir que el modelo cumpla en tantos frentes los valores posibles para las masas de las nuevas partículas quedan bastante restringidos: si

---

queremos observar una señal en los experimentos de  $0\nu\beta\beta$  queremos que las masas de las nuevas partículas no sean muy pesadas, lo cual es bueno, porque las pone al alcance del LHC; sin embargo, masas *demasiado* ligeras para las nuevas partículas hacen más difícil ajustar las masas de los neutrinos, además de entrar en tensión con otras cotas experimentales. Teniéndolo todo en cuenta, las nuevas partículas habrían de tener masas entre unos pocos TeV y algunas decenas de TeV, lo cual las situaría un poco por encima de lo que el LHC va a poder observar. Si renunciamos a alguna de nuestras exigencias, como por ejemplo que se observe una señal de  $0\nu\beta\beta$  inminentemente, la situación se vuelve más laxa: las nuevas partículas pueden ser más pesadas, quedando igualmente lejos del LHC pero dando más margen en la generación de masas de neutrinos.

En el capítulo 8, pues, vemos un buen ejemplo de lo que requiere el análisis de modelos: considerar todas las consecuencias observables de las nuevas partículas que estás analizando y ver hasta qué punto pueden cumplir todas tus expectativas. Habitualmente hay que renunciar a alguna de esas expectativas para que el modelo resulte viable; en este caso ha habido suerte y hemos dado con un modelo versátil que puede acomodar, aunque con estrecheces, un escenario bastante optimista. Ahora, para que el optimismo sea completo, sólo faltaría que el modelo fuera cierto.

## 11. AGRADECIMIENTOS

Esto no es un adiós. Pero sería deshonesto pretender que no se le parece, aunque sólo sea un poco. No recuerdo cuándo supe que la ciencia iba a ser mi vida. Recuerdo el día que en el colegio nos enseñaron la tabla del dos – “multiplicar”, me dije, “guau, esto son matemáticas de verdad”; es uno de mis recuerdos emocionales más antiguos. Recuerdo también haber estado rodeado siempre de libros de zoología: interminables catálogos de insectos, aves rapaces, anfibios, reptiles – y tortugas; muchas tortugas, claro. No descarto que mi afición por lo enciclopédico derive de haber devorado con afán insensato listas y listas de bichos diversos, descripciones de sus libreas, especificaciones sobre sus hábitos, consejos para combatir sus enfermedades. Finalmente, recuerdo el día en que en la biblioteca descubrí, más bien por azar, *El electrón es zurdo* de Isaac Asimov; era un volumen vetusto, de desvencijada tapa dura, con el olor a rancio y el color moreno que sólo los buenos jamones conocen. Si usted no lo ha leído, entonces yo poco le puedo decir; sólo que un descubrimiento le está esperando, y que no se arrepentirá si da el paso. Después de *El electrón...* vino el inimitable *El Universo*, y luego un irracionalmente exhaustivo volumen que repasaba la ciencia de los últimos 400 años y cuyo título no consigo recordar. Al maestro Asimov le debo sin duda el estar escribiendo estas líneas. Pero no sólo a él; también se lo debo a otros maestros, gente que por aquel entonces acertó a enseñarme que esto de la ciencia tenía su gracia. Recuerdo con especial cariño el estilo impulsivo de Asun, que me enseñó mi primer teorema; los chistes de Elvira, la polvorienta geología de Tere. Y la física con María Dolores. Lo hacía bien. Para ser química. También por esa época, recuerdo, el padre Javier me descubrió a un señor llamado Albert Camus, que daría para otra historia, y conocí *Cosmos*, de Carl Sagan. Recuerdo que no le

presté mucha atención entonces. Cosas de niños, supongo.

Luego vino la carrera. Es sorprendente que aquello saliera tan bien; elegí Física casi a ciegas, sin saber dónde me metía –tan lejana es la enseñanza de instituto de la física real–, y no estaba en absoluto seguro de que ésta fuese la carrera para mí. Unos meses después, sin embargo, no podía imaginarme en otro sitio ni rodeado de otra gente. En esta facultad me han enseñado a pensar, a ser crítico y humilde, a buscar en los libros las respuestas que las personas no tienen, y sobre todo –porque éste es el trabajo de un físico– que cuando los problemas son grandes y complejos podemos aspirar a atacarlos si los sabemos transformar en otras cosas, más pequeñas, que sí conocemos. También he jugado mucho al mus y he aprendido que puede haber mentes muy brillantes en personas muy oscuras. Destacar a toda la gente que ha sido importante para mí en esta facultad sería imposible, son demasiados años. Pero aun así me enfangaré y citaré a una selección; después de tantas páginas de tesis las cosas no pueden ir a peor. . .

Entre el profesorado no olvidaré a Pepe Bernabéu, que daba clase con pasión y nos enseñó aquello de “nunca hay que empezar un cálculo cuyo resultado no conoces de antemano”; a Pepe Navarro, cuyas lecciones fueron para mí el comienzo de las altas matemáticas; a Adolfo de Azcárraga, que enseñaba con un detallismo casi erudito; a Toni Pich, que jugaba en sus clases con lo que sabíamos y lo que queríamos saber, como los buenos *thrillers* hacen. Y en fin, sólo me faltan Eugenio y Germán, con los que di mis primeros bocados a la investigación y aprendí cosas que aún uso, tanto sobre la ciencia como sobre las personas.

And speaking about science and people, there’s a bunch of scientists who are also a little bit responsible for this story: my collaborators, Kyungwook, Subha, Paco, Nuria and Juan; Sacha, Vincenzo and Michael, who so kindly hosted me at Lyon and Los Alamos and tried to extract some science out of me. And maybe especially José Wudka, whose ideas and momentum were fundamental for the birth of these works. To all of them I feel indebted, and this work is also somewhat theirs.

En el mismo orden de cosas no puedo dejar de mencionar a las personas que han evaluado esta tesis, colegas y amigos que han dedicado

una parte de su apretada agenda a leer este texto que ha quedado tan largo y a aportarle lo mejor que han podido. Muchas gracias por vuestro esfuerzo y generosidad.

Ésta ha sido una etapa de maduración científica, pero también –me atrevería a decir que sobre todo– humana. Los testigos más cualificados para dar fe de esto son mi familia y amigos. A mis padres y mis hermanas les debo que se hayan mantenido al pie del cañón a pesar de mi humor insoportable y mi tendencia a preferir la soledad de mi habitación al salón de casa. Tengo la sensación de que todo esto puede haber pasado por delante de vuestros ojos sin que hayáis entendido mucho qué estaba sucediendo, ni por qué ni cómo; me tranquiliza un poco pensar que en realidad tampoco necesitabais entenderlo: lo que queríais era que yo fuera feliz y que pudiera compartir esa alegría con vosotros. Temo en este punto no haber estado siempre a la altura. Sólo puedo daros las gracias por vuestra paciencia y el tozudo cariño que siempre me dais. No desfallezcáis, ya veis que hasta yo puedo hacerme mayor.

Hay amigos que son casi como si fueran familia; gente que si durante una invasión zombi te dijeran “tírate por esa ventana” no tendrías otra que hacerles caso. Gente que, a menudo, te conoce mejor que tú mismo. Pienso en Carl, Apa, David, Sergio, Marta, Juan, Joaquín, Antonio. Para vosotros tengo lo único que vale la pena dar: todo mi cariño. Mirando atrás creo que sois lo que ha hecho que esta andadura valga la pena; con vosotros he aprendido a vivir y por vosotros me he convertido en alguien mejor, y ahora me miro al espejo y me alegro del paso de los años. No voy a repasar nuestros mejores momentos, no voy a elevar grandes deseos de que esto dure para siempre; pienso que lo nuestro está por encima de esas cosas. Os diré simplemente que gracias. Que me mantenéis unido a este mundo. Que mañana nos veremos, y que probablemente será un día mejor que hoy.

Junto a ellos está la legión; gente y más gente que han sido, fueron, son o serán importantes. Sus méritos han sido reír, montar telescopios, comprar botellón, ver películas, hablar de política y de física, comer mucho y bien, copiarse, dejar copiar, escuchar siempre, ser sinceros junto a una lumbre o una cerveza. Hoy me siento especialmente incompetente intentando haceros justicia. A mis amigos de Castellón

---

les diré que han sido los cimientos de todo; os recordaré las tardes hablando de agujeros negros en algún parque, lo extraño que me sentía entrando a una discoteca de estrangis, lo a gusto que me siento ahora. A Carlos, Paula, Luis y Juan les diré que les quiero; que es por vosotros que soy un poco de letras; que hemos pasado mucho frío en ese putito portal, leches; y que sólo consigo acordarme de buenos momentos. A Bernat le agradeceré ser mi familia durante seis años, las tertulias por la noche, los partidos de Champions, aguantar mis rarezas y ser práctico con los problemas; para Pepe y para Berta iré una parte alícuota de estas mismas cosas. A los Caballeros de la Orden les diré que me hicisteis sentir en casa por primera vez, que será difícil encontrar otra gente con la que sea tan sencillo ser yo mismo; también que creo que nunca he cumplido tantos sueños de la infancia como la noche del Hyundai. A Pepón le diré que no conozco a nadie que vea las matemáticas como tú lo haces, y que si la ciencia va a echar de menos tus teoremas me alegro de que al menos pueda disfrutar tus poemas; al fin y al cabo, como todo el mundo sabe, la poesía y las matemáticas son la misma cosa. A la gente de la Asociación de Astronomía les agradeceré la paciencia, la generosidad que hace fácil lo difícil, el entusiasmo por enseñar; y les diré que este punto azul pálido es demasiado pequeño para que no estemos, de una manera o de otra, cerca. A Avelino, Rika, los Javis, las Susanas, Ferrándiz, Víctor y todos los demás les confesaré que si no os hubiera conocido no habría logrado recuperarle el pulso a la carrera, que la habría terminado de cualquier manera; sé que pensaréis que exagero, pero eso es porque siempre fuisteis demasiado generosos. Puedo decir sin inmutarme que sois el mejor grupo humano que he conocido, y que formar parte de él ha sido –sigue siendo– una verdadera alegría. A toda la gente de iGEM Valencia 2006 les contaré lo que ya saben: que ese verano fue mágico, que hicimos muchas más cosas que ciencia, que lo que construimos ha sido duradero; y añadiré que si hoy hubiese de decidir cuándo comenzó el cambio creo que lo situaría en aquel verano extraño en el que aprendí que existe un mundo más allá de la física. A Francesc, Manu, Paco, Vicent, María y el resto les diré que siempre sonríe con vosotros; que nos hemos juntado poco y que somos un grupo heterogéneo, pero que todas nuestras reuniones son un buen momento. A toda la gente del

Departamento, desde a mis compañeros de despacho a los profesores pasando por la gente de secretaría les agradeceré que me hayan hecho las cosas tan fáciles; que pudiendo ser mis compañeros de trabajo se hayan convertido en mis amigos; y les diré que si he tenido que huir no ha sido porque estuviera a disgusto, sino porque es *imposible* escribir una tesis estando tan a gusto. A Dani, Gustavo, Paco, Álex y Clarilla... no os puedo decir nada, porque no me habéis visto el pelo! Hablando en serio, ya lo sabéis: mi vida es un completo desorden, y quizá por eso pongo tanto esfuerzo en que al menos la casa esté ordenada; haciendo gala de estas costumbres que conocéis tan bien, estas líneas las estoy escribiendo a las ocho y pico de la noche en un edificio semidesierto, y mañana es fiesta. Realmente quizá haya cosas que nunca cambian. A los últimos en llegar: David, Clari, Oliver, Javi, Beni, Diana, os diré que habéis conocido una versión depauperada de mí mismo y que, pese a ello, habéis hecho lo posible por sacarme a flote; os diré también que ha funcionado, está funcionando. Por ello, pues, gracias; nada me hará más feliz que el día en que *no* tenga que devolveros el favor porque todo os vaya bien.

Todas las cosas se acaban, incluso las malas. Ésta, sin embargo, no puede terminar hasta que haya hablado de Arcadi. Escoger un director de tesis no es necesariamente un asunto fácil, y menos cuando hay mucha oferta: todos los proyectos, en el fondo, suenan bien, porque en realidad no tienes ni idea de cómo evaluarlos, y no puedes comprender cuáles son los aspectos relevantes hasta que estés dentro. Cuando escogí a Arcadi lo hice porque me gustaba la física que me ofrecía, pero también porque parecía un hombre de fiar, una buena persona. En lo que respecta a la física, Arcadi, tú la ves con mucha mayor claridad de lo que yo nunca la veré. Has intentado enseñarme, señalarme cuáles eran las estrategias más inteligentes, y no ha sido un esfuerzo infructuoso porque creo que algo he aprendido; sin embargo, no puedo dejar de pensar que te he tenido desaprovechado, porque en serio, creo que eres uno de los físicos más brillantes que he conocido. Ha sido un placer descubrir cosas a tu lado. En lo humano... bueno, sé que va a sonar a coba, pero el nivel ha sido igual o mejor. Eres mi director de tesis, sí, pero sobre todo eres mi amigo, y te he contado cosas que creo que la mayor parte de gente no le contaría a su jefe.

---

Eso es relevante; eso tiene peso. Eso, aunque me suspendan el día de la defensa, seguirá existiendo – bueno vale, entenderé que te enfades si me suspenden, tampoco vamos a exagerar. En fin, que muchas gracias por este viaje; espero que, como yo, pienses que el viaje no ha sido en vano.

Es hora de echar el cierre. Antes he dicho que los últimos tiempos han visto una versión depauperada de mí mismo. Lo sigo pensando. La redacción de este texto que aquí termina y otras tantas complicaciones que ahora no vienen al caso han hecho de estos dos últimos años un periodo difícil. La suerte es que junto con esas dificultades han venido otras cosas que no dejan de empujar para seguir adelante; quizá la más sorprendente y la más importante sea la gente de La Brújula, a la que mando un saludo desde aquí. He dicho antes también que esto no era un adiós, y es cierto. Tiendo a pensar en la vida como en una partida de cartas: jugamos bien o jugamos mal, pero al final siempre acabamos con unas cuantas cartas en la mano. ¿Cómo vas a decir adiós si al final sigues jugando, como al principio? Yo no siempre he jugado bien; no me hacen feliz los errores, pero sí atesoro unos cuantos aciertos. Si estás leyendo esto es porque eres uno de esos aciertos. Hasta siempre.



## BIBLIOGRAPHY

- [1] Alberto Aparici, Kyungwook Kim, Arcadi Santamaria, and Jose Wudka, “Right-handed neutrino magnetic moments,” *Phys.Rev.* **D80**, 013010 (2009), [arXiv:0904.3244 \[hep-ph\]](#) [Back to page iii](#), [234](#), [235](#), or [236](#)
- [2] Alberto Aparici, Arcadi Santamaria, and Jose Wudka, “A model for right-handed neutrino magnetic moments,” *J.Phys.* **G37**, 075012 (2010), [arXiv:0911.4103 \[hep-ph\]](#) [Back to page iii](#), [234](#), or [236](#)
- [3] Alberto Aparici, Kyung-Wook Kim, Arcadi Santamaria, and Jose Wudka, “Right-handed neutrino magnetic moments,” *J.Phys.Conf.Ser.* **259**, 012089 (2010) [Back to page iii](#)
- [4] Francisco del Aguila, Alberto Aparici, Subhaditya Bhattacharya, Arcadi Santamaria, and Jose Wudka, “A realistic model of neutrino masses with a large neutrinoless double beta decay rate,” *JHEP* **1205**, 133 (2012), [arXiv:1111.6960 \[hep-ph\]](#) [Back to page iii](#) or [240](#)
- [5] Francisco del Aguila, Alberto Aparici, Subhaditya Bhattacharya, Arcadi Santamaria, and Jose Wudka, “Effective Lagrangian approach to neutrinoless double beta decay and neutrino masses,” *JHEP* **1206**, 146 (2012), [arXiv:1204.5986 \[hep-ph\]](#) [Back to page iii](#) or [238](#)
- [6] F. del Águila, A. Aparici, S. Bhattacharya, A. Santamaria, and J. Wudka, “Neutrinoless double  $\beta$  decay with small neutrino masses,” *PoS Corfu2012*, 028 (2013), [arXiv:1305.4900 \[hep-ph\]](#) [Back to page iii](#)

- 
- [7] S.L. Glashow, “Partial symmetries of weak interactions,” *Nucl.Phys.* **22**, 579–588 (1961) [Back to page 3](#) or [4](#)
- [8] Peter W. Higgs, “Broken symmetries and the masses of gauge bosons,” *Phys.Rev.Lett.* **13**, 508–509 (1964) [Back to page 3](#)
- [9] F. Englert and R. Brout, “Broken symmetry and the mass of gauge vector mesons,” *Phys.Rev.Lett.* **13**, 321–323 (1964) [Back to page 3](#)
- [10] G.S. Guralnik, C.R. Hagen, and T.W.B. Kibble, “Global conservation laws and massless particles,” *Phys.Rev.Lett.* **13**, 585–587 (1964) [Back to page 3](#)
- [11] Peter W. Higgs, “Spontaneous symmetry breakdown without massless bosons,” *Phys.Rev.* **145**, 1156–1163 (1966) [Back to page 3](#)
- [12] T.W.B. Kibble, “Symmetry breaking in non-Abelian gauge theories,” *Phys.Rev.* **155**, 1554–1561 (1967) [Back to page 3](#)
- [13] Steven Weinberg, “A model of leptons,” *Phys.Rev.Lett.* **19**, 1264–1266 (1967) [Back to page 3](#) or [4](#)
- [14] Abdus Salam, “Weak and electromagnetic interactions,” *Conf.Proc.* **C680519**, 367–377 (1968) [Back to page 3](#) or [4](#)
- [15] M.Y. Han and Yoichiro Nambu, “Three-triplet model with double  $su(3)$  symmetry,” *Phys.Rev.* **139**, B1006–B1010 (1965) [Back to page 3](#)
- [16] H. Fritzsch, Murray Gell-Mann, and H. Leutwyler, “Advantages of the color octet gluon picture,” *Phys.Lett.* **B47**, 365–368 (1973) [Back to page 3](#)
- [17] Murray Gell-Mann, “Quarks,” *Acta Phys.Austriaca Suppl.* **9**, 733–761 (1972) [Back to page 3](#)
- [18] Harald Fritzsch and Murray Gell-Mann, “Current algebra: Quarks and what else?,” eConf **C720906V2**, 135–165 (1972), [arXiv:hep-ph/0208010 \[hep-ph\]](#) [Back to page 3](#)

- 
- [19] Antonio Pich, “The standard model of electroweak interactions,” (2012), [arXiv:1201.0537 \[hep-ph\]](#) Back to page [3](#), [7](#), or [12](#)
- [20] Antonio Pich, “Aspects of quantum chromodynamics,” (1999), [arXiv:hep-ph/0001118 \[hep-ph\]](#) Back to page [3](#)
- [21] E. Fermi, “Trends to a theory of beta radiation. (in Italian),” [Nuovo Cim.](#) **11**, 1–19 (1934) Back to page [4](#)
- [22] E. Fermi, “An attempt of a theory of beta radiation. 1.” [Z.Phys.](#) **88**, 161–177 (1934) Back to page [4](#)
- [23] Fred L. Wilson, “Fermi’s theory of beta decay,” [American Journal of Physics](#) **36**, 1150–1160 (1968) Back to page [4](#)
- [24] C.S. Wu, E. Ambler, R.W. Hayward, D.D. Hoppes, and R.P. Hudson, “Experimental test of parity conservation in beta decay,” [Phys.Rev.](#) **105**, 1413–1414 (1957) Back to page [4](#)
- [25] T.D. Lee and Chen-Ning Yang, “Question of parity conservation in weak interactions,” [Phys.Rev.](#) **104**, 254–258 (1956) Back to page [4](#)
- [26] T.P. Cheng and L.F. Li, *Gauge theory of elementary particle physics* (Oxford University Press, 1984) ISBN 978-0198519614 Back to page [5](#), [7](#), [10](#), or [12](#)
- [27] R. Jackiw and A. Kerman, “Time-dependent variational principle and the effective action,” [Phys.Lett.](#) **A71**, 158–162 (1979) Back to page [9](#)
- [28] R. Jackiw, “Functional evaluation of the effective potential,” [Phys.Rev.](#) **D9**, 1686 (1974) Back to page [9](#)
- [29] John M. Cornwall, R. Jackiw, and E. Tomboulis, “Effective action for composite operators,” [Phys.Rev.](#) **D10**, 2428–2445 (1974) Back to page [9](#)
- [30] Howard Georgi, *Lecture notes on weak interactions*, <http://www.people.fas.harvard.edu/~hgeorgi/weak.pdf> Back to page [9](#)

- 
- [31] Sydney Coleman, *Aspects of symmetry* (Cambridge University Press, 1985) [Back to page 9](#)
- [32] J. Beringer *et al.* (Particle Data Group), “Review of particle physics (RPP),” *Phys.Rev.* **D86**, 010001 (2012) [Back to page 9](#), [27](#), [65](#), [79](#), [85](#), [123](#), [182](#), [195](#), or [230](#)
- [33] Georges Aad *et al.* (ATLAS Collaboration), “Observation of a new particle in the search for the Standard Model Higgs boson with the ATLAS detector at the LHC,” *Phys.Lett.* **B716**, 1–29 (2012), [arXiv:1207.7214 \[hep-ex\]](#) [Back to page 9](#) or [92](#)
- [34] Serguei Chatrchyan *et al.* (CMS Collaboration), “Observation of a new boson at a mass of 125 GeV with the CMS experiment at the LHC,” *Phys.Lett.* **B716**, 30–61 (2012), [arXiv:1207.7235 \[hep-ex\]](#) [Back to page 9](#) or [92](#)
- [35] E.S. Abers and B.W. Lee, “Gauge theories,” *Phys.Rept.* **9**, 1–141 (1973) [Back to page 10](#)
- [36] Arcadi Santamaria, “Masses, mixings, Yukawa couplings and their symmetries,” *Phys.Lett.* **B305**, 90–97 (1993), [arXiv:hep-ph/9302301 \[hep-ph\]](#) [Back to page 12](#) or [33](#)
- [37] Steven Weinberg, “Phenomenological Lagrangians,” *Physica* **A96**, 327 (1979) [Back to page 18](#)
- [38] H. Georgi, “Effective field theory,” *Ann.Rev.Nucl.Part.Sci.* **43**, 209–252 (1993) [Back to page 18](#) or [69](#)
- [39] David B. Kaplan, “Effective field theories,” (1995), [arXiv:nucl-th/9506035 \[nucl-th\]](#) [Back to page 18](#)
- [40] C.P. Burgess, “An ode to effective Lagrangians,” *Proceedings of RADCOR 98(1998)*, [arXiv:hep-ph/9812470 \[hep-ph\]](#) [Back to page 18](#)
- [41] Aneesh V. Manohar, “Effective field theories,” in *Perturbative and Nonperturbative Aspects of Quantum Field Theory*, Lecture

- Notes in Physics, Vol. 479, edited by H. Latal and W. Schweiger (Springer Berlin Heidelberg, 1997) pp. 311–362, ISBN 978-3-540-62478-3, [arXiv:hep-ph/9606222 \[hep-ph\]](#) Back to page [18](#)
- [42] Antonio Pich, “Effective field theory,” , 949–1049(1998), [arXiv:hep-ph/9806303 \[hep-ph\]](#) Back to page [18](#)
- [43] Jose Wudka, “Electroweak effective Lagrangians,” *Int.J.Mod.Phys.* **A9**, 2301–2362 (1994), [arXiv:hep-ph/9406205 \[hep-ph\]](#) Back to page [18](#) or [69](#)
- [44] R.N. Mohapatra, S. Antusch, K.S. Babu, G. Barenboim, Mu-Chun Chen, *et al.*, “Theory of neutrinos: A white paper,” *Rept.Prog.Phys.* **70**, 1757–1867 (2007), [arXiv:hep-ph/0510213 \[hep-ph\]](#) Back to page [25](#) or [26](#)
- [45] R.N. Mohapatra and P.B. Pal, *Massive neutrinos in physics and astrophysics*, 3rd ed., Lecture Notes in Physics, Vol. 72 (World Scientific, 2004) ISBN 978-9812380708 Back to page [25](#), [26](#), or [29](#)
- [46] Carlo Giunti and Chung W. Kim, *Fundamentals of Neutrino Physics and Astrophysics* (Oxford University Press, 2007) ISBN 978-0198508717 Back to page [25](#)
- [47] Zhi-zhong Xing and Shun Zhou, *Neutrinos in particle physics, astronomy and cosmology* (Springer, 2011) ISBN 978-3642175596 Back to page [25](#)
- [48] G.G. Raffelt, *Stars as laboratories for fundamental physics: the astrophysics of neutrinos, axions, and other weakly interacting particles* (University of Chicago Press, 1996) ISBN 978-0226702728 Back to page [25](#), [39](#), [67](#), [93](#), [94](#), or [95](#)
- [49] Alessandro Strumia and Francesco Vissani, “Neutrino masses and mixings and....” (2006), [arXiv:hep-ph/0606054 \[hep-ph\]](#) Back to page [26](#)
- [50] M.C. Gonzalez-Garcia and Michele Maltoni, “Phenomenology with massive neutrinos,” *Phys.Rept.* **460**, 1–129 (2008), [arXiv:0704.1800 \[hep-ph\]](#) Back to page [26](#), [31](#), or [39](#)

- 
- [51] Paul Dirac, “The quantum theory of electron,” *Proc. Roy. Soc. Lond.* **A117**, 610–624 (1928) [Back to page 26](#)
- [52] Paul Dirac, “The quantum theory of electron. 2.” *Proc. Roy. Soc. Lond.* **A118**, 351 (1928) [Back to page 26](#)
- [53] Ettore Majorana, “Theory of the symmetry of electrons and positrons,” *Nuovo Cim.* **14**, 171–184 (1937) [Back to page 26](#)
- [54] Steven Weinberg, “Baryon and lepton nonconserving processes,” *Phys.Rev.Lett.* **43**, 1566–1570 (1979) [Back to page 28](#) or [110](#)
- [55] H.A. Weldon and A. Zee, “Operator analysis of new physics,” *Nucl.Phys.* **B173**, 269 (1980) [Back to page 28](#)
- [56] Rabindra N. Mohapatra and Goran Senjanovic, “Neutrino masses and mixings in gauge models with spontaneous parity violation,” *Phys.Rev.* **D23**, 165 (1981) [Back to page 29](#)
- [57] T.P. Cheng and Ling-Fong Li, “Neutrino masses, mixings and oscillations in  $SU(2) \otimes U(1)$  models of electroweak interactions,” *Phys.Rev.* **D22**, 2860 (1980) [Back to page 29](#) or [60](#)
- [58] A. Zee, “Quantum numbers of Majorana neutrino masses,” *Nucl.Phys.* **B264**, 99 (1986) [Back to page 29](#)
- [59] J.I. Silva-Marcos, “Alternative to the seesaw mechanism,” *Phys.Rev.* **D59**, 091301 (1999) [Back to page 29](#) or [59](#)
- [60] Ernest Ma, “Verifiable radiative seesaw mechanism of neutrino mass and dark matter,” *Phys.Rev.* **D73**, 077301 (2006), [arXiv:hep-ph/0601225 \[hep-ph\]](#) [Back to page 29](#)
- [61] D. Ibanez, S. Morisi, and J.W.F. Valle, “Inverse tri-bimaximal type III seesaw and lepton flavor violation,” *Phys.Rev.* **D80**, 053015 (2009), [arXiv:0907.3109 \[hep-ph\]](#) [Back to page 29](#)
- [62] Alberto Aparici, Juan Herrero-Garcia, Nuria Rius, and Arcadi Santamaria, “Neutrino masses from new generations,” *JHEP* **1107**, 122 (2011), [arXiv:1104.4068 \[hep-ph\]](#) [Back to page 29](#)

- 
- [63] E. Peinado and A. Vicente, “Neutrino masses from R-parity violation with a  $Z_3$  symmetry,” *Phys.Rev.* **D86**, 093024 (2012), [arXiv:1207.6641 \[hep-ph\]](#) [Back to page 29](#)
- [64] R. Davis, “Solar neutrinos. II: Experimental,” *Phys.Rev.Lett.* **12**, 303–305 (1964) [Back to page 30](#) or [39](#)
- [65] B.T. Cleveland, Timothy Daily, Jr. Davis, Raymond, James R. Distel, Kenneth Lande, *et al.*, “Measurement of the solar electron neutrino flux with the Homestake chlorine detector,” *Astrophys.J.* **496**, 505–526 (1998) [Back to page 30](#) or [39](#)
- [66] Y. Fukuda *et al.* (Kamiokande Collaboration), “Solar neutrino data covering solar cycle 22,” *Phys.Rev.Lett.* **77**, 1683–1686 (1996) [Back to page 30](#) or [39](#)
- [67] W. Hampel *et al.* (GALLEX Collaboration), “GALLEX solar neutrino observations: Results for GALLEX IV,” *Phys.Lett.* **B447**, 127–133 (1999) [Back to page 30](#) or [39](#)
- [68] Y. Fukuda *et al.* (Super-Kamiokande Collaboration), “Measurements of the solar neutrino flux from Super-Kamiokande’s first 300 days,” *Phys.Rev.Lett.* **81**, 1158–1162 (1998), [arXiv:hep-ex/9805021 \[hep-ex\]](#) [Back to page 30](#) or [39](#)
- [69] Q.R. Ahmad *et al.* (SNO Collaboration), “Measurement of the rate of  $\nu_e + d \rightarrow p + p + e^-$  interactions produced by  $^8\text{B}$  solar neutrinos at the Sudbury Neutrino Observatory,” *Phys.Rev.Lett.* **87**, 071301 (2001), [arXiv:nucl-ex/0106015 \[nucl-ex\]](#) [Back to page 30](#) or [39](#)
- [70] J.N. Abdurashitov *et al.* (SAGE Collaboration), “Solar neutrino flux measurements by the Soviet-American Gallium Experiment (SAGE) for half the 22 year solar cycle,” *J.Exp.Theor.Phys.* **95**, 181–193 (2002), [arXiv:astro-ph/0204245 \[astro-ph\]](#) [Back to page 30](#) or [39](#)
- [71] M. Altmann *et al.* (GNO COLLABORATION), “Complete results for five years of GNO solar neutrino observations,” *Phys.Lett.*

- 
- B616**, 174–190 (2005), [arXiv:hep-ex/0504037 \[hep-ex\]](#) Back to page [30](#) or [39](#)
- [72] F. Reines, M.F. Crouch, T.L. Jenkins, W.R. Kropp, H.S. Gurr, *et al.*, “Evidence for high-energy cosmic ray neutrino interactions,” [Phys.Rev.Lett.](#) **15**, 429–433 (1965) Back to page [30](#) or [40](#)
- [73] C.V. Achar *et al.*, “Detection of muons produced by cosmic ray neutrinos deep underground,” [Physics Letters](#) **18**, 196 – 199 (1965), ISSN 0031-9163 Back to page [30](#) or [40](#)
- [74] M. Aglietta *et al.* (NUSEX Collaboration), “Experimental study of atmospheric neutrino flux in the NUSEX experiment,” [Euro-phys.Lett.](#) **8**, 611–614 (1989) Back to page [30](#) or [40](#)
- [75] K. Daum *et al.* (Frejus Collaboration.), “Determination of the atmospheric neutrino spectra with the Fréjus detector,” [Z.Phys.](#) **C66**, 417–428 (1995) Back to page [30](#) or [40](#)
- [76] R. Becker-Szendy, C.B. Bratton, D. Casper, S.T. Dye, W. Gajewski, *et al.*, “The electron-neutrino and muon-neutrino content of the atmospheric flux,” [Phys.Rev.](#) **D46**, 3720–3724 (1992) Back to page [30](#) or [40](#)
- [77] Y. Fukuda *et al.* (Kamiokande Collaboration), “Atmospheric muon-neutrino / electron-neutrino ratio in the multiGeV energy range,” [Phys.Lett.](#) **B335**, 237–245 (1994) Back to page [30](#) or [40](#)
- [78] Q.R. Ahmad *et al.* (SNO Collaboration), “Direct evidence for neutrino flavor transformation from neutral current interactions in the Sudbury Neutrino Observatory,” [Phys.Rev.Lett.](#) **89**, 011301 (2002), [arXiv:nucl-ex/0204008 \[nucl-ex\]](#) Back to page [31](#) or [39](#)
- [79] Carlo Giunti and Chung W. Kim, “Quantum mechanics of neutrino oscillations,” [Found.Phys.Lett.](#) **14**, 213–229 (2001), [arXiv:hep-ph/0011074 \[hep-ph\]](#) Back to page [31](#) or [37](#)
- [80] Carlo Giunti, “Neutrino flavor states and the quantum theory of neutrino oscillations,” [AIP Conf.Proc.](#) **1026**, 3–19 (2008), [arXiv:0801.0653 \[hep-ph\]](#) Back to page [31](#) or [37](#)



- 
- [81] Chris Waltham, “Teaching neutrino oscillations,” *Am.J.Phys.* **72**, 742–752 (2004), [arXiv:physics/0303116 \[physics.ed-ph\]](#) [Back to page 31](#)
- [82] T. Araki *et al.* (KamLAND Collaboration), “Measurement of neutrino oscillation with KamLAND: Evidence of spectral distortion,” *Phys.Rev.Lett.* **94**, 081801 (2005), [arXiv:hep-ex/0406035 \[hep-ex\]](#) [Back to page 32](#) or [42](#)
- [83] B. Pontecorvo, “Mesonium and anti-mesonium,” *Sov.Phys.JETP* **6**, 429 (1957), [http://puhep1.princeton.edu/~mcdonald/examples/EP/pontecorvo\\_spjetp\\_6\\_429\\_57.pdf](http://puhep1.princeton.edu/~mcdonald/examples/EP/pontecorvo_spjetp_6_429_57.pdf) [Back to page 32](#)
- [84] B. Pontecorvo, “Inverse beta processes and nonconservation of lepton charge,” *Sov.Phys.JETP* **7**, 172–173 (1958) [Back to page 32](#)
- [85] Ziro Maki, Masami Nakagawa, and Shoichi Sakata, “Remarks on the unified model of elementary particles,” *Prog.Theor.Phys.* **28**, 870–880 (1962) [Back to page 32](#)
- [86] M. Nakagawa, H. Okonogi, S. Sakata, and A. Toyoda, “Possible existence of a neutrino with mass and partial conservation of muon charge,” *Prog.Theor.Phys.* **30**, 727–729 (1963) [Back to page 32](#)
- [87] J. Schechter and J.W.F. Valle, “Neutrino masses in  $SU(2) \otimes U(1)$  theories,” *Phys.Rev.* **D22**, 2227 (1980) [Back to page 32](#) or [60](#)
- [88] P.F. Harrison, D.H. Perkins, and W.G. Scott, “Tri-bimaximal mixing and the neutrino oscillation data,” *Phys.Lett.* **B530**, 167 (2002), [arXiv:hep-ph/0202074 \[hep-ph\]](#) [Back to page 36](#)
- [89] V. Antonelli, L. Miramonti, C. Pena Garay, and A. Serenelli, “Solar neutrinos,” *Adv.High Energy Phys.* **2013**, 351926 (2013), [arXiv:1208.1356 \[hep-ex\]](#) [Back to page 39](#)
- [90] L. Wolfenstein, “Neutrino oscillations in matter,” *Phys.Rev.* **D17**, 2369–2374 (1978) [Back to page 39](#)

- 
- [91] L. Wolfenstein, “Neutrino oscillations and stellar collapse,” *Phys.Rev.* **D20**, 2634–2635 (1979) [Back to page 39](#)
- [92] S.P. Mikheev and A. Yu. Smirnov, “Resonant amplification of neutrino oscillations in matter and solar neutrino spectroscopy,” *Nuovo Cim.* **C9**, 17–26 (1986) [Back to page 39](#)
- [93] S.P. Mikheev and A. Yu. Smirnov, “Resonance amplification of oscillations in matter and spectroscopy of solar neutrinos,” *Sov.J.Nucl.Phys.* **42**, 913–917 (1985) [Back to page 39](#)
- [94] A. Yu. Smirnov, “The MSW effect and matter effects in neutrino oscillations,” *Phys.Scripta* **T121**, 57–64 (2005), [arXiv:hep-ph/0412391 \[hep-ph\]](#) [Back to page 39](#)
- [95] Takaaki Kajita, “Atmospheric neutrinos,” *Adv.High Energy Phys.* **2012**, 504715 (2012) [Back to page 40](#)
- [96] Y. Fukuda *et al.* (Super-Kamiokande Collaboration), “Evidence for oscillation of atmospheric neutrinos,” *Phys.Rev.Lett.* **81**, 1562–1567 (1998), [arXiv:hep-ex/9807003 \[hep-ex\]](#) [Back to page 41](#)
- [97] M. Ambrosio *et al.* (MACRO Collaboration), “Matter effects in upward-going muons and sterile neutrino oscillations,” *Phys.Lett.* **B517**, 59–66 (2001), [arXiv:hep-ex/0106049 \[hep-ex\]](#) [Back to page 41](#)
- [98] Mayly C. Sanchez *et al.* (Soudan 2 Collaboration), “Measurement of the L/E distributions of atmospheric neutrinos in Soudan 2 and their interpretation as neutrino oscillations,” *Phys.Rev.* **D68**, 113004 (2003), [arXiv:hep-ex/0307069 \[hep-ex\]](#) [Back to page 41](#)
- [99] S. Adrian-Martinez *et al.* (ANTARES collaboration), “Measurement of atmospheric neutrino oscillations with the ANTARES neutrino telescope,” *Phys.Lett.* **B714**, 224–230 (2012), [arXiv:1206.0645 \[hep-ex\]](#) [Back to page 41](#)
- [100] M.G. Aartsen *et al.* (IceCube Collaboration), “Measurement of atmospheric neutrino oscillations with IceCube,” *Phys.Rev.Lett.* **111**, 081801 (2013), [arXiv:1305.3909 \[hep-ex\]](#) [Back to page 41](#)

- 
- [101] S.T. Petcov and T. Schwetz, “Determining the neutrino mass hierarchy with atmospheric neutrinos,” *Nucl.Phys.* **B740**, 1–22 (2006), [arXiv:hep-ph/0511277 \[hep-ph\]](#) [Back to page 41](#)
- [102] Olga Mena, Irina Mocioiu, and Soebur Razzaque, “Neutrino mass hierarchy extraction using atmospheric neutrinos in ice,” *Phys.Rev.* **D78**, 093003 (2008), [arXiv:0803.3044 \[hep-ph\]](#) [Back to page 41](#)
- [103] T. Lasserre and H.W. Sobel, “Reactor neutrinos,” *Comptes Rendus Physique* **6**, 749–757 (2005), [arXiv:nucl-ex/0601013 \[nucl-ex\]](#) [Back to page 41](#)
- [104] G. Zacek *et al.* (CALTECH-SIN-TUM COLLABORATION), “Neutrino oscillation experiments at the Gosgen nuclear power reactor,” *Phys.Rev.* **D34**, 2621–2636 (1986) [Back to page 42](#)
- [105] G.S. Vidyakin, V.N. Vyrodov, Yu.V. Kozlov, A.V. Martemyanov, V.P. Martemyanov, *et al.*, “Limitations on the characteristics of neutrino oscillations,” *JETP Lett.* **59**, 390–393 (1994) [Back to page 42](#)
- [106] Y. Declais, J. Favier, A. Metref, H. Pessard, B. Achkar, *et al.*, “Search for neutrino oscillations at 15-meters, 40-meters, and 95-meters from a nuclear power reactor at Bugey,” *Nucl.Phys.* **B434**, 503–534 (1995) [Back to page 42](#)
- [107] M. Apollonio *et al.* (CHOOZ Collaboration), “Limits on neutrino oscillations from the CHOOZ experiment,” *Phys.Lett.* **B466**, 415–430 (1999), [arXiv:hep-ex/9907037 \[hep-ex\]](#) [Back to page 42](#)
- [108] A. Piepke (Palo Verde Collaboration), “Final results from the Palo Verde neutrino oscillation experiment,” *Prog.Part.Nucl.Phys.* **48**, 113–121 (2002) [Back to page 42](#)
- [109] K. Eguchi *et al.* (KamLAND Collaboration), “First results from KamLAND: Evidence for reactor anti-neutrino disappearance,” *Phys.Rev.Lett.* **90**, 021802 (2003), [arXiv:hep-ex/0212021 \[hep-ex\]](#) [Back to page 42](#)

- 
- [110] Y. Abe *et al.* (DOUBLE-CHOOZ Collaboration), “Indication for the disappearance of reactor electron antineutrinos in the Double Chooz experiment,” *Phys.Rev.Lett.* **108**, 131801 (2012), [arXiv:1112.6353 \[hep-ex\]](#) Back to page [42](#) or [210](#)
- [111] F.P. An *et al.* (DAYA-BAY Collaboration), “Observation of electron-antineutrino disappearance at Daya Bay,” *Phys.Rev.Lett.* **108**, 171803 (2012), [arXiv:1203.1669 \[hep-ex\]](#) Back to page [42](#) or [210](#)
- [112] J.K. Ahn *et al.* (RENO collaboration), “Observation of reactor electron antineutrino disappearance in the RENO experiment,” *Phys.Rev.Lett.* **108**, 191802 (2012), [arXiv:1204.0626 \[hep-ex\]](#) Back to page [42](#) or [210](#)
- [113] G.J. Feldman, J. Hartnell, and T. Kobayashi, “Long-baseline neutrino oscillation experiments,” *Adv.High Energy Phys.* **2013**, 475749 (2013), [arXiv:1210.1778 \[hep-ex\]](#) Back to page [42](#)
- [114] N. Agafonova *et al.* (OPERA Collaboration), “Search for  $\nu_\mu \rightarrow \nu_\tau$  oscillation with the OPERA experiment in the CNGS beam,” *New J.Phys.* **14**, 033017 (2012) Back to page [43](#)
- [115] N. Di Marco (OPERA Collaboration), “Recent results of the OPERA experiment,” *Nucl.Phys.Proc.Suppl.* **237-238**, 187–189 (2013) Back to page [43](#)
- [116] M.H. Ahn *et al.* (K2K Collaboration), “Measurement of neutrino oscillation by the K2K experiment,” *Phys.Rev.* **D74**, 072003 (2006), [arXiv:hep-ex/0606032 \[hep-ex\]](#) Back to page [43](#)
- [117] J.K. de Jong (MINOS Collaboration), “Near-to-final MINOS oscillation results,” *Nucl.Phys.Proc.Suppl.* **237-238**, 166–169 (2013) Back to page [43](#)
- [118] S. Yamamoto *et al.* (K2K Collaboration), “An improved search for  $\nu_\mu \rightarrow \nu_e$  oscillation in a long-baseline accelerator experiment,” *Phys.Rev.Lett.* **96**, 181801 (2006), [arXiv:hep-ex/0603004 \[hep-ex\]](#) Back to page [43](#)

- 
- [119] P. Adamson *et al.* (MINOS Collaboration), “Improved search for muon-neutrino to electron-neutrino oscillations in MINOS,” [Phys.Rev.Lett.](#) **107**, 181802 (2011), [arXiv:1108.0015 \[hep-ex\]](#) Back to page [43](#)
- [120] M.G. Catanesi (T2K Collaboration), “T2K results and perspectives,” [Nucl.Phys.Proc.Suppl.](#) **237-238**, 129–134 (2013) Back to page [43](#)
- [121] N. Agafonova *et al.* (OPERA collaboration), “Search for  $\nu_\mu \rightarrow \nu_e$  oscillations with the OPERA experiment in the CNGS beam,” [JHEP](#) **1307**, 004 (2013), [arXiv:1303.3953 \[hep-ex\]](#) Back to page [43](#)
- [122] P. Shanahan (NOVA Collaboration), “Status and prospects of the NOVA experiment,” [Nucl.Phys.Proc.Suppl.](#) **221**, 254–259 (2011) Back to page [43](#)
- [123] A. Aguilar-Arevalo *et al.* (LSND Collaboration), “Evidence for neutrino oscillations from the observation of  $\bar{\nu}_e$  appearance in a  $\bar{\nu}_\mu$  beam,” [Phys.Rev.](#) **D64**, 112007 (2001), [arXiv:hep-ex/0104049 \[hep-ex\]](#) Back to page [43](#)
- [124] B. Armbruster *et al.* (KARMEN Collaboration), “Upper limits for neutrino oscillations  $\bar{\nu}_\mu \rightarrow \bar{\nu}_e$  from muon decay at rest,” [Phys.Rev.](#) **D65**, 112001 (2002), [arXiv:hep-ex/0203021 \[hep-ex\]](#) Back to page [43](#)
- [125] A.A. Aguilar-Arevalo *et al.* (MiniBooNE Collaboration), “A search for electron neutrino appearance at the  $\Delta m^2 \sim 1 \text{ eV}^2$  scale,” [Phys.Rev.Lett.](#) **98**, 231801 (2007), [arXiv:0704.1500 \[hep-ex\]](#) Back to page [43](#)
- [126] R.G. Van de Water (MiniBooNE Collaboration), “MiniBooNE search for  $\bar{\nu}_\mu \rightarrow \bar{\nu}_e$  oscillations,” [Nucl.Phys.Proc.Suppl.](#) **229-232**, 45–49 (2012) Back to page [43](#)
- [127] Stephen F. King and Christoph Luhn, “Neutrino mass and mixing with discrete symmetry,” [Rept.Prog.Phys.](#) **76**, 056201 (2013), [arXiv:1301.1340 \[hep-ph\]](#) Back to page [44](#)

- 
- [128] D.V. Forero, M. Tortola, and J.W.F. Valle, “Global status of neutrino oscillation parameters after Neutrino-2012,” *Phys.Rev.* **D86**, 073012 (2012), [arXiv:1205.4018 \[hep-ph\]](#) Back to page [44](#), [46](#), [209](#), or [210](#)
- [129] V.N. Aseev *et al.* (Troitsk Collaboration), “An upper limit on electron antineutrino mass from Troitsk experiment,” *Phys.Rev.* **D84**, 112003 (2011), [arXiv:1108.5034 \[hep-ex\]](#) Back to page [46](#) or [47](#)
- [130] P.A.R. Ade *et al.* (Planck Collaboration), “Planck 2013 results. XVI. Cosmological parameters,” (2013), [arXiv:1303.5076 \[astro-ph.CO\]](#) Back to page [46](#) or [49](#)
- [131] M. Auger *et al.* (EXO Collaboration), “Search for neutrinoless double-beta decay in  $^{136}\text{Xe}$  with EXO-200,” *Phys.Rev.Lett.* **109**, 032505 (2012), [arXiv:1205.5608 \[hep-ex\]](#) Back to page [46](#), [58](#), or [193](#)
- [132] M. Agostini *et al.* (GERDA Collaboration), “Results on neutrinoless double beta decay of  $^{76}\text{Ge}$  from GERDA Phase I,” *Phys.Rev.Lett.* **111**, 122503 (2013), [arXiv:1307.4720 \[nucl-ex\]](#) Back to page [46](#), [58](#), or [193](#)
- [133] G. Drexlin, V. Hannen, S. Mertens, and C. Weinheimer, “Current direct neutrino mass experiments,” *Adv.High Energy Phys.* **2013**, 293986 (2013), [arXiv:1307.0101 \[physics.ins-det\]](#) Back to page [45](#) or [47](#)
- [134] Julien Lesgourgues and Sergio Pastor, “Neutrino mass from cosmology,” *Adv.High Energy Phys.* **2012**, 608515 (2012), [arXiv:1212.6154 \[hep-ph\]](#) Back to page [48](#)
- [135] J. Lesgourgues, G. Mangano, G. Miele, and S. Pastor, *Neutrino Cosmology* (Cambridge University Press, 2013) ISBN 9781107013957 Back to page [48](#)
- [136] A.S. Barabash, “Average and recommended half-life values for two-neutrino double beta decay: Upgrade’05,” *Czech.J.Phys.* **56**, 437–445 (2006), [arXiv:nucl-ex/0602009 \[nucl-ex\]](#) Back to page [50](#)

- 
- [137] N. Ackerman *et al.* (EXO-200 Collaboration), “Observation of two-neutrino double-beta decay in  $^{136}\text{Xe}$  with EXO-200,” *Phys.Rev.Lett.* **107**, 212501 (2011), [arXiv:1108.4193 \[nucl-ex\]](#)  
Back to page [50](#)
- [138] W.H. Furry, “On transition probabilities in double beta disintegration,” *Phys.Rev.* **56**, 1184–1193 (1939) Back to page [50](#)
- [139] Frank T. Avignone, Steven R. Elliott, and Jonathan Engel, “Double beta decay, Majorana neutrinos, and neutrino mass,” *Rev.Mod.Phys.* **80**, 481–516 (2008), [arXiv:0708.1033 \[nucl-ex\]](#)  
Back to page [50](#) or [54](#)
- [140] J.J. Gomez-Cadenas, J. Martin-Albo, M. Mezzetto, F. Monrabal, and M. Sorel, “The Search for neutrinoless double beta decay,” *Riv.Nuovo Cim.* **35**, 29–98 (2012), [arXiv:1109.5515 \[hep-ex\]](#) Back to page [50](#), [54](#), [58](#), or [127](#)
- [141] S.M. Bilenky and Carlo Giunti, “Neutrinoless double beta decay: A brief review,” *Mod.Phys.Lett.* **A27**, 1230015 (2012), [arXiv:1203.5250 \[hep-ph\]](#) Back to page [50](#) or [57](#)
- [142] Frank F. Deppisch, Martin Hirsch, and Heinrich Päs, “Neutrinoless Double Beta Decay and Physics Beyond the Standard Model,” *J.Phys.* **G39**, 124007 (2012), [arXiv:1208.0727 \[hep-ph\]](#)  
Back to page [50](#)
- [143] J. Schechter and J.W.F. Valle, “Neutrinoless double beta decay in  $SU(2) \otimes U(1)$  theories,” *Phys.Rev.* **D25**, 2951 (1982) Back to page [53](#), [128](#), or [238](#)
- [144] H. Päs, M. Hirsch, H.V. Klapdor-Kleingrothaus, and S.G. Kovalenko, “Towards a superformula for neutrinoless double beta decay,” *Phys.Lett.* **B453**, 194–198 (1999) Back to page [54](#) or [143](#)
- [145] H. Päs, M. Hirsch, H.V. Klapdor-Kleingrothaus, and S.G. Kovalenko, “A superformula for neutrinoless double beta decay. 2. The short-range part,” *Phys.Lett.* **B498**, 35–39 (2001), [arXiv:hep-ph/0008182 \[hep-ph\]](#) Back to page [54](#), [144](#), [145](#), [192](#), or [193](#)

- 
- [146] H.V. Klapdor-Kleingrothaus, A. Dietz, L. Baudis, G. Heusser, I.V. Krivosheina, *et al.*, “Latest results from the Heidelberg-Moscow double beta decay experiment,” *Eur.Phys.J.* **A12**, 147–154 (2001), [arXiv:hep-ph/0103062 \[hep-ph\]](#) Back to page [58](#) or [193](#)
- [147] H.V. Klapdor-Kleingrothaus, A. Dietz, H.L. Harney, and I.V. Krivosheina, “Evidence for neutrinoless double beta decay,” *Mod.Phys.Lett.* **A16**, 2409–2420 (2001), [arXiv:hep-ph/0201231 \[hep-ph\]](#) Back to page [58](#)
- [148] H.V. Klapdor-Kleingrothaus and I.V. Krivosheina, “The evidence for the observation of  $0\nu\beta\beta$  decay: the identification of  $0\nu\beta\beta$  events from the full spectra,” *Mod.Phys.Lett.* **A21**, 1547–1566 (2006) Back to page [58](#)
- [149] Murray Gell-Mann, Pierre Ramond, and Richard Slansky, “Complex spinors and unified theories,” *Conf.Proc.* **C790927**, 315–321 (1979), published in *Supergravity*, P. van Nieuwenhuizen and D.Z. Freedman (eds.), North Holland Publ. Co., 1979, [arXiv:1306.4669 \[hep-th\]](#), [http://tuvalu.santafe.edu/~mgm/Site/Publications\\_files/MGM%2086.pdf](http://tuvalu.santafe.edu/~mgm/Site/Publications_files/MGM%2086.pdf) Back to page [59](#)
- [150] Pierre Ramond, “The family group in grand unified theories,” , 265–280(1979), retro-Preprint (1979 unpublished Caltech preprint no: CALT-68-709). Invited talk at the Sanibel Symposia, Feb 1979, [arXiv:hep-ph/9809459 \[hep-ph\]](#) Back to page [59](#)
- [151] Peter Minkowski, “ $\mu \rightarrow e\gamma$  at a rate of one out of 1-billion muon decays?,” *Phys.Lett.* **B67**, 421 (1977) Back to page [59](#)
- [152] Tsutomu Yanagida, “Horizontal symmetry and masses of neutrinos,” *Prog. Theor. Phys.* **64**, 1103–1105 (1980) Back to page [59](#)
- [153] Rabindra N. Mohapatra and Goran Senjanovic, “Neutrino mass and spontaneous parity violation,” *Phys.Rev.Lett.* **44**, 912 (1980) Back to page [59](#)



- 
- [154] D. Wyler and L. Wolfenstein, “Massless neutrinos in left-right-symmetric models,” *Nucl.Phys.* **B218**, 205 (1983) [Back to page 59](#)
- [155] R.N. Mohapatra, “Mechanism for understanding small neutrino mass in superstring theories,” *Phys.Rev.Lett.* **56**, 561–563 (1986) [Back to page 59](#)
- [156] R.N. Mohapatra and J.W.F. Valle, “Neutrino mass and baryon number nonconservation in superstring models,” *Phys.Rev.* **D34**, 1642 (1986) [Back to page 59](#)
- [157] W. Konetschny and W. Kummer, “Nonconservation of total lepton number with scalar bosons,” *Phys.Lett.* **B70**, 433 (1977) [Back to page 60](#)
- [158] George Lazarides, Q. Shafi, and C. Wetterich, “Proton lifetime and fermion masses in an  $so(10)$  model,” *Nucl.Phys.* **B181**, 287 (1981) [Back to page 60](#)
- [159] M. Magg and C. Wetterich, “Neutrino mass problem and gauge hierarchy,” *Phys.Lett.* **B94**, 61 (1980) [Back to page 60](#)
- [160] R. Foot, H. Lew, X.G. He, and G. C. Joshi, “Seesaw neutrino masses induced by a triplet of leptons,” *Z.Phys.* **C44**, 441 (1989) [Back to page 63](#)
- [161] Ernest Ma and D.P. Roy, “Heavy triplet leptons and new gauge boson,” *Nucl.Phys.* **B644**, 290–302 (2002), [arXiv:hep-ph/0206150 \[hep-ph\]](#) [Back to page 63](#)
- [162] Graham G. Ross, *Grand unified theories*, Frontiers in Physics (Westview Press, 2003) ISBN 978-0805369687 [Back to page 65](#)
- [163] M. Fukugita and T. Yanagida, *Physics of neutrinos and applications to astrophysics* (Springer, 2003) ISBN 978-3540438007 [Back to page 66](#)

- 
- [164] Boris Kayser, F. Gibrat-Debu, and F. Perrier, *The Physics of massive neutrinos*, Lecture Notes in Physics, Vol. 25 (World Scientific, 1989) ISBN 978-9971506612 [Back to page 66](#)
- [165] Sacha Davidson, Martin Gorbahn, and Arcadi Santamaria, “From transition magnetic moments to Majorana neutrino masses,” *Phys.Lett.* **B626**, 151–160 (2005), [arXiv:hep-ph/0506085 \[hep-ph\]](#) [Back to page 66](#)
- [166] Nicole F. Bell, Vincenzo Cirigliano, Michael J. Ramsey-Musolf, Petr Vogel, and Mark B. Wise, “How magnetic is the Dirac neutrino?,” *Phys.Rev.Lett.* **95**, 151802 (2005), [arXiv:hep-ph/0504134 \[hep-ph\]](#) [Back to page 66](#)
- [167] Georg G. Raffelt, “Particle physics from stars,” *Ann.Rev.Nucl.Part.Sci.* **49**, 163–216 (1999), [arXiv:hep-ph/9903472 \[hep-ph\]](#) [Back to page 67](#)
- [168] G.G. Raffelt, “New bound on neutrino dipole moments from globular cluster stars,” *Phys.Rev.Lett.* **64**, 2856–2858 (1990) [Back to page 67](#), [68](#), or [93](#)
- [169] Steven Weinberg, “Effective gauge theories,” *Phys.Lett.* **B91**, 51 (1980) [Back to page 69](#)
- [170] M.J.G. Veltman, “The infrared-ultraviolet connection,” *Acta Phys.Polon.* **B12**, 437 (1981) [Back to page 70](#)
- [171] Andre de Gouvea, James Jenkins, and Nirmala Vasudevan, “Neutrino phenomenology of very-low-energy seesaws,” *Phys.Rev.* **D75**, 013003 (2007), [arXiv:hep-ph/0608147 \[hep-ph\]](#) [Back to page 70](#)
- [172] A. Ibarra, E. Molinaro, and S.T. Petcov, “TeV-scale seesaw mechanisms of neutrino mass generation, the Majorana nature of the heavy singlet neutrinos and  $(\beta\beta)_{0\nu}$  decay,” *JHEP* **1009**, 108 (2010), [arXiv:1007.2378 \[hep-ph\]](#) [Back to page 70](#)

- 
- [173] Aneesh Manohar and Howard Georgi, “Chiral quarks and the nonrelativistic quark model,” *Nucl.Phys.* **B234**, 189 (1984) Back to page [74](#)
- [174] Howard Georgi, “Generalized dimensional analysis,” *Phys.Lett.* **B298**, 187–189 (1993), [arXiv:hep-ph/9207278 \[hep-ph\]](#) Back to page [74](#)
- [175] Benjamin W. Lee, C. Quigg, and H.B. Thacker, “Weak interactions at very high-energies: The role of the Higgs boson mass,” *Phys.Rev.* **D16**, 1519 (1977) Back to page [83](#), [106](#), or [196](#)
- [176] John M. Cornwall, David N. Levin, and George Tiktopoulos, “Derivation of gauge invariance from high-energy unitarity bounds on the S matrix,” *Phys.Rev.* **D10**, 1145 (1974) Back to page [83](#) or [106](#)
- [177] Mark Terwort (ATLAS Collaboration, CMS Collaboration), “Searches for GMSB at the LHC,” *Proceedings of DIS 2008*, 110–113(2008), [arXiv:0805.2524 \[hep-ex\]](#) Back to page [83](#)
- [178] Piotr Zalewski, “Search for GMSB NLSPs at LHC,” *Proceedings of SUSY 2007*, 314–317(2007), [arXiv:0710.2647 \[hep-ph\]](#), <http://www-ekp.physik.uni-karlsruhe.de/~susy07/Proceedings/proceedings/susy07.pdf> Back to page [83](#)
- [179] Damien Prieur, “GMSB SUSY models with non pointing photons signatures in ATLAS at the LHC,” (2005), [arXiv:hep-ph/0507083 \[hep-ph\]](#) Back to page [83](#)
- [180] P. Abreu *et al.* (DELPHI Collaboration), “Search for neutral heavy leptons produced in  $Z$  decays,” *Z.Phys.* **C74**, 57–71 (1997) Back to page [85](#) or [86](#)
- [181] O. Adriani *et al.* (L3 Collaboration), “Search for isosinglet neutral heavy leptons in  $Z^0$  decays,” *Phys.Lett.* **B295**, 371–382 (1992) Back to page [85](#) or [86](#)

- 
- [182] M.Z. Akrawy *et al.* (OPAL Collaboration), “Limits on neutral heavy lepton production from  $Z^0$  decay,” *Phys.Lett.* **B247**, 448–457 (1990) Back to page [85](#) or [86](#)
- [183] M. Dittmar, A. Santamaria, M.C. Gonzalez-Garcia, and J.W.F. Valle, “Production mechanisms and signatures of isosinglet neutral heavy leptons in  $Z^0$  decays,” *Nucl.Phys.* **B332**, 1 (1990) Back to page [85](#)
- [184] J. Abdallah *et al.* (DELPHI Collaboration), “Photon events with missing energy in  $e^+e^-$  collisions at  $\sqrt{s} = 130$  to 209 GeV,” *Eur.Phys.J.* **C38**, 395–411 (2005), [arXiv:hep-ex/0406019 \[hep-ex\]](#) Back to page [85](#), [86](#), or [87](#)
- [185] P. Achard *et al.* (L3 Collaboration), “Single photon and multi-photon events with missing energy in  $e^+e^-$  collisions at LEP,” *Phys.Lett.* **B587**, 16–32 (2004), [arXiv:hep-ex/0402002 \[hep-ex\]](#) Back to page [85](#), [86](#), or [87](#)
- [186] G. Abbiendi *et al.* (OPAL Collaboration), “Search for anomalous photonic events with missing energy in  $e^+e^-$  collisions at  $\sqrt{s} = 130$  GeV, 136 GeV and 183 GeV,” *Eur.Phys.J.* **C8**, 23–40 (1999), [arXiv:hep-ex/9810021 \[hep-ex\]](#) Back to page [85](#), [86](#), or [87](#)
- [187] Gary J. Feldman and Robert D. Cousins, “A unified approach to the classical statistical analysis of small signals,” *Phys.Rev.* **D57**, 3873–3889 (1998), [arXiv:physics/9711021 \[physics.data-an\]](#) Back to page [86](#)
- [188] P. Abreu *et al.* (DELPHI Collaboration), “Search for new phenomena using single photon events in the DELPHI detector at LEP,” *Z.Phys.* **C74**, 577–586 (1997) Back to page [86](#)
- [189] John M. Campbell, J.W. Huston, and W.J. Stirling, “Hard interactions of quarks and gluons: A primer for LHC physics,” *Rept.Prog.Phys.* **70**, 89 (2007), [arXiv:hep-ph/0611148 \[hep-ph\]](#) Back to page [89](#) or [125](#)

- 
- [190] J. Pumplin, D.R. Stump, J. Huston, H.L. Lai, Pavel M. Nadolsky, *et al.*, “New generation of parton distributions with uncertainties from global QCD analysis,” *JHEP* **0207**, 012 (2002), [arXiv:hep-ph/0201195 \[hep-ph\]](#) Back to page [89](#) or [125](#)
- [191] A. Pukhov, E. Boos, M. Dubinin, V. Edneral, V. Ilyin, *et al.*, “CompHEP: a package for evaluation of Feynman diagrams and integration over multiparticle phase space,” (1999), [arXiv:hep-ph/9908288 \[hep-ph\]](#) Back to page [89](#) or [125](#)
- [192] E. Boos *et al.* (CompHEP Collaboration), “CompHEP 4.4: Automatic computations from Lagrangians to events,” *Nucl.Instrum.Meth.* **A534**, 250–259 (2004), [arXiv:hep-ph/0403113 \[hep-ph\]](#) Back to page [89](#) or [125](#)
- [193] Diptimoy Ghosh, Rohini Godbole, Monoranjan Guchait, Kir-timaan Mohan, and Dipan Sengupta, “Looking for an invisible Higgs signal at the LHC,” *Phys. Lett. B* **725**, 344 (2013), [arXiv:1211.7015 \[hep-ph\]](#) Back to page [92](#)
- [194] G. Belanger, B. Dumont, U. Ellwanger, J.F. Gunion, and S. Kraml, “Status of invisible Higgs decays,” *Phys.Lett.* **B723**, 340–347 (2013), [arXiv:1302.5694 \[hep-ph\]](#) Back to page [92](#)
- [195] Serguei Chatrchyan *et al.* (CMS Collaboration), “Search for the standard model Higgs boson produced in association with a W or a Z boson and decaying to bottom quarks,” (2013), [arXiv:1310.3687 \[hep-ex\]](#) Back to page [92](#) or [99](#)
- [196] Georges Aad *et al.* (ATLAS Collaboration), “Measurements of Higgs boson production and couplings in diboson final states with the ATLAS detector at the LHC,” *Phys.Lett.* **B726**, 88–119 (2013), [arXiv:1307.1427 \[hep-ex\]](#) Back to page [92](#) or [99](#)
- [197] V. Castellani and S. Degl’Innocenti, “Stellar evolution as a probe of neutrino properties,” *Astrophys.J.* **402**, 574–578 (1993) Back to page [93](#)

- 
- [198] M. Catelan, J. A. de Freitas Pacheco, and J. E. Horvath, “The helium-core mass at the helium flash in low-mass red giant stars: Observations and theory,” *Astrophys. J.* **461**, 231 (1996), [arXiv:astro-ph/9509062](#) Back to page 93
- [199] Martin Haft, Georg Raffelt, and Achim Weiss, “Standard and nonstandard plasma neutrino emission revisited,” *Astrophys. J.* **425**, 222–230 (1994), [arXiv:astro-ph/9309014 \[astro-ph\]](#) Back to page 93
- [200] Georg G. Raffelt, “Core mass at the helium flash from observations and a new bound on neutrino electromagnetic properties,” *Astrophys. J.* **365**, 559 (1990) Back to page 93
- [201] Georg Raffelt and Achim Weiss, “Nonstandard neutrino interactions and the evolution of red giants,” *Astron. Astrophys.* **264**, 536–546 (1992), <http://adsabs.harvard.edu/abs/1992A&A...264..536R> Back to page 93
- [202] Alexander Heger, Alexander Friedland, Maurizio Giannotti, and Vincenzo Cirigliano, “The impact of neutrino magnetic moments on the evolution of massive stars,” *Astrophys. J.* **696**, 608–619 (2009), [arXiv:0809.4703 \[astro-ph\]](#) Back to page 93
- [203] Naoki Iwamoto, Letao Qin, Masataka Fukugita, and Sachiko Tsuruta, “Neutrino magnetic moment and neutron star cooling,” *Phys. Rev.* **D51**, 348–352 (1995) Back to page 94
- [204] G.G. Raffelt, “Limits on neutrino electromagnetic properties: an update,” *Phys. Rept.* **320**, 319–327 (1999) Back to page 94
- [205] G. Steigman, “Observational tests of antimatter cosmologies,” *Ann. Rev. Astron. Astrophys.* **14**, 339–372 (1976) Back to page 95
- [206] Andrew G. Cohen, A. De Rujula, and S.L. Glashow, “A matter-antimatter universe?,” *Astrophys. J.* **495**, 539–549 (1998), [arXiv:astro-ph/9707087 \[astro-ph\]](#) Back to page 95

- 
- [207] A.D. Sakharov, “Violation of CP invariance, C asymmetry and baryon asymmetry of the universe,” *Pisma Zh.Eksp.Teor.Fiz.* **5**, 32–35 (1967) [Back to page 95](#)
- [208] M.B. Gavela, P. Hernandez, J. Orloff, and O. Pene, “Standard model CP violation and baryon asymmetry,” *Mod.Phys.Lett.* **A9**, 795–810 (1994), [arXiv:hep-ph/9312215 \[hep-ph\]](#) [Back to page 95](#)
- [209] M.B. Gavela, P. Hernandez, J. Orloff, O. Pene, and C. Quimbay, “Standard model CP violation and baryon asymmetry. Part 2: Finite temperature,” *Nucl.Phys.* **B430**, 382–426 (1994), [arXiv:hep-ph/9406289 \[hep-ph\]](#) [Back to page 95](#)
- [210] Patrick Huet and Eric Sather, “Electroweak baryogenesis and standard model CP violation,” *Phys.Rev.* **D51**, 379–394 (1995), [arXiv:hep-ph/9404302 \[hep-ph\]](#) [Back to page 95](#)
- [211] M. Fukugita and T. Yanagida, “Baryogenesis without grand unification,” *Phys.Lett.* **B174**, 45 (1986) [Back to page 95](#)
- [212] Marion Flanz, Emmanuel A. Paschos, Utpal Sarkar, and Jan Weiss, “Baryogenesis through mixing of heavy Majorana neutrinos,” *Phys.Lett.* **B389**, 693–699 (1996), [arXiv:hep-ph/9607310 \[hep-ph\]](#) [Back to page 95](#)
- [213] A.D. Dolgov, “NonGUT baryogenesis,” *Phys.Rept.* **222**, 309–386 (1992) [Back to page 96](#)
- [214] Sacha Davidson, Enrico Nardi, and Yosef Nir, “Leptogenesis,” *Phys.Rept.* **466**, 105–177 (2008), [arXiv:0802.2962 \[hep-ph\]](#) [Back to page 96](#)
- [215] V.A. Rubakov and M.E. Shaposhnikov, “Electroweak baryon number nonconservation in the early universe and in high-energy collisions,” *Usp.Fiz.Nauk* **166**, 493–537 (1996), [arXiv:hep-ph/9603208 \[hep-ph\]](#) [Back to page 96](#) or [219](#)

- 
- [216] Apostolos Pilaftsis, “CP violation and baryogenesis due to heavy Majorana neutrinos,” *Phys.Rev.* **D56**, 5431–5451 (1997), [arXiv:hep-ph/9707235 \[hep-ph\]](#) [Back to page 96](#)
- [217] Apostolos Pilaftsis and Thomas E.J. Underwood, “Resonant leptogenesis,” *Nucl.Phys.* **B692**, 303–345 (2004), [arXiv:hep-ph/0309342 \[hep-ph\]](#) [Back to page 96](#)
- [218] A. De Rujula, S.L. Glashow, and U. Sarid, “Charged dark matter,” *Nucl.Phys.* **B333**, 173 (1990) [Back to page 118](#)
- [219] Savas Dimopoulos, David Eichler, Rahim Esmailzadeh, and Glenn D. Starkman, “Getting a charge out of dark matter,” *Phys.Rev.* **D41**, 2388 (1990) [Back to page 118](#)
- [220] J.L. Basdevant, R. Mochkovitch, J. Rich, M. Spiro, and A. Vidal-Madjar, “Is there room for charged dark matter?,” *Phys.Lett.* **B234**, 395 (1990) [Back to page 118](#)
- [221] T.K. Hemmick, D. Elmore, T. Gentile, P.W. Kubik, S.L. Olsen, *et al.*, “A search for anomalously heavy isotopes of low-Z nuclei,” *Phys.Rev.* **D41**, 2074–2080 (1990) [Back to page 118](#)
- [222] T. Yamagata, Y. Takamori, and H. Utsunomiya, “Search for anomalously heavy hydrogen in deep sea water at 4000 m,” *Phys.Rev.* **D47**, 1231–1234 (1993) [Back to page 118](#)
- [223] Andrew Gould, Bruce T. Draine, Roger W. Romani, and Shmuel Nussinov, “Neutron stars: Graveyard of charged dark matter,” *Phys.Lett.* **B238**, 337 (1990) [Back to page 118](#)
- [224] R. Sekhar Chivukula, Andrew G. Cohen, Savas Dimopoulos, and Terry P. Walker, “Bounds on halo particle interactions from interstellar calorimetry,” *Phys.Rev.Lett.* **65**, 957–959 (1990) [Back to page 118](#)
- [225] Stephen Wolfram, “Abundances of stable particles produced in the early universe,” *Phys.Lett.* **B82**, 65 (1979) [Back to page 118](#)



- 
- [226] Leonid Chuzhoy and Edward W. Kolb, “Reopening the window on charged dark matter,” *JCAP* **0907**, 014 (2009), [arXiv:0809.0436 \[astro-ph\]](#) Back to page [118](#)
- [227] Karsten Jedamzik, “Bounds on long-lived charged massive particles from Big Bang nucleosynthesis,” *JCAP* **0803**, 008 (2008), [arXiv:0710.5153 \[hep-ph\]](#) Back to page [119](#) or [122](#)
- [228] Karsten Jedamzik, “The cosmic  ${}^6\text{Li}$  and  ${}^7\text{Li}$  problems and BBN with long-lived charged massive particles,” *Phys.Rev.* **D77**, 063524 (2008), [arXiv:0707.2070 \[astro-ph\]](#) Back to page [119](#) or [122](#)
- [229] Mikhail S. Bilenky and Arcadi Santamaria, “One loop effective Lagrangian for a Standard Model with a heavy charged scalar singlet,” *Nucl.Phys.* **B420**, 47–93 (1994), [arXiv:hep-ph/9310302 \[hep-ph\]](#) Back to page [122](#)
- [230] J. Adam *et al.* (MEG Collaboration), “New constraint on the existence of the  $\mu \rightarrow e\gamma$  decay,” (2013), [arXiv:1303.0754 \[hep-ex\]](#) Back to page [123](#)
- [231] Hajime Nishiguchi (MEG Collaboration), “MEG experiment: new result and prospects,” *AIP Conf.Proc.* **1382**, 239–241 (2011) Back to page [123](#)
- [232] C. Dohmen *et al.* (SINDRUM II Collaboration.), “Test of lepton flavor conservation in  $\mu - e$  conversion on titanium,” *Phys.Lett.* **B317**, 631–636 (1993) Back to page [124](#)
- [233] Yoshitaka Kuno (COMET Collaboration), “A search for muon-to-electron conversion at J-PARC: The COMET experiment,” *PTEP* **2013**, 022C01 (2013) Back to page [124](#)
- [234] J. Pasternak (PRISM Task Force), “Recent studies on the PRISM FFAG ring,” *J.Phys.Conf.Ser.* **408**, 012080 (2013) Back to page [124](#)
- [235] M. Fairbairn, A.C. Kraan, D.A. Milstead, T. Sjostrand, Peter Z. Skands, *et al.*, “Stable massive particles at colliders,” *Phys.Rept.* **438**, 1–63 (2007), [arXiv:hep-ph/0611040 \[hep-ph\]](#) Back to page [125](#)

- 
- [236] Jie Chen and Todd Adams, “Searching for high speed long-lived charged massive particles at the LHC,” *Eur.Phys.J.* **C67**, 335–342 (2010), [arXiv:0909.3157 \[hep-ph\]](#) Back to page [125](#)
- [237] Roberto Franceschini, Thomas Hambye, and Alessandro Strumia, “Type III seesaw at LHC,” *Phys.Rev.* **D78**, 033002 (2008), [arXiv:0805.1613 \[hep-ph\]](#) Back to page [125](#)
- [238] F. de Campos, O.J.P. Eboli, M.B. Magro, and D. Restrepo, “Searching supersymmetry at the LHCb with displaced vertices,” *Phys.Rev.* **D79**, 055008 (2009), [arXiv:0809.0007 \[hep-ph\]](#) Back to page [125](#)
- [239] K.S. Babu and Chung Ngoc Leung, “Classification of effective neutrino mass operators,” *Nucl.Phys.* **B619**, 667–689 (2001), [arXiv:hep-ph/0106054 \[hep-ph\]](#) Back to page [128](#)
- [240] Ki-woon Choi, Kwang Sik Jeong, and Wan Young Song, “Operator analysis of neutrinoless double beta decay,” *Phys.Rev.* **D66**, 093007 (2002), [arXiv:hep-ph/0207180 \[hep-ph\]](#) Back to page [128](#)
- [241] J. Engel and P. Vogel, “Effective operators for double beta decay,” *Phys.Rev.* **C69**, 034304 (2004), [arXiv:nucl-th/0311072 \[nucl-th\]](#) Back to page [128](#)
- [242] Andre de Gouvea and James Jenkins, “A survey of lepton number violation via effective operators,” *Phys. Rev.* **D77**, 013008 (2008), [arXiv:0708.1344 \[hep-ph\]](#) Back to page [128](#)
- [243] A.S. Barabash, “Double beta decay experiments,” *Phys.Part.Nucl.* **42**, 613–627 (2011), [arXiv:1107.5663 \[nucl-ex\]](#) Back to page [141](#) or [193](#)
- [244] K. Muto, E. Bender, and H.V. Klapdor, “Nuclear structure effects on the neutrinoless double beta decay,” *Z.Phys.* **A334**, 187–194 (1989) Back to page [143](#)
- [245] T.D. Lee, “A theory of spontaneous T violation,” *Phys.Rev.* **D8**, 1226–1239 (1973) Back to page [159](#)

- 
- [246] G.C. Branco, P.M. Ferreira, L. Lavoura, M.N. Rebelo, Marc Sher, *et al.*, “Theory and phenomenology of two-Higgs-doublet models,” *Phys.Rept.* **516**, 1–102 (2012), [arXiv:1106.0034 \[hep-ph\]](#) Back to page [159](#)
- [247] Monika Blanke, Andrzej J. Buras, Bjoern Duling, Anton Poschenrieder, and Cecilia Tarantino, “Charged lepton flavour violation and  $(g - 2)_\mu$  in the littlest Higgs model with T-parity: A clear distinction from supersymmetry,” *JHEP* **0705**, 013 (2007), [arXiv:hep-ph/0702136 \[hep-ph\]](#) Back to page [169](#)
- [248] F. del Aguila, J.I. Illana, and M.D. Jenkins, “Precise limits from lepton-flavour-violating processes on the Littlest Higgs model with T-parity,” *JHEP* **0901**, 080 (2009), [arXiv:0811.2891 \[hep-ph\]](#) Back to page [169](#)
- [249] Toru Goto, Yasuhiro Okada, and Yasuhiro Yamamoto, “Tau and muon lepton flavor violations in the littlest Higgs model with T-parity,” *Phys.Rev.* **D83**, 053011 (2011), [arXiv:1012.4385 \[hep-ph\]](#) Back to page [169](#)
- [250] F. del Aguila, J.I. Illana, and M.D. Jenkins, “Muon to electron conversion in the Littlest Higgs model with T-parity,” *JHEP* **1009**, 040 (2010), [arXiv:1006.5914 \[hep-ph\]](#) Back to page [169](#)
- [251] S.L. Glashow, J. Iliopoulos, and L. Maiani, “Weak interactions with lepton-hadron symmetry,” *Phys.Rev.* **D2**, 1285–1292 (1970) Back to page [173](#)
- [252] F. del Aguila, L. Ametller, Gordon L. Kane, and J. Vidal, “Vector-like fermion and standard Higgs production at hadron colliders,” *Nucl.Phys.* **B334**, 1 (1990) Back to page [173](#)
- [253] J.A. Aguilar-Saavedra, “Heavy lepton pair-production at LHC: model discrimination with multi-lepton signals,” *Nucl.Phys.* **B828**, 289–316 (2010), [arXiv:0905.2221 \[hep-ph\]](#) Back to page [173](#)
- [254] Francisco del Aguila, Adrian Carmona, and Jose Santiago, “Tau custodian searches at the LHC,” *Phys.Lett.* **B695**, 449–453 (2011), [arXiv:1007.4206 \[hep-ph\]](#) Back to page [173](#)

- 
- [255] F. del Aguila, J.A. Aguilar-Saavedra, J. de Blas, and M. Perez-Victoria, “Electroweak constraints on seesaw messengers and their implications for LHC,” Proceedings of the 43rd Rencontres de Moriond **I - Standard Model**, 45–52 (2008), [arXiv:0806.1023 \[hep-ph\]](#), <https://indico.in2p3.fr/internalPage.py?pageId=10&confId=420> Back to page [183](#)
- [256] M.B. Einhorn, D.R.T. Jones, and M.J.G. Veltman, “Heavy Particles and the rho Parameter in the Standard Model,” *Nucl.Phys.* **B191**, 146 (1981) Back to page [183](#)
- [257] Mitchell Golden, “An upper limit on the masses of the charged Higgs bosons in the Gelmini-Roncadelli model,” *Phys.Lett.* **B169**, 248 (1986) Back to page [183](#)
- [258] Shinya Kanemura and Kei Yagyu, “Radiative corrections to electroweak parameters in the Higgs triplet model and implication with the recent Higgs boson searches,” *Phys.Rev.* **D85**, 115009 (2012), [arXiv:1201.6287 \[hep-ph\]](#) Back to page [183](#)
- [259] Miguel Nebot, Josep F. Oliver, David Palao, and Arcadi Santamaria, “Prospects for the Zee-Babu model at the CERN LHC and low energy experiments,” *Phys.Rev.* **D77**, 093013 (2008), [arXiv:0711.0483 \[hep-ph\]](#) Back to page [194](#)
- [260] Martti Raidal and Arcadi Santamaria, “Muon-electron conversion in nuclei versus  $\mu \rightarrow e\gamma$ : An effective field theory point of view,” *Phys.Lett.* **B421**, 250–258 (1998), [arXiv:hep-ph/9710389 \[hep-ph\]](#) Back to page [194](#)
- [261] Steven Weinberg, *The quantum theory of fields, Vol. 1: Foundations* (Cambridge University Press, 2005) ISBN 978-0521670531 Back to page [196](#)
- [262] Benjamin W. Lee, C. Quigg, and H.B. Thacker, “The strength of weak interactions at very high-energies and the Higgs boson mass,” *Phys.Rev.Lett.* **38**, 883–885 (1977) Back to page [196](#)

- 
- [263] Michael S. Chanowitz, M.A. Furman, and I. Hinchliffe, “Weak interactions of ultraheavy fermions. 2..” *Nucl.Phys.* **B153**, 402 (1979) [Back to page 196](#)
- [264] Thomas Schwetz, Mariam Tortola, and J.W.F. Valle, “Where we are on  $\theta_{13}$ : addendum to ‘Global neutrino data and recent reactor fluxes: status of three-flavour oscillation parameters’,” *New J.Phys.* **13**, 109401 (2011), [arXiv:1108.1376 \[hep-ph\]](#) [Back to page 208](#) or [209](#)
- [265] J.F. Gunion, J. Grifols, A. Mendez, Boris Kayser, and Fredrick I. Olness, “Higgs bosons in left-right symmetric models,” *Phys.Rev.* **D40**, 1546 (1989) [Back to page 217](#)
- [266] K. Huitu, J. Maalampi, A. Pietila, and M. Raidal, “Doubly charged Higgs at LHC,” *Nucl.Phys.* **B487**, 27–42 (1997), [arXiv:hep-ph/9606311 \[hep-ph\]](#) [Back to page 217](#) or [218](#)
- [267] J.F. Gunion, C. Loomis, and K.T. Pitts, “Searching for doubly charged Higgs bosons at future colliders,” eConf **C960625**, LTH096 (1996), [arXiv:hep-ph/9610237 \[hep-ph\]](#) [Back to page 217](#)
- [268] A.G. Akeroyd and Mayumi Aoki, “Single- and pair-production of doubly-charged Higgs bosons at hadron colliders,” *Phys.Rev.* **D72**, 035011 (2005), [arXiv:hep-ph/0506176 \[hep-ph\]](#) [Back to page 217](#)
- [269] G. Azuelos, K. Benslama, and J. Ferland, “Prospects for the search for a doubly-charged Higgs in the left-right symmetric model with ATLAS,” *J.Phys.* **G32**, 73–92 (2006), [arXiv:hep-ph/0503096 \[hep-ph\]](#) [Back to page 217](#)
- [270] F. del Aguila and J.A. Aguilar-Saavedra, “Distinguishing seesaw models at LHC with multi-lepton signals,” *Nucl.Phys.* **B813**, 22–90 (2009), [arXiv:0808.2468 \[hep-ph\]](#) [Back to page 217](#)
- [271] A.G. Akeroyd, Cheng-Wei Chiang, and Naveen Gaur, “Leptonic signatures of doubly charged Higgs boson production at the

- LHC,” *JHEP* **1011**, 005 (2010), [arXiv:1009.2780 \[hep-ph\]](#) Back to page [217](#)
- [272] B. Dion, T. Gregoire, David London, L. Marleau, and H. Nadeau, “Bilepton production at hadron colliders,” *Phys.Rev.* **D59**, 075006 (1999), [arXiv:hep-ph/9810534 \[hep-ph\]](#) Back to page [217](#)
- [273] Frank Cuypers and Sacha Davidson, “Bileptons: Present limits and future prospects,” *Eur.Phys.J.* **C2**, 503–528 (1998), [arXiv:hep-ph/9609487 \[hep-ph\]](#) Back to page [217](#)
- [274] F. del Aguila, J.A. Aguilar-Saavedra, and J. de Blas, “Trilepton signals: the golden channel for seesaw searches at LHC,” *Acta Phys.Polon.* **B40**, 2901–2911 (2009), [arXiv:0910.2720 \[hep-ph\]](#) Back to page [217](#)
- [275] Francisco del Aguila, Juan Antonio Aguilar-Saavedra, and Jorge de Blas, “New neutrino interactions at large colliders,” *PoS ICHEP2010*, 296 (2010), [arXiv:1012.1327 \[hep-ph\]](#) Back to page [217](#)
- [276] Pran Nath, Brent D. Nelson, Hooman Davoudiasl, Bhaskar Dutta, Daniel Feldman, *et al.*, “The hunt for new physics at the large hadron collider,” *Nucl.Phys.Proc.Suppl.* **200-202**, 185–417 (2010), [arXiv:1001.2693 \[hep-ph\]](#) Back to page [217](#)
- [277] CMS collaboration, “Inclusive search for doubly charged higgs in leptonic final states at  $\sqrt{s} = 7$  TeV,” CMS-PAS-HIG-11-007 (2011), <http://cdsweb.cern.ch/record/1369542> Back to page [217](#)
- [278] J. Abdallah *et al.* (DELPHI Collaboration), “Search for doubly charged Higgs bosons at LEP-2,” *Phys.Lett.* **B552**, 127–137 (2003), [arXiv:hep-ex/0303026 \[hep-ex\]](#) Back to page [217](#)
- [279] G. Abbiendi *et al.* (OPAL Collaboration), “Search for doubly-charged Higgs bosons with the OPAL detector at LEP,” *Phys.Lett.* **B526**, 221–232 (2002), [arXiv:hep-ex/0111059 \[hep-ex\]](#) Back to page [217](#)

- 
- [280] P. Achard *et al.* (L3 Collaboration), “Search for doubly-charged Higgs bosons at LEP,” *Phys.Lett.* **B576**, 18–28 (2003), [arXiv:hep-ex/0309076 \[hep-ex\]](#) Back to page [217](#)
- [281] G. Abbiendi *et al.* (OPAL Collaboration), “Search for the single production of doubly-charged Higgs bosons and constraints on their couplings from Bhabha scattering,” *Phys.Lett.* **B577**, 93–108 (2003), [arXiv:hep-ex/0308052 \[hep-ex\]](#) Back to page [217](#)
- [282] V.M. Abazov *et al.* (D0 Collaboration), “Search for doubly-charged Higgs boson pair-production in the decay to  $\mu^+\mu^+\mu^-\mu^-$  in  $p\bar{p}$  collisions at  $\sqrt{s} = 1.96$  TeV,” *Phys.Rev.Lett.* **93**, 141801 (2004), [arXiv:hep-ex/0404015 \[hep-ex\]](#) Back to page [217](#)
- [283] D. Acosta *et al.* (CDF Collaboration), “Search for doubly-charged Higgs bosons decaying to dileptons in  $p\bar{p}$  collisions at  $\sqrt{s} = 1.96$  TeV,” *Phys.Rev.Lett.* **93**, 221802 (2004), [arXiv:hep-ex/0406073 \[hep-ex\]](#) Back to page [217](#)
- [284] D. Acosta *et al.* (CDF Collaboration), “Search for long-lived doubly-charged Higgs bosons in  $p\bar{p}$  collisions at  $\sqrt{s} = 1.96$  TeV,” *Phys.Rev.Lett.* **95**, 071801 (2005), [arXiv:hep-ex/0503004 \[hep-ex\]](#) Back to page [217](#)
- [285] Alejandra Melfo, Miha Nemevsek, Fabrizio Nesti, Goran Senjanovic, and Yue Zhang, “Type II seesaw at LHC: the roadmap,” *Phys.Rev.* **D85**, 055018 (2012), [arXiv:1108.4416 \[hep-ph\]](#) Back to page [218](#)
- [286] Ya.B. Zeldovich, I. Yu. Kobzarev, and L.B. Okun, “Cosmological consequences of the spontaneous breakdown of discrete symmetry,” *Zh.Eksp.Teor.Fiz.* **67**, 3–11 (1974) Back to page [218](#)
- [287] T.W.B. Kibble, “Topology of cosmic domains and strings,” *J.Phys.* **A9**, 1387–1398 (1976) Back to page [218](#)
- [288] Alexander Vilenkin, “Cosmic strings and domain walls,” *Phys.Rept.* **121**, 263 (1985) Back to page [218](#)

- 
- [289] Y. Chikashige, Rabindra N. Mohapatra, and R.D. Peccei, “Are there real Goldstone bosons associated with broken lepton number?” *Phys.Lett.* **B98**, 265 (1981) [Back to page 219](#)
- [290] Kiwoon Choi and A. Santamaria, “Majorons and supernova cooling,” *Phys.Rev.* **D42**, 293–306 (1990) [Back to page 219](#)
- [291] Y. Chikashige, Rabindra N. Mohapatra, and R.D. Peccei, “Spontaneously broken lepton number and cosmological constraints on the neutrino mass spectrum,” *Phys.Rev.Lett.* **45**, 1926 (1980) [Back to page 219](#)
- [292] Kiwoon Choi and A. Santamaria, “17-KeV neutrino in a singlet - triplet majoron model,” *Phys.Lett.* **B267**, 504–508 (1991) [Back to page 219](#)
- [293] Lorenzo Basso, *Phenomenology of the minimal B-L extension of the Standard Model at the LHC*, Ph.D. thesis, University of Southampton (2011), [arXiv:1106.4462 \[hep-ph\]](#) [Back to page 219](#)
- [294] Stanisław Lem, *Solaris* (Impedimenta, 2011) ISBN 9788415130093, edición en español; traducción del polaco por Joanna Orzechowska [Back to page 230](#)
- [295] Wikipedia, The Free Encyclopedia, “List of particles,” [Online; accessed 30-September-2013], [http://en.wikipedia.org/wiki/List\\_of\\_subatomic\\_particles](http://en.wikipedia.org/wiki/List_of_subatomic_particles) [Back to page 230](#)
- [296] Particle Data Group, “Summary tables of the PDG,” [Online; accessed 30-September-2013], [http://pdg.lbl.gov/2013/tables/contents\\_tables.html](http://pdg.lbl.gov/2013/tables/contents_tables.html) [Back to page 230](#)



